RADIOLOGIC EVALUATION OF BREAST DISORDERS RELATED TO TUBERCULOSIS AMONGST WOMEN IN DURBAN, KWAZULU-NATAL, SOUTH AFRICA

Dibuseng P. Ramaema MBChB, FCRAD DIAG (SA)

RADIOLOGIC EVALUATION OF BREAST DISORDERS RELATED TO TUBERCULOSIS AMONGST WOMEN IN DURBAN, KWAZULU-NATAL, SOUTH AFRICA

Dibuseng P. Ramaema MBChB, FCRAD DIAG (SA)

Thesis submitted in fulfilment of the requirements for the doctor of Philosophy in the School of Clinical Medicine, University of KwaZulu-Natal

Supervisor

Prof Richard J Hift

School of Clinical Medicine, University of KwaZulu-Natal, South Africa

Co-supervisor

Prof Sat Somers

Department of Radiology, McMaster University, Hamilton, Ontario, Canada

February 2016

PREFACE

Developing countries bear the burden of tuberculosis infections. In particular, South Africa ranks high among these countries with KwaZulu-Natal province having the highest incidence. This high prevalence of tuberculosis (TB) infection is associated with the increasing human immunodeficiency virus (HIV). Whilst many research studies have been conducted on TB, most have focused on pulmonary TB (PTB) or other body parts rather than on the breast. It appears like the presence of breast TB (BTB) has been overlooked by research teams. Sadly, there is no national breast cancer screening, and women who have BTB end up with complications from various factors including: being frightened to seek help because of the belief that it might be cancer; being misdiagnosed by their healthcare-worker as having simple mastitis; and being misdiagnosed at hospital as having pyogenic breast infection. It is for these factors that we embarked on attempting to raise awareness of the disease, specifically to study the radiological appearances on various radiology modalities, and to improve pertinent differentiating features between BTB and breast cancer, with the aim of increasing practitioner's level of confidence in diagnosing the condition.

DECLARATION

I, Dr Dibuseng P. Ramaema, declare as follows:

1. That the work described in this thesis has not been submitted to UKZN or other tertiary institution for purposes of obtaining an academic qualification, whether by myself or any other party.
2. That my contribution to the project was as follows:
    1. The preparation of the protocol, recruitment of participants including personally obtaining signed consent forms. Supervision of radiology investigations and interpretation and processing of the radiology images. Drafting and submission of manuscripts for publication. Writing of the thesis document.
    2. That the contribution of others to the project were as follows:

- Richard Hift: Assisted with conceptualising the project and protocol preparation. He contributed to the editing of the manuscripts and thesis chapters.
- Ines Buccimazza: Assisted with data extraction for the retrospective analysis. She was further instrumental in identifying patients who were newly diagnosed with BTB.
- Sat Somers: Assisted with protocol advice, and commented on one manuscript, in which he was the co-author.
- Nischal Soni: Assisted with the interpretation of PET-CT images.

Signed Date (Student)

12th February, 2017

Signed Date (Supervisor)

12th February, 2017

DEDICATION

I dedicate this work to my beloved daughter, Dieketseng.

ACKNOWLEDGEMENTS

When I decided to enrol for a PhD in 2012, I had very little knowledge of the research methodologies and the tough road ahead that I was embarking upon. Nonetheless, once I found myself halfway through the gruelling protocol writing, there were many times when I would have given up were it not for the immense support I received from family, friends and colleagues.

I would like to thank my supervisors and mentors, specifically Richard Hift for his mentoring skills and guiding me through getting rid of the biostatistics phobia.

My family has been my rock, both my daughter Dieketseng and husband Tony were the pillars of support and courage to persevere. I thank all my friends who were constantly supportive throughout the project, especially Pili Mpikashe and Lerato Marishane. A very supportive colleague Ncoza Dlova deserves special thanks for always having solutions to my countless problems. I further thank a colleague Ines Buccimazza for being supportive during the gruelling recruitment period. Much gratitude to Prof Benn Sartorius for providing statistical advice.

I am very grateful to the funders Medical Education Partnership Initiative (MEPI-REMETH) and University of KwaZulu-Natal (UKZN) College of Health Sciences (CHS) strategic funds. The MEPI provided seed funding and research education in the form of various workshops which were very useful, whilst the UKZN operational funds enabled me to attend a conference in Vienna where I presented a poster.

All the radiographers at participating hospitals played an important role, in particular I thank the Addington and King Edward mammographers. Much thanks to the radiographers and administrative staff at Inkosi Albert Luthuli Central Hospital (IALCH) MRI and Nuclear Medicine departments. The surgical breast clinic staff at Addington hospital assisted in finding patients records and I wish to give special thanks to them.

My sincere gratitude goes to the KwaZulu-Natal (KZN) Department of Health (DoH), participating hospital managers, and UKZN institution for providing me with the necessary permissions to carry out the project. Finally, but not least, I give sincere thanks to the participants who sacrificed their valuable time by coming to hospital for further radiology

investigations. The project would otherwise not have been possible without their full commitment and participation.

TABLE OF CONTENTS

Preface		i
Declaration		ii
Dedication		iii
Acknowledgements		iv
List of tables		vii
Abbreviations		viii
Abstract		ix
Chapter 1.	Introduction, literature review, aim, objectives and outline of methodology.	1
Chapter 2.	Prevalence of breast tuberculosis: Retrospective analysis of 65 patients attending a tertiary hospital in Durban, South Africa.	23
Chapter 3.	The role of ^{18}F-FDG-PET-CT in breast tuberculosis: Patterns and assessment of response to treatment.	29
Chapter 4.	The role of multiparametric MRI in breast tuberculosis: Morphological appearances and the evaluation of treatment response.	64
Chapter 5.	Utility of ^{18}F-FDG-PET-CT in differentiating breast cancer from breast tuberculosis.	92
Chapter 6.	Differentiation of breast tuberculosis and breast cancer using diffusion-weighted, T2W and dynamic contrast-enhanced MRI.	116
Chapter 7.	Comparative study of breast lesion size evaluation using DCE-MRI at 1.5T and ^{18}F-FDG- PET-CT in seven patients with breast tuberculosis or breast cancer.	142
Chapter 8.	Synthesis and discussion	166
References		180
Appendix	Breast tuberculosis: radiology spectrum with clinical correlation -a retrospective analysis of 65 patients *(Poster presented at European Congress of Radiology, Vienna, Austria: March 2015)*	194

TABLES

Table 1.1	Classification of breast tuberculosis	5
Table 1.2	Retrospective studies of breast tuberculosis since 1995	7
Table 8.1	Proposed clinical-radiological classification of BTB, based on clinical mammography and ultrasound examination	170
Table 8.2	MRI differential diagnosis of breast lesion in a patient suspected of having either BTB or BCA	172

ABBREVIATIONS

18F-FDG-PET-CT	(Fluorine-18)-fluoro-2-deoxy-D-glucose (18F-FDG) positron emission tomography (PET) integrated with computed tomography (CT)
3-D	3 Dimensional
ADC value	Apparent Diffusion Coefficient value
BCA	Breast cancer
BTB	Breast tuberculosis
CT	Computed Tomography
DCE-MRI	Dynamic Contrast Enhanced Magnetic Resonance Imaging
Dmax	Maximum diameter of a lesion
DWI	Diffusion Weighted Imaging MRI
FDG	F-18 2-fluorodeoxy-D-glucose
HIV	Human Immune-deficiency Virus
MRI	Multiparametric Magnetic Resonance Imaging
PET	Positron Emission Tomography
SUVmax	Maximum Standardised Uptake Value
T1W	T1 Weighted MRI
T2SI	T2 Weighted Signal Intensity
T2W	T2 Weighted MRI

ABSTRACT

Women in KwaZulu-Natal Province, South Africa, are at high risk of developing breast tuberculosis (BTB) due to the increased incidence of HIV. However, there is a general lack of knowledge regarding the various diseases that can affect the breast. This is compounded by lack of the national breast screening program. As a result, many patients with breast cancer (BCA) and BTB are initially misdiagnosed by clinicians. It was evident from the study that much still has to be done in educating the public and healthcare workers about breast diseases.

This project endeavoured to compare the effectiveness of various radiological technologies to identify breast problems. The study consisted of three phases all based at Ethekwini Municipality tertiary referral hospitals. The first phase aimed to determine the prevalence of the BTB using retrospective data over a period of 13 years. The same data further provided information of the clinical and radiological manifestations of BTB. This study concluded that while BTB is not common, it shares the clinical and radiology features with BCA, and is difficult to diagnose with current pathology methods.

The second phase was done prospectively by recruiting patients who were newly diagnosed with BTB. The aim was to evaluate the use of modern imaging techniques to further describe the radiology patterns of BTB and to determine the radiological parameters that may be used in disease monitoring. The results provided insight into disease extent, and showed that it is usually more severe than perceived with current diagnostic methods.

The third phase was performed using retrospective image analysis of patients who had BCA and BTB by using modern radiology techniques. The purpose was to identify the salient features that can differentiate BTB from the BCA. Several radiology parameters were identified as possible biomarkers for differentiation between the two conditions. The knowledge of their respective features would aid in the timeous diagnosis of both conditions, particularly in cases where the pathology results are inconclusive for various reasons.

Overall the study highlights the lack of evidence based information on BTB. Recommendations and conclusions are provided in the last chapter.

CHAPTER 1
INTRODUCTION

INTRODUCTION

EXTRAPULMONARY TUBERCULOSIS

It is estimated that in 2014, 9.6 million people were infected with *Mycobacterium tuberculosis* worldwide, the causative agent of tuberculosis (TB), and that the prevalence had increased since the previous year, 2013, when there were 9.0 million estimated cases (*World Health Organisation.* 2014, 2015). Although TB may affect any organ in the body, pulmonary tuberculosis (PTB) accounts for 80% of all cases (*Akbulut et al.* 2011; *Centre for Disease Control and Prevention.* 2013; *Kulchavenya* 2014). Extrapulmonary tuberculosis (EPTB) affects organs outside the lungs and has a reported incidence of 18-20% (*Akbulut et al.* 2011; *Leeds et al.* 2012; *Mirsaeidi et al.* 2007). The reported incidence of EPTB varies, depending on the geographical location and socioeconomic status of the population under study. Gunal *et al.* (2011) found the most common types of EPTB in Turkey to be genitourinary TB (27.2%) and meningeal TB (19.4%), with the other types ranging in incidence from 9.7% to 10.7% during the period 2001-2007 (*Gunal et al.* 2011). In the United States, the spectrum of EPTB from 1993-2006 was found to include lymphatic (40.4%), pleural (19.8%), bone and joint (11.3%), genitourinary (6.5%), meningeal (5.4%), peritoneal (4.9%) and unclassified EPTB (11.8%) (*Peto et al.* 2009).

Meningeal TB and disseminated TB are more severe forms of TB and occur most commonly in children and immunocompromised adults (*Aurum Institute* 2013). Disseminated TB follows the widespread haematogenous spread of TB bacilli, which may be due to an exacerbation of recent primary infection or a complication of a pre-existing tuberculous focus which has eroded into a blood-vessel (*Aurum Institute* 2013).

The impact of HIV on EPTB

There has been a resurgence of EPTB in last 33 years due to the worldwide increasing incidence of Human Immune Deficiency Virus (HIV) infection (*Leeds et al.* 2012). The severity of the immunodeficiency in HIV infected individuals has led to the increased susceptibility to opportunistic infections, including TB (*Department of Health South Africa.* 2009). The level of immunosuppression determines the nature of opportunistic infections. EPTB occurs more frequently in patients with a low CD4 count of < 100

cells/mm^3 (*Department of Health South Africa.* 2009). The development of EPTB in a HIV infected patient has been classified as WHO stage 4 (*World Health Organization.* 2005).

BREAST TUBERCULOSIS

Among other forms of tuberculosis infections, TB of the breast occurs and was initially described in 1829 by Sir Astley Cooper, an English surgeon and anatomist in 1829. In his two-part book entitled "Illustrations of diseases of the breast", in a section named "Scrofulous Tumours of the Breast" he described finding tumours in the breasts of young women with enlarged cervical glands. He suggested that the tumours were of the inflammatory nature and were not to be regarded as malignant (*Cooper* 1829). Other reports and case series followed. The first classification was by Velpeau A (1854), who classified breast tuberculosis (BTB) into three forms: a) disseminated tubercles; b) multiple lymphatic tumours; and c) lymphatic suppurating (or caseating) tumours. To this point management consisted of the surgical removal of the diseased breast or breast tissue, and the diagnosis was based on clinical and surgical findings only. The first histological diagnosis of BTB was made by Lancereaux and Charley (1860) when they studied the structure of the removed part of the breast under the microscope . Subsequently, histological and bacteriological evidence for the diagnosis was reported by Gautier from his thesis in which he analysed seventy-seven previously published cases. He demonstrated the presence of tubercles containing giant cells (*Gautier* 1896). Around the same period, Dubar L-E (1881) reclassified the disease based on the microscopic and the histological appearances, classifying BTB as *Isolated* or *disseminated nodular TB*; and *confluent TB* on anatomical pathological grounds. Much later, McKeown and Wilkinson (1952) re-classified BTB into five types: *nodular, disseminated, sclerosing, acute miliary tuberculous mastitis* and *tuberculous mastitis obliterans*. They based their classifications on the clinical presentation reported in five case series they reviewed. The most recent formal classification is that of Tewari and Shukla (2005) who classified BTB into *nodular-caseous, disseminated/confluent* and *abscess* varieties. They

found nodular-caseous variety to be the most common. The two classifications are compared in Table 1.1 below.

The route of breast infection

BTB is termed *primary* if there is no other demonstrable focus elsewhere in the body. Several isolated cases of primary BTB have been reported since 1999 (*Bhosale* 2012; *Chalazonitis et al.* 2003; *Chauhan et al.* 2006; *Gupta et al.* 2012; *Jah et al.* 2004; *Sen et al.* 2009; *Zandrino et al.* 2000). If there is a focus elsewhere, BTB is termed *secondary*. The primary focus may be from the lung, lymph nodes including axillary, paratracheal and internal mammary nodes (2013; *Halstead & Lecount* 1898; *Khanna et al.* 2002; *Mirsaeidi et al.* 2007; *Winzer et al.* 2005). BTB may also arise secondarily from haematogenous spread and from the contiguous spread of infection from adjacent organs such as chest wall, ribs and sternum (*Winzer et al.* 2005). It is generally accepted that the lymphatic spread is by retrograde extension from the axillary nodes (*Baharoon* 2008; *Domingo et al.* 1990). This hypothesis has been supported by frequent unilateral ipsilateral axillary nodes involvement in 50-70% of tuberculous mastitis cases (*Baharoon* 2008).

Old classification (*McKeown & Wilkinson* 1952)	**New classification (*Tewari & Shukla* 2005)**
Nodular tubercular mastitis (most common)	Nodular-caseous tubercular mastitis approx. (72%)
Disseminated/ confluent tubercular mastitis	Tubercular breast abscess approx. (26%)
Sclerosing tubercular mastitis (mimics cancer, common in older women)	Disseminated/confluent tubercular mastitis (approx. 2%)
Tuberculous mastitis obliterans	
Acute miliary tubercular mastitis	

Table 1. 1 Classification of BTB

THE INCIDENCE AND PREVALENCE OF BTB

As with other forms of TB, the incidence of BTB is dependent on the level of economic development of a country. In first world countries, the incidence of BTB is reported to be less than 0.1% of all surgically treated breast disease. On the other hand, developing countries have an incidence of approximately 3-4.5% among surgical breast cases (*Kalaç et al.* 2002). The high rate of HIV infections in developing countries further contributes to increasing the incidence of EPTB including BTB (*Tewari & Shukla* 2005; *World Health Organisation.* 2015). In a study done at Khuzestan Health Centre, Iran, where TB is considered endemic, only 9 BTB cases among 2235 patients with TB were found over a five year period from 2005-2009 (*Shushtari et al.* 2011). Other studies include those of Mehta *et al.* (2010), who reviewed 63 BTB cases among 5200 TB patients during the period 1992-2008, whilst Tewari and Shukla (2005) reported 30 cases from a total of 1180 TB patients over a 20 year period. Makanjuola reported 6 cases identified among 1152 mammograms during a 3 year period in 1996 (*Makanjuola et al.* 1996). A summary of retrospective studies on BTB is provided in Table 1.2.

Study	Country	Number of BTB cases	Period of review
Hiremath and Subramaniam (2015)	India	7	2012-2014
Tandon *et al.* (2014)	Not available	22	Not available
Khodabakhshi and Mehravar (2014)	Iran	22	2002-2012
Meerkotter *et al.* (2011)	South Africa	21	2002-2008
(2013); Shushtari *et al.* (2011)	Iran	9 (Total TB 2235)	2005-2009
Mehta *et al.* (2010)	India	63 1 male (Total TB 5200)	1992-2008
Afridi *et al.* (2009)	India	30	1999-2007
Da Silva *et al.* (2009)	Brazil	20	1994-2007
Atamanalp *et al.* (2010)	Turkey	7	1988-2007
Harris *et al.* (2006)	India	38 (1 male)	1998-2003
Ben Hassouna *et al.* (2005)	Tunisia	65	1980-2001
Tewari and Shukla (2005)	India	30 (Total TB 1180)	1983-2003
Bani-Hani *et al.* (2005)	Jordan	9	1994-2003
Sakr *et al.* (2004)	Egypt	10	1999-2001
Khanna *et al.* (2002)	India	52	1986-2000
Al-Marri *et al.* (2000)	Qatar	13	1988-1998
Oh *et al.* (1998)	China	17	1983-1995
Makanjuola *et al.* (1996)	Saudi Arabia	6 (Total mammograms 1152)	3 year period (no date)

Table 1.2 Retrospective studies of BTB since 1995. Where the total TB population from which the BTB cases are drawn is reported, is listed here.

RISK FACTORS FOR THE DEVELOPMENT OF BTB

Reported risk factors include multiparity (*Al-Marri et al.* 2000); lactation (*Harris et al.* 2006; *Kalaç et al.* 2002) and HIV (*Hartstein & Leaf* 1992). Age of onset varies widely, including adolescence (*Indumathi et al.* 2007), young adult (*Afridi et al.* 2009) and the elderly (*Da Silva et al.* 2009; *Maroulis et al.* 2008). BTB has occasionally been reported in male patients (*Mehta et al.* 2010; *Rajagopala & Agarwal* 2008).

DIAGNOSIS OF BTB

Diagnosis may be based on clinical breast examination, radiological tests and pathological investigations. The clinical appearance of an irregular mass associated with axillary lymphadenopathy is similar to breast cancer presentation, while the mammographic appearance of an irregular dense mass with enlarged dense axillary nodes mimic breast cancer is often provisionally reported by the radiologist as cancer. The lack of specific clinical and radiological appearances compounds the problem of misdiagnosis (*Ben Hassouna et al.* 2005). Early diagnosis and efficient distinction between BTB and breast cancer (BCA) is imperative, especially because BTB is a treatable condition.

Clinical appearances

A wide range of the breast symptoms and signs have been described. These include lump or mass, breast swelling, fluctuating mass, breast pain, nipple discharge, axillary lymph nodes, discharging sinuses, ulcers, cutaneous fistulae, fibrotic changes with breast atrophy and breast deformities (*Makanjuola et al.* 1996; *Tewari & Shukla* 2005). Constitutional symptoms are not common, except in patients who also have PTB (*Mehta et al.* 2010). Because constitutional symptoms such as fever are not always present, differentiation from cancer is not always possible when using clinical findings alone. In a recent study of six cases, symptoms included loss of weight and appetite, pain, weakness and fever. The fever was present in only two patients (*Gill et al.* 2012). The signs are nonspecific, can be insidious and often mimic those of BCA (*Akcay et al.* 2007; *Bani-Hani et al.* 2005; *Farrokh et al.* 2010; *Gill et al.* 2012; *Kapan et al.* 2010; *Maroulis et al.* 2008; *Woyke et al.* 1980) and pyogenic breast abscess (*Al-Roomi et al.* 2009; *Chauhan et al.* 2006; *Mathur* 2009). Furthermore, BTB can co-exist with BCA (*Akbulut et al.* 2011). During an extensive

literature review, Akbulut *et al* found twenty nine cases of co-existing BTB and BCA from 1899 to 2011 (*Akbulut et al.* 2011); with the inclusion of their own case report, there were thirty cases altogether.

Pathological diagnosis

Pathological methods in current use include fine needle aspiration cytology (FNAC) (*Sriram et al.* 2008), wide bore core biopsy/histopathology (*Gupta et al.* 2012), smear acid fast bacilli (AFB) on Ziehl-Neelsen (ZN) stain (*Harris et al.* 2006)**,** TB culture (*Deepa et al.* 2011), polymerase chain reaction (PCR) (*Chia BS* 2012), QuantiFERON gold test for TB (*Mazurek et al.* 2005), interferon release assay (*Sen et al.* 2009), and incision/excision biopsy (*Tewari & Shukla* 2005).

Fine needle aspiration cytology (FNAC)

Although aspiration cytology cannot determine the etiological agent, the presence of epithelioid cell granulomas and necrosis is considered adequate for diagnosis, often allowing a diagnosis in up to 73% of cases (*Sriram et al.* 2008). However, the absence of necrosis on FNAC does not exclude BTB because of the small quantity of sample material, and FNAC is therefore of limited value (*Akcay et al.* 2007).

Wide bore core biopsy/histopathology

Core biopsy yields an adequately sized sample, and often yields a positive diagnosis (*Tewari & Shukla* 2005). The diagnosis is readily established by the presence of caseating granuloma, epithelioid cells, Langhans' type giant cells and lympho-histiocytic aggregates (*Harris et al.* 2006; *Khanna et al.* 2002). Gupta *et al.* (2012) have stressed the importance of always performing a tissue biopsy even in cases where the clinical impression is of a non-TB breast abscess

Smear acid fast bacilli (AFB) on Ziehl-Neelsen (ZN) stain

Abscess fluid and nipple discharge should be subjected to microscopy using ZN stain and AFB sought. The yield has been low, with Harris *et al.* (2006) reporting a 2% rate of positive ZN smears for AFB. The low number of bacilli in EPTB further complicates the diagnosis,

since 1,000 to 10,000 mycobacterium per gram of tissue are required in order to obtain a positive smear (*Mathur* 2009). Nor is an AFB-positive smear always adequate evidence for a definitive diagnosis of *M. tuberculosis*, as it should be differentiated from other mycobacterium species (*Akcay et al.* 2007)..

TB culture (FNA and core biopsy): detection of m tuberculosis

Detection of *M. tuberculosis* by culture takes time, and there is a significant possibility of false negative results, with some authors reporting a 50% false negative rate in samples with low mycobacterial counts. In a series of 14 cases, Deepa *et al.* (2011) showed the presence of acid-fast bacteria in 5 of 9 patients with a tuberculous breast.

Furthermore, not all Mycobacteria are *Mycobacterium tuberculosis (MTB).* One case of atypical *Mycobacterium* causing breast infection has been reported (*Verfaillie et al.* 2004). This was an 85 year old man in whom FNAC of a breast mass revealed AFB and culture yielded *Mycobacterium kansasii* (*Verfaillie et al.* 2004). In another unusual case, bilateral BTB developed in a 25-year-old HIV-negative woman whilst she was on anti-tuberculous therapy (ATT) for PTB. She represented with fever, bilateral breast nodules and axillary lymphadenopathy. Breast ultrasound showed bilateral infective type lesion whilst FNAC demonstrated AFB. Culture revealed a mycobacterium complex consisting of *Mycobacterium tuberculosis, Mycobacterium bovis, Mycobacterium africanum and Mycobacterium microti* which were sensitive to second line ATT (*Kaneria MV* 2006).

Polymerase chain reaction (PCR): (nucleic acid amplification tests/NAAT)

PCR detects *MTB*. It is also beneficial in detecting mutations that give rise to drug resistance, and can identify multi drug resistant tuberculosis (MDR-TB) using Multiplex Allele-Specific Polymerase Chain Reaction (MAS-PCR) (*Chia BS* 2012).

Interferon release assays (IGRAs)

Whole-blood enzyme-linked immunosorbent interferon release assays detect interferon secreted by T cells in response to antigens encoded in the region of difference 1 of *MTB*, a genomic segment from Bacillus Calmette-Guerin (BCG) and most environmental Mycobacteria. It has higher specificity than tuberculin skin test, and results are available

within 24hrs (*Sen et al.* 2009). The IGRAs which have been approved by the United States (U.S) Food and Drug Administration (FDA) are the QuantiFERON-TB Gold In-Tube test (QFT-GIT) and the T-SPOT.TB blood test (Oxford Immunotec Global PLC, Abingdon, England) (*Centre for Disease Control and Prevention.* 2014).

Incision/Excision biopsy

This is a more invasive procedure compared to core biopsy and FNAC and is hence reserved for cases where diagnosis cannot be achieved by either method. It can be done for a lump, ulcer, sinus or wall of an abscess cavity, whereby diagnosis is almost always confirmed (*Tewari & Shukla* 2005). Extreme care is required with histological interpretation as not all granulomas demonstrate necrosis. In a study of lymph-node granulomas, Khurram *et al.* (2007) found *M. tuberculosis* DNA in 50% of granulomas with necrosis, and in 50% of granulomas without necrosis

DIFFERENTIAL DIAGNOSIS

BCA and idiopathic granulomatous mastitis (IGM) are commonly included in the differential diagnosis of BTB, (*Afridi et al.* 2010; *Baharoon* 2008; *Lacambra et al.* 2011). There have been several reports of BTB mimicking BCA both clinically and radiologically (*Akcay et al.* 2007; *Farrokh et al.* 2010; *Gill et al.* 2012; *Goyal et al.* 1998; *Kant et al.* 2008; *Kapan et al.* 2010; *Maroulis et al.* 2008; *Woyke et al.* 1980). The distinction between TB mastitis and IGM is important because the treatment is different: ATT and steroid treatment respectively.

The distinction between BTB and IGM is based on histological features because clinically the two conditions are not easily distinguishable. Predominantly neutrophilic inflammation with a lack of caseous necrosis favours IGM rather than TB (*Akcay et al.* 2007). In cases where IGM was confused with cancer, the histopathologic association of benign ductolobular units that is seen with IGM can help to differentiate the two (*Cheng et al.* 2010). However, Baharoon recommends the addition of *Mycobacterium Tuberculosis* (MTB) PCR as part of routine investigation, because both ZN for AFB can be negative in FNAC, and histopathology may not demonstrate necrosis in cases of BTB (*Baharoon* 2008).

There are other causes of granulomatous lesions of the breast, and although they are not common, they should be considered and excluded before diagnosis of idiopathic lobular granulomatous mastitis is considered (*Bakaris et al.* 2006). Breast mass with discharging sinuses can occur in actinomycosis, with the presence of sulphur granules in the pus differentiating it from TB (*Akcay et al.* 2007). Some cases have been confused with pyogenic abscesses, leading to delays in treatment (*Al-Roomi et al.* 2009; *Chauhan et al.* 2006). Other differentials include fibroadenoma and fibrocystic change based on ultrasound appearances (*Akcakaya et al.* 2005). Radiological appearances can also be similar to traumatic fat necrosis, plasma cell mastitis and mammary dysplasia. Clinically and radiologically discharging sinuses can also be seen in other fungal infection such as blastomycosis (*Da Silva et al.* 2009). Histologically non caseating granulomas without draining sinuses can occur in sarcoidosis (*Fiorucci et al.* 2006). Granulomatous vasculitis, such as giant cell arteritis and Wegener's granulomatosis also need to be ruled out (*McKendry &* 1990). One confirmed case of Wegener's granulomatosis of the breast was reported by (*Veerysami et al.* 2006).

IMAGING OF BTB

Following clinical examination, radiology is the first line of investigation for patients presenting with breast symptoms.

Mammography (including Full Field Digital Mammography: FFDM)

Mammography and ultrasound are the standard radiological modalities in use for breast diagnosis and for monitoring of disease and of treatment response (*The Royal College of Radiologists* 2013). Mammography was developed in 1960, and has been a recognised and established modality since 1969 (*Gold* 1992). By 1976 screening with mammography had become standard practice given its role in detecting early stage breast cancer (*Moskowitz et al.* 1976).

Mammograms have been mainly used to define disease extent, but not to differentiate BTB from other differentials (*Baharoon* 2008). However, specific signs such as the skin bulge and sinus tract sign have been described (*Makanjuola et al.* 1996), this being the result of contracted Cooper's ligament. Subsequent to this, Harris *et al* and Khanna provisionally

diagnosed BTB on the basis of mammographic findings of skin thickening with sinus tracts, which were communicating with intramammary masses (*Harris et al.* 2006; *Khanna et al.* 2002). Other mammographic appearances include irregular mass lesions, smooth well defined mass lesions, intramammary nodes, axillary nodes, asymmetric density, duct ectasia, skin thickening with nipple retraction, microcalcification and skin sinuses (*Sakr et al.* 2004). Some authors have termed the round mass appearance as pseudotumoral image, due to its lack of classic halo seen in benign lesions like fibroadenoma (*del Agua et al.* 2006). Non-specific stromal thickening has also been found (*Khanna et al.* 2002).

Mammography limitations reduced sensitivity for cancer detection in women with mammographically dense breasts (*Kolb et al.* 2002). Furthermore, the risk of radiation has resulted in guidelines restriction for mammograms to be performed in women above 35 years of age, with an exception being made for those younger patients who are classified as high risk (*NHS Breast Screening Programme* 2013).

Digital Breast Tomosynthesis (DBT)

In a recent study by Michell *et al.* (2012), the use of DBT additional to full field digital mammography (FFDM) and film-screen mammography combined, and film-screen mammography alone was found to increase the accuracy of breast lesion detection and characterisation. They screened 788 women. The area under the curve (AUC) values showed significant increase in diagnostic accuracy with DBT addition to FFDM and film-screen mammography compared to FFDM plus film-screen mammography, and film screen mammography alone. The use of DBT has not been explored in the diagnosis of BTB. Another limitation is increased radiologist reading time per study (*Dang et al.* 2014).

Ultrasound

Patients below 35 years of age are investigated with ultrasound only, with an exception being made for those younger patients who are classified as high risk (*NHS Breast Screening Programme* 2013). The reason being to avoid exposure of young breast tissues to ionising radiation (*Hendrick* 2010). Mammography and ultrasound are both used in those over 35 years of age. The appearances of BTB vary depending on the morphological subtype. Nodular caseous subtype appears as a hypoechoic mass, which may be irregular in outline, or be well defined. Diffuse subtype may appear as diffuse trabecular tissue thickening or

microcysts with oedema. The abscess subtype appears as a complex hypoechoic fluid collection, and may be connected to skin sinuses and fistulae (*Kalaç et al.* 2002).

Ultrasound has a limitation of being operator dependent, which has the potential to increase imaging interpretation inter-observer variability

Computed Tomography (CT scan)

The value of CT scan needs to be further explored. No authors have extensively explored this valuable modern modality in evaluating breast infection. New multi-detector scanners with three-dimensional tube modulation together with adaptive x-ray shutters have led to significant dose reduction to the patients while improving image quality. This is due to the use of optimized reconstruction algorithms (*Rogalla P* 2008).

The cases described in the literature limited the use of CT scan to evaluate the possibility of disease extension into the chest wall (*Chalazonitis et al.* 2003; *Tewari & Shukla* 2005). The other benefit of CT scan is that it can investigate the presence of pulmonary disease at the same time (*Kalaç et al.* 2002). CT scan machine make use of ionising radiation to generate images, it therefore has a relative contraindication in pregnant women. There are no dedicated mammo CT scanners in the market, hence it is currently not the modality of choice for breast related disorders.

Magnetic Resonance Imaging scan (MRI)

As with the CT scan, the usefulness of MRI needs to be explored. The literature indicated that it had mainly been used to identify TB outside breast, specifically in the thoracic wall (*Chalazonitis et al.* 2003; *Tewari & Shukla* 2005). One author used MRI to evaluate response to treatment in a patient with BTB. MRI before and after six months of ATT demonstrated full response (*Fellah et al.* 2006). In a study by Al-Khawari *et al.* (2011), ten patients who had granulomatous mastitis (GM) were evaluated by MRI. Final histology showed tuberculous mastitis in four patients, unknown aetiology GM in four and duct ectasia related GM in two patients. Because the MRI appearances were similar in all ten patients, they concluded that MRI could not differentiate BTB from GM (*Al-Khawari et al.* 2011). MRI is also useful in looking at the extent of disease spread beyond the breast. Both T1 weighted and T2 weighted MRI sequences are routinely acquired during MRI investigation.

Proton Magnetic Resonance Spectroscopy (MRS)

This technique has proved useful in differentiating BTB from BCA in four cases where mammography, ultrasound and MRI indicated BCA rather than BTB. The absence of choline peak and the presence of strong lipid peak was suggestive of tuberculosis, which was later confirmed on FNA (*Popli et al.* 2010).

F-18 2-fluorodeoxy-D-glucose positron emission tomography (^{18}F-FDG-PET-CT) scan

Sathekge *et al.* (2012) conducted a prospective study to evaluate the use of ^{18}F-FDG-PET CT in assessing response after 4 months of ATT in 20 patients with TB-HIV coinfection, specifically using lymph nodes (LN) parameters. They evaluated relationships between FDG-PET, CT and treatment outcome. They concluded that responding and nonresponding LNs could be differentiated using SUV_{max} cut off value of 4.5 and presence of at least one LN basin with peripheral rim enhancement and central low attenuation (PRECLO). However, in another study by the same author, it was found that dual phase ^{18} F-FDG-PET-CT could not differentiate malignant lymph nodes from tuberculous nodes in 30 patients with solitary pulmonary nodule (*Sathekge et al.* 2010).

Radiological diagnosis of BTB in the South African setting

Despite the high incidence of TB in South Africa, there is little published information on the radiological appearance of BTB. Furthermore, all studies concerning the radiology of BTB in the last fifteen years have been retrospective due to the low incidence and prevalence of the disease. Meerkotter *et al.* (2011) conducted a retrospective chart review of 21 patients with BTB over a six year period from 2002–2008 in Johannesburg, recording presenting clinical, ultrasound and mammographic features. Their study was mainly descriptive and the statistics used was simple proportions with no reference to sensitivity or specificity. They described the appearances of BTB as nodular, disseminated and sclerosing types. This description differs from the most recent classification by Tewari and Shukla (2005), namely, nodular-caseous, disseminated/confluent and abscess varieties. Some important findings reported by Meerkotter included the presence of chest wall mass and ipsilateral axillary lymph nodes as the predominant presenting symptom.

Similarly Tewari and Shukla (2005) conducted a retrospective study of 30 BTB patients seen over a twenty year period (1983–2003), recording presenting features, pathological diagnosis and treatment The authors did not determine sensitivity or specificity. There were 30 cases out of a total of 1180, and they mention an incidence of 2.5%, although this appears like a 20-year period prevalence.

MANAGEMENT OF BREAST TUBERCULOSIS

Most patients respond to standard ATT. Early diagnosis and treatment of BTB may prevent debilitating complications including discharging sinuses and cutaneous fistulae, fibrosis and breast deformities (*Bani-Hani et al.* 2005; *Sen et al.* 2009). There is however little information in the literature regarding the morbidity and mortality rate. In TB endemic areas, patients presenting with a breast mass in whom histology showed granulomatous mastitis, should be candidates for ATT, even if culture results are negative for TB (*Shushtari et al.* 2011). The disadvantage of this empirical treatment is that IGM is treated with steroids, therefore patients who have IGM may not respond to ATT. The South African National TB guidelines recommend 6 months' treatment for PTB whilst that for EPTB is 9 months (*Department of Health (South Africa)* 2014). Our local institution protocol is as follows.

<u>Initiation phase: 2 months</u>

- Rifafour (daily)
    - 38 – 54kg: 3 tablets
    - 55 – 70kg: 4 tablets
    - 71kg and above: 5 tablets
- Pyridoxine (daily)
    - 25mg

<u>Maintenance phase: 7 months</u>

- Rifinah $^{150/75}$ (daily)
    - 38 – 54kg: 3 tablets

rifinah $^{300/150}$ (daily)

≥ 55kg: 2 tablets

- Pyridoxine (daily)
    - 25mg

Clinical response

Follow up is monthly for the first two months to assess clinical response, followed by follow up every three months for the duration of the treatment. If there is no clinical response during the follow up visits, a repeat biopsy is performed, the sample obtained is sent for microbiology, culture and sensitivity to evaluate for drug resistance.

Radiological response

Mammography and breast ultrasound may be repeated if the referring clinician has concern. Although there are no documented criteria for radiological response, lack of reduction in size of lesion as well as lack of mammographic change in appearance may be indicative of non-response and possible drug resistance. Whereas most patients who presented with painful breast mass demonstrate a complete clinical and radiological response after six months of standard therapy (*Akcay et al.* 2007), there have been cases not responsive to standard treatment who may require surgical intervention (*Shushtari et al.* 2011). (*Mehta et al.* 2010) reviewed 63 cases and reported that only 18 cases (28%) responded to ATT alone. Over half the cases (55%) were complicated by the presence of sinuses, fistulae and deformities, requiring surgical intervention, typically by primary localised excision; one patient required a simple mastectomy.

PROBLEM STATEMENT

While BTB would appear to be uncommon, cases are likely to be encountered on a regular basis in developing countries such as South Africa subject to a higher background prevalence of TB. As shown in the foregoing literature review, literature on BTB is sparse, and in particular, information on its radiological appearances is lacking. Since the first line of investigation following clinical examination for most forms of breast disease is radiological imaging, there is a need for the radiology of BTB to be far better characterised. Though there is some information on mammography and ultrasound, very little is known about the appearances of BTB on the newer modalities of MRI and ^{18}F-FDG-PET scanning.

AIM OF THE STUDY

The aim of this study was to report our experience with BTB in Durban, South Africa, to assess the incidence of BTB as a proportion of all women attending the main referral clinics for breast disease, to study the appearances of BTB on MRI and PET-CT and to investigate their role in diagnosis and in the monitoring of response to ATT.

OBJECTIVES

The study had the following objectives:

1. To assess the prevalence of BTB amongst patients attending the major surgical breast referral clinics in Durban, South Africa.
2. To describe the clinical and radiological findings in patients with BTB, including an evaluation of current treatment methods.
3. To describe the appearances of BTB on ^{18}F-FDG-PET-CT and to study its potential utility in the assessment of treatment response.
4. To describe the appearances of BTB on MRI and to study its potential utility in the assessment of treatment response.
5. To explore the role of ^{18}F-FDG-PET-CT as a non-invasive assessment method to differentiate BTB from BCA.
6. To evaluate the value of diffusion weighted imaging (DWI), T2 Weighted (T2W) and dynamic contrast enhanced magnetic resonance imaging (DCE-MRI) in differentiating BCA from BTB.
7. To compare the values of breast lesion volume as measured by DCE-MRI and prone ^{18}F-FDG-PET-CT imaging.

Study design and methodology

The study settings were at the Addington, King Edward and Inkosi Albert Luthuli Central Hospitals (IALCH) breast clinics, Durban, South Africa. The work is reported as seven sub-studies, using a selection of methodologies appropriate to each, which are fully described in Chapters 2-7.

Subjects

The BTB patient cohort studied in Chapter 2 here were not analysed for any subsequent study. The same cohort of BTB patients were studied in Chapters 3-7. Different groups of patients with BCA were studied in chapters 5-7. There is no overlap.

STRUCTURE OF THE THESIS

Chapter 1

Introduction, literature review, aim, objectives and outline of methodology.

Chapter 2

Prevalence of breast tuberculosis: Retrospective analysis of 65 patients attending a tertiary hospital in Durban, South Africa.

This chapter presents the literature review, methodology, results and discussion for Objectives 1 and 2, specifically determination of the prevalence of BTB, a description of the clinical and radiological patterns observed in these patients and the outcome of therapy.

This was published as: Ramaema DP, Buccimazza I, Hift RJ. Prevalence of breast tuberculosis: Retrospective analysis of 65 patients attending a tertiary hospital in Durban, South Africa. *S. Afr. Med. J. 2015; **105**: 866-9.*

Chapter 3

The role of ^{18}F-FDG-PET-CT in breast tuberculosis: Patterns and assessment of response to treatment.

This chapter presents the literature review, methodology, results and discussion for Objective 3, a description of the appearances of BTB on ^{18}F-FDG-PET-CT and a preliminary study of its potential utility in the assessment of treatment response.

The work is presented in manuscript form as: Ramaema DP, Hift RJ, Somers S, Soni N. The role of ^{18}F-FDG-PET-CT in breast tuberculosis: Patterns and assessment of response to treatment.

Chapter 4

The role of multiparametric MRI in breast tuberculosis: Morphological appearances and the evaluation of treatment response.

This chapter presents the literature review, methodology, results and discussion for Objective 4, a description of the appearances of BTB on MRI and a preliminary study of its potential utility in the assessment of treatment response.

The work is presented in manuscript form as: Ramaema DP, Hift RJ. The role of multiparametric MRI in breast tuberculosis: Morphological appearances and the evaluation of treatment response.

Chapter 5

Utility of ^{18}F-FDG-PET-CT in differentiating breast cancer from breast tuberculosis.

This chapter presents the literature review, methodology, results and discussion for Objective 5, an exploration of the role of ^{18}F-FDG-PET-CT as a non-invasive assessment method to differentiate BTB from BCA.

The work is presented in manuscript form as: Ramaema DP, Hift RJ. Utility of ^{18}F-FDG-PET-CT in differentiating breast cancer from breast tuberculosis.

Chapter 6

Differentiation of breast tuberculosis and breast cancer using diffusion-weighted, T2W and dynamic contrast-enhanced MRI.

This chapter presents the literature review, methodology, results and discussion for Objective 6, an evaluation of the value of diffusion weighted imaging (DWI), T2W and DCE-MRI in differentiating BCA from BTB.

The work is presented in manuscript form as: Ramaema DP, Hift RJ. Differentiation of breast tuberculosis and breast cancer using diffusion-weighted, T2W and dynamic contrast-enhanced MRI.

Chapter 7

Comparative study of breast lesion size evaluation using DCE-MRI at 1.5T and ^{18}F-FDG-PET-CT in seven patients with breast tuberculosis or breast cancer.

This chapter presents the literature review, methodology, results and discussion for Objective 7, a comparison of the values of breast lesion volume as measured by dynamic contrast-enhanced breast MRI (DCE-MRI) and prone ^{18}F-FDG-PET-CT imaging.

The work is presented in manuscript form as: Ramaema DP, Hift RJ. Comparative study of breast lesion size evaluation using DCE-MRI at 1.5T and ^{18}F-FDG-PET-CT.

Chapter 8

Synthesis and discussion

References

CHAPTER 2

Prevalence of breast tuberculosis: Retrospective analysis of 65 patients attending a tertiary hospital in Durban, South Africa

Prevalence of breast tuberculosis: Retrospective analysis of 65 patients attending a tertiary hospital in Durban, South Africa

D P Ramaema,[1] FCRad (Diag) SA; **I Buccimazza**,[2] FCS (SA), FACS; **R J Hift**,[3] MMed (Med), PhD, FCRP, FCP (SA)

[1] *Division of Radiation Medicine (Radiology), School of Clinical Medicine, College of Health Sciences, Nelson R Mandela School of Medicine, University of KwaZulu-Natal, Durban, South Africa*
[2] *Division of General Surgery, School of Clinical Medicine, College of Health Sciences, Nelson R Mandela School of Medicine, University of KwaZulu-Natal, Durban, South Africa*
[3] *Division of Medicine, School of Clinical Medicine, College of Health Sciences, Nelson R Mandela School of Medicine, University of KwaZulu-Natal, Durban, South Africa*

Corresponding author: *D P Ramaema (ramaema@ukzn.ac.za)*

Background. Breast tuberculosis (BTB) is uncommon, but not rare. Knowledge of the ways in which it can present can prevent unnecessary invasive procedures and delay in diagnosis.
Objectives. To describe the clinical and radiological findings in patients with BTB, including evaluation of current treatment methods.
Methods. We retrospectively analysed 65 patients diagnosed with BTB at Addington and King Edward VIII hospitals, Durban, South Africa, between 2000 and 2013. Demographic, clinical and radiological findings and treatment outcomes were noted.
Results. A total of 11 092 patients underwent breast investigations between 2009 and 2013, with a prevalence of BTB for the period of 0.3% (30 patients). Of the 65 patients diagnosed between 2000 and 2013, 64 were female (98.5%) and one was male (1.5%). The age range was 23 - 69 years (mean 38.5). The most common mammographic pattern was density (39.4%) and the least common a mass (6.1%). Isolated axillary lymphadenitis was found in 12.1%. Abscess was the commonest ultrasound pattern (39.0%). Of the 47 patients with a known history of pulmonary tuberculosis (TB), 68.1% (*n*=32) did not have radiological evidence of previous or concurrent pulmonary TB, nor was there evidence of TB elsewhere. Of 47 patients with known HIV status, 34 were HIV-positive. Fine-needle aspiration cytology had sensitivity of only 28% compared with 94% for histology. Of those treated, 72.7% obtained full resolution following 9 months of TB treatment; 25.0% did not complete treatment, and 2.3% (*n*=1) died while on treatment. Follow-up data on relapse rates after treatment completion and disease resolution are scanty.
Conclusion. Understanding and being aware of the various presentations of BTB make it possible to treat most patients successfully.

S Afr Med J 2015;105(10):866-869. DOI:10.7196/SAMJnew.7704

It is estimated that over 1 billion people worldwide have tuberculosis (TB).[1] However, breast tuberculosis (BTB) is a rare condition. The incidence has been reported as <0.1% of all surgical breast lesions seen in developed countries and 3 - 4.5% of breast lesions in countries where BTB is endemic,[2,3] although even in this setting, carcinoma is far more commonly encountered.[4] While BTB is considered a manifestation of extrapulmonary tuberculosis (EPTB), it represents only about 0.1% of the disease burden of EPTB. However, there has been a resurgence of EPTB as a result of HIV, with estimated incidences as high as 50% in countries where HIV infection is endemic.[5]

The right and left breasts are equally affected by BTB, which may be bilateral in ~3% of cases.[6] Up to 70% of patients may have associated axillary lymphadenopathy, often with visible axillary swelling.[7] Constitutional symptoms are unusual in the absence of systemic and particularly pulmonary TB.[4]

No clinical or radiological features are absolutely diagnostic of BTB. The diagnosis is usually readily confirmed by biopsy with histological examination or fine-needle aspiration and staining for acid-fast bacilli (AFB), mycobacterial culture or polymerase chain reaction (PCR) testing. While the main differential diagnosis is carcinoma, other considerations are idiopathic granulomatous mastitis and fungal infections. Most patients respond to standard anti-TB therapy (ATT).[8] It has been suggested that patients in endemic areas who have a breast mass with granulomatous inflammation on histological examination should receive ATT, even if culture results are negative for TB.[9] There have been reports that sinuses, fistulas and deformities may occasionally require primary localised excision or simple mastectomy, but this is not standard care.[4]

Objectives

To identify the various radiological patterns of BTB, and to assess available treatment options and response to treatment.

Methods

We identified 64 patients with a histological or cytological confirmed diagnosis of BTB. One patient with discharging axillary nodes and breast oedema was included even though cytological findings were not confirmatory; 65 patients were therefore included in the data analysis. Patients were diagnosed between 2000 and 2013. Data were collected from Addington (*n*=60 patients) and King Edward VIII hospitals (*n*=5), Durban, South Africa. The study was approved by the Bioethics Research Committee at the University of KwaZulu-Natal, Durban (Reference No. BF213/13). A retrospective chart and radiology review focused on demographic, clinical, mammographic and ultrasound patterns and diagnostic and treatment methods.

Mammograms (mediolateral oblique (MLO) and craniocaudal views) were done using a standard Mecatronica analogue mammographic unit (± digital processing). Ultrasound images

were obtained on the various standard units using a 7.5 - 12.5 MHz linear probe. Mammographic patterns were classified as follows: asymmetrical density, asymmetrical density with axillary nodes, inflammation with axillary nodes, mass, mass with axillary nodes, nodes only, and normal. Ultrasound patterns were classified as abscess, abscess with axillary nodes, mass, mass with axillary nodes, oedema, oedema with nodes, thickening, nodes only, and normal.

Histological and microbiological diagnosis was done by obtaining core biopsy samples using a 14-gauge needle. Cytological diagnosis was done by FNA biopsy. Lesion localisation was either achieved by palpation or ultrasound guided.

Descriptive statistics using proportions were used to analyse results.

Table 1. Demographic and clinical features (*N*=65)

Characteristics	
Gender, *n* (%)	
Female	64 (98.5)
Male	1 (1.5)
Age at presentation (years)	
Range	23 - 69
Mean (SD)	38.5 (10.3)
Side, *n* (%)	
Left	30 (46.2)
Right	33 (50.8)
Unknown	2 (3.1)
Axillary nodes, *n* (%)	
Yes	21 (33.9)
No	41 (66.1)
Clinical presentation, *n* (%)	
Abscess	2 (3.1)
Adenitis + oedema	16 (24.6)
Mass (nodular) form	17 (26.2)
Inflammatory mass (disseminated)	26 (40.0)
Occult mass	1 (1.5)
Unknown	3 (4.6)

SD = standard deviation.

Results

Sixty-four records of patients with pathology-proven BTB and one with strong clinical but inconclusive cytological findings were identified during the period 2000 - 2013. Accurate clinic attendance records were available for the years 2009 - 2013, and during this 5-year period a total of 11 092 patients underwent breast investigations and 30 were diagnosed with BTB (prevalence for the period 0.3%). Demographics and clinical presentation are described in Table 1. The age range was 23 - 69 years (mean 38.5 years). Of the 65 patients, 26 presented with an inflammatory mass or disseminated form of BTB. Other associated clinical features are set out in Table 2. Of the 65 patients, only one was lactating. HIV status was known in 47 patients, of whom 34 were HIV-positive. While 47 patients had a history of previous pulmonary TB, only 15 had radiological evidence of either previous or concurrent pulmonary TB.

Table 2. Associated clinical features

Characteristics	*n* (%)
History of pulmonary TB (*N*=47)	
CXR normal	32 (49.2)
CXR abnormal	15 (23.1)
Pregnant/lactating assessed (*N*=65)	
No	64 (98.5)
Yes	1 (1.5)
HIV status (*N*=47)	
Negative	12 (18.5)
Positive	34 (52.3)
Refused testing	1 (1.5)

CXR = chest radiograph.

Radiological features on mammograms and ultrasound scans are summarised in Fig. 1 (a and b, respectively). Of the 33 patients who had mammograms, 16 demonstrated ipsilateral or bilateral axillary lymphadenopathy. A density pattern was seen in 13 cases. Ultrasound scans were done in 41 patients. The commonest pattern was that of an abscess (16 cases, 39.0%).

Sensitivity for fine-needle aspiration cytology (FNAC) was 28% as opposed to 94% for histology. AFB were seen in 10.3% of the FNAC specimens and 29.7% of the histology specimens. Of the 65 patients, 59 received medical treatment, 3 received surgical intervention, and 3 were lost to follow-up after diagnosis. Of those who were treated, 72.7% obtained full resolution, 25.0% did not complete treatment, and 2.3% died (*n*=1).

Discussion

Clinical and radiological findings

Inflammatory/disseminated

This pattern was the most common clinical presentation of BTB. However, among patients who had mammograms, this pattern was seen in 21.2% (Fig. 2, a). The mammogram typically demonstrated nonspecific diffuse stromal thickening. We noted that all cases with an inflammatory/disseminated form also

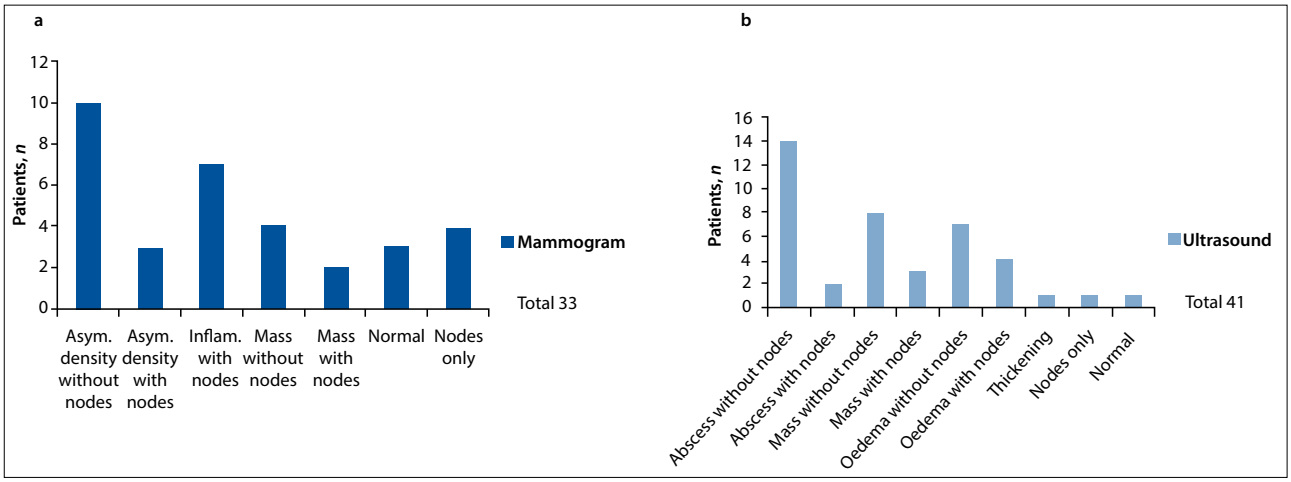

Fig. 1. (a) Of 33 patients who had mammograms, 16 demonstrated ipsilateral or bilateral axillary lymphadenopathy. An asymmetrical density pattern was seen in 13 cases. (b) Ultrasound scans were performed in 41 patients. The commonest pattern was an abscess variety in (16 cases, 39%).

had nodes. This supports the hypothesis that this form may be due to either reactive oedema or retrograde spread from the axillary lymph nodes.[10] To date, no study has specifically determined whether AFB are present in the oedematous or diffusely inflamed breast. Because of the appearances, it has been suggested that this in fact represents the clinical spectrum from inflammatory mass/disseminated to oedema. The major differential diagnosis of this form is inflammatory breast cancer. However, the combination of an inflammatory breast lesion and sinuses or fistulas favours BTB rather than cancer.[3] On the ultrasound scan, some disseminated forms appeared as diffuse trabecular thickening and oedema (Fig. 2, c), whereas others demonstrated a diffuse inflammatory mass.

Oedema with adenitis

The clinical presentation of oedema was noted in 24.6% of cases, and an ultrasound pattern of oedema was seen in 26.9% (*n*=11). In contrast to the disseminated/inflammatory form, where all had associated axillary lymph nodes, seven patients in this group (17.1%) did not have associated lymphadenopathy. This pattern can be found in other forms of mastitis.

Abscess variety

Even though clinical evaluation classified an abscess variety of BTB in only 3.1%, this was the most common pattern on ultrasound, seen in 39.0% (*n*=18), with or without adenitis. Ultrasound scans demonstrated complex solid-cystic heterogeneous hypoechoic masses and fluid collections. In our study, asymmetrical density was the commonest mammographic pattern (39.4%, *n*=13) associated with this classification. Three patients only had ultrasound diagnosis. The differential diagnosis was a pyogenic abscess, and some of our patients had in fact received treatment with antibiotics; it was only after lack of response to this that the diagnosis of tubercular abscess was considered. It is therefore important to obtain samples specifically for TB analysis in all cases of non-lactational breast abscess, even if there is no history of TB elsewhere.

Nodular (focal mass)

Clinically this form of BTB presented as a focal mass. On the mammograms the focal mass opacities had variable outlines, some having smooth margins while others were irregular. Some were single mass lesions, and others were multiple (Fig. 3). This was the third most common mammographic pattern, seen in 18.2% of patients. On ultrasound this form appeared as a hypoechoic solid or heterogeneous mass with a variable outline ranging from well-defined round to irregular. Lesion size based on ultrasound ranged from 0.9 cm to 6.1 cm. The differential diagnosis of this form can range from benign fibroadenoma to breast cancer, depending on the lesion character on imaging. We did not find microcalcification to be a feature in our study.

Tuberculous lymphadenitis

Although isolated lymphadenitis was not reported on clinical presentation, it was seen in 12.1% of mammograms (*n*=4) and 2.4% of ultrasound scans (*n*=1). Nodes were intramammary, axillary, or both. Clinically, large nodes can extend to the skin surface to form discharging sinuses (Fig. 4, a). The intramammary nodes appeared as well-defined round, dense masses on the mammogram. These can be confused with a breast mass when they are solitary. Radiological differentiation of tuberculous axillary nodes from metastatic nodes

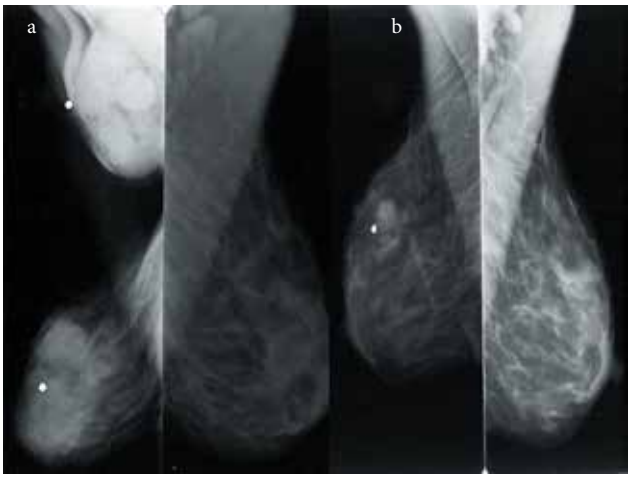

Fig. 3. Nodular form of BTB. Mammogram, MLO views. (a) At presentation – multiple rounded mass opacities in the right breast, and enlarged dense right axillary nodes. (b) After 4 months of treatment with ATT, one small round mass opacity remains in the upper part.

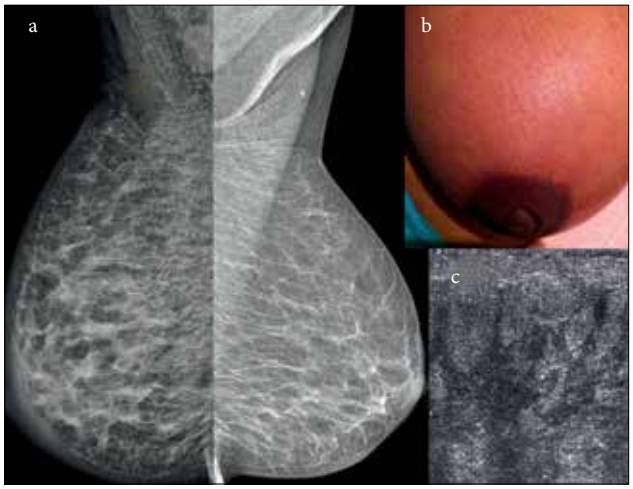

Fig. 2. Inflammatory/disseminated BTB, images taken from various patients. (a) mammogram, MLO views. The right breast is enlarged. Diffuse stromal thickening and skin oedema is evident. (b) Photograph of the left breast, showing inflammation of the skin. (c) Ultrasound images showing diffuse trabecular thickening with oedema as hypoechoic bands in between hyperechoic fibrofatty tissue.

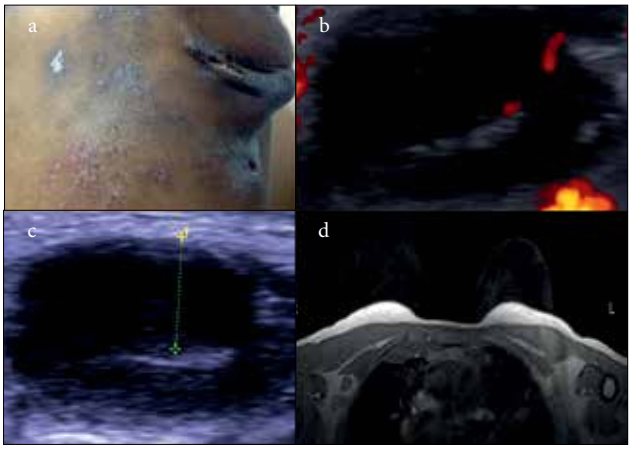

Fig. 4. Tuberculous lymphadenitis. (a) Left axilla, enlarged nodes discharging onto skin sinuses. (b) Ultrasound Doppler scan showing hilum vessel and thick cortex. (c) Ultrasound scan showing node with thick 7 mm cortex (callipers). (d) Breast MRI T1 post-contrast axial image. Right axillary lymph nodes have peripheral rim enhancement and central low signal (PRECLO).

remains difficult. In our series, ultrasound scanning of axillary nodes demonstrated oval, hypoechoic solid masses with thick cortices and loss of normal fatty hilum (Fig. 4, b and c). This appearance cannot be differentiated from that of a malignant or metastatic lymph node. Post-contrast magnetic resonance imaging (MRI) showed peripheral enhancement with a central low signal (Fig. 4, d). Another author described nodes as having peripheral enhancement with central low attenuation (PRECLO) on positive emission tomography with fluorodeoxyglucose integrated with computed tomography (^{18}F-FDG PET/CT).[11]

Pathological findings

We found FNAC to be only 28% sensitive, whereas the sensitivity of histopathology was 94%. Necrotising granulomatous inflammation was seen in histological specimens. In support of the literature, the yield of AFB in our study was low, being positive in 10.3% of cytology and 29.6% of histology specimens. In one case, AFB were detected histologically by PCR testing. Harris *et al.*[12] reported a 2% rate of positive Ziehl-Neelsen smears for AFB from tuberculous breast abscess fluid. Furthermore, an AFB-positive smear is not always adequate for a definitive diagnosis of *Mycobacterium tuberculosis*, as it should be differentiated from other *Mycobacterium* species.

Treatment

Of the 65 patients, 59 received medical treatment comprising 9 months of standard ATT, 3 received both medical and surgical intervention involving abscess drainage, and 3 were lost to follow-up and were never treated following diagnosis. Of those who were treated, 72.7% obtained full clinical resolution, 25.0% did not complete treatment, and one patient died. Response to treatment was assessed by clinical examination and repeated radiological investigations (ultrasound, mammography or both). Although there are no documented criteria for radiological response, drug resistance may be suspected when lesions fail to reduce in size or change their appearance on ultrasound or mammography. Ultrasound is especially useful in monitoring the abscess form of BTB, to detect residual fluid collections. In single studies, both MRI[13] and ^{18}F-FDG PET/CT[11] have shown promise as tools for monitoring response.

Risk factors

Our data demonstrate the varied spectrum of BTB presentation, both clinical and radiological, as well as good outcome with medical treatment. Furthermore, the study illustrates some association of BTB with HIV. Although most patients with BTB are females, male patients are occasionally affected. Our study supports this, with only one of 65 patients (1.5%) being male. The mean age of the patients in our study was 38.5 years, with a range of 23 - 69 years, demonstrating that BTB is not limited to females of reproductive age, as has been reported in the literature.[14] Several risk factors for BTB have been described, including lactation, multiparity and HIV/AIDS.[12] We found only one patient (1.5%) to be lactating. HIV status was known in 47 of our patients, of whom 72.3% (n=34) were HIV-positive. Although HIV infection has been associated with an increased incidence of EPTB, BTB still remains rare. BTB has been classified as primary or secondary. Whereas most studies report that the primary form of BTB is rare,[9] we found the opposite. A history of pulmonary TB was obtained from 47 patients, of whom 68.1% (n=32) had a normal chest radiograph and no evidence of pulmonary or concurrent TB or of TB elsewhere in the body. This finding suggests that half of our cohort had the primary form of BTB.

Study limitations

Limitations due to the retrospective nature of the study include incomplete data on follow-up after treatment completion, even though patients were scheduled for further visits.

Conclusions

Our findings demonstrate the varied clinical and radiological presentations of BTB. Early diagnosis can lead to full response following treatment with standard ATT, resulting in avoidance of more invasive surgical treatment which can potentially cause breast disfigurement. Clinicians need to be aware of these patterns and to have a high index of suspicion in order to prevent misdiagnosis and inappropriate management.

Sources of support. The University of KwaZulu-Natal (UKZN)'s Medical Education Partnership Initiative (MEPI) Enhancing Training, Research and Education (ENTRÉE) programme (Grant No. 5R24TW008863) provided seed funding and support for the development of this study. MEPI is a National Institutes of Health/PEPFAR-funded grant awarded to UKZN in 2010 that aims to develop or expand and enhance models of medical education in sub-Saharan Africa.

Acknowledgements. Part of the material from this article was presented at the European Congress of Radiology (ECR 2015) as the Electronic Poster Online Submission (EPOS).[15] The authors thank the staff at the breast units at Addington and King Edward VIII hospitals, who facilitated access to radiological and clinical information on study participants.

Conflict of interest. Some of the material in this article was presented at ECR 2015 as the EPOS.[15]

References

1. Gupta R, Singal RP, Gupta A, Singal S, Shahi SR, Singal R. Primary tubercular abscess of the breast – an unusual entity. J Med Life 2012;5(1):98-100.
2. Meerkotter D, Spiegel K, Page-Shipp LS. Imaging of tuberculosis of the breast: 21 cases and a review of the literature. J Med Imaging Radiat Oncol 2011;55(5):453-460. [http://dx.doi.org/10.1111/j.1754-9485.2011.02306.x]
3. Tewari M, Shukla SH. Breast tuberculosis: Diagnosis, clinical features and management. Indian J Med Res 2005;122(2):103-110.
4. Mehta G, Mittal A, Verma S. Breast tuberculosis – clinical spectrum and management. Indian J Surg 2010;72(6):433-437. [http://dx.doi.org/10.1007/s12262-010-0166-5]
5. Akbulut S, Sogutcu N, Yagmur Y. Coexistence of breast cancer and tuberculosis in axillary lymph nodes: A case report and literature review. Breast Cancer Res Treat 2011;130(3):1037-1042. [http://dx.doi.org/10.1007/s10549-011-1634-8]
6. Baslaim MM, Al-Amoudi SA, Al-Ghamdi MA, Ashour AS, Al-Numani TS. Case report: Breast cancer associated with contralateral tuberculosis of axillary lymph nodes. World J Surg Oncol 2013;11:43. [http://dx.doi.org/10.1186/1477-7819-11-43]
7. Kumar M, Chand G, Nag VL, et al. Breast tuberculosis in immunocompetent patients at tertiary care center: A case series. J Res Med Sci 2012;17(2):199-202.
8. Tanrikulu AC, Abakay A, Abakay O, Kapan M. Breast tuberculosis in southeast Turkey: Report of 27 cases. Breast Care (Basel) 2010;5(3):154-157. [http://dx.doi.org/10.1159/000314267]
9. Shushtari MHS, Alavi SM, Talaeizadeh A. Breast tuberculosis: Report of nine cases of extra pulmonary tuberculosis with breast mass. Pak J Med Sci 2011;27(3):582-585.
10. Oh KK, Kim JH, Kook SH. Imaging of tuberculous disease involving breast. Eur Radiol 1998;8(8):1475-1480. [http://dx.doi.org/10.1007/s003300050578]
11. Sathekge M, Maes A, D'Asseler Y, Vorster M, Gongxeka H, van de Wiele C. Tuberculous lymphadenitis: FDG PET and CT findings in responsive and nonresponsive disease. Eur J Nucl Med Mol Imaging 2012;39(7):1184-1190.. [http://dx.doi.org/10.1007/s00259-012-2115-y]
12. Harris SH, Khan MA, Khan R, Haque F, Syed A, Ansari MM. Mammary tuberculosis: Analysis of thirty eight patients. ANZ J Surg 2006;76(4):234-237. [http://dx.doi.org/10.1111/j.1445-2197.2006.03692.x]
13. Fellah L, Leconte I, Weynand B, Donnez J, Berlière M. Breast tuberculosis imaging. Fertil Steril 2006;86(2):460-461. [http://dx.doi.org/10.1016/j.fertnstert.2006.03.020]
14. Afridi SP, Memon A, Rehman SU, Baig N. Spectrum of breast tuberculosis. J Coll Physicians Surg Pak 2009;19(3):158-161. [http://dx.doi.org/03.2009/jcpsp.158161]
15. Ramaema DP, Buccimazza I, Hift RJ. Breast tuberculosis: Radiology spectrum with clinical correlation – a retrospective analysis of 65 patients. ESR EPOS™. [http://dx.doi.org/10.1594/ecr2015/C-1154]

Accepted 18 June 2015.

CHAPTER 3

The role of ^{18}F-FDG-PET-CT in breast tuberculosis: Patterns and assessment of response to treatment – Pilot study

TITLE

The role of ^{18}F-FDG-PET-CT in breast tuberculosis: Patterns and assessment of response to treatment: a pilot study.

AUTHORS

Dibuseng P Ramaema MBChB (UCT) FCRad (Diag) SA[1]
Richard J Hift MMed (Med) PhD FCP (SA) FRCP (UK)[2]
Sat Somers FRCPC, FFRRCSI (Hon.) FACR[3]
Nischal Soni MBCHB (Medunsa) FCNP (SA)[4]

AFFILIATIONS

1. Division of Radiation Medicine (Radiology), Nelson R Mandela School of Medicine, University of KwaZulu-Natal, Durban, South Africa.
2. Division of Medicine, Nelson R Mandela School of Medicine, University of KwaZulu-Natal, Durban, South Africa.
3. Department of Radiology, McMaster University, Hamilton, Ontario, Canada.
4. Discipline of Radiation Medicine (Nuclear Medicine), School of Clinical Medicine, University of KwaZulu Natal, Durban, South Africa.

CORRESPONDING AUTHOR

Dr Dibuseng P Ramaema
Discipline of Radiation Medicine (Diagnostic Radiology)
Nelson R Mandela School of Medicine
University of KwaZulu-Natal
Private Bag 7, Congella, Durban
South Africa, 4013

Email: Ramaema@ukzn.ac.za
Tel: +27 31 260 4301

RUNNING TITLE

Patterns of breast tuberculosis on ^{18}F-FDG-PET-CT

KEYWORDS

^{18}F-FDG-PET-CT
Axillary lymphadenitis
Breast tuberculosis
Treatment response

ABBREVIATIONS

ATT	anti-tuberculosis treatment
^{18}F-FDG-PET-CT	(Fluorine-18)-fluoro-2-deoxy-D-glucose (^{18}F-FDG) positron emission tomography (PET) integrated with computed tomography (CT)
BTB	breast tuberculosis
D_{max}	maximum diameter
EPEMEN	extra-pulmonary extra-mammary extra-nodal
EPTB	extrapulmonary tuberculosis
ROI	region of interest;
$SUV_{max,}$	maximum standardised uptake value.
TB	tuberculosis

WORD, FIGURE AND TABLE COUNT

Abstract	263
Words	2977
Tables	3
Figures	5

ABSTRACT

Aim

The purpose of our study was to describe the appearances of breast tuberculosis (BTB) on ^{18}F-FDG-PET-CT and to study its potential utility in the assessment of treatment response.

Methods

Five patients who presented with pathologically proven BTB were studied. All underwent a non-contrast enhanced whole body ^{18}F-FDG-PET-CT baseline scan within two weeks of diagnosis. A follow-up scan was performed approximately 4 months after initiation of anti-tuberculous treatment (ATT). We compared the imaging patterns on ^{18}F-FDG-PET-CT scan of the responders and non-responders.

Results

Two metabolic activity distribution patterns were identified. In the breast only pattern (*n=1*), the patient had activity localised to the breast. In the combined breast/lymphatic pattern (*n=4*), patients showed spread beyond the breast including enlarged ^{18}F-FDG avid lymph nodes. Three of the five patients demonstrated a clinical response to ATT, whilst two were non-responsive at 4 months. The change in SUV_{max} between the two groups was not significant ($p=0.08$). However, by linear regression, the responders had a highly statistically significant decrease in the SUV_{max} values compared to this same change in the non-responders from their baseline, ($p<0.001$). The proportional change in the maximum diameter (D_{max}) between the responders and the non-responders was not significant, ($p=0.08$). The number of lymph nodes basins and 3-D volume did not differ significantly between the two groups ($p=1.000$).

Conclusions

Two metabolic activity distribution patterns of BTB on ^{18}F-FDG-PET-CT, namely a breast only and a combined breast/lymphatic patterns were identified. The SUV_{max} and D_{max} may

be useful markers for identifying patients with BTB with a suboptimal response to antituberculous therapy.

INTRODUCTION

There has been a resurgence of extra-pulmonary tuberculosis (EPTB), precipitated by the increasing prevalence of Human Immune Deficiency-Acquired Immune Deficiency Syndrome (HIV-AIDS) [1]. EPTB is an AIDS-defining condition, [2, 3] and the risk of EPTB increases with decreasing CD4 counts [4, 5]. Breast tuberculosis (BTB) is rare. A study in India identified 30 BTB cases out of a total of 1180 breast lesions over a 20 year period [6]. Another study also in India found 63 BTB cases out of a total of 5200 breast cases over a 16 year period [7]. In a recent study in South Africa, 65 BTB cases out of a total of 11092 patients attending breast clinic were identified over a 5 year period, with a BTB period prevalence of 0.3% in this cohort [8]. The role of (fluorine-18)-fluoro-2-deoxy-D-glucose (^{18}F-FDG) positron emission tomography (PET) integrated with computed tomography (^{18}F-FDG-PET-CT) in oncology is well established [9-11], with other applications being neurology, infections and inflammation [12-15]. Some interest in its application in TB has been developed in the past decade [16-18]. TB infection elicits an inflammatory response in which the macrophages and neutrophils predominantly metabolise glucose, and this increased glucose metabolism is detected with ^{18}F-FDG. The intensity of ^{18}F-FDG uptake is proportional to the intensity of the inflammatory response [19]. There are studies that have investigated the role of ^{18}F-FDG-PET-CT in monitoring treatment response in both pulmonary TB (PTB) [20-22] and EPTB patients [16, 22, 23]. Coleman *et al* demonstrated quantitative PET-CT imaging changes in the five patients infected with pulmonary extremely drug resistant (XDR) TB who had linezolid added to their treatment regimen, and found correlation between reduction in lesion ^{18}F-FDG activity and therapeutic response [20]. We have not found a study which focused on the ^{18}F-FDG-PET-CT findings in patients with BTB.

Several diagnostic tools have been employed in the diagnosis and monitoring of treatment response in BTB, including clinical [24], histological assessment [25], mammography , ultrasonography [26] and magnetic resonance imaging (MRI) [27, 28]. There are no documented data on the radiological treatment monitoring with the use of mammography and ultrasound, however these two modalities are known to be non-specific, hence may not be reliable in measuring disease resolution [27, 29, 30]. To our knowledge, there has not been a reported study or case report that has specifically evaluated the usefulness of ^{18}F-FDG-PET-CT in diagnosing and evaluating the treatment response of BTB. The purpose of

our study was to explore the role of ^{18}F-FDG-PET-CT in the non-invasive assessment of BTB.

PATIENTS AND METHODS

Study design

We conducted a non-randomized prospective observational study between January 2014 and January 2015. Ethical clearance was obtained from the institution Biomedical Research Ethics Committee (BREC) (Ref BF213/13). All participants provided written, informed consent.

Patients

Five patients who presented with BTB were recruited. All of them had pathologically proven tuberculosis. Four had conclusive histology from either the breast or the axillary lymph nodes. Of these three had concurrent pulmonary TB (PTB). One patient had proven pulmonary TB and had already received 8 weeks of anti-tuberculous treatment (ATT), which might have contributed to the histology being inconclusive. This patient had clinical and radiological features compatible with BTB, and continued to demonstrate response of both the breast and the axillary nodes. Therefore we are confident that the breast and axillary nodes were part of the TB spectrum. The remaining four patients were immediately initiated on first line ATT at the time of diagnosis confirmation. All patients reported compliance with ATT.

Methods

All patients had undergone screening investigations at the referring breast clinic, including ultrasonography, with or without mammograms depending on the patient's age. Following histological confirmation of BTB, patients were invited for a baseline ^{18}F-FDG-PET-CT scan, which was timed to allow the breast and axillary node biopsy sites to heal, thereby minimising biopsy-associated injury as a confounder.

The baseline scan was done within two weeks of commencement on ATT, and the follow-up scan was done after 4 months, as recommended by the Centre for Disease Control and Prevention of TB Guidelines [31]. At the time of the follow up scan the patients' response to treatment was evaluated on the following criteria: improvement or worsening symptoms including pain, enlargement or reduction of the breast lesion or axillary lymph nodes, requirement for surgical intervention to alleviate signs and symptoms. Pain threshold was divided into mild, moderate and severe.

The patients were divided into two groups as responders and non-responders to first line ATT. Those who demonstrated reduction in the size of breast lesion or axillary nodes together with improvement of symptoms were classed as responders. The patients who had enlargement of breast lesion or axillary nodes with or without symptom worsening, and those who needed surgical intervention to alleviate signs and symptoms were classed as non-responders.

^{18}F-FDG-PET-CT image acquisition:

The patients fasted for at least 6 hours prior to intravenous administration of ^{18}F-FDG. They received 4 MBq/kg body weight (range 192-261MBq, 5.17-7.05mCi). Glucose values were obtained before I.V. injection. The department protocol requires glucose level to not exceed 11.1mmol/L/, in order to reduce the competition of high plasma glucose with ^{18}F-FDG and a diversion of the latter into muscle with reduced uptake by the inflammatory cells. None of our patients had glucose levels higher than acceptable.

A whole body PET-CT scan was performed using a PET-CT scanner (*Siemens Biograph 16 slice, Erlangen, Germany*). The scan was timed to commence between 60 and 90 min post injection of ^{18}F-FDG. The PET images were acquired for a maximum of 8 bed positions at 3 minutes per field of view in the craniocaudal direction, starting at the vertex of the skull and ending at the mid-femur point. The images were acquired at a zoom of 1 and a matrix of 168 x 168. An iterative reconstruction using 2 iterations and 24 subsets was used for post-acquisition image processing.

A diagnostic non-contrasted CT scan was acquired in the craniocaudal direction with the following parameters: 4D CARE dose for 100mAs, 120 kVp and 5 mm slice thickness, pitch

of 0.75 for a scan time of 25s. A CT Image multiplanar reconstruction was obtained using a kernel of B31f, abdomen window, slice thickness of 4 mm and a recon increment of 2 mm.

Combined ^{18F}-FDG-PET-CT analysis

All the images were interpreted by two experienced nuclear medicine physicians and one experienced radiologist. The nuclear medicine physicians were blinded to the patient's clinical treatment response status during the follow-up scan, but the radiologist was not blinded and the images were read in consensus.

^{18F}-FDG-PET-CT Quantitative analysis

True-D software with automatic multi-planar orthogonal display of the regions of interest (ROI) in axial, sagittal and coronal planes was used to analyse the fused PET-CT images. 3-D ROI were drawn around ^{18}F-FDG-avid areas, and the maximum standardised uptake value (SUV_{max}) of all the ^{18}F-FDG-avid lesions were recorded: For this cohort, the most avid lesions were found to be either the axillary lymph nodes or the breast. The maximum diameter (D_{max}) of the most avid lesion and the number of the ^{18}F-FDG-avid lymph nodes basins were recorded. If there were many adjacent nodes in a basin, these were considered as one, and the SUV_{max} of the whole basin was taken. The CT images were analysed for bilateral whole breast 3-D volume.

^{18}F-FDG-PET-CT Morphological analysis of lesion and disease extent

The breast morphological pattern was analysed according to the BTB classifications as; abscess, disseminated/inflammatory, mass and axillary lymphadenitis with breast oedema [8]. The axillary lymph nodes were assessed for the presence of matted necrotic nodes. The chest/lung was evaluated on lung and mediastinal windows, and the following parameters were recorded: lung nodules; lung consolidation; lung cavitation; pleural thickening; and pleural effusion. The presence of extra-pulmonary, extra-mammary and extra-nodal (EPEMEN) hypermetabolic foci, which included liver, spleen, bones, and subcutaneous soft tissues were recorded. Based on the visual analysis, we observed the two patterns: the breast pattern and the combined breast/ lymphatic pattern [32].

Statistical analysis

Data were entered into Epi-Info [33] and were subsequently transferred to STATA *(StataCorp. 2015: Stata Statistical Software, Release 14* College Station, TX) for analysis. The patients were classified as responders and non-responders. Summary statistics were used to analyse the demographics, clinical and initial basic radiological investigations. Non-parametric Wilcoxon rank-sum was used to compare the mean change in the SUV_{max} levels at the two time points for each participant, and the Mann-Whitney U tests were applied to assess differences in the mean SUV_{max} between the responders and non-responders. The linear regression model was used to determine the mean change in the SUV_{max} when a follow up was undertaken between the two groups. 1 sided Fisher exact test was used for the differences of the lymph nodes. Results were considered significant where p values<0.05.

RESULTS

All the patients were female, with an age range of 23 to 42 years, Table 1. ^{18}F-FDG-PET-CT scan quantitative findings are summarised in Table 2.

^{18}F-FDG-PET-CT lesions and disease extent of breast tuberculosis patients

We identified two patterns of disease in patients with BTB. In the *breast only* pattern (*n=1*), the patient had predominant activity localised to the breast region. This patient responded to treatment. In the *combined breast/lymphatic* pattern (*n=4*), patients demonstrated a combination of localised breast and spread beyond the breast including lymph node activity. This group consisted of two responders and two non-responders. Two patients with the combined breast/lymphatic pattern were HIV-infected on anti-retroviral treatment (ART) and had moderately low CD4 counts (233 and 289 cells/mm3). None of the patients demonstrated the lung pattern as defined by Soussan *et al.* [32] Three of the five patients were responsive to ATT, whilst two were non-responsive at 4 months of treatment with ATT. The patterns of disease encountered on PET-CT scan are described in more detail in Table 3.

^{18}F-FDG-PET-CT markers of treatment response

When the SUV_{max} for the two time points per patient is plotted, there is a clear pattern illustrating that the rate of increase is higher for the non-responders compared to the responders (Fig. 2). For the non-responders at baseline, the mean SUV_{max} was 7.97±2.43, (range 6.25-9.69), and at 4 months, the mean SUV_{max} had increased to 16.79±0.34, (range 16.55-17.03). For the responders at M0, the mean SUV_{max} was 8.64±2.29, (range 6.93-11.25), and at 4months, the mean SUV_{max} had declined to 6.63±4.24, (range 1.74-9.40).

The difference in both the proportional and the absolute change in SUV_{max} between the two groups was not significant, ($p=0.08$) (Fig. 1). On linear regression, responders had a significant decrease (mean relative decrease of 10.84) in their SUV compared to the change in the non-responders in relation to their baseline value ($p<0.001$).

Similarly, the proportional change in the D_{max} of the most avid lesion, for this cohort being either the breast or the axillary nodes, between the responders and the non-responders was not significant, ($p=0.08$) (Fig. 3). The number of lymph nodes basins was found not to differ significantly between the two groups ($p=1.000$). Similarly, the whole breast 3-D volume as measured on CT images did not differ between the responders and the non-responders ($p=1.000$).

A total of 10 EPEMEN hypermetabolic foci were observed in the two non-responders, and not in the other patients. Both non-responders were HIV-TB co-infected. The foci in patient 1 included liver, spleen, four areas of bone involvement and one subcutaneous tissue. The second patient (patient 2) demonstrated 3 EPEMEN foci involving subcutaneous soft tissues.

The presence of matted nodes did not discriminate between the two groups. All patients were followed up until declared disease-free, the longest duration being 16 months (*n=1*), whilst others received 9 months of treatment and disease resolution was confirmed (*n=4*). One of the two patients classified as non-responders in our study was managed with surgical debridement of the axilla, whilst the second non-responder received a prolonged 16 months of supportive treatment in addition to the ATT due to the severity of the disseminated TB.

Fig. 4 and Fig 5 show the ^{18}F-FDG-PET-CT images of patient 2 (non-responder) with combined breast/lymphatic pattern and patient 4 (responder) with breast only pattern, at two time points respectively.

DISCUSSION

In developing countries TB has high mortality in HIV infected individuals [1, 34, 35]. HIV-infected patients are more susceptible to TB including EPTB and may present more severely [4]. Furthermore drug-resistant forms of TB with associated complications are increasing, especially in the context of HIV-TB co-infection [1]. Thus, it is critical to have these potentially life-threatening strains recognised early in order to switch the treatment from the first line tuberculostatics to the second or the third line treatment. The utility of ^{18}F-FDG-PET-CT in demonstrating a response to treatment in the early stage of pulmonary TB has been shown [36]. In this study we aimed to evaluate the potential use of ^{18}F-FDG-PET-CT in monitoring treatment response in patients with BTB and to further evaluate the disease extent and identify patterns of organ involvement.

^{18}F-FDG-PET-CT patterns and extent of disease in patients with breast tuberculosis

We identified two metabolic distribution patterns based on the combined analysis of CT and ^{18}F-FDG-PET. The *breast only* pattern was observed when the ^{18}F-FDG activity was localised to the breast region, with lack of strong uptake elsewhere and no evidence of pulmonary infection on CT. There was an association of this pattern with good response to treatment and a generally well patient. The *combined breast/lymphatic pattern* comprised a combination of breast disease with ^{18}F-FDG avidity and additional significant extra-mammary systemic uptake, which could include lymph nodes, bone, hepato-splenic and subcutaneous tissues. Although lung nodules were present, they did not conform in distribution and number to the pattern described by Soussan *et al*. [32]. This combined pattern was seen in patients who were generally unwell, with two demonstrating poor response to ATT at 4 months. There are limited data regarding the patterns of TB on ^{18}F-FDG-PET-CT, and our search revealed only three studies [23, 32, 37]. Both Soussan *et al*. [32] and Martinez *et al*. [23] studies studied the findings on ^{18}F-FDG-PET-CT in two patients with PTB. They identified two patterns: the lung pattern and the lymphatic pattern, the former being related to predominant lung infection whilst the latter was more associated with

severe systemic disease. Mehta [37] evaluated patterns of systemic uptake of ^{18}F-FDG-PET-CT in eleven patients with ocular TB, and described two patterns: one with no detectable systemic uptake, and a second with detectable systemic uptake which they further subcategorised as chest only, disseminated and extrapulmonary only. Our study describes another pattern; the breast only pattern.

^{18}F-FDG-PET-CT in treatment monitoring of breast tuberculosis patients

One of the two patients classified as non-responders in our study was managed with surgical debridement of the axilla, whilst the second non-responder received a prolonged 16 months of supportive treatment in addition to the ATT due to the severity of the disseminated TB. Neither of them received second line ATT and both were followed up until completion of treatment and disease resolution. Both non-responders were HIV-infected on ART, which is likely to have affected the severity of the disease. Thus, though a lack of response should always raise concern about the possible development of drug resistance, which would require a switch to second line ATT [38] , it appears that in our cases the slow response was due to the severity and extent of the disease rather than resistance.

Although ^{18}F-FDG uptake is not specific for TB, the change in the SUV_{max} from the baseline to the follow up scan has been shown to be a good indicator of evaluating response and resistance to first line ATT [16, 21]. Our study demonstrated a significant change in the SUV_{max} on ^{18}F-FDG-PET-CT at different time points during ATT for each patient. It also showed that the intensity of ^{18}F-FDG uptake by the most avid lesion at 4 months is significantly higher in the non-responders than in the responders. We suggest therefore that the SUV_{max} can be used as a disease marker for serial quantification of disease activity.

The proportional change in the maximum diameter (D_{max}) of the most avid lesion appears to have potential in monitoring the response to treatment, confirming the suggestion of [39]. The difference in proportional change between responders and non-responders approached statistical significance. We found that the 3-D breast volume was not predictive in assessing clinical response.

The number of lymph node basins did not differ significantly in this study, in contrast with the findings of [21] who reported that a cut-off of 5 or more lymph node basins had 88%

sensitivity and 81% specificity for separating ATT responders from non-responders in patients with HIV-TB coinfection.

The presence of EPEMEN hypermetabolic foci, which are part of the EPTB spectrum, appears to be a marker of severity. We observed EPEMEN uptake only in the non-responders who also had HIV-TB co-infection. Anatomically these foci included the liver, spleen, bone and subcutaneous tissues. The liver and splenic lesions in our patients consisted of multiple tiny hypermetabolic cysts consistent with military TB [40]. In contrast, local hepatic TB is associated with focal lesions which are usually greater than 2mm [41]. We are unaware of any study, prior to the current study, in which breast involvement was described as part of the spectrum of EPTB in which the use of ^{18}F-FDG-PET-CT has been explored.

Study limitations

The small sample size is related to the low prevalence of BTB and the prospective study design.

Conclusion

Our study identified two distinct metabolic activity distribution patterns of BTB on ^{18}F-FDG-PET-CT which include a *breast only* pattern and a *combined breast/lymphatic pattern*. We have further shown that ^{18}F-FDG-PET-CT at 4 months after initiation of treatment of breast TB may be useful in evaluating the response to treatment. The SUV_{max} and the D_{max} may be useful biomarkers in BTB for separating patients who are likely to respond to the standard first line tuberculostatics from those who require more aggressive treatment interventions including surgical and prolonged ATT period.

CONFLICT OF INTEREST

The authors declare no conflict of interest.

ACKNOWLEDGEMENTS

This publication was made possible by grant number: R24TW008863 from the Office of the U.S. Global AIDS Coordinator and the U. S. Department of Health and Human Services, National Institutes of Health (NIH OAR and NIH ORWH). Its contents are solely the responsibility of the authors and do not necessarily represent the official views of the government. Further funding for operational costs was obtained from the UKZN strategic funds

REFERENCES

1. Global tuberculosis report 2015. In: *Secondary*: World Health Organization)

2. Centre for Disease Control and Prevention. AIDS-Defining Conditions. In: *Secondary,*

3. Peto HM, Pratt RH, Harrington TA, LoBue PA ,Armstrong LR, Epidemiology of extrapulmonary tuberculosis in the United States, 1993-2006. Clinical infectious diseases : an official publication of the Infectious Diseases Society of America 2009·49(9): 1350-7

4. Leeds IL, Magee MJ, Kurbatova EV, del Rio C, Blumberg HM, *et al.*, Site of extrapulmonary tuberculosis is associated with HIV infection. Clinical infectious diseases : an official publication of the Infectious Diseases Society of America 2012·55(1): 75-81

5. Yang Z, Kong Y, Wilson F, Foxman B, Fowler AH, *et al.*, Identification of risk factors for extrapulmonary tuberculosis. Clinical infectious diseases : an official publication of the Infectious Diseases Society of America 2004·38(2): 199-205

6. Tewari M, Shukla HS, Breast tuberculosis: diagnosis, clinical features & management. The Indian Journal Of Medical Research 2005·122(2): 103-10

7. Mehta G, Mittal A ,Verma S, Breast Tuberculosis- Clinical Spectrum and Management. Indian Journal of Surgery 2010·72(6): 433-7

8. Ramaema DP, Buccimazza I, Hift RJ, Prevalence of breast tuberculosis: Retrospective analysis of 65 patients attending a tertiary hospital in Durban, South Africa. S. Afr. Med. J. 2015·105(10): 866-9

9. Agrawal A, Rangarajan V, Appropriateness criteria of FDG PET/CT in oncology. The Indian journal of radiology & imaging 2015·25(2): 88-101

10. Quak E, Le Roux PY, Hofman MS, Robin P, Bourhis D, *et al.*, Harmonizing FDG PET quantification while maintaining optimal lesion detection: prospective

multicentre validation in 517 oncology patients. Eur J Nucl Med Mol Imaging 2015·42(13): 2072-82

11. Society of Nuclear Medicine. 18F-fluorodeoxyglucose (FDG) PET and PET/CT Practice Guidelines in Oncology. In: *Secondary,*

12. Basu S, Ranade R, 18-Fluoro-deoxyglucose-PET/Computed Tomography in Infection and Aseptic Inflammatory Disorders: Value to Patient Management. PET clinics 2015·10(3): 431-9

13. Hess S, Hansson SH, Pedersen KT, Basu S ,Hoilund-Carlsen PF, FDG-PET/CT in Infectious and Inflammatory Diseases. PET clinics 2014·9(4): 497-519, vi-vii

14. Sathekge M, Warwick JM, Doruyter A ,Vorster M, Appropriate indications for positron emission tomography/computed tomography: College of Nuclear Physicians of the Colleges of Medicine of South Africa. S. Afr. Med. J. 2015·105(11): 894-6

15. Zhuang H, Codreanu I, Growing applications of FDG PET-CT imaging in non-oncologic conditions. Journal of biomedical research 2015·29(3): 189-202

16. Dureja S, Sen IB ,Acharya S, Potential role of F18 FDG PET-CT as an imaging biomarker for the noninvasive evaluation in uncomplicated skeletal tuberculosis: a prospective clinical observational study. European spine journal : official publication of the European Spine Society, the European Spinal Deformity Society, and the European Section of the Cervical Spine Research Society 2014·23(11): 2449-54

17. Sathekge M, Maes, A., Van de Wiele, C, FDG-PET imaging in HIV infection and tuberculosis. Semin Nucl Med 2013·43(5): 349-66

18. Soussan M, Cyrta J, Pouliquen C, Chouahnia K, Orlhac F, *et al.*, Fluorine 18 fluorodeoxyglucose PET/CT volume-based indices in locally advanced non-small cell lung cancer: prediction of residual viable tumor after induction chemotherapy. Radiology 2014·272(3): 875-84

19. Love C, Tomas MB, Tronco GG ,Palestro CJ, FDG PET of infection and inflammation. Radiographics : a review publication of the Radiological Society of North America, Inc 2005·25(5): 1357-68

20. Coleman M, Chen RY, Lee M, Lin PL, Dodd LE, *et al.*, PET/CT imaging reveals a therapeutic response to oxazolidinones in macaques and humans with tuberculosis. Sci. Transl. Med. 2014·6(265): 9

21. Sathekge M, Maes, A., Kgomo, M., Stoltz, A., Van de Wiele, C, Use of 18F-FDG PET to predict response to first-line tuberculostatics in HIV-associated tuberculosis. J Nucl Med 2011·52(6): 880-5

22. Stelzmueller I, Huber H, Wunn R, Hodolic M, Mandl M, *et al.*, 18F-FDG PET/CT in the Initial Assessment and for Follow-up in Patients With Tuberculosis. Clin. Nucl. Med. 2015·10.1097/rlu.0000000000001102:

23. Martinez V, Castilla-Lievre MA, Guillet-Caruba C, Grenier G, Fior R, *et al.*, (18)F-FDG PET/CT in tuberculosis: an early non-invasive marker of therapeutic response. Int J Tuberc Lung Dis 2012·16(9): 1180-5

24. Khodabakhshi B, Mehravar F, Breast tuberculosis in northeast Iran: review of 22 cases. BMC women's health 2014·14: 72

25. Zhong L, Zhou XL, Li J, Zhang YM, Jiao YF, *et al.*, The T-SPOT.TB Test for Diagnosis of Breast Tuberculosis. Laboratory medicine 2015·46(1): 14-9

26. Meerkotter D, Spiegel K ,Page-Shipp LS, Imaging of tuberculosis of the breast: 21 cases and a review of the literature. Journal of Medical Imaging & Radiation Oncology 2011·55(5): 453-60

27. Oh KK, Kim JH, Kook SH ,, Imaging of tuberculous disease involving breast Eur. Radiol. 1998·8(8): 6

28. Popli MB, Kumari A ,Popli V, Proton magnetic resonance spectroscopy in breast tuberculosis. European Journal of Radiology Extra 2010·74(3): e59-e63

29. Makanjuola D, Murshid K, Sulaimani SA ,Saleh MA, Mammographic features of breast tuberculosis: The skin bulge and sinus tract sign. Clinical Radiology 1996·51(5): 354-8

30. Mirsaeidi SM, Masjedi MR, Mansouri SD ,Velayati AA, Tuberculosis of the breast: report of 4 clinical cases and literature review. East Mediterr Health J 2007·13(3): 670-6

31. American Thoracic Society, Treatment of tuberculosis. MMWR Recomm. Rep. 2003·52(Rr-11): 1-77

32. Soussan M, Brillet PY, Mekinian A, Khafagy A, Nicolas P, *et al.*, Patterns of pulmonary tuberculosis on FDG-PET/CT. European journal of radiology 2012·81(10): 2872-6

33. Carstensen B, Plummer M, Laara E ,Hills M Epi: A Package for Statistical Analysis in Epidemiology. R package version 2.0. . In: *Secondary,*

34. Global tuberculosis report 2014. In: *Secondary*: World Health Organization)year; p 171

35. Global tuberculosis report 2013. In: *Secondary*: World Health Organization)

36. Skoura E, Zumla A ,Bomanji J, Imaging in tuberculosis. International journal of infectious diseases : IJID : official publication of the International Society for Infectious Diseases 2015·32: 87-93

37. Mehta S, Patterns of systemic uptake of 18-FDG with positron emission tomography/computed tomography (PET/CT) studies in patients with presumed ocular tuberculosis. Ocular immunology and inflammation 2012·20(6): 434-7

38. Health Systems Trust, Management of Drug-Resistant Tuberculosis - Policy Guidelines. http://www.hst.org.za/publications/management-drug-resistant-tuberculosis-policy-guidelines(2012).

39. Sathekge M, Maes, A., D'Asseler, Y., Vorster, M., Gongxeka, H., Van de Wiele, C, Tuberculous lymphadenitis: FDG PET and CT findings in responsive and

nonresponsive disease. European Journal of Nuclear Medicine and Molecular Imaging 2012·39(7): 7

40. Lee WK, Van Tonder F, Tartaglia CJ, Dagia C, Cazzato RL, *et al.*, CT appearances of abdominal tuberculosis. Clin Radiol 2012·67(6): 596-604

41. Hickey AJ, Gounder L, Moosa MY ,Drain PK, A systematic review of hepatic tuberculosis with considerations in human immunodeficiency virus co-infection. BMC infectious diseases 2015·15: 209

FIGURE LEGENDS

Figure 1

Boxplots showing the absolute change of SUV_{max} values for the responders and the non-responders.

Figure 2

The SUV_{max} for the two time points per patient demonstrating that the rate of increase is higher for the non-responders compared to the responders. Red=non-responders, Blue=responders.

Figure 3

Boxplots demonstrating the proportional change in the D_{max} of the presenting lesion (breast or axillary nodes) between the responders and the non-responders.

Figure 4

^{18}F-FDG-PET-CT scan of a non-responder (Patient 2): Combined Breast/Lymphatic pattern. *Axial ^{18}F-FDG-PET images at breast level (A and B).* A) *Baseline scan*: Diffusely enlarged left breast, and multiple matted large ^{18}F-FDG avid left axillary nodes. B) *4 month follow-up scan:* Two metabolically active subcutaneous nodules in the posterior chest wall were present. The activity in the left axillary nodes had increased. Corresponding coronal whole body fused ^{18}F-FDG-PET-CT images *(C and D).* C) *Baseline scan*: Widespread nodal disease. D) *4 months follow up scan*: Progressive left breast oedema and enlargement as well as increased intensity and size of left axillary nodes.

Figure 5

^{18}F-FDG-PET-CT scan of a (Patient 4): Breast only pattern: *Axial ^{18}F-FDG-PET images at breast level (A and B).* A) *Baseline scan*: showed an 8.7cm left breast mass with thick metabolically active rim and hypodense photopaenic necrotic centre, with deep extension into the chest where there was invasion of the intercostal muscle and the pleural space. B) *4*

month follow-up scan: showed a separation of the breast mass from the pleura. The left breast mass had lost the necrotic centre and now appeared as a uniform, and had separated from pleura. Size reduced to 3.9cm. Corresponding coronal whole body fused ^{18}F-FDG-PET-CT images *(C and D).* C) *Baseline scan*: D) *4 months follow up scan*.

TABLE 1

Patient demographic, clinical, mammography and ultrasound features. ALBE= axillary lymphadenitis and breast oedema; BAbsc=Breast abscess. MAL= matted axillary lymphadenopathy. AL= axillary lymphadenopathy. FM= focal mass.

Patient	Age	Prior PTB	Concomitant PTB	Pain	Predominant presentation	HIV status	ESR (mm/hr)	CD4 (cells/mm^3)	Follow-up duration (months)	Mammographic pattern	Ultrasound pattern	BIRADS score	Response
1	23	yes	yes	severe	BAbsc	POS on ART	120	465	16		BAbsc, MAL	3	No
2	36	yes	yes	severe	ALBE, BAbsc	POS on ART	131	289	9	ALBE, FM	ALBE	5	No
3	38	no	no	severe	AL	-	32	-	9	AL	MAL	3	Yes
4	40	no	no	moderate	BAbsc cold	NEG	40	-	9	FM	BAbsc	3	Yes
5	42	yes	yes	severe	ALBE	POS on ART	-	233	9	ALBE	ALBE	4	Yes

TABLE 2

Quantitative data of breast tuberculosis patients on 18F-FDG-PET-CT. M0=Baseline at start of the treatment, M1=follow up scan after 4 months of ATT. EPEMEN: Extra-pulmonary extra-mammary extra-nodal hypermetabolic foci. *One new lymph node basin was present in the follow-up scan. # Coincidental MFU not considered as EPEMEN.

Patient	Lymph node basins (n)	D_{max}0 presenting lesion	D_{max}1 presenting lesion	Breast CT vol 0 (cm^3)	Whole breast CT vol 1 (cm^3)	SUV_{max} M0	SUV_{max}M1	Delta SUV_{max}	EPEMEN foci	Response
1	5	14.1	11.6	15.59	7.8	6.25	17.03	10.78	7	No
2	19*	14.8	13.9	42.53	70.18	9.69	16.55	6.86	3	No
3	6	7.3	5.8	9.74	6.87	11.25	9.4	-1.85	0	Yes
4	6	5.3	3.3	9.35	10.81	7.75	8.75	1.00	0	Yes
5	12	5.2	0.7	15.45	11.99	6.93	1.74	-5.2	0#	Yes

TABLE 3

^{18}F-FDG-PET-CT lesions and disease extent of breast tuberculosis patients. Lt: left, RT: right.

Patient	Sites of TB involvement on ^{18}F-FDG-PET-CT	Chest findings	Pattern	Breast SUV_{max}M0	Breast SUV_{max}M1	Matted axillary nodes	Axillary nodes SUV_{max}M0	Axillary nodes SUV_{max}M1	Response	HIV status	CD4 count
1	Rt Breast, Lymph nodes (Lt supraclavicular, Rt axillary, Lt hilar, preaortic,), liver, spleen, skeletal, subcutaneous	Bilateral lung nodules	Breast/ lymphatic	6.25	17.03	no	3.05	3.92	No	POS on ART	465
2	Lt Breast, Lymph nodes (Rt cervical level *111*, Lt cervical *Va*, Lt supraclavicular, Rt parotid, Rt & Lt axillary, thorax preaortic, para-aortic, porta hepatis, abdominal para-aortic, caval, abdominal lt para-aortic, mesenteric, Rt & Lt common iliac, Rt & lt	Occasional pleural nodules	Breast/ lymphatic	2.67	3.9	yes	9.69	16.55	No	POS on ART	289

	external iliac, Rt & Lt internal obturator), subcutaneous										
3	Rt Breast, Lymph nodes (Rt axillary, Lt hilar, Rt internal obturator, Rt & Lt inguinal)	Normal	Breast/ lymph atic	1.84	1.54	yes	11.25	9.40	Yes	Not avail able	
4	Lt Breast, Lymph nodes (Rt & Lt cervical level *11*, Rt &Lt axillary, Lt internal mammary)	Occasional pleural nodule	Breast	7.75	8.75	no	2.07	1.47	Yes	NEG	Not avail able
5	Rt Breast, Lymph nodes (Rt & Lt axillary,& Lt hilar, preaortic, subcarinal, Lt cervical level *11*, Lt parotid, Rt & Lt internal obturator, Rt & Lt inguinal)	One basal nodule	Breast/ lymph atic	1.64	1.48	yes	6.93	1.73	Yes	POS on ARV	233

FIGURE 1

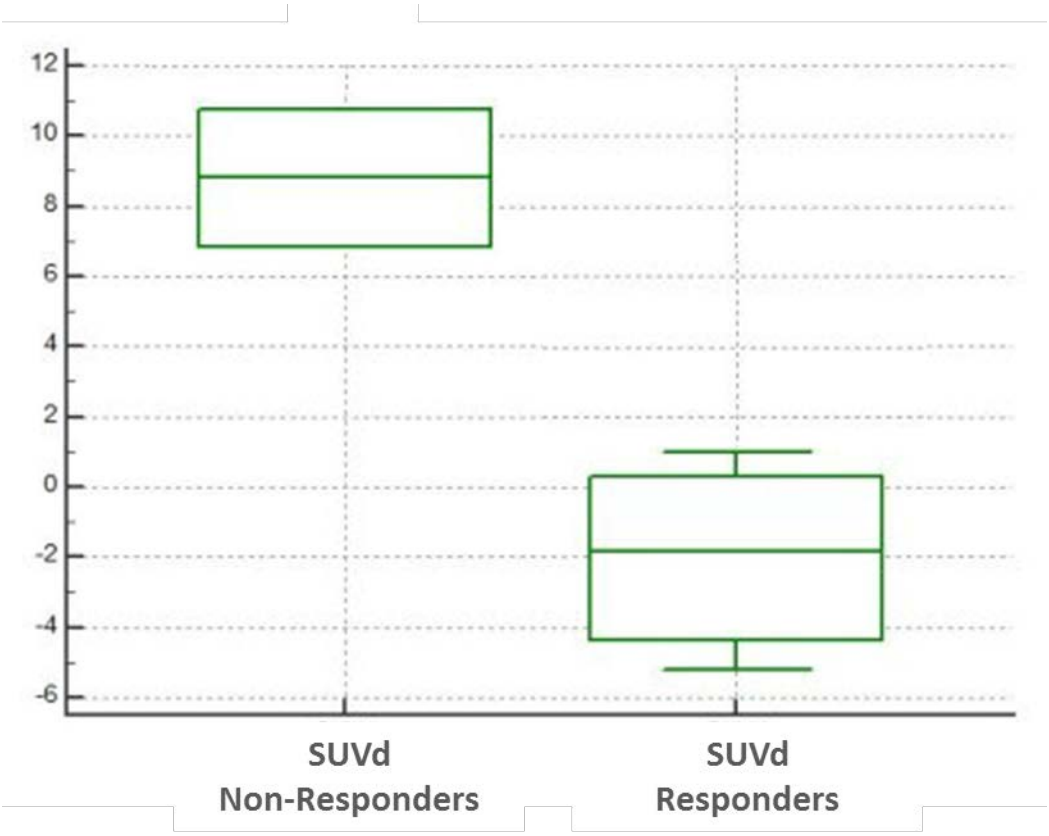

FIGURE 2

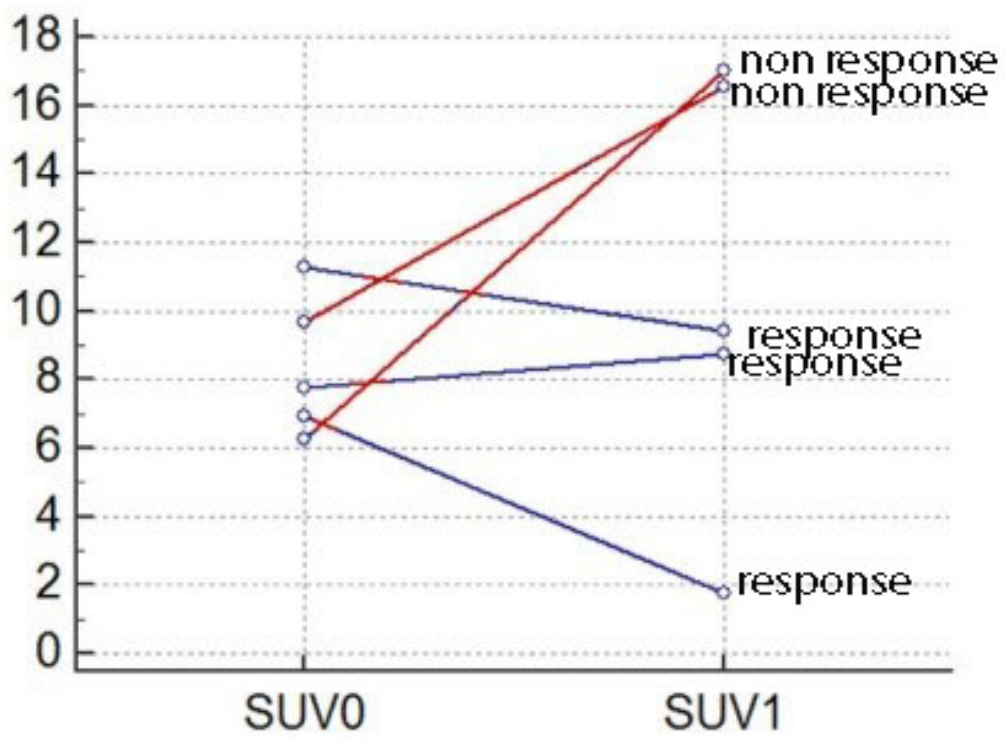
18
16
14
12
10
8
6
4
2
0
SUV0
SUV1
non response
non response
response
response
response

FIGURE 3

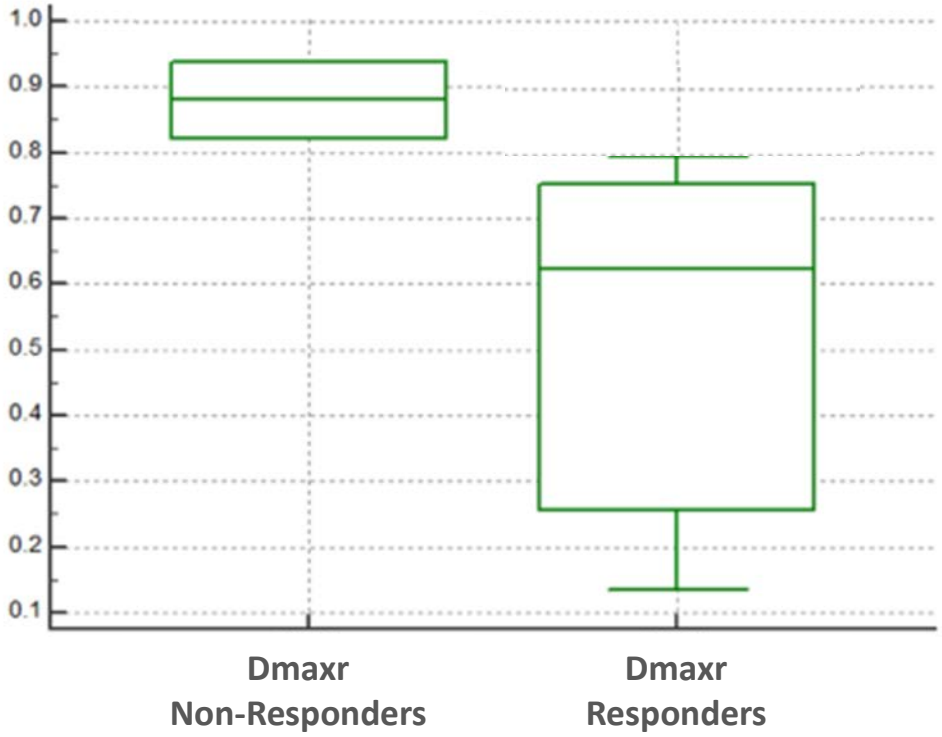
1.0
0.9
0.8
0.7
0.6
0.5
0.4
0.3
0.2
0.1
Dmaxr
Non-Responders
Dmaxr
Responders

FIGURE 4

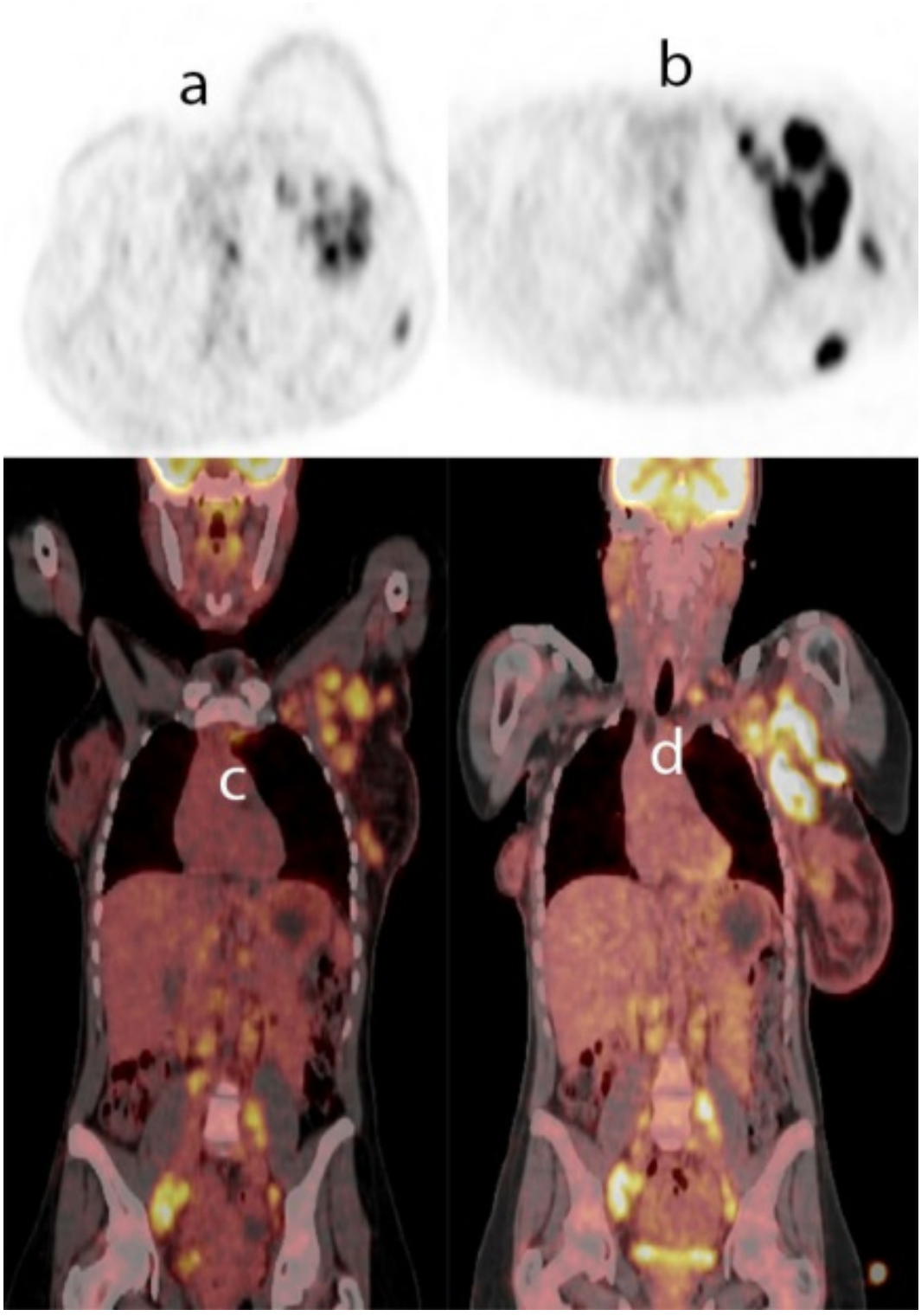

FIGURE 5

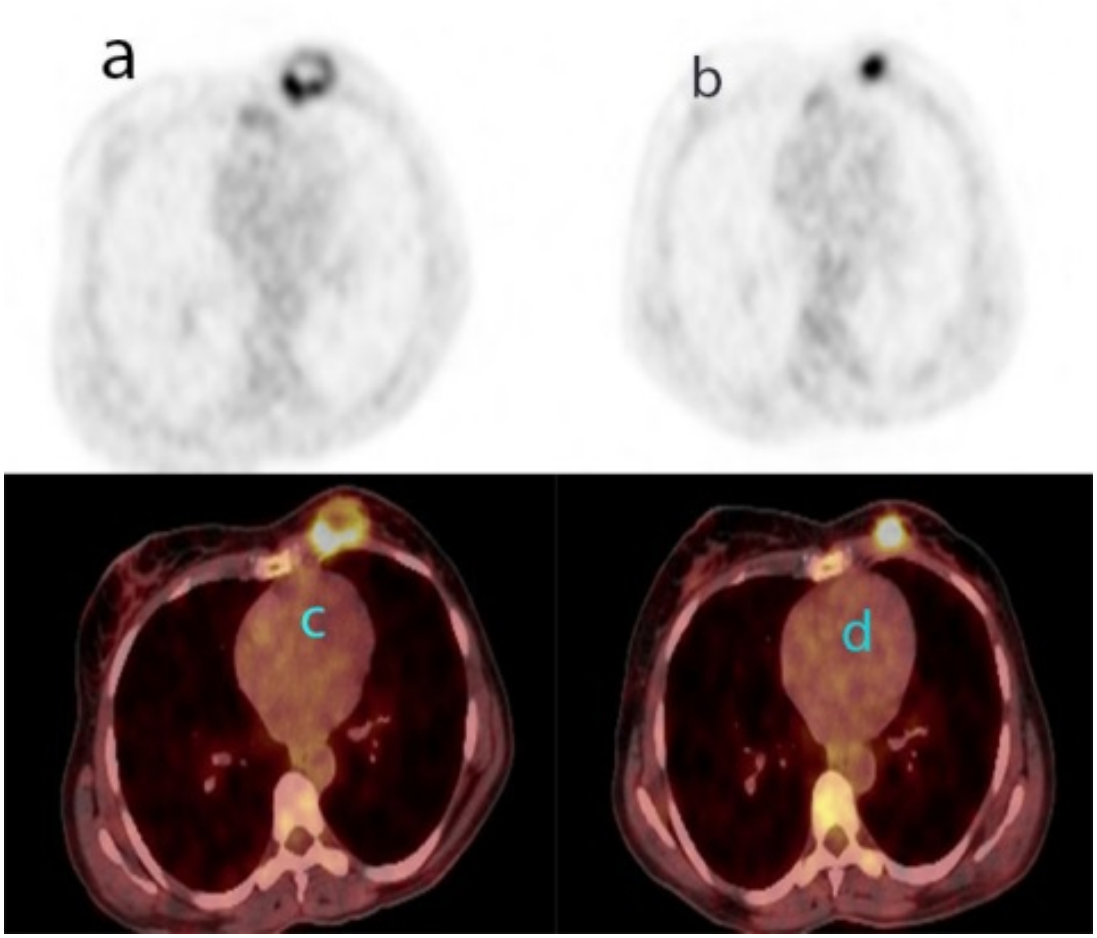

CHAPTER 4

The role of multiparametric MRI in breast tuberculosis: Morphological appearances and the evaluation of treatment response.

TITLE

The role of multiparametric MRI in breast tuberculosis: Morphological appearances and the evaluation of treatment response.

AUTHORS

Dibuseng P Ramaema MBChB (UCT) FCRad (Diag) SA[1]
Richard J Hift MMed (Med) PhD FCP (SA) FRCP (UK)[2]

AFFILIATIONS

1 Discipline of Radiation Medicine (Diagnostic Radiology), School of Clinical Medicine, University of KwaZulu Natal, Durban, South Africa.
2 Discipline of Medicine, School of Clinical Medicine, University of KwaZulu Natal, Durban, South Africa.

CORRESPONDING AUTHOR

Dr Dibuseng P Ramaema
Discipline of Radiation Medicine (Diagnostic Radiology)
Nelson R Mandela School of Medicine
University of KwaZulu-Natal
Private Bag 7 Congella
Durban, South Africa
4013

Email: Ramaema@ukzn.ac.za
Tel: +27 31 260 4301

RUNNING TITLE

MRI in the diagnosis and evaluation of breast tuberculosis.

KEYWORDS

Breast tuberculosis
BI-RADS Lexicon
Dynamic contrast-enhanced MRI

ABBREVIATIONS

ADC	apparent diffusion coefficient
BTB	breast tuberculosis
DCE-MRI	dynamic contrast enhanced magnetic resonance imaging
DWI	diffusion weighted imaging.
MRI	magnetic resonance imaging, multiparametric
ROI	region of interest
T1W	T1 weighted MRI sequence
T2SI	T2 signal intensity
T2W	T2 weighted MRI sequence

WORD, FIGURE AND TABLE COUNT

Abstract	265
Words	2310
Tables	4
Figures	2

ABSTRACT

Aim

The aim of this study was to describe the appearances of breast tuberculosis on MRI and to study its potential utility in the assessment of treatment response.

Methods

We included 6 consecutive patients with pathologically proven breast tuberculosis who underwent a contrast enhanced MRI scan within two weeks of diagnosis. The repeat scan was timed at 4 months after initiation of the anti-tuberculous treatment. The patients were classified as responders or non-responders.

Results

All the patients were female with an age range of 23-43 years. All the lesions were hypointense on the pre-contrast T1W. The responders had uniformly hyperintense lesions on the pre-contrast T2W, whilst the non-responders had mixed signal intensity lesions. The enhancement patterns of foci and rim were present in equal proportions in both groups. All the patients demonstrated rim enhancing axillary nodes. The enhancement distribution in both groups included diffuse, focal and multifocal patterns. The differences (delta) between the two time points at the baseline and the follow-up were determined for the three parameters, ADC, T2SI and the breast lesion maximum diameter (D_{max}). The mean delta ADC and the mean Delta T2SI were not statistically significant between the responders and the non-responders (p=0.901) and (p=0.282) respectively. In contrast, the mean delta D_{max} showed statistically significant differences between the responders and the non-responders (p=0.024).

Conclusions

Our results indicate that the lesion maximum diameter can be valuable in monitoring the response to treatment of patients with breast tuberculosis. Furthermore, the combination of

rim enhancing breast lesions and axillary nodes on DCE-MRI appear to favour breast tuberculosis rather than breast cancer as a diagnosis.

INTRODUCTION

Breast tuberculosis (BTB) is an uncommon manifestation of extrapulmonary tuberculosis (EPTB) [1]. Because of the low prevalence of BTB, there have been few studies on the disease [2, 3]. BTB has been classified into five distinct patterns based on mammography and ultrasound findings: inflammatory/disseminated, oedema with adenitis, abscess, nodular and axillary tuberculous lymphadenitis [4]. Whilst the abscess pattern can readily point the physician to the possible diagnosis of an infective cause, other patterns are still easily confused with malignancy at presentation [5, 6].

The diagnosis of the disease has been achieved through the clinical, radiological and pathological assessment [7, 8]. Mammography and breast ultrasound scans are widely used radiological tests in all women who present with breast disease [9]. Confirmatory diagnosis is obtained from various pathological methods which may include histology, culture, fine needle aspiration cytology (FNAC), the interferon release assays tests [10, 11] and the nucleic acid amplification tests (NAATs) [12]. Newer tests which have proved particularly useful in EPTB diagnosis include the urinary lipoarabinomannan (LAM) for patients with CD4 counts less than 100/mm^3 [13, 14]. The South African treatment guidelines for TB permit the discretionary extension of the standard 6 month-treatment regimen to 9 months or longer in the case of extrapulmonary tuberculosis, which is the protocol followed in our patients [15, 16].

Response to treatment of BTB is currently monitored with a combination of clinical, mammography and ultrasound at scheduled return visits. Resistance to treatment may be suspected when there is no improvement in signs and symptoms [5]. To date, we could not find data of a study which specifically evaluated BTB response to treatment by radiological means. It is well documented that mammography features are not specific for BTB [17] hence identifying patients not responding to treatment may prove difficult with the use of this mammography alone.

The use of magnetic resonance imaging (MRI) in treatment monitoring is well established in breast cancer management [18, 19], with some of the common indications being; for the pre-operative staging, in patients receiving neo-adjuvant chemotherapy at the baseline and

the follow-ups to evaluate the efficacy of therapy [20, 21]. It is also used as a screening tool to monitor young patients with a strong family history [22].

MRI has an established role in monitoring treatment response of EPTB involving the central nervous system (CNS) [23, 24], the musculoskeletal system (MSK) [25, 26] and abdominal TB [27]. We found one case report [28] which describes the use of MRI in evaluating response to treatment of BTB. The authors used contrast enhanced breast MRI in one patient to assess the resolution of BTB on completion of therapy, rather than for disease monitoring during treatment [28]. Comparison was made between the baseline and follow-up scan after six months of anti-tuberculous treatment (ATT), and complete radiological response was demonstrated [28]. Another study used magnetic resonance spectroscopy (MRS) in four patients with BTB but there was no follow-up to assess the response [29]. The technique was used to differentiate BTB from breast carcinoma (BCA) in four cases where mammography, ultrasound and MRI indicated breast cancer rather than TB. The absence of choline peak and the presence of strong lipid peak was suggestive of tuberculosis, which was later confirmed on FNAC[29].

There is evidence that the breast morphological appearance on the dynamic contrast enhanced MRI (DCE-MRI) is an important characteristic for predicting the likelihood of malignancy [30]. There is paucity of literature on the appearances of BTB on DCE-MRI, we found only one study that was performed on 6 patients with BTB in 1998 [31]. The study evaluated a total of seven breast lesions, four of which demonstrated ring/rim enhancement, two had internal enhancement, and one lesion did not have any enhancement[31]. The purpose of our study was to determine the morphological patterns of BTB on multiparametric MRI, which includes T1W, T2W, DWI and DCE-MRI, as well as to use quantitative parameters to assess response to treatment.

PATIENTS AND METHODS

We recruited six consecutively identified patients with BTB who were newly diagnosed with BTB between January 2014 and January 2015. Ethical clearance was obtained from our institution’s Biomedical Research Ethics Committee (Reference number BF213/13). Five patients had conclusive histology either from the breast or the axillary lymph nodes. One patient had inconclusive histology from the breast and the axilla, but had microbiologically

proven pulmonary TB for which she had received 8 weeks of ATT. Her clinical and radiological features were compatible with BTB and she continued to demonstrate positive response to treatment. All the participants provided written informed consent.

All patients had undergone preliminary clinical and radiological investigations at the breast clinic. Following histological confirmation of BTB, the patients were invited for a baseline MRI scan. A follow up scan was performed approximately 4 four months after the initiation of ATT. One patient declined to have a follow-up MRI scan, however, she agreed to come for follow-up mammograms, therefore her treatment response was evaluated based on the clinical, mammographic and ultrasound results. Her results were evaluated in relation to the qualitative morphological features at start of treatment but not in the quantitative evaluation of treatment response. The patients were divided into two groups as either responders or non-responders at the time of their follow-up scan. Response was based on the following criteria: improvement in symptoms; reduction in size of the breast lesion and/or axillary lymph nodes; no requirement for surgical intervention for alleviation of symptoms.

MRI imaging

MRI was performed on a 1.5T machine *(Siemens, Erlangen, Germany)* using a dedicated breast coil. The patients were scanned in the prone position. Power injection of 20 ml intravenous (I.V) *Magnevist® (Gadopentetate Dimeglumine, Bayer)* Standard 469 mg/mL (0.5 mmol/mL) at a dosage of 0.1 mmol/kg was administered to all the patients. The IV contrast rate was 3ml/sec followed by a 20 ml saline flush administered as a bolus. The T1 dynamic phase scan time was 6 minutes 41 seconds, during which 5 dynamic sequences were obtained in the axial position at various time points. The technical parameters are shown in Table 1.

MRI image analysis

All the images were read by one of the authors (DPR), an experienced breast radiologist with 15 years of experience. There was no blinding to clinical information. The images were viewed and analysed on the *Syngo-via* post-processing workstation (*Siemens*, *Erlangen*, *Germany*). Where indicated, the region of interest (ROI) was placed around the lesion to cover the entire circumference.

The following quantitative parameters were measured for each patient: Apparent diffusion coefficient (ADC value), T2 signal intensity (T2SI) value and breast lesion maximum diameter (D_{max}). Qualitative MRI characteristics used included the current Breast Imaging-Reporting and Data System (BI-RADS) descriptors [32]. We recorded; the side; pre-contrast T1 and T2 signal intensity; breast lesion enhancement pattern; and axillary node enhancement pattern. Signal intensity was classed as hyperintense; isointense; hypointense; and mixed. The enhancement pattern was classified according to the three main BI-RADS descriptors as a) Focus or foci (<5mm); b) Mass and c) Non-mass enhancement (NME). The mass pattern internal enhancement characteristic was grouped as: i) solid-cystic; ii) rim; iii) homogeneous; and iv) heterogeneous; The axillary node enhancement pattern was classed as either ring/rim or homogeneous. The enhancement distribution was classified as a) diffuse; b) unifocal; and c) multifocal; all with or without chest wall involvement.

Statistical analysis

Data were entered into an Excel spreadsheet (*Microsoft Excel 2013*. Redmond, WA) and analysed using the STATA software package *(StataCorp. 2015: Stata Statistical Software, Release 14*. College Station, TX). Differences were evaluated with a two-tailed t-test. A *p* value of < 0.05 was considered significant.

RESULTS

Patient demographics and qualitative MRI features

All the patients were female with an age range of 23-43 years. One patient, Patient 5, was studied at baseline only as she declined a follow-up study. She is known however to be a responder, since this was demonstrated on serial mammography. She has therefore been included as a responder, and the data available for her analysed accordingly.

Four of these patients had right-sided involvement, and two left-sided. Four patients were identified as responders. Two patients were identified as non-responders due to reported increasing breast pain, visual breast and axillary nodes enlargement in both, and one required surgical intervention to debride the axillary tuberculous abscesses. Both non-responders

were HIV positive. Amongst the four responders, one was HIV positive, two HIV negative and one patient had an unknown status.

The appearances of pre and post-contrast BTB lesions in a responder vs a non-responder are depicted in Fig. 1. All the lesions were hypointense on the pre-contrast T1 (Fig. 1a). All four responders had hyperintense lesions on pre-contrast T2 (Fig. 1b), whilst the two non-responders had mixed signal intensity lesions (Fig. 1e). The observed enhancement patterns in the responders were NME (Fig. 2a) and mass: rim (Fig. 2b) in equal proportions. Similarly, these two patterns were observed in the non-responders in equal proportions. All patients demonstrated rim enhancing axillary nodes (Fig. 2c). The results are summarised in Table 2.

Quantitative imaging features

The differences (*delta*) between the two time points at the baseline and the follow-ups were determined for the three MRI parameters, ADC, T2SI and D_{max}. Differences in the mean Delta ADC and the mean Delta T2SI did not differ statistically between the responders and the non-responders (p=0.901 and p=0.282 respectively). In contrast, the mean Delta D_{max} showed a statistically significant difference between the responders and the non-responders (p=0.024). These results are summarised in Table 3 and 4.

DISCUSSION

The incidence of tuberculosis is rising and the disease remains a challenge in developing countries [33, 34].Treatment can be effective in most cases if the disease is diagnosed early [16], though the development of drug resistant strains has compounded the complication of managing patients with TB [34]. In this study we have demonstrated the variable morphological appearance of BTB when assessed on the DCE-MRI, and explored the potential biomarkers which may be utilised in treatment monitoring.

Characteristics of breast TB on MRI

All the lesions were hypointense on pre-contrast T1 weighted (T1W), whereas on pre-contrast T2 weighted (T2W) all the responders had uniformly hyperintense lesions and the non-responders demonstrated mixed signal intensity lesions. None of the lesions were

uniformly hypointense on T2. This observation can play an important role in differentiating BTB from BCA because the majority of BCA are hypointense on T2 weighted imaging [35-37]. There is limited literature on the appearances of BTB on DCE-MRI, we found only one study that was performed on 6 patients with BTB in 1998 [31]. The authors reported similar findings to our study, they had a total of seven breast lesions, all lesions were hypointense on pre-contrast T1W, however they did not mention T2W appearances [31].

It is important to note that other benign lesions such as cysts, lymph nodes and fibroadenoma are usually hyperintense on T2 [38]. However, cysts generally, do not enhance post-contrast unless they have a complex component [39]. Lymph nodes [40]and fibroadenomas [41] have their own distinct morphological appearances on other sequences and on post contrast imaging [36]. Following the administration of the I.V. contrast, the enhancement pattern was either NME or rim enhancing mass. None of the BTB lesions demonstrated solid-cystic, homogeneous or heterogeneous enhancing mass pattern. Again, this might be an important differentiating factor from BCA, especially if the breast cancer has cystic elements. The presence of solid elements in a cystic mass may favour breast cancer instead of BTB. Oh *et al* found four out of a total of seven BTB lesions demonstrated ring/rim enhancement, however in contrast to ours, two had internal enhancement, and one lesion did not have any enhancement [31]. The differences could be due to advancement in imaging techniques since 1998.

All the lymph nodes showed rim-enhancement with the central low signal consistent with typical necrotic nodes found in TB [27, 42]. The enhancement distribution ranged from diffuse, focal and multifocal with and without the chest wall involvement in both responders and non-responders and these patterns can all occur in breast cancer [32].

Changes in morphology and quantitative markers with treatment

On the morphological analysis, whereas all BTB lesions were hypointense on pre-contrast T1W, all the responders had uniformly hyperintense lesions and the non-responders demonstrated mixed signal intensity lesions on pre-contrast T2 weighted (T2W) sequence.

There is data regarding the use of breast MRI quantitative parameters in the evaluation of the response to cancer treatment, especially in patients receiving neoadjuvant chemotherapy (NAC) [43-45] . Hahn *et al* evaluated the role of DWI as an adjunct to DCE-MRI in

evaluating residual BCA following NAC. The investigators found that the accuracy for the detection of residual cancer improved with a combination of both modalities instead of each individual modality [44]. We have not found a study in which the ADC, the T2SI value or the D_{max} were used to evaluate response to BTB treatment. In our study, we found that the D_{max} is the best discriminator between the responders and the non-responders (p=0.024). The other two biomarkers, namely the ADC value and T2SI were not useful in differentiating the responders from the non-responders.

Our preliminary results therefore suggest that the combination of the DCE-MRI morphological patterns and the D_{max} may have a potential role in the diagnosis of breast tuberculosis, particularly in terms of differentiating it from breast cancer, and in the monitoring of response to treatment.

There were several limitations to our study: Firstly, the small sample size reflects the low prevalence of BTB. Secondly, the images were read by one radiologist. Confirmation of these preliminary results will require a larger, multicentre study with formal assessment of inter-reader agreements.

Conclusions

Our results indicate that the lesion maximum diameter can be valuable in treatment monitoring in breast tuberculosis patients. Furthermore, the morphological features of T2W hyperintensity, DCE-MRI rim-enhancing ***breast lesions*** associated with ***ring/rim-enhancing axillary nodes*** favour breast tuberculosis than breast cancer and may play a role in differentiating these two conditions.

ACKNOWLEDGEMENTS

This publication was made possible by grant number: R24TW008863 from the Office of the U.S. Global AIDS Coordinator and the U. S. Department of Health and Human Services, National Institutes of Health (NIH OAR and NIH ORWH). Its contents are solely the responsibility of the authors and do not necessarily represent the official views of the government. Further funding for operational costs was obtained from the UKZN strategic funds.

CONFLICT OF INTEREST

The authors declare no conflict of interest.

REFERENCES

1. Akbulut S, Sogutcu N, Yagmur Y. Coexistence of breast cancer and tuberculosis in axillary lymph nodes: a case report and literature review. *Breast Cancer Research and Treatment* 2011; **130**: 1037-42.

2. Meerkotter D, Spiegel K, Page-Shipp LS. Imaging of tuberculosis of the breast: 21 cases and a review of the literature. *Journal of Medical Imaging & Radiation Oncology* 2011; **55**: 453-60.

3. Mehta G, Mittal A, Verma S. Breast Tuberculosis- Clinical Spectrum and Management. *Indian Journal of Surgery* 2010; **72**: 433-7.

4. Ramaema DP, Buccimazza I, Hift RJ. Prevalence of breast tuberculosis: Retrospective analysis of 65 patients attending a tertiary hospital in Durban, South Africa. *South African Medical Journal* 2015; **105**: 866-9.

5. Hiremath BV, Subramaniam N. Primary breast tuberculosis: Diagnostic and therapeutic dilemmas. *Breast Disease* 2015; **35**: 187-93.

6. Kant S, Mahajan V, Verma SK. Tubercular mastitis mimicking malignancy. *Internet Journal of Pulmonary Medicine* 2008; **9**: 5-.

7. Deepa H, Vijay S, Mishra P, Jai J, Chitra DH. Tubercular Mastitis is Common in Garhwal Region of Uttarakhand: Clinico athological Features of 14 Cases. *Journal of Clinical and Diagnostic Research* 2011; **5**: 5.

8. McKeown K, Wilkinson K. Tuberculous disease of the breast. *British Journal of Surgery* 1952; **39**: 420.

9. NHS Breast Screening Programme. Guidelines on organising the surveillance of women at higher risk of developing breast cancer in an NHS Breast Screening Programme. England2013; Available from: https://www.gov.uk/government/uploads/system/uploads/attachment_data/file/439634/nhsbsp73.pdf.

10. Afridi SP, Memon A, Rehman SU, Baig N. Spectrum of breast tuberculosis. *Journal of the College of Physicians and Surgeons, Pakistan* 2009; **19**: 158-61.

11. Meldau R, Peter J, Theron G, Calligaro G, Allwood B, *et al.* Comparison of same day diagnostic tools including Gene Xpert and unstimulated IFN-gamma for the evaluation of pleural tuberculosis: a prospective cohort study. *BMC Pulmonary Medicine* 2014; **14**: 58.

12. Nalini G, Kusum S, Barwad A, Gurpreet S, Arvind R. Role of polymerase chain reaction in breast tuberculosis. *Breast Disease* 2015; **35**: 129-32.

13. Shah M, Dowdy D, Joloba M, Ssengooba W, Manabe YC, *et al.* Cost-effectiveness of novel algorithms for rapid diagnosis of tuberculosis in HIV-infected individuals in Uganda. *AIDS* 2013; **27**: 2883-92.

14. Sun D, Dorman S, Shah M, Manabe YC, Moodley VM, *et al.* Cost utility of lateral-flow urine lipoarabinomannan for tuberculosis diagnosis in HIV-infected African adults. *International Journal of Tuberculosis and Lung Disease* 2013; **17**: 552-8.

15. Aurum Institute. Managing TB in a new era of diagnosis. Johannesburg, South Africa: Aurum Institute; 2013; Available from: http://www.sahivsoc.org/upload/documents/Aurum%20Managing%20TB%20in%20an%20era%20of%20new%20diagnostics.pdf.

16. Department of Health. National TB Management Guidelines. 2014.

17. Khandelwal R, Jain I. Breast tuberculosis mimicking a malignancy: a rare case report with review of literature. *Breast Disease* 2013; **34**: 53-5.

18. Dialani V, Chadashvili T, Slanetz PJ. Role of imaging in neoadjuvant therapy for breast cancer. *Annals of Surgical Oncology* 2015; **22**: 1416-24.

19. Wu LA, Chang RF, Huang CS, Lu YS, Chen HH, *et al.* Evaluation of the treatment response to neoadjuvant chemotherapy in locally advanced breast cancer using combined magnetic resonance vascular maps and apparent diffusion coefficient. *Journal of Magnetic Resonance Imaging* 2015; **42**: 1407-20.

20. Mann RM, Balleyguier C, Baltzer PA, Bick U, Colin C, *et al.* Breast MRI: EUSOBI recommendations for women's information. *European Radiology* 2015; **25**: 3669-78.

21. Mann RM, Kuhl CK, Kinkel K, Boetes C. Breast MRI: guidelines from the European Society of Breast Imaging. *European Radiology* 2008; **18**: 1307-18.

22. Alonso Roca S, Jimenez Arranz S, Delgado Laguna AB, Quintana Checa V, Grifol Clar E. [Breast cancer screening in high risk populations]. *Radiologia* 2012; **54**: 490-502.

23. Engin G, Acunas B, Acunas G, Tunaci M. Imaging of extrapulmonary tuberculosis. *Radiographics* 2000; **20**: 471-88; quiz 529-30, 32.

24. Torres C, Riascos R, Figueroa R, Gupta RK. Central nervous system tuberculosis. *Topics in Magnetic Resonance Imaging* 2014; **23**: 173-89.

25. Rasouli MR, Mirkoohi M, Vaccaro AR, Yarandi KK, Rahimi-Movaghar V. Spinal tuberculosis: diagnosis and management. *Asian Spine J* 2012; **6**: 294-308.

26. Saraf SK, Tuli SM. Tuberculosis of hip: A current concept review. *Indian Journal of Orthopaedics* 2015; **49**: 1-9.

27. Williams A, Stockely H, Filobbos R. A pictorial review of the imaging findings in abdominal tuberculosis. European Congress of Radiology; Vienna2010.

28. Fellah L, Leconte I, Weynand B, Donnez J, Berlière M. Breast tuberculosis imaging. *Fertility and Sterility* 2006; **86**: 460-1.

29. Popli MB, Kumari A, Popli V. Proton magnetic resonance spectroscopy in breast tuberculosis. *European Journal of Radiology Extra* 2010; **74**: e59-e63.

30. Machida Y, Tozaki M, Shimauchi A, Yoshida T. Two Distinct Types of Linear Distribution in Nonmass Enhancement at Breast MR Imaging: Difference in Positive Predictive Value between Linear and Branching Patterns. *Radiology* 2015; **276**: 686-94.

31. Oh KK, Kim JH, Kook SH, . Imaging of tuberculous disease involving breast *European Radiology* 1998; **8**: 6.

32. D'Orsi C, Sickles E, Mendelson E, Morris E. ACR BI-RADS Atlas: Breast Imaging Reporting and Data System. Reston, VA: American College of Radiology 2013.

33. World Health Organisation. Global Tuberculosis report 2014. World Health Organization: 2014.

34. World Health Organisation. Global tuberculosis report 2015. World Health Organisation: 2015.

35. Gribbestad IS, Nilsen G, Fjosne HE, Kvinnsland S, Haugen OA, *et al.* Comparative signal intensity measurements in dynamic gadolinium-enhanced MR mammography. *Journal of Magnetic Resonance Imaging* 1994; **4**: 477-80.

36. Kuhl CK. MRI of breast tumors. *European Radiology* 2000; **10**: 46-58.

37. Malich A, Fischer DR, Wurdinger S, Boettcher J, Marx C, *et al.* Potential MRI interpretation model: differentiation of benign from malignant breast masses. *AJR: American Journal of Roentgenology* 2005; **185**: 964-70.

38. Santamaria G, Velasco M, Bargallo X, Caparros X, Farrus B, *et al.* Radiologic and pathologic findings in breast tumors with high signal intensity on T2-weighted MR images. *Radiographics* 2010; **30**: 533-48.

39. Petralia G, Bonello L, Priolo F, Summers P, Bellomi M. Breast MR with special focus on DW-MRI and DCE-MRI. *Cancer Imaging* 2011; **11**: 76-90.

40. de Felice C, Cipolla V, Stagnitti A, Porfiri LM, Guerrieri D, *et al.* Diagnostic accuracy of 1.5 Tesla breast magnetic resonance imaging in the pre-operative assessment of axillary lymph nodes. *European Journal of Gynaecological Oncology* 2015; **36**: 447-51.

41. Hochman MG, Orel SG, Powell CM, Schnall MD, Reynolds CA, *et al.* Fibroadenomas: MR imaging appearances with radiologic-histopathologic correlation. *Radiology* 1997; **204**: 123-9.

42. Lee WK, Van Tonder F, Tartaglia CJ, Dagia C, Cazzato RL, *et al.* CT appearances of abdominal tuberculosis. *Clinical Radiology* 2012; **67**: 596-604.

43. Boes JL, Hoff BA, Hylton N, Pickles MD, Turnbull LW, *et al.* Image registration for quantitative parametric response mapping of cancer treatment response. *Translational Oncology* 2014; **7**: 101-10.

44. Hahn SY, Ko EY, Han BK, Shin JH, Ko ES. Role of diffusion-weighted imaging as an adjunct to contrast-enhanced breast MRI in evaluating residual breast cancer following neoadjuvant chemotherapy. *European Journal of Radiology* 2014; **83**: 283-8.

45. Vignati A, Giannini V, Carbonaro LA, Bertotto I, Martincich L, *et al.* A new algorithm for automatic vascular mapping of DCE-MRI of the breast: Clinical application of a potential new biomarker. *Computer Methods and Programs in Biomedicine* 2014; **117**: 482-8.

FIGURE LEGENDS

Figure 1

(A-F): Axial pre-and post-contrast breast MRI images of two patients with breast tuberculosis (BTB), (A-C) a responder and (D-E) non-responder. **a)** Pre-contrast T1 hypointense lesion in the left breast of a responder. **b)** Pre-contrast T2 hyperintense lesion in the left breast. **c)** Post-contrast T1 showing rim enhancing lesion. **d**) Pre-contrast T1 hypointense lesions in the right breast of a non-responder. **e)** Pre-contrast T2 mixed signal intensity lesions in the right breast. **f)** Post-contrast lesions in the right breast of a non-responder demonstrating multiple rim-enhancing lesions.

Figure 2

(A-C): Axial T1 post-contrast subtracted breast MRI images of various patients with breast tuberculosis (BTB). **a)** Non-mass enhancement (NME) pattern in the unilaterally enlarged left breast. **b)** Rim-enhancing breast lesions in the shrunken left breast. **c)** Rim-enhancing right axillary nodes.

TABLE 1

Local dynamic contrast-enhanced breast MRI protocol technical parameters. TSE=Turbo Spin Echo; GE=Gradient Echo; STIR=Short Tau Inversion Recovery.

MRI sequence	Acquisition plane	Repetition time (TR) (msec)	Echo Time (TE) (msec)	Inversion time (msec)	Matrix size	Field of view (FoV) (mm)	Slice thickness (mm)	Voxel size (mm)
Localizer	sagittal	7.6	3.53	-	384 x 512	400	6	2.1x1.6x6.0
T1 precontrast GE 3D	axial	8.6	4.70	-	299 x 384	320	1	1.0x0.7x1.0
T1 GE 3D dynamic sequences (1 pre& 5post contrast)	axial	9.1	4.76	-	299 x 284	340	1.5	1.1x0.9x1.5
T1 3D Dixon	axial	7.20	first 2.38; second 4.76	-	320 x 320	340	1.8	1.1x1.1x1.8
T1 fat sat	axial	680	10	-	224 x 320	320	4	1.4x1.0x4.0
T2 STIR	axial	5600	59.0	170	314 x 320	340	4	1.1x1.1x4.0
T2 TSE	axial	6100	111	-	384 x 512	320	4	1.7x1.3x4.0
DWI b values 0 & 800s/mm^2	axial	9200	86	180	150 x 192	380	4	2.0x2.0x4.0

TABLE 2

MRI qualitative characteristic of breast tuberculosis patients at the baseline scan. The descriptive categories employed are listed in the text under *Methods*.

Characteristic	**Responder (n=4)**	**Non responder (n=2)**
T1 (precontrast)		
Hyperintense		
Isointense		
Hypointense	4	2
T2 (precontrast)		
Hyperintense	4	
Isointense		
Hypointense		
Mixed hyper/iso/hypointense		2
Enhancement pattern		
Focus/Foci (<5mm)		
Non-mass enhancement-NME	2	1
Mass:		
Solid-cystic		
Rim	2	1
Homogeneous		
Heterogeneous		
Axillary nodes enhancement		
Rim	4	2
Homogeneous		
Enhancement distribution		
Diffuse, *and* chest wall ext.		
Diffuse, *No* chest wall ext.	2	1

Characteristic	Responder (n=4)	Non responder (n=2)
Focal, and chest wall ext.		
Focal, No chest wall ext.	1	
Multifocal, *and* chest wall ext.		
Multifocal, *No* chest wall ext	1	1

TABLE 3

MRI quantitative parameters of breast tuberculosis patients.ADC-0, T2SI-0, Dmax-0: corresponding values at baseline. ADC-1, T2SI-1, Dmax-1: corresponding values at 4 month follow-up examination. Units are: ADC: x10-6mm2/sec); Dmax: cm. Patient 5, was studied at baseline only as she declined a follow-up study. She is known however to be a responder, since this was demonstrated on serial mammography. She has therefore been included as a responder, and the data available for her analysed accordingly.

Responder (yes/no)	**Patient**	**HIV status**	**ADC-0 (n=6) Mean (SD)**	**ADC-1 (n=5) Mean (SD)**	**Delta ADC (n=5) Mean (SD)**	**T2SI-0 (n=6) Mean (SD)**	**T2SI-1 (n-5) Mean (SD)**	**Delta T2SI (n-5) Mean (SD)**	**D_{max}-0**	**D_{max}-1**	**Delta (D_{max})**
No	1	pos	993.38	2084.36	-1090.98	790.2	379.63	410.57	3.9	3.9	0
No	2	pos	1994.58	2168.03	-173.45	945.13	1074.11	-128.98	1.7	3.4	-1.7
Yes	3	Not tested	972.75	199.54	773.21	400.39	144.07	256.32	4.5	2.4	2.1
Yes	4	pos	1558.79	1725.81	-167.02	863.47	753.12	110.35	8.9	7.1	1.8
Yes	5	pos	2135.96	-	-	857.09	-	-	3	-	-
Yes	6	neg	2489.15	1293.32	1195.83	870.19	438.85	431.34	3	1.2	1.8

TABLE 4

Delta Mean MRI parameter values between the responders and the non-responders patients with breast tuberculosis.

MRI parameter	**Non-Responders (n=2)**	**Responders (n=3)**	***p* value**
Delta ADC Mean ± SD ($x10^{-6}mm^2/sec$)	-632.21 ± 648.79 (95% CI,-6461.37-5196.94)	600.67 ± 697.61 (95% CI,-1132.29-2333.64)	0.901
Delta T2SI Mean ± SD	140.79 ± 381.51 (95% CI,-3287.02-3568.61)	266.00 ± 160.71 (95% CI,-133.23-665.23)	0.282
Delta Lesion diameter ($D_{max)}$ Mean ± SD (cm)	-0.85 ± 1.2 (95% CI,-11.65-9.95)	1.90 ± 0.17 (95% CI, 1.46-2.33)	0.024

FIGURE 1

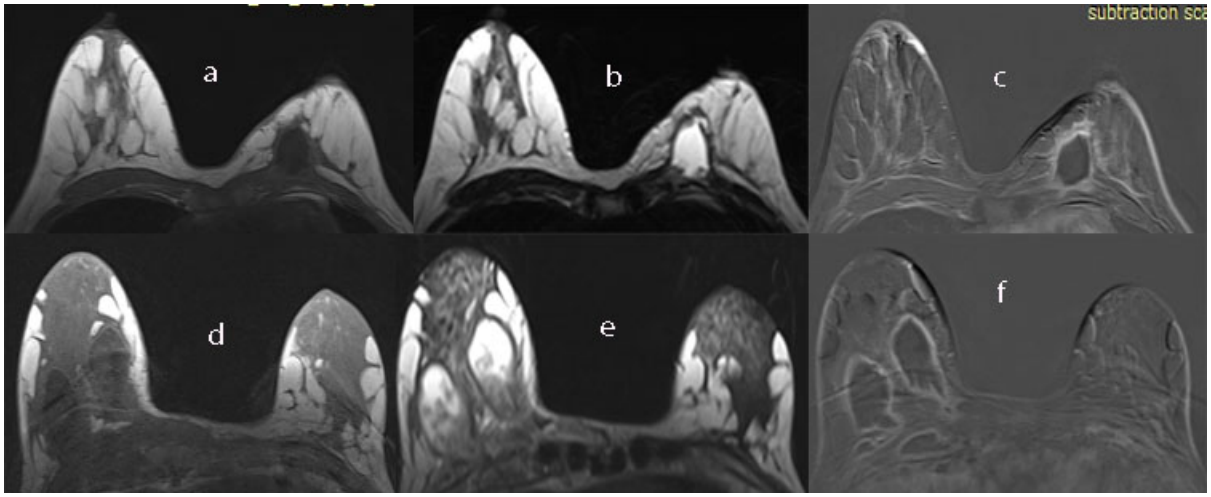

FIGURE 2

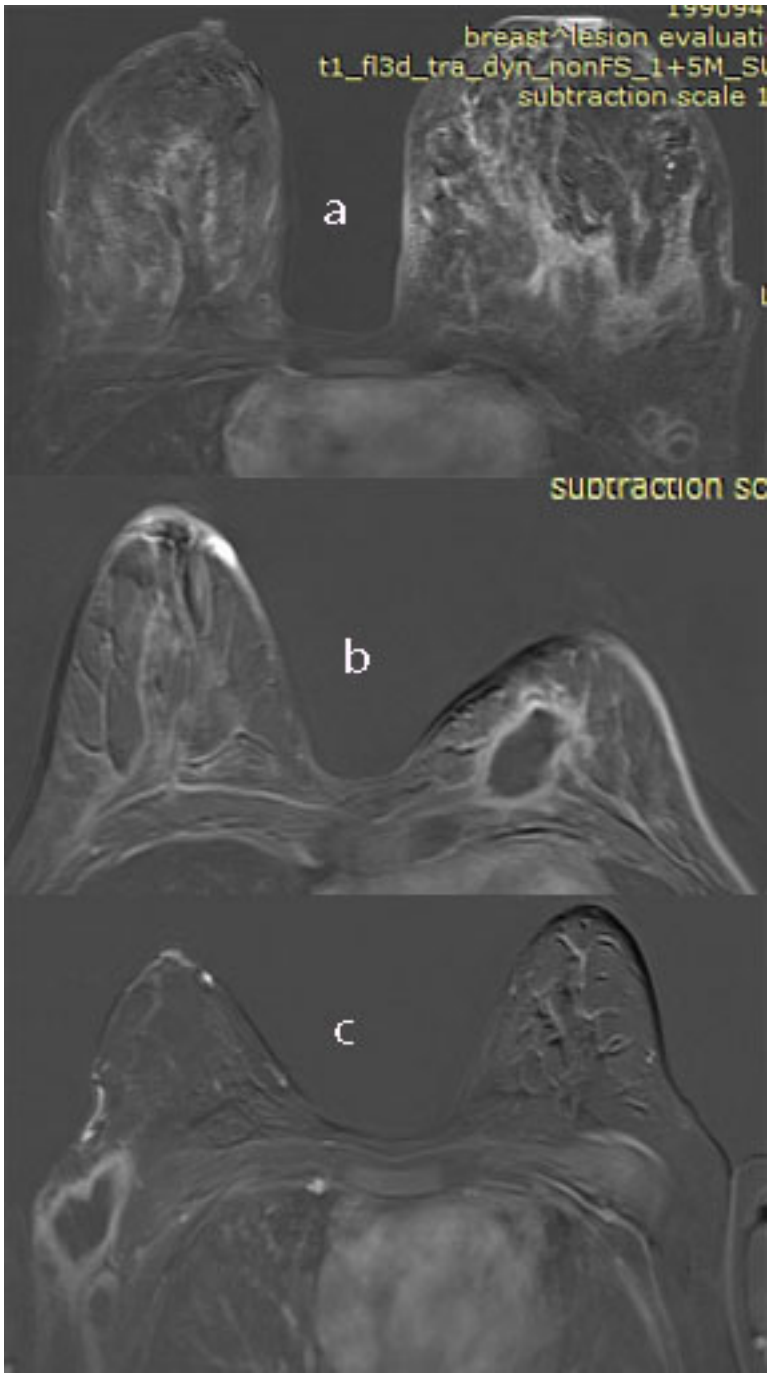
breast^lesion evaluati
t1_fl3d_tra_dyn_nonFS_1+5M_S
subtraction scale 1
a
subtraction sc
b
c

CHAPTER 5

Utility of ^{18}F-FDG-PET-CT in differentiating breast cancer from breast tuberculosis

TITLE

Utility of ^{18}F-FDG-PET-CT in differentiating breast cancer from breast tuberculosis.

AUTHORS

Dibuseng P Ramaema MBChB (UCT) FCRad (Diag) SA[1]
Richard J Hift MMed (Med) PhD FCP (SA) FRCP (UK)[2]

AFFILIATIONS:

1. Division of Radiation Medicine (Radiology), Nelson R Mandela School of Medicine, University of KwaZulu-Natal, Durban, South Africa.
2. Division of Medicine, Nelson R Mandela School of Medicine, University of KwaZulu-Natal, Durban, South Africa.

*CORRESPONDING AUTHOR:

Dr Dibuseng P Ramaema
Discipline of Radiation Medicine (Diagnostic Radiology)
Nelson R Mandela School of Medicine
University of KwaZulu-Natal
Private Bag 7 Congella
Durban, South Africa
4013

Email: Ramaema@ukzn.ac.za
Tel: +27 31 260 4301

RUNNING TITLE

Utility of ^{18}F-FDG-PET-CT in differentiating breast cancer from breast tuberculosis

KEYWORDS

^{18}F-FDG-PET-CT
Breast cancer
Breast tuberculosis

ABBREVIATIONS

^{18}F-FDG	(Fluorine-18)-fluoro-2-deoxy-D-glucose
^{18}F-FDG PET-CT	(Fluorine-18)-fluoro-2-deoxy-D-glucose (^{18}F-FDG) positron emission tomography (PET) integrated with computed tomography (CT)
ATT	anti-tuberculous therapy
BTB	breast tuberculosis
CT	computed tomography
FDG	(Fluorine-18)-fluoro-2-deoxy-D-glucose
HU	Hounsfield units
ROI	region of interest
$SUV_{max,}$	maximum standardised uptake value
TB	tuberculosis

WORD, FIGURE AND TABLE COUNT

Abstract	219
Words	1913
Tables	2
Figures	5

ABSTRACT

Aim

The purpose of our study was to explore the role of ^{18}F-FDG-PET-CT as a non-invasive assessment method to differentiate breast tuberculosis (BTB) from breast cancer (BCA).

Methods

We reviewed ^{18}F-FDG-PET-CT findings of twenty nine patients, 24 with BCA and 5 with BTB. The maximum standardised uptake value (SUV_{max}) and the CT density in Hounsfield units (HU) of the breast lesions and axillary nodes were measured. The demographics and pertinent PET-CT morphological appearances were recorded.

Results

All patients were female. The age of the patients with BTB ranged from 23 to 42 years, and of those with BCA from 34 to 76 years. The commonest morphological pattern for the cancer group was that of a mass, whereas for the BTB group there were equal proportions for the mass and oedema morphologies. The mean (SD) SUV_{max} of the ***breast lesions*** in the BCA patients were significantly higher than in those of the BTB patients, 12.59±8.11 vs 3.14±1.55 (p=0.016). There was no statistically significant difference in the mean SUV_{max} of the ***axillary lymph nodes***, the breast lesion density (HU) or the axillary lymph nodes density.

Conclusions

The SUV_{max} was useful for distinguishing the breast lesions in cancer and tuberculosis patients, but not for the axillary nodes. The Hounsfield density was not useful for differentiating either the breast lesions or the axillary nodes.

INTRODUCTION

While breast cancer (BCA) is globally one of the commonest cancers in women [1], the incidence of breast tuberculosis (BTB) is low [2-4]. There is a significant overlap in the clinical presentation of the two conditions, creating the possibility for incorrect diagnosis [3]. This is complicated by the poor specificity of the currently available routine imaging modalities, including mammography and ultrasound, in distinguishing the two conditions [5].

^{18}F-FDG-PET-CT has established a role in managing advanced, recurrent and metastatic BCA [6], and there is emerging evidence regarding the use of this modality in early breast cancer [7, 8]. It has also been studied as a modality for differentiating pulmonary tuberculosis (PTB) from malignant conditions with varying results [9-11]. In recent years, there has been increasing evidence for the utility of ^{18}F-FDG-PET-CT in diagnosing inflammatory and infective conditions [12-15]. In areas where TB is endemic, one study has found that ^{18}F-FDG-PET-CT was not useful to differentiate benign from malignant pulmonary nodule [16]. Similarly in another study performed in China where TB is endemic, the authors found lower specificity (61.1%) for ^{18}F-FDG-PET due to the high percentage (57.14%) of false positives from TB. The specificity of CT was slightly higher than that of ^{18}F-FDG-PET. The authors concluded that the combined ^{18}F-FDG-PET-CT offered greater diagnostic accuracy than that for PET or CT alone. Caution in the interpretation of PET-positive SPN in regions where granulomatous pulmonary disease prevails is mentioned [17]. Owing to the hybrid imaging offered by ^{18}F-FDG-PET-CT in combining the morphological appearances on CT and the metabolic behaviour of organs on PET, it has an advantage over the use of either modality alone [18]. Most studies which utilised ^{18}F-FDG-PET-CT to evaluate variables that may be useful in predicting malignancy were directed at solitary pulmonary nodules [10, 11, 16]. We are unaware of any previous studies of the value of ^{18}F-FDG-PET-CT in diagnosing breast tuberculosis. In this study we evaluate the utility of ^{18}F-FDG-PET-CT in differentiating BTB from BCA.

PATIENTS AND METHODS

Study design

We conducted a non-randomized prospective observational study between January 2014 and January 2015. Ethical clearance was obtained from our institutions Biomedical Research Ethics Committee (Reference number BF213/13).

Patients

The study consisted of 29 patient's ^{18}F-FDG-PET-CT images from two cohorts, one with histologically proven BCA and the other with histologically proven BTB.

Twenty four patients with histologically proven BCA who underwent pre-operative ^{18}F-FDG-PET-CT during the period January 2014 to September 2015 were retrospectively identified in our hospital's database. The ^{18}F-FDG-PET-CT images were retrieved from the picture archiving and communication system (PACS) and analysed retrospectively. Inclusion criteria were: histologically proven breast cancer, a radiologically proven breast lesion on the staging scan for either primary or recurrent breast cancer. In all cases of restaging, if the original baseline scan was done prior to treatment, this was sourced and used in the analysis. Pathology reports were reviewed and the following information was recorded; the histological type, and whether the breast cancer was newly diagnosed, recurrent or examination was for restaging following treatment was noted.

Five consecutively identified patients with pathologically proven BTB were recruited and invited to have ^{18}F-FDG-PET-CT after giving signed written consent to participate in the study. Four had conclusive histology, while one had inconclusive histology from breast and axilla, but had microbiologically proven pulmonary TB, for which she was receiving anti-tuberculous therapy (ATT). Her clinical and radiological features were compatible with BTB. The biopsy was performed at the initial visit, and patients underwent ^{18}F-FDG-PET-CT scanning approximately three weeks after the initial visit, hence there was sufficient time to allow the biopsy sites to heal, thereby minimising interference with the PET-CT scan interpretation.

Methods

^{18}F-FDG-PET-CT image acquisition

All patients fasted for at least six hours prior to an intravenous administration of ^{18}F-FDG at a dose of 4 MBq/kg body weight. Glucose values were assessed before injection, with the maximum allowable glucose level prior to scan being 11.1 mmol/L. This was done in order to minimise the competition of high plasma glucose with ^{18}F-FDG, which can result in the diversion of ^{18}F-FDG into muscle, with a subsequent reduction in uptake by the inflammatory cells [19].

A whole body PET-CT scan (Siemens, Erlangen, Germany) Biograph 16 slice was performed between 60 and 90 minutes after the injection. The PET images were acquired for a maximum of 8 bed positions at 3 minutes per field of view (FoV) in the craniocaudal direction, from the skull vertex to the mid-femur point. Images were acquired at a zoom of 1 and a matrix of 168 x 168. An iterative reconstruction using 2 iterations and 24 subsets was used for post-acquisition image processing.

A diagnostic non-contrasted CT scan was acquired in the craniocaudal direction with the following parameters: 4D CARE dose for 100 mAs, 120 KVp and 5 mm slice thickness, pitch of 0.75 for a scan time of 25s. A CT image multiplanar reconstruction was obtained using a kernel of B31f, abdomen window, slice thickness of 4 mm and a recon increment of 2 mm.

Combined ^{18}F-FDG-PET-CT analysis

The images were read by two experienced nuclear medicine physicians with ten years' and five years' experience respectively, and one of the authors, an experienced radiologist with 15 years' experience (DPR). Readings were agreed by consensus and there was no blinding.

Quantitative analysis

True-D software (*Siemens, Erlangen, Germany*) with automatic multi-planar orthogonal display of the 3-D regions of interest (ROI) in axial, sagittal and coronal planes, was used to analyse the fused and unfused ^{18}F-FDG-PET-CT images. 3-D ROI were drawn over the ^{18}F-FDG avid areas, and the maximum standardised uptake value (SUV_{max}) of the FDG avid

breast lesions and axillary nodes were recorded. Bilateral axillary nodes were evaluated, and the highest SUV_{max} value was recorded. The corresponding CT images were evaluated for the density of the breast lesion and the axillary nodes in Hounsfield units (HU). If there were many adjacent nodes in a basin, these were considered as one, and the SUV_{max} and the HU of the whole basin was taken.

Morphological analysis

The lesions were grouped into four patterns: a mass, oedema, mass-oedema and thickening. The morphological characteristics were classified as solid, solid-cystic, axillary lymphadenopathy breast-oedema (ALBE) and thickening.

Statistical analysis

The two-sample t test with equal variances was used for differentiating the two groups. The results were considered significant where p values were <0.05. The relative frequencies of the various radiological patterns and morphologies were calculated using the *Freeman-Halton* extension of the Fisher exact probability test for a two-rows by four-column contingency table and an online calculator (http://vassarstats.net/newcs.html).

RESULTS

Patient demographics and ^{18}F-FDG-PET-CT qualitative findings

All the patients were female, with age range for the BTB group being 23 to 42 years, and for the BCA cohort being 34 to 76. Amongst the BTB patients, three were HIV positive, one HIV negative and one not tested. BTB patients showed a mass (*n*=2), oedema (*n*=2) or thickening (*n*=1) pattern, while the majority of BCA patients had mass patterns (n=18). The mass-oedema pattern was only observed in the BCA group (*n*=4). There is a significant difference in the frequency of these patterns between the two groups (p=0.05).

For morphological analysis, the solid morphology was only seen in the BCA group (*n*=17) (Fig. 1), whereas the ALBE morphology was only observed in the BTB group (*n*=2) (Fig. 2). Both groups demonstrated solid-cystic morphology, with the BCA group having 6 (*n*=6) and the BTB group having 2 (*n*=2) (Fig. 3). Similarly, both groups had thickening

morphology, with one BCA (*n*=1) and one BTB patient (*n*=1) Fig. 4). These features are summarised in (Table 1). There is a highly significant difference in the frequency of these morphologies between the two groups (p=0.0007).

The BCA pathological subtype were invasive ductal cancer (IDC) (n=22), invasive ductal adenocarcinoma (IDA) (n=1) and differentiated neuroendocrine (DNE) tumour (n=1). Of the 29 women, 58.3% had ^{18}F-FDG-PET-CT following prior treatment, whilst 41.7% had the scan prior to any treatment. The findings are summarised in (Fig. 5).

Quantitative ^{18}F-FDG-PET-CT findings

The mean (SD) SUV_{max} of the ***breast lesions*** in the BCA patients were significantly higher than those of the BTB patients at baseline, 12.59±8.11 vs 3.14±1.55 respectively, (*p*=0.016). There was no statistically significant difference in the baseline mean SUV_{max} of the ***axillary lymph nodes***, the breast lesions density (HU) and the axillary lymph nodes density (HU). These are summarised in Table 2.

DISCUSSION

BTB is an uncommon manifestation of extra-pulmonary tuberculosis (EPTB); and may have a more severe presentation when associated with HIV infection [20, 21]. BTB can be effectively treated medically in most cases [4], making early diagnosis important. The features of BTB are similar to and may overlap those of BCA [22]. Furthermore BCA and BTB can co-exist, and patients with TB-HIV co-infection who develop BCA are at risk of being misdiagnosed [23-25]. The importance of discriminating these two conditions can therefore be challenging, particularly in the setting of TB-HIV co-infection.

Our results show that the mean SUV_{max} for the ***breast lesion*** is higher in patients with BCA than in those with BTB. SUV_{max} appears to be a strong discriminator between breast cancer and breast tuberculosis when the lesion is located within the breast or chest wall, (*p*=0.016). This result is in keeping with some recent studies utilising ^{18}F-FDG-PET-CT in assessing solitary pulmonary nodules (SPN). Lopez *et al* retrospectively analysed ^{18}F-FDG-PET-CT scans of fifty-five patients with SPN using a combination of quantitative parameters; maximum diameter on CT (D_{max}) and SUV_{max}; and demographic variables. Their study found the predictive model incorporating SUV_{max} values and patient age was the best

discriminator between benign and malignant SPN [10]. In another study, Yilmaz *et al* retrospectively reviewed ^{18}F-FDG-PET-CT of 241 patients with SPN, and found the mean SUV_{max} value was statistically significantly higher in patients with the SPN diameter ≥ 1cm hence was useful for differentiating benign from malignant nodules above this size [11].

On the other hand, in our study the SUV_{max} was not useful in differentiating between tuberculous and metastatic ***axillary lymphadenopathy*** (p=0.411). This is in agreement with a study that attempted to differentiate benign from malignant solitary pulmonary nodules in a population in which TB is endemic, where ^{18}F-FDG-PET-CT failed to distinguish the two conditions [16]. It therefore appears that the SUV_{max} is a good discriminator of BTB and BCA for the intra-mammary breast lesions and not for axillary lymph nodes. Lesion density HU was not useful in differentiating between the ***breast lesions*** (p=0.566) and the ***axillary nodes*** (p=0.101) of the BTB and BCA patients.

The three morphological patterns of mass, oedema and thickening were observed in both the BTB and the BCA patients. However, mass-oedema was only observed in the BCA patients. Although our numbers are small, this may suggest that breast masses associated with oedema on ^{18}F-FDG-PET-CT are more likely to be cancer than TB. Similarly, although the solid-cystic and the thickening morphologies were present in both groups, the solid morphology was only observed in the BCA group, and the ALBE pattern only in the BTB group. It therefore appears that when the breast oedema without a mass is associated with axillary lymphadenopathy, it is more likely to be TB than cancer.

Owing to the low prevalence of BTB, the small sample size cannot at this stage do more than flag possible areas of divergence of the two diseases. The changes we have shown however suggest that a pooled multinational study with larger numbers may be useful in developing diagnostic algorithms for the radiological diagnosis of BTB.

STUDY LIMITATIONS

Given the small sample size, our conclusions are preliminary.

ACKNOWLEDGEMENTS

This publication was made possible by grant number R24TW008863 from the Office of the U.S. Global AIDS Coordinator and the U. S. Department of Health and Human Services, National Institutes of Health (NIH OAR and NIH ORWH). Its contents are solely the responsibility of the authors and do not necessarily represent the official views of the government. Further funding for operational costs was obtained from the UKZN strategic funds.

CONFLICT OF INTEREST:

The authors declare no conflict of interest.

REFERENCES

1. American Cancer Society. Breast Cancer Facts & Figures 2013-2014. Atlanta: American Cancer Society: 2014.

2. Kalaç N, Özkan B, Bayiz H, Dursun AB, Demirağ F. Breast tuberculosis. *The Breast* 2002; **11**: 346-9.

3. Mehta G, Mittal A, Verma S. Breast tuberculosis- clinical spectrum and management. *The Indian Journal Of Surgery* 2010; **72**: 433-7.

4. Ramaema DP, Buccimazza I, Hift RJ. Prevalence of breast tuberculosis: Retrospective analysis of 65 patients attending a tertiary hospital in Durban, South Africa. *South African Medical Journal* 2015; **105**: 866-9.

5. Khodabakhshi B, Mehravar F. Breast tuberculosis in northeast Iran: review of 22 cases. *BMC Women's Health* 2014; **14**: 72.

6. Society of Nuclear Medicine. 18F-fluorodeoxyglucose (FDG) PET and PET/CT Practice Guidelines in Oncology. 2013; Available from: http://www.snm.org/docs/PET_PROS/OncologyPracticeGuidelineSummary.pdf.

7. Choi YJ, Shin YD, Kang YH, Lee MS, Lee MK, *et al.* The effects of preoperative (18)F-FDG PET/CT in breast cancer patients in comparison to the conventional imaging study. *Journal of Breast Cancer* 2012; **15**: 441-8.

8. Jung NY, Kim SH, Kim SH, Seo YY, Oh JK, *et al.* Effectiveness of breast MRI and (18)F-FDG PET/CT for the peoperative staging of invasive lobular carcinoma versus ductal carcinoma. *Journal of Breast Cancer* 2015; **18**: 63-72.

9. Khalaf M, Abdel-Nabi H, Baker J, Shao Y, Lamonica D, *et al.* Relation between nodule size and 18F-FDG-PET SUV for malignant and benign pulmonary nodules. *Journal of Hematology & Oncology* 2008; **1**: 13.

10. Van Gomez Lopez O, Garcia Vicente AM, Honguero Martinez AF, Jimenez Londono GA, Vega Caicedo CH, *et al.* (18)F-FDG-PET/CT in the assessment of pulmonary solitary nodules: comparison of different analysis methods and risk variables in the prediction of malignancy. *Transl Lung Cancer Res* 2015; **4**: 228-35.

11. Yilmaz F, Tastekin G. Sensitivity of (18)F-FDG PET in evaluation of solitary pulmonary nodules. *International Journal of Clinical and Experimental Medicine* 2015; **8**: 45-51.

12. Basu S, Ranade R. 18-Fluoro-deoxyglucose-PET/Computed Tomography in Infection and Aseptic Inflammatory Disorders: Value to Patient Management. *PET Clin* 2015; **10**: 431-9.

13. Dong A, Dong H, Wang Y, Cheng C, Zuo C, *et al.* (18)F-FDG PET/CT in differentiating acute tuberculous from idiopathic pericarditis: preliminary study. *Clinical Nuclear Medicine* 2013; **38**: e160-5.

14. Hess S, Hansson SH, Pedersen KT, Basu S, Hoilund-Carlsen PF. FDG-PET/CT in Infectious and Inflammatory Diseases. *PET Clin* 2014; **9**: 497-519, vi-vii.

15. Vaidyanathan S, Patel CN, Scarsbrook AF, Chowdhury FU. FDG PET/CT in infection and inflammation--current and emerging clinical applications. *Clinical Radiology* 2015; **70**: 787-800.

16. Sathekge M, Maes A, Pottel H, Stoltz A, Van de Wiele C. Dual time-point FDG PET/CT for differentiating benign from malignant solitary pulmonary nodules in a TB endemic area. *South African Medical Journal* 2010; **100**: 4.

17. Li Y, Su M, Li F, Kuang A, Tian R. The value of (1)(8)F-FDG-PET/CT in the differential diagnosis of solitary pulmonary nodules in areas with a high incidence of tuberculosis. *Annals of Nuclear Medicine* 2011; **25**: 804-11.

18. Pennant M, Takwoingi Y, Pennant L, Davenport C, Fry-Smith A, *et al.* A systematic review of positron emission tomography (PET) and positron emission tomography/computed tomography (PET/CT) for the diagnosis of breast cancer recurrence. *Health Technology Assessment* 2010; **14**: 1-103.

19. Lindholm H, Brolin F, Jonsson C, Jacobsson H. The relation between the blood glucose level and the FDG uptake of tissues at normal PET examinations. *EJNMMI Res* 2013; **3**: 50.

20. Leeds IL, Magee MJ, Kurbatova EV, del Rio C, Blumberg HM, *et al.* Site of extrapulmonary tuberculosis is associated with HIV infection. *Clinical Infectious Diseases* 2012; **55**: 75-81.

21. Yang Z, Kong Y, Wilson F, Foxman B, Fowler AH, *et al.* Identification of risk factors for extrapulmonary tuberculosis. *Clinical Infectious Diseases* 2004; **38**: 199-205.

22. Makanjuola D, Murshid K, Sulaimani SA, Saleh MA. Mammographic features of breast tuberculosis: The skin bulge and sinus tract sign. *Clinical Radiology* 1996; **51**: 354-8.

23. Akbulut S, Sogutcu N, Yagmur Y. Coexistence of breast cancer and tuberculosis in axillary lymph nodes: a case report and literature review. *Breast Cancer Research and Treatment* 2011; **130**: 1037-42.

24. Alzaraa A, Dalal N. Coexistence of carcinoma and tuberculosis in one breast. *World Journal of Surgical Oncology* 2008; **6**: 29.

25. Baslaim MM, Al-Amoudi SA, Al-Ghamdi MA, Ashour AS, Al-Numani TS. Case report: Breast cancer associated with contralateral tuberculosis of axillary lymph nodes. *World Journal of Surgical Oncology* 2013; **11**: 43.

FIGURE LEGENDS

Figure 1

Axial ^{18}F-FDG-PET-CT image of an 86 year old woman with left breast cancer, demonstrating a rounded strongly ^{18}F-FDG avid mass and perilesional increased metabolic activity in the left breast consistent with the solid morphological characteristic. The left breast is significantly larger than the right. Moderate metabolic activity present adjacent to the calcified fibrotic right lung changes from old PTB.

Figure 2

Axial ^{18}F-FDG-PET-CT image of a 36 year old woman with left breast tuberculosis, showing left breast enlargement and hypermetabolic ^{18}F-FDG avid enlarged left axillary nodes consistent with axillary lymphadenopathy and breast oedema (ALBE).

Figure 3

Axial ^{18}F-FDG-PET-CT image of **a)** A 45 year old woman with left breast cancer and **b)** A 23 year old woman with right breast tuberculosis, extending into the underlying chest wall. The white arrows in both images demonstrate photopaenic areas which represent the cystic/necrotic centres, whilst the blue arrows show the ^{18}F-FDG avid solid components of the solid-cystic morphology.

Figure 4

Axial ^{18}F-FDG-PET-CT images of a) A 76 year old woman with right breast cancer and b) A 38 year old woman with right breast tuberculosis. The blue arrows on both images demonstrate the thickening in the axillary tail. The white arrow on image b) represents the metabolically active right axillary nodes.

Figure 5

Morphological characteristics of breast tuberculosis (*n*=5) and breast cancer (*n*=24) patients on ^{18}F-FDG-PET-CT. IDC=invasive ductal cancer; IDA=invasive ductal adenocarcinoma; DNE=differentiated neuroendocrine tumour.

TABLE 1

^{18}F-FDG-PET-CT Qualitative features for breast cancer and breast tuberculosis patients. ALBE" Axillary lymphadenopathy and breast oedema.

Qualitative feature	**BTB patients *(n=5)***	**BCA patients *(n=24)***
Patterns		
Mass	2	18
Oedema	2	1
Mass-oedema	0	4
Thickening	1	1
Morphology character		
Solid	0	17
Solid-cystic	2	6
ALBE	2	0
Thickening	1	1

TABLE 2

^{18}F-FDG-PET-CT Quantitative parameters for breast cancer and breast tuberculosis patients. SD: standard deviation.

Parameter	BTB (baseline)	BCA	*P* value
Mean±SD SUV_{max} breast lesion	3.14±1.55 (95% CI, 1.21-5.06)	12.59±8.11 (95% CI, 9.16-16.01)	0.016*
Mean±SD SUV_{max} axillary nodes	6.99±3.51 (95% CI, 2.62-11.36)	9.91±7.55 (95% CI, 6.64-13.17)	0.411
Mean±SD HU breast lesion	331.60±269.11 (95% CI, -2.54-665.74)	405.16±255.61 (95% CI, 297.23-513.10)	0.566
Mean±SD HU axillary nodes	192.4±285.94 (95% CI, -162.65-547.45)	393.60±230.53 (95% CI, 293.91-493.29)	0.101

FIGURE 1

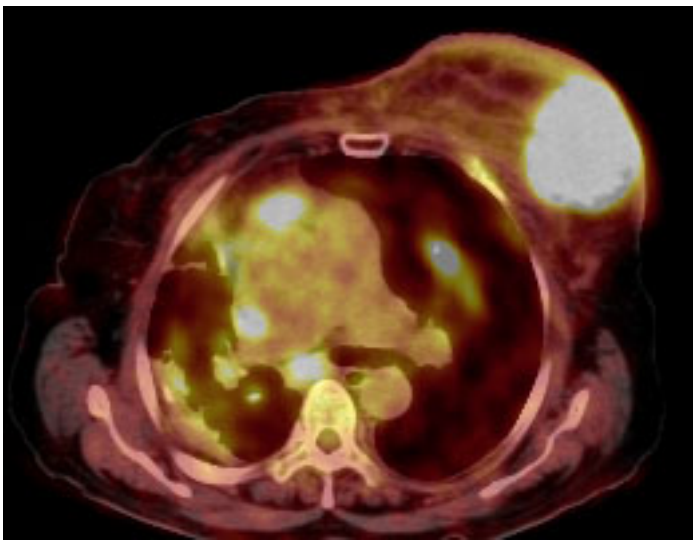

FIGURE 2

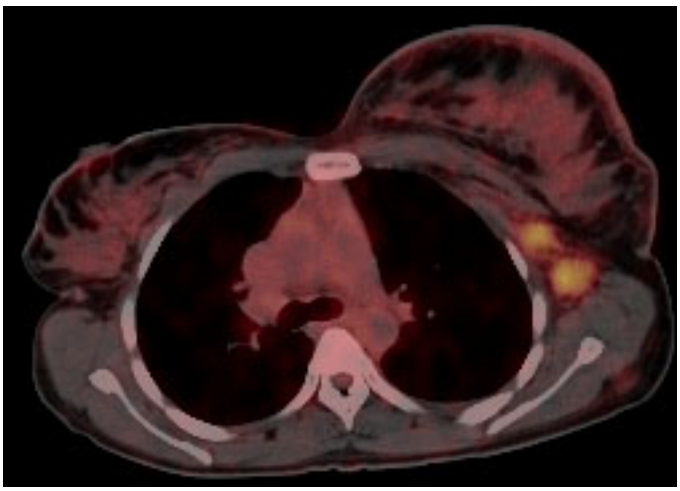

FIGURE 3

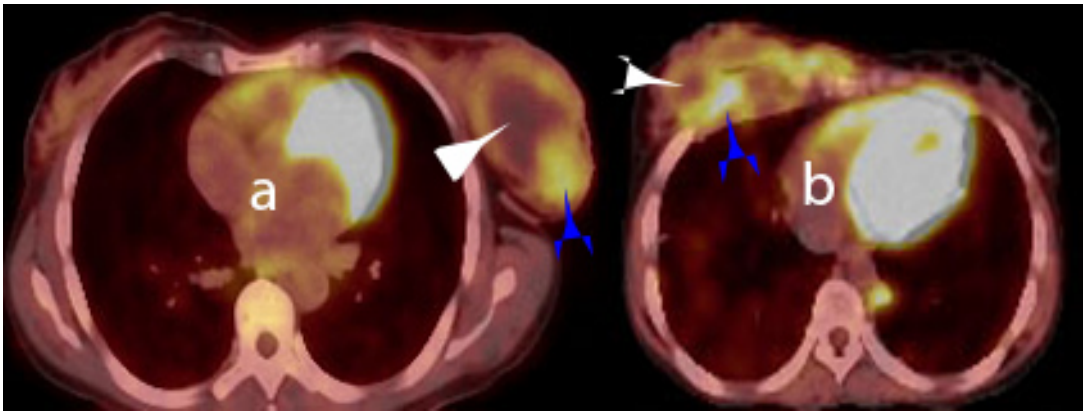

FIGURE 4

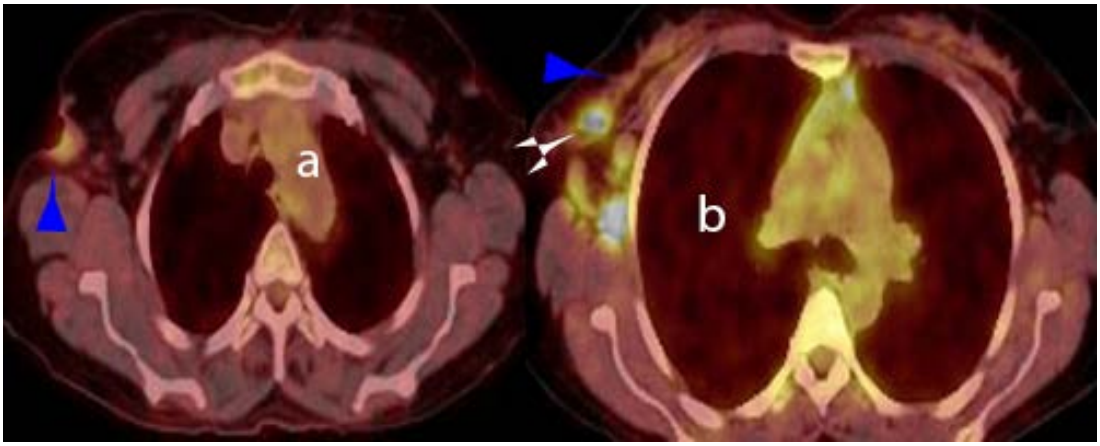

FIGURE 5

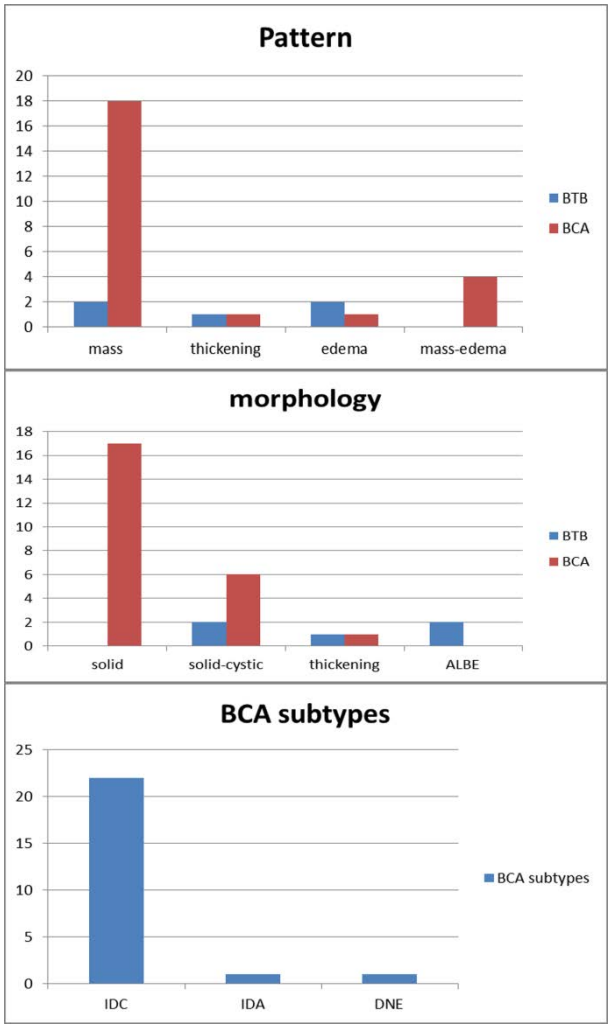
Pattern
20
18
16
14
12
10
8
6
4
2
0
mass
thickening
edema
mass-edema
BTB
BCA
morphology
18
16
14
12
10
8
6
4
2
0
solid
solid-cystic
thickening
ALBE
BTB
BCA
BCA subtypes
25
20
15
10
5
0
IDC
IDA
DNE
BCA subtypes

CHAPTER 6

Differentiation of breast tuberculosis and breast cancer using diffusion-weighted, T2W and dynamic contrast-enhanced MRI

TITLE

Differentiation of breast tuberculosis and breast cancer using diffusion-weighted, T2W and dynamic contrast-enhanced MRI.

AUTHORS

Dibuseng P Ramaema MBChB (UCT) FCRad (Diag) SA[1]
Richard J Hift MMed (Med) PhD FCP (SA) FRCP (UK)[2]

AFFILIATIONS

1. Division of Radiation Medicine (Radiology), Nelson R Mandela School of Medicine, University of KwaZulu-Natal, Durban, South Africa.
2. Division of Medicine, Nelson R Mandela School of Medicine, University of KwaZulu-Natal, Durban, South Africa.

CORRESPONDING AUTHOR

Dr Dibuseng P Ramaema
Discipline of Radiation Medicine (Diagnostic Radiology)
Nelson R Mandela School of Medicine
University of KwaZulu-Natal
Private Bag 7 Congella
Durban, South Africa
4013

Email: Ramaema@ukzn.ac.za
Tel: +27 31 260 4301

RUNNING TITLE

Differentiation of breast tuberculosis and breast cancer using DWI, T2W and DCE-MRI.

ABBREVIATIONS

ADC	apparent diffusion coefficient
BCA	breast cancer
BTB	breast tuberculosis
DCE-MRI	dynamic contrast-enhanced magnetic resonance imaging
DWI	diffusion-weighted imaging
MRI	multiparametric magnetic resonance imaging
ROI	region of interest
T1W	T1 weighted
T2SI	T2 weighted signal intensity.
T2W	T2 weighted

KEYWORDS

Breast cancer
Breast tuberculosis
Diffusion weighted imaging
Magnetic resonance imaging

WORD, FIGURE AND TABLE COUNT

Abstract	215
Words	2570
Tables	2
Figures	4

ABSTRACT

Aim

The aim of this study was to evaluate the value of diffusion weighted imaging (DWI), T2W and dynamic contrast enhanced magnetic resonance imaging (DCE-MRI) in differentiating breast cancer (BCA) from breast tuberculosis (BTB).

Methods

We retrospectively studied images of 18 patients with BCA who had undergone pre-operative MRI and 6 patients with pathologically proven BTB who underwent dynamic contrast enhanced (DCE-MRI) during the period January 2014 to January 2015.

Results

All patients were female, with the age range of BTB patients being 23-43 years, and the BCA patients being 31-74 years. BCA patients had a statistically significant lower mean apparent diffusion coefficient (ADC) value (1072.10±365.14) compared to the BTB group (1690.77±624.05, p=0.006). The mean T2 weighted signal intensity (T2SI) was lower for the BCA group (521.56±233.73) than the BTB group (787.74±196.04, p=0.020). An ADC mean cut-off value of 1558.79 yielded 66% sensitivity and 94% specificity whilst the T2SI cut-off value of 790.20 yielded 83% sensitivity and 83% specificity for differentiating between BTB and BCA. Our results suggest that these parameters were better able to distinguish the two groups when a morphological enhancement pattern was one of a mass lesion, rather than non-mass enhancement (NME).

Conclusions

Multi-parametric MRI incorporating the DWI, T2W and the DCE-MRI may be a useful tool to differentiate BCA from BTB.

INTRODUCTION

While breast cancer (BCA) is the most prevalent malignancy amongst South African women, accounting for 20.62% [1], the prevalence of breast tuberculosis (BTB) is by contrast very much lower, with reported ranges between 0.3% - 0.4% [2, 3]. BTB is a manifestation of extra-pulmonary tuberculosis (EPTB), a condition which has become considerably more commonly encountered as a consequence of the human immunodeficiency virus (HIV) pandemic [4, 5], yet studies and guidelines on the management of EPTB frequently do not mention the breast as a potential site for tuberculosis [6-8]. Given the infrequency with which BTB is diagnosed, little research has been performed on the disease. BTB and BCA may present clinically in a very similar fashion leading to potential misdiagnosis [9, 10]; given that an accurate diagnosis is essential if the patient is to receive correct and timely treatment, this may be problematic [8]

Conventional imaging with mammography and ultrasound has limited ability to differentiate between BTB and BCA [11]. It is therefore appropriate to investigate the use of newer and more complex imaging modalities in the differentiation of BCA and BTB. Studies that have used MRI to differentiate EPTB from malignant lesions are those which focused on other body parts such as the central nervous system (CNS) [12-14] and the musculoskeletal system [15, 16]. Peng *et al* used the diffusion weighted imaging (DWI) and magnetic resonance spectroscopy (MRS) to differentiate intracranial tuberculomas from high grade gliomas and found significant differences. The diagnostic accuracy was higher when using the minimum ADC value from the DWI than the maximum MRS ratios of Cho/Cr, Cho/NAA, and Cho/Cho [13]. MRI has also been utilised in pulmonary tuberculosis (PTB) to differentiate between tuberculoma nodules and the malignant ones [17-20]. Only one study was found in the literature which aimed to differentiate BTB from BCA with the use of magnetic resonance spectroscopy (MRS) in four BTB patients with no comparison group [21]. The authors suggested that the absence of choline peak and the presence of a strong lipid peak favoured BTB rather than BCA [21].

The studies that focused on using MRI in discriminating malignant breast lesions from benign breast disease do exist [22-27]. Rong-Feng Qu *et al* recently conducted a meta-analysis of the differential diagnosis of benign and malignant breast tumours. The authors

found that the ADC values of normal breast tissues were higher than those of benign tissues, and that the values of benign lesions were higher than of malignant tumours [23].

DWI measures the microscopic movement of water molecules in biological tissues, with the pathologic processes altering their mobility, the detection of these changes aid in lesion characterisation [28]. The apparent diffusion coefficient (ADC) maps from the DWI are automatically displayed on the MRI workstations. Tissues with high ADC values, due to increased diffusion, display a brighter signal, whereas those with lower ADC values appear darker, due to restricted diffusion [29]. Most malignant lesions display lower ADC values when compared to benign or inflammatory lesions [26].

Breast DCE-MRI involves administration of magnetic compatible intravenous (I.V) contrast agent in order to detect and characterise lesions [30]. Further advantage is the ability to evaluate the breast lesion enhancement parameters and kinetic curves [31]. It has been shown that the kinetic parameters have correlation with the immuno-histochemical surrogates of tumour neovascularity [32].

The T2 weighted (T2W) MRI uses the tissue transverse relaxation times to generate the signal [33]. The displayed T2 signal intensity (T2SI) is used in the characterisation of tissues and lesions [33]. Studies that used the T2SI in the discrimination of benign and malignant breast lesions mainly analysed the morphologic T2SI appearance rather than the quantitative values [34, 35]. Majority of breast cancers appear hypointense on T2W compared to most benign lesions which appear hyperintense [36].

The purpose of our study was to evaluate the use of the DWI parameter of ADC, the DCE-MRI enhancement morphologic characteristics and the T2W parameter of T2 signal intensity value to differentiate BCA from BTB.

PATIENTS AND METHODS

We retrospectively identified 25 patients with histologically proven BCA (including ductal carcinoma in situ (DCIS) and lobular carcinoma in situ (LCIS) who underwent DWI, T2W and DCE-MRI during the period January 2014 to December 2014. Seven patients did not have a full set of images on the picture archiving and communication system (PACS) and were excluded from the study, which resulted in the final total of 18 patients.

For the BTB group, we included six prospectively and consecutively identified patients with proven BTB who also underwent the DWI, T2W and DCE-MRI. While five had conclusive histology from either the breast or the axillary lymph nodes, one had inconclusive histology from breast and axilla, but had proven concurrent PTB, for which she was receiving anti-tuberculous therapy (ATT). Her clinical and radiological features were compatible with BTB, and both the breast and the axillary nodes responded satisfactorily to ATT. All BTB patients had undergone screening investigations at the referring breast clinic, including ultrasonography, with or without mammograms, depending on their age. Following the histological confirmation of BTB, the patients were invited for a baseline MRI scan within two weeks of confirmation of diagnosis. Scans were not performed within two weeks of a biopsy in order to avoid the presence of haematoma and/or inflammation confounding our results.

MRI image acquisition

MRI images were retrospectively analysed following retrieval from the hospital's picture archiving and communication system (PACS). MRI was performed on a 1.5T machine *(Siemens, Erlangen, Germany)* using a dedicated breast coil. The patients were scanned in the prone position. A power injection of 20 ml intravenous (I.V) *Magnevist® (Gadopentetate Dimeglumine, Bayer)* Standard 469 mg/mL (0.5 mmol/mL) at a dosage of 0.1 mmol/kg was administered to all the patients. The IV contrast rate was 3ml/sec followed by a 20 ml saline flush administered as a bolus. The T1 dynamic phase scan time was 6 minutes 41 seconds, during which 5 dynamic sequences were obtained in the axial position at various time points. The DWI images with the ADC map were also acquired during the same scan. The technical parameters are reported in Table 1.

MRI image analysis

All the images were read by one of the authors (DPR), a radiologist with more than ten years' experience of breast radiology. The following qualitative parameters were recorded: The breast cancer pathological subtype from the pathology records; The DCE-MRI parameters included: the enhancement pattern, the lesion morphology and the distribution pattern. The enhancement pattern was classified as either mass like enhancement (MASS) or non-mass enhancement (NME) [37]; the lesion morphology was classified as solid, solid-cystic, focal,

necrotic or axillary nodes; and the distribution pattern as unifocal, multifocal, multicentric, segmental or diffuse [37]. We further recorded the apparent diffusion coefficient (ADC) values ($x10^{-6}mm^2/sec$) derived from the DWI images; and T2SI value derived the T2W. For the quantitative parameters, the region of interest (ROI) was drawn on the axial images around the lesion circumference. All images were analysed on the dedicated *Syngo-via (Siemens, Erlangen, Germany)* reading platform.

Statistical analysis

Data were entered into an Excel spreadsheet (*Microsoft Excel 2013*. Redmond, WA) and analysed using the STATA software package *(StataCorp. 2015: Stata Statistical Software, Release 14*. College Station, TX). Differences in ADC value and T2SI between the two groups were assessed with a two-tailed unpaired t test. Differences in ADC value and T2SI with enhancement pattern matching were assessed using analysis of variance (ANOVA). The results were considered significant where $p < 0.05$.

Ethical clearance

Ethical clearance was obtained from the institution Biomedical Research Ethics Committee (BREC) (Reference number BF213/13).

RESULTS

Patient characteristics

All the patients were female. The ages of the BTB patients ranging from 23-43 years, for those with BCA 31-74 years. Three BTB patients, were HIV positive, one HIV negative and one not tested. The BCA subtypes included; 12 cases of invasive ductal cancer (IDC) (67.5%), three cases of DCIS (16.5%), of whom one had high grade DCIS, and one case each (5.5%) of invasive lobular cancer (ILC), invasive ductal adenocarcinoma (IDA), and lobular carcinoma in situ (LCIS).

Radiologic findings

The MRI morphological characteristics of the patients are summarised in (Fig. 1). We found significant differences in both ADC and mean T2SI values between the two groups. BCA patients had a significantly lower mean ADC value (1072.1±365.1) compared to those with BTB (1690.8±624.1), (p=0.006). The BCA group had a lower mean T2SI (521.6±233.7) compared with the BTB group (787.7±196.0) (p=0.020). These findings are summarised in (Table 2). In terms of predictive ability, we performed a preliminary ROC curve analysis and showed a 67% sensitivity and 94% specificity for an ADC cut-off value of 1558, with an AUC of 0.81 (95% CI 0.57-1.05) (Fig. 2). The corresponding values for a T2SI cut-off value of 790 were sensitivity 83% and specificity 83%, with an AUC of 0.77 (95% CI 0.54-0.96) (Fig. 3). Our total number of observations is however small, and a larger test sample will be necessary to play such a test on a firm footing. The representative images demonstrating data extraction for ADC values and T2SI measurements of the BCA and BTB patients are depicted in (Fig. 4).

Breast cancer versus breast tuberculosis with matched patterns

These differences persisted when the two groups were matched for the patterns of mass-like enhancement (MASS) and non-mass enhancement (NME) and compared with ANOVA. Significance was shown for both mean ADC value (p=0.040) and T2SI (p=0.015). Tukey post-hoc test comparisons identified a number of pairings for which the difference is significant as follows;

For ADC: BTB (mass-like enhancement) versus BCA (mass-like enhancement) (p=0.037) and BTB (non-mass enhancement) versus BCA (mass-like enhancement), (p=0.016); and ***for T2SI***: BTB (mass-like enhancement) versus BCA (mass-like enhancement) (p=0.021); BTB (non-mass enhancement) versus BCA (mass-like enhancement) (p=0.011); and BCA (mass-like enhancement) versus BCA (non-mass enhancement) (p=0.027).

DISCUSSION

This study evaluated the ability of the two quantitative MRI markers, the ADC value and the T2SI and the qualitative dynamic post contrast enhancement patterns to discriminate

between BCA and BTB. We have shown that BCA patients have significantly lower mean ADC and T2SI values compared to the BTB. This outcome is explicable in that malignant lesions have high cellularity with resulting restricted diffusion, yielding lower ADC values, a parameter derived from the DWI. This finding has been shown to be consistent across many studies [23-27, 38, 39], with few exceptions [12]. Woodhams *et al.* [24] found malignant breast tumours to have higher ADC values than the benign lesions furthermore the invasive ductal cancers (IDC) displayed lower values when compared to the non-invasive ductal cancer (NIDC). In contrast, Chatterjee *et al.* [12] found similar ADC values for brain tuberculomas and brain metastases. In our study the ADC value appeared to be the better discriminator between BCA and BTB. A preliminary ROC curve suggested an optimal ADC cut-off value at 1558.8 and a T2SI cut-off at 790.20 with a sensitivity and specificity of 66% and 94% respectively. The confidence intervals are however wide and further validation is required before these can be accepted as accurate figures for discrimination.

The studies that utilised the T2SI to discriminate the benign from the malignant breast lesions predominantly focused on the qualitative T2 signal morphologic appearance rather than the quantitative value as in our study [34, 35]. The data on the use of quantitative T2SI as a discriminator between benign and malignant breast lesions is scanty [40]. Other studies in which T2SI quantitative values were used in differentiating benign from malignant lesions involve other parts of the body and not the breast [41, 42]. Henz Concatto *et al.* [41] investigated pulmonary nodules with MRI using quantitative parameters ADC and T2SI in a granulomatous endemic area. They found both the mean T2SI ratio and the ADC to be significant in differentiating the benign from the malignant pulmonary nodules.

Given the limitations of post-hoc analysis, our study may suggest that discriminatory performance is not homogeneous across all morphological enhancement patterns exhibited by lesions; the discriminatory value of tests based on ADC and T2SI may be higher for some morphological appearances than for others. Our findings suggest that these tests are more discriminatory for a mass-pattern post-contrast appearance rather than when the pattern is of non-mass enhancement (NME). The Breast imaging-reporting and data system (BI-RADS)[37] morphologic descriptor and internal enhancement patterns of non-mass enhancement have been found to be unreliable in predicting the likelihood of malignancy by other studies [43, 44]. In a study of 258 MRI examinations of suspicious BI-RADS category 4 and 5 lesions, the differences in lesion size, margins and enhancement patterns were useful

in predicting malignancy for masses, but were not useful for non-mass enhancement [43]. We have shown that the T2SI was better able to detect a significant difference (p=0.027), than the ADC (p=0.276) when the BCA mass pattern was compared with the BCA NME pattern. Although there is data from many studies [22, 25, 27] that used the ADC value to differentiate benign from malignant breast lesions, they did not incorporate the enhancement pattern matching into the methodology. There is paucity of studies [38, 45] which evaluated the value of ADC in discriminating benign from malignant breast lesions with inclusion of the enhancement pattern. Partridge *et al* suggested that the ADC values may be more beneficial for mass lesions than for the NME [45], which is similar to our finding. Similarly, Imamura *et al* found the use of ADC values did not adequately improve DCE-MRI performance for the differential diagnosis of non-mass-like breast lesions however, the addition of the ADC value criteria to the DCE-MRI pattern analysis improved sensitivity, NPV and accuracy [38].

The BI-RADS lexicon defines the NME pattern as an area of enhancement that is distinct from the surrounding parenchyma. It does not represent a space-occupying mass (<5mm), and is typically interspersed with non-enhancing fatty or glandular breast tissue [37]. This leads us to believe that the ADC value of the tumour cells and the intervening normal breast tissues cannot be reliably measured when the tumour cells are scattered randomly in a NME pattern, rather than grouped discreetly into a mass. The differential diagnosis of the NME pattern includes both benign [46, 47] and malignant causes [39, 48, 49]. Therefore it is clear that the NME pattern on its own cannot be used to differentiate between benign and malignant conditions. However, when other imaging markers are taken into account, the use of NME patterns can be useful. The T2SI measures the transverse relaxation times of tissues in order to provide image contrast [33]: it is unclear why the T2SI does not appear to be influenced by the enhancing pattern.

The enhancement morphological pattern of completely solid mass and the distribution pattern of segmental, multifocal and multicentric were exclusive for BCA. On the other hand both the BCA and the BTB lesions displayed the unifocal and the diffuse distribution patterns. These qualitative features can be used as descriptors for separating the two conditions when the other imaging or pathology results are equivocal.

Based on our findings, we conclude that the combination of dynamic contrast enhanced MRI morphologic enhancement pattern, the quantitative T2SI and the quantitative DWI ADC values may provide some useful non-invasive information in distinguishing malignant from non-malignant illness (in this case, BTB) in patients with suspicious breast lesions. Development of accurate diagnostic algorithms will require the accumulation of a larger patient database for BTB in particular; more broadly however, continued investigation is appropriate in terms of the development of tests to distinguish malignant from benign disease more generally.

CONFLICT OF INTEREST:

The authors declare no conflict of interest.

REFERENCES

1. Cancer association of South Africa. Fact sheet on the top ten cancers per population group. South Africa: CANSA.: 2010.

2. Shushtari MHS, Alavi SM, Talaeizadeh A. Breast tuberculosis: Report of nine cases of extra pulmonary tuberculosis with breast mass. *Pakistan Journal of Medical Sciences* 2011; **27**: 582-5.

3. Ramaema DP, Buccimazza I, Hift RJ. Prevalence of breast tuberculosis: Retrospective analysis of 65 patients attending a tertiary hospital in Durban, South Africa. *South African Medical Journal* 2015; **105**: 866-9.

4. Akbulut S, Sogutcu N, Yagmur Y. Coexistence of breast cancer and tuberculosis in axillary lymph nodes: a case report and literature review. *Breast Cancer Research and Treatment* 2011; **130**: 1037-42.

5. Yang Z, Kong Y, Wilson F, Foxman B, Fowler AH, *et al.* Identification of risk factors for extrapulmonary tuberculosis. *Clinical Infectious Diseases* 2004; **38**: 199-205.

6. Aurum Institute. Managing TB in a new era of diagnosis. Johannesburg, South Africa: Aurum Institute; 2013; Available from: http://www.sahivsoc.org/upload/documents/Aurum%20Managing%20TB%20in%20an%20era%20of%20new%20diagnostics.pdf.

7. Leeds IL, Magee MJ, Kurbatova EV, del Rio C, Blumberg HM, *et al.* Site of extrapulmonary tuberculosis is associated with HIV infection. *Clinical Infectious Diseases* 2012; **55**: 75-81.

8. Department of Health (South Africa). National tuberculosis management guidelines 2014. Pretoria: Department of Health; 2014 [cited 2015 3 December 2015]; Available from: http://www.hst.org.za/sites/default/files/NTCP_Adult_TB-Guidelines-27.5.2014.pdf.

9. Gill M, Chabbra S, Sangwan M, Singh S, Praveen, *et al.* Tuberculous mastitis–A great mimicker. *Asian Pacific Journal of Tropical Disease* 2012; **2**: 348-51.

10. Kapan M, Toksöz Mt, BakIr ŞD, Sak ME, Evsen MS, *et al.* Tuberculosis of breast. *European Journal of General Medicine* 2010; **7**: 216-9.

11. Baharoon S. Tuberculosis of the breast. *Annals of Thoracic Medicine* 2008; **3**: 110-4.

12. Chatterjee S, Saini J, Kesavadas C, Arvinda HR, Jolappara M, *et al.* Differentiation of tubercular infection and metastasis presenting as ring enhancing lesion by diffusion and perfusion magnetic resonance imaging. *Journal of Neuroradiology Journal de Neuroradiologie* 2010; **37**: 167-71.

13. Peng J, Ouyang Y, Fang WD, Luo TY, Li YM, *et al.* Differentiation of intracranial tuberculomas and high grade gliomas using proton MR spectroscopy and diffusion MR imaging. *European Journal of Radiology* 2012; **81**: 4057-63.

14. Sankhe S, Baheti A, Ihare A, Mathur S, Dabhade P, *et al.* Perfusion magnetic resonance imaging characteristics of intracerebral tuberculomas and its role in differentiating tuberculomas from metastases. *Acta Radiologica* 2013; **54**: 307-12.

15. Lang N, Su MY, Yu HJ, Yuan H. Differentiation of tuberculosis and metastatic cancer in the spine using dynamic contrast-enhanced MRI. *European Spine Journal* 2015; **24**: 1729-37.

16. Pui MH, Mitha A, Rae WI, Corr P. Diffusion-weighted magnetic resonance imaging of spinal infection and malignancy. *Journal of Neuroimaging* 2005; **15**: 164-70.

17. Chung MH, Lee HG, Kwon SS, Park SH. MR imaging of solitary pulmonary lesion: emphasis on tuberculomas and comparison with tumors. *Journal of Magnetic Resonance Imaging* 2000; **11**: 629-37.

18. Donmez FY, Yekeler E, Saeidi V, Tunaci A, Tunaci M, *et al.* Dynamic contrast enhancement patterns of solitary pulmonary nodules on 3D gradient-recalled echo MRI. *AJR: American Journal of Roentgenology* 2007; **189**: 1380-6.

19. Peng G, Cai Z, Gao Y. [The value of CT and MRI in differentiating malignant nodule from tuberculoma]. *Zhonghua Jie He He Hu Xi Za Zhi Chinese Journal of Tuberculosis and Respiratory Diseases* 1995; **18**: 218-20, 55.

20. Schaefer JF, Vollmar J, Wiskirchen J, Erdtmann B, D VR, *et al.* Differentiation between malignant and benign solitary pulmonary nodules with proton density weighted and ECG-gated magnetic resonance imaging. *European Journal of Medical Research* 2006; **11**: 527-33.

21. Popli MB, Kumari A, Popli V. Proton magnetic resonance spectroscopy in breast tuberculosis. *European Journal of Radiology Extra* 2010; **74**: e59-e63.

22. Dorrius MD, Dijkstra H, Oudkerk M, Sijens PE. Effect of b value and pre-admission of contrast on diagnostic accuracy of 1.5-T breast DWI: a systematic review and meta-analysis. *European Radiology* 2014; **24**: 2835-47.

23. Qu RF, Guo DR, Chang ZX, Meng J, Sun Y, *et al.* Differential Diagnosis of Benign and Malignant Breast Tumors Using Apparent Diffusion Coefficient Value Measured Through Diffusion-Weighted Magnetic Resonance Imaging. *Journal of Computer Assisted Tomography* 2015; **39**: 513-22.

24. Woodhams R, Matsunaga K, Kan S, Hata H, Ozaki M, *et al.* ADC mapping of benign and malignant breast tumors. *Magnetic Resonance in Medical Sciences* 2005; **4**: 35-42.

25. Yamaguchi K, Schacht D, Nakazono T, Irie H, Abe H. Diffusion weighted images of metastatic as compared with nonmetastatic axillary lymph nodes in patients with newly diagnosed breast cancer. *Journal of Magnetic Resonance Imaging* 2015; **42**: 771-8.

26. Yili Z, Xiaoyan H, Hongwen D, Yun Z, Xin C, *et al.* The value of diffusion-weighted imaging in assessing the ADC changes of tissues adjacent to breast carcinoma. *BMC Cancer* 2009; **9**: 18.

27. Zhao J, Guan H, Li M, Gu H, Qin J, *et al.* Significance of the ADC ratio in the differential diagnosis of breast lesions. *Acta Radiologica* 2015; 0284185115590286.

28. Thomassin-Naggara I, De Bazelaire C, Chopier J, Bazot M, Marsault C, *et al.* Diffusion-weighted MR imaging of the breast: advantages and pitfalls. *European Journal of Radiology* 2013; **82**: 435-43.

29. Petralia G, Bonello L, Priolo F, Summers P, Bellomi M. Breast MR with special focus on DW-MRI and DCE-MRI. *Cancer Imaging* 2011; **11**: 76-90.

30. Tozaki M. Interpretation of breast MRI: correlation of kinetic and morphological parameters with pathological findings. *Magnetic Resonance in Medical Sciences* 2004; **3**: 189-97.

31. Hnilicova P, Jaunky T, Baranovicova E, Heckova E, Dobrota D. A new approach in DCE MRI data analysis for differentiating benign and malignant breast lesions. *Klin Onkol* 2015; **28**: 44-50.

32. Padhani AR. Dynamic contrast-enhanced MRI in clinical oncology: current status and future directions. *Journal of Magnetic Resonance Imaging* 2002; **16**: 407-22.

33. Nelson KL, Runge VM. Basic principles of MR contrast. *Topics in Magnetic Resonance Imaging* 1995; **7**: 124-36.

34. Huang YH, Chang YC, Huang CS, Wu TJ, Chen JH, *et al.* Computer-aided diagnosis of mass-like lesion in breast MRI: differential analysis of the 3-D morphology between benign and malignant tumors. *Computer Methods and Programs in Biomedicine* 2013; **112**: 508-17.

35. Tan SL, Rahmat K, Rozalli FI, Mohd-Shah MN, Aziz YF, *et al.* Differentiation between benign and malignant breast lesions using quantitative diffusion-weighted sequence on 3 T MRI. *Clinical Radiology* 2014; **69**: 63-71.

36. Malich A, Fischer DR, Wurdinger S, Boettcher J, Marx C, *et al.* Potential MRI interpretation model: differentiation of benign from malignant breast masses. *AJR: American Journal of Roentgenology* 2005; **185**: 964-70.

37. D'Orsi C, Sickles E, Mendelson E, Morris E. ACR BI-RADS Atlas: Breast Imaging Reporting and Data System. Reston, VA: American College of Radiology 2013.

38. Imamura T, Isomoto I, Sueyoshi E, Yano H, Uga T, *et al.* Diagnostic performance of ADC for Non-mass-like breast lesions on MR imaging. *Magnetic Resonance in Medical Sciences* 2010; **9**: 217-25.

39. Yabuuchi H, Matsuo Y, Kamitani T, Setoguchi T, Okafuji T, *et al.* Non-mass-like enhancement on contrast-enhanced breast MR imaging: lesion characterization using combination of dynamic contrast-enhanced and diffusion-weighted MR images. *European Journal of Radiology* 2010; **75**: e126-32.

40. Li C, Meng S, Yang X, Wang J, Hu J. The value of T2* in differentiating metastatic from benign axillary lymph nodes in patients with breast cancer--a preliminary in vivo study. *PloS One* 2014; **9**: e84038.

41. Henz Concatto N, Watte G, Marchiori E, Irion K, Felicetti JC, *et al.* Magnetic resonance imaging of pulmonary nodules: accuracy in a granulomatous disease-endemic region. *European Radiology* 2015;

42. Peng Y, Jiang Y, Antic T, Giger ML, Eggener SE, *et al.* Validation of quantitative analysis of multiparametric prostate MR images for prostate cancer detection and aggressiveness assessment: a cross-imager study. *Radiology* 2014; **271**: 461-71.

43. Gutierrez RL, DeMartini WB, Eby PR, Kurland BF, Peacock S, *et al.* BI-RADS lesion characteristics predict likelihood of malignancy in breast MRI for masses but not for nonmasslike enhancement. *AJR: American Journal of Roentgenology* 2009; **193**: 994-1000.

44. Newell D, Nie K, Chen JH, Hsu CC, Yu HJ, *et al.* Selection of diagnostic features on breast MRI to differentiate between malignant and benign lesions using computer-aided diagnosis: differences in lesions presenting as mass and non-mass-like enhancement. *European Radiology* 2010; **20**: 771-81.

45. Partridge SC, DeMartini WB, Kurland BF, Eby PR, White SW, *et al.* Quantitative diffusion-weighted imaging as an adjunct to conventional breast MRI for improved positive predictive value. *AJR: American Journal of Roentgenology* 2009; **193**: 1716-22.

46. Giess CS, Raza S, Birdwell RL. Patterns of nonmasslike enhancement at screening breast MR imaging of high-risk premenopausal women. *Radiographics* 2013; **33**: 1343-60.

47. Thomassin-Naggara I, Trop I, Chopier J, David J, Lalonde L, *et al.* Nonmasslike enhancement at breast MR imaging: the added value of mammography and US for lesion categorization. *Radiology* 2011; **261**: 69-79.

48. Bartella L, Liberman L, Morris EA, Dershaw DD. Nonpalpable mammographically occult invasive breast cancers detected by MRI. *AJR: American Journal of Roentgenology* 2006; **186**: 865-70.

49. Machida Y, Tozaki M, Shimauchi A, Yoshida T. Two Distinct Types of Linear Distribution in Nonmass Enhancement at Breast MR Imaging: Difference in Positive Predictive Value between Linear and Branching Patterns. *Radiology* 2015; **276**: 686-94.

ACKNOWLEDGEMENTS

This publication was made possible by grant number: R24TW008863 from the Office of the U.S. Global AIDS Coordinator and the U. S. Department of Health and Human Services, National Institutes of Health (NIH OAR and NIH ORWH). Its contents are solely the responsibility of the authors and do not necessarily represent the official views of the government. Further funding for operational costs was obtained from the UKZN strategic funds

FIGURE LEGENDS:

Figure 1

Morphological characteristics of the breast cancer and breast tuberculosis patients on DCE-MRI demonstrating; **a)** The enhancement pattern. **b)** The morphological pattern. **c)** The distribution pattern.

Figure 2

Preliminary ROC curve analysis of the ADC value of the breast lesions for differentiating cancer from tuberculosis.

Figure 3

Preliminary ROC curve analysis of the T2 signal intensity of the breast lesions for differentiating cancer from tuberculosis.

Figure 4

ADC value and the T2SI measurements.

(A-C): Axial DCE-MRI, DWI and T2W-MRI images of a 61 year old woman patient with left breast cancer. **a)** Axial T1post-contrast subtracted image demonstrate strongly enhancing mass with neovascularity in the left breast; **b)** Corresponding axial DWI-MRI ADC map image shows dark signal; and **c)** Axial T2 weighted image shows the tumour hypointensity.

(D-F): Axial DCE-MRI, DWI and T2W-MRI images of a 41 year old woman patient with left breast tuberculosis. **d)** Axial T1post-contrast subtracted image demonstrate a hypointense rim-enhancing mass in left breast; **e)** Corresponding axial DWI-MRI ADC map image demonstrate a bright signal; and **f)** Axial T2 weighted image shows a uniformly hyperintense signal.

TABLE 1

Local dynamic contrast-enhanced breast MRI protocol technical parameters. TSE=Turbo Spin Echo; GE=Gradient Echo; STIR=Short Tau Inversion Recovery.

MRI sequence	Acquisition plane	Repetition time (TR) (msec)	Echo Time (TE) (msec)	Inversion time (msec)	Matrix size	Field of view (FoV) (mm)	Slice thickness (mm)	Voxel size (mm)
Localizer	sagittal	7.6	3.53	-	384 x 512	400	6	2.1x1.6x6.0
T1 precontrast GE 3D	axial	8.6	4.70	-	299 x 384	320	1	1.0x0.7x1.0
T1 GE 3D dynamic sequences (1 pre& 5post contrast)	axial	9.1	4.76	-	299 x 284	340	1.5	1.1x0.9x1.5
T1 3D Dixon	axial	7.20	first 2.38; second 4.76	-	320 x 320	340	1.8	1.1x1.1x1.8
T1 fat sat	axial	680	10	-	224 x 320	320	4	1.4x1.0x4.0
T2 STIR	axial	5600	59.0	170	314 x 320	340	4	1.1x1.1x4.0
T2 TSE	axial	6100	111	-	384 x 512	320	4	1.7x1.3x4.0
DWI b values 0 & 800s/mm^2	axial	9200	86	180	150 x 192	380	4	2.0x2.0x4.0

TABLE 2

Comparison of the DWI and T2W-MRI imaging quantitative parameters for the breast tuberculosis and breast cancer patients.

Parameter	**BTB (Mean ± SD) (*n* = 6)**	**BCA (Mean ± SD) (*n* = 18)**	***P* value**
ADC ($x10^{-6}mm^2/sec$)	1690.8±624.1 (95% CI 1035.9 – 2345.7)	1072.1±365.1 (95% CI 890.5 – 1253.7)	0.006
T2 signal intensity value (T2SI)	787.7±196.0 (95% CI 582.0 – 993.5)	521.6±233.7) (95% CI 405.33 – 637.8)	0.020

FIGURE 1

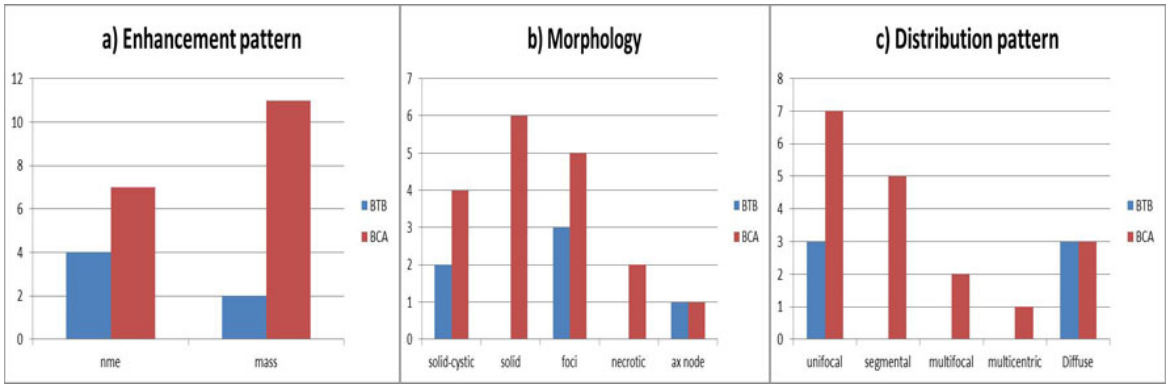
a) Enhancement pattern
12
10
8
6
4
2
0
nme
mass
BTB
BCA
b) Morphology
7
6
5
4
3
2
1
0
solid-cystic
solid
foci
necrotic
ax node
BTB
BCA
c) Distribution pattern
8
7
6
5
4
3
2
1
0
unifocal
segmental
multifocal
multicentric
Diffuse
BTB
BCA

FIGURE 2

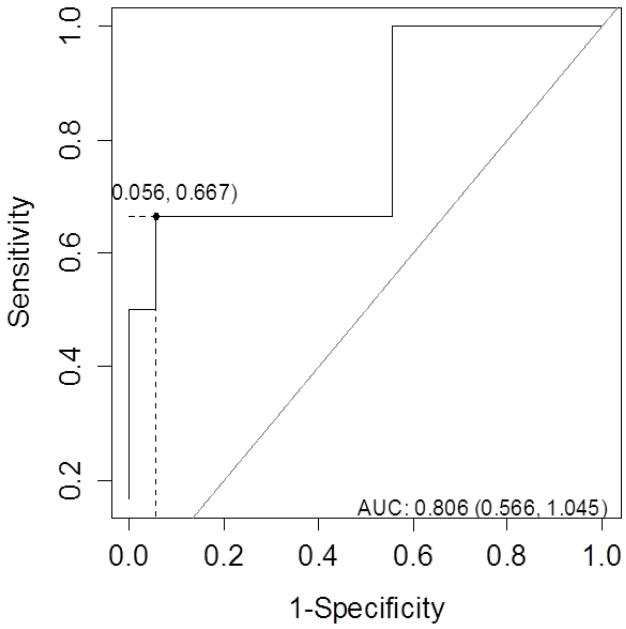
Sensitivity
1-Specificity
0.0
0.2
0.4
0.6
0.8
1.0
0.056, 0.667)
AUC: 0.806 (0.566, 1.045)

FIGURE 3

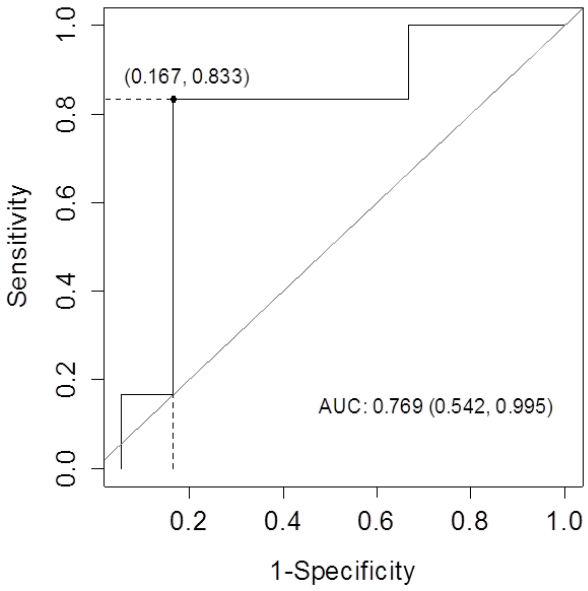
(0.167, 0.833)
AUC: 0.769 (0.542, 0.995)
Sensitivity
1-Specificity
0.0
0.2
0.4
0.6
0.8
1.0

FIGURE 4

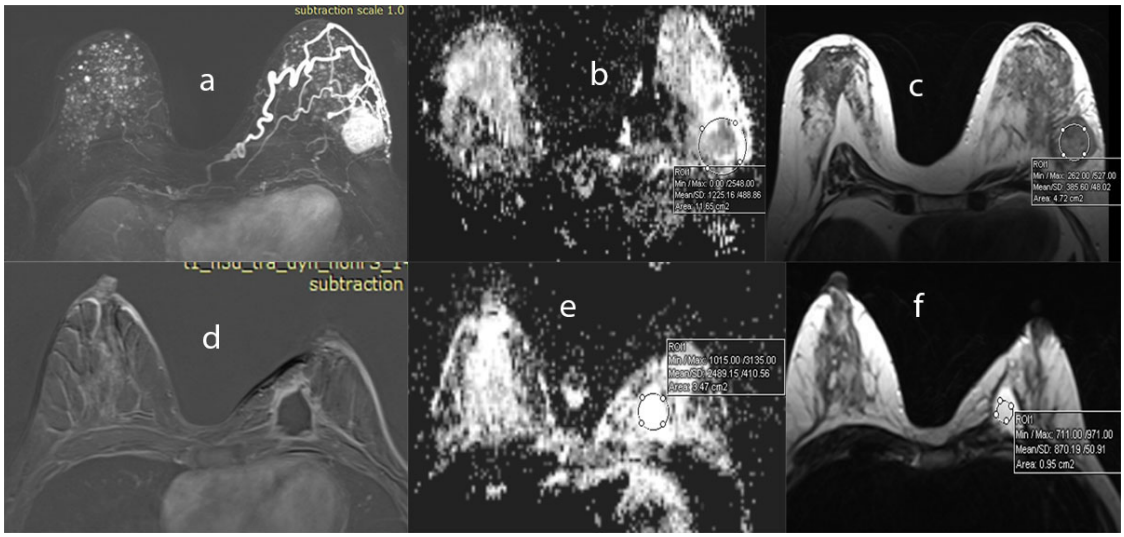

CHAPTER 7

Comparative study of breast lesion size evaluation using DCE-MRI at 1.5T and ^{18}F-FDG- PET-CT in seven patients with breast tuberculosis or breast cancer

TITLE

Comparative study of breast lesion size evaluation using DCE-MRI at 1.5T and ^{18}F-FDG- PET-CT in seven patients with breast tuberculosis or breast cancer.

AUTHORS

Dibuseng P Ramaema MBChB (UCT) FCRad (Diag) SA[1]
Richard J Hift MMed (Med) PhD FCP (SA) FRCP (UK)[2]

AFFILIATIONS

1. Division of Radiation Medicine (Radiology), Nelson R Mandela School of Medicine, University of KwaZulu-Natal, Durban, South Africa.
2. Division of Medicine, Nelson R Mandela School of Medicine, University of KwaZulu-Natal, Durban, South Africa.

CORRESPONDING AUTHOR

Dr Dibuseng P Ramaema
Discipline of Radiation Medicine (Diagnostic Radiology)
Nelson R Mandela School of Medicine
University of KwaZulu-Natal
Private Bag 7 Congella
Durban, South Africa
4013

Email: Ramaema@ukzn.ac.za
Tel: +27 31 260 4301

RUNNING TITLE

Comparative study of breast lesion size evaluation using DCE-MRI at 1.5T and ^{18}F-FDG PET-CT.

KEYWORDS

Breast cancer

Breast tuberculosis

^{18}F-FDG-PET-CT

MRI

ABBREVIATIONS

^{18}F-FDG	(Fluorine-18)-fluoro-2-deoxy-D-glucose
^{18}F-FDG-PET-CT	(Fluorine-18)-fluoro-2-deoxy-D-glucose (^{18}F-FDG) positron emission tomography (PET) integrated with computed tomography (CT)
CT	computed tomography
DCE-MRI	dynamic contrast-enhanced magnetic resonance imaging
FDG	(Fluorine-18)-fluoro-2-deoxy-D-glucose
MRI	multiparametric magnetic resonance imaging
PET	positron emission tomography
SUV_{max}	maximum standardised uptake value

WORD, FIGURE AND TABLE COUNT

Abstract	220
Words	2403
Tables	2
Figures	3

ABSTRACT

Aim

The aim of the study was to compare the values of breast lesion volume and maximum diameter as measured by dynamic contrast-enhanced breast MRI (DCE-MRI) and prone ^{18}F-FDG-PET-CT imaging.

Methods

7 patients who underwent both ^{18}F-FDG-PET-CT and DCE-MRI with an interval not exceeding one month were studied. For both modalities, True-D software was used and the 3-D volume of interest (VOI) was drawn around the ^{18}F-FDG avid areas on PET-CT. We recorded the breast lesion volume and maximum diameter (D_{max}).

Results

A total of 9 lesions from the 7 patients were found. The mean D_{max} was 8.1 ± 3.6 cm and 9.7 ± 5.1 cm when using DCE-MRI and ^{18}F-FDG-PET-CT respectively. The mean lesion volume was 281.0 ± 406.8 cm^3 for DCE-MRI and 319.4 ± 421.8 cm^3 for ^{18}F-FDG-PET-CT. For both lesion volume and D_{max}, there was a strong correlation between modalities with coefficients of determination ($R^{2)}$ of 0.986 and 0.931 respectively (p <0.0001). However ^{18}F-FDG-PET-CT returned significantly higher values for both the D_{max} and the lesion volume, (p=0.032) and (p=0.05) respectively.

Conclusion

Breast lesion volume and maximum diameter measured by ^{18}F-FDG-PET-CT and DCE-MRI show a strong correlation between the two modalities. Both can be used in the treatment monitoring of breast lesions. There is however a difference in the absolute measurements, and they should not be used interchangeably.

INTRODUCTION

The management of breast cancer is being constantly updated in line with advances in imaging technologies which improve the correct staging [1]. The basic radiological tests for breast cancer staging are mammography and ultrasound [2, 3], however the move towards individual targeted therapy has contributed to the increasing use of both ^{18}F-FDG-PET-CT and breast DCE-MRI in management algorithms [4, 5]. In view of the continually evolving diagnostic and staging methods, the international guidelines for breast cancer management are regularly revised [2]. Since 2008, the newer imaging modality of hybrid PET-MRI has been studied for use in breast cancer management [6]; using either sequential image acquisition as in PET-CT, or simultaneous image acquisition in an integrated device [7].

Indications for the use of DCE-MRI in breast cancer management include both screening and management of manifest disease [3, 8]. MRI screening has been recommended for women with a life time breast cancer risk of more than 20%; and for those who have had previous breast augmentation in whom mammographic screening is difficult [2, 8]. MRI indications in symptomatic disease include: the preoperative staging of newly diagnosed breast cancer; further evaluation of equivocal clinical and radiological findings; for baseline and monitoring of neoadjuvant chemotherapy (NAC); for the investigation of unknown primary; and for the evaluation of local tumour recurrence when conventional imaging is equivocal [1, 2, 8, 9].

Although there are other PET tracers in use or under study [7, 10], ^{18}F-FDG is the most commonly used and has an established role in oncology [11]. ^{18}F-FDG-PET indications in breast oncology include: baseline staging in locally advanced breast cancer in which the tumour is large but operable (stages 11B and 111A) or there is skin, chest wall and/or high burden nodal disease (stages 111B and 111C) [5]; the suspicion of metastatic disease when conventional imaging is equivocal [5, 11] and the follow-up of metastases or recurrence when conventional imaging is equivocal; [11]. ^{18}F-FDG-PET has additionally been recommended for monitoring response to NAC although it has been mentioned as optional by the National Comprehensive Cancer Network Clinical Practice Guidelines in Oncology (NCCN Guidelines®) version 3, 2014 [12].

^{18}F-FDG-PET-CT hybrid imaging in breast cancer has the advantage of providing information on the morphological CT features and the metabolic nature of the primary tumour, as well as evaluating for distant disease [13]. In contrast to dedicated breast MRI, it has the further

advantage of imaging the whole body and not just the immediate breast region except in facilities where whole body MRI is available and routinely applied in the staging pathway [10]. Breast DCE-MRI has the advantage of providing good soft tissue contrast and definition of morphological features of the primary tumour [2, 14]. Furthermore MRI does not use ionising radiation hence it is a safer option in paediatric and pregnant patients than PET-CT [15].

Studies comparing the diagnostic performance of PET-CT and breast DCE-MRI suggest that MRI is more sensitive in the evaluation of tumour size and breast lesion detection [16-21]. However, equivalent diagnostic performance between MRI and PET-CT for the evaluation of the axillary lymph nodes was found in some studies [20, 22].

The correct measurement and documentation of the local tumour size with various imaging modalities in patients with breast cancer is critical because it influences treatment choices and decisions [9]. In this study, our aim was to evaluate whether there is correlation between the parameters, namely: the breast lesion volume and the maximum diameter measured on ^{18}F-FDG-PET-CT and dedicated breast DCE-MRI.

PATIENTS AND METHODS

Nine lesions from seven patients who underwent ^{18}F-FDG-PET-CT between January 2014 and July 2015 were analysed. All patients had undergone both prone ^{18}F-FDG-PET-CT and prone breast DCE-MRI within two weeks of each other. Ethical clearance was obtained from our institution's Biomedical Research Ethics Committee (Ref BF213/13).

The five breast tuberculosis patients had undergone screening investigations at the referring breast clinic, including ultrasonography with or without mammograms depending on the patient's age. Following the histological confirmation of BTB, the patients were invited for a baseline ^{18}F-FDG-PET-CT and DCE-MRI scans. The other two patients' records were retrieved from the database between January 2014 and December 2014 and this was done by identifying those patients who had had both modalities performed within two weeks of each other. A total of nine lesions in seven patients were studied.

^{18}F-FDG PET-CT image acquisition

All patients fasted for at least 6 hours prior to the intravenous administration of ^{18}F-FDG in a dose of 4 MBq/kg body weight (range 192-261MBq, 5.17-7.05mCi). Glucose values were obtained before injection. All the patients had an acceptable glucose level not exceeding 11.1mmol/L in order to minimise the competition of high plasma glucose with ^{18}F-FDG, which can result in the diversion of ^{18}F-FDG into muscle [23].

A whole body PET-CT scan with 16 slice Biograph (Siemens, Erlangen, Germany) was performed between 60 and 90 minutes after the injection. The PET images were acquired for a maximum of 8 prone bed positions at 3 minutes per field of view (FoV) in the cranio-caudal direction commencing at the skull vertex and terminating at the mid-femur point. The images were acquired at a zoom of 1 and a matrix of 168 x 168. An iterative reconstruction using 2 iterations and 24 subsets was used for the post-acquisition image processing.

A diagnostic non-contrasted CT scan was acquired in the cranio-caudal direction using the following parameters: 4D CARE dose for 100mAs, 120 KVp and 5 mm slice thickness, pitch of 0.75 for a scan time of 25s. A CT Image multiplanar reconstruction was obtained using a kernel of B31f, abdomen window, slice thickness of 4 mm and a recon increment of 2 mm.

Quantitative ^{18}F-FDG-PET-CT and DCE-MRI image analysis

All the images were read by one experienced nuclear medicine physician with ten years of experience and one of the authors, an experienced radiologist with 20 years of experience (DPR). Agreement was reached by consensus.

True-D software with automatic multi-planar orthogonal display of the volume of interest (VOI) in axial, sagittal and coronal planes, was used to analyse the fused ^{18}F-FDG-PET-CT images and the DCE-MRI images. 3-D VOI were drawn around circumference of ^{18}F-FDG avid areas on PET. A visual correlation of the same anatomical lesion on subtracted dynamic post contrast T1 breast DCE-MRI images was performed. The 3-D VOI was drawn around the circumference of the enhancing lesion (Fig. 1). For MRI, the lesion anatomical borders were used to determine diameter and volume. For FDG-PET-CT, the volume of interest (VOI's) were mapped visually to cover borders of the lesion, and isocontours of 20% SUV_{max} were generated.

The following parameters were recorded; a) lesion volume, b) lesion maximum diameter (D_{max}).

MRI image acquisition

MRI was performed on a 1.5T machine (Siemens, Erlangen, Germany) using the dedicated breast coil. Scans were done in the prone position. MRI was performed on a 1.5T machine *(Siemens, Erlangen, Germany)* using a dedicated breast coil. The patients were scanned in the prone position. Power injection of 20 ml intravenous (I.V) *Magnevist® (Gadopentetate Dimeglumine, Bayer)* Standard 469 mg/mL (0.5 mmol/mL) at a dosage of 0.1 mmol/kg was administered to all the patients. The IV contrast rate was 3 ml/sec followed by a 20 ml saline flush administered as a bolus. The T1 dynamic phase scan time was 6 minutes 41 seconds, during which 5 dynamic sequences were obtained in the axial position at various time points. The technical parameters are shown in Table 1.

Statistical analysis

Data were entered into a Microsoft Excel spreadsheet (Microsoft Excel 2013, Microsoft Corporation, Redmond, WA) and analysed using MedCalc for Windows, version 15.11.4 (MedCalc Software, Ostend, Belgium). The correlation of lesion volume (VL) and lesion maximum diameter (D_{max}) on the two modalities of ^{18}F-FDG-PET-CT and DCE-MRI was assessed using linear regression. The paired t test was used to compare differences in means between the two tests. A p value <0.05 was considered significant.

RESULTS

All the patients were female with an age range of 23 to 48 years. There were two malignant lesions and seven TB lesions. Patient ID number 2 on table 2 had three lesions. Amongst the five BTB patients, three were HIV positive, one negative and one unknown.

The results are summarised in Table 2. The measured maximum diameter of the lesions was significantly larger on ^{18}F-FDG-PET-CT than on DCE-MRI (p=0.03). Similarly, the measured lesion volume was significantly larger on ^{18}F-FDG-PET-CT than on DCE-MRI

(p=0.05). In both cases the measured dimensions correlated highly between the two modalities (R^2 for D_{max}=0.931, R^2 for volume=0.986, p<0.0001).

DISCUSSION

The use of ^{18}F-FDG-PET-CT and DCE-MRI in the staging of breast cancer influences treatment decisions [1]. The breast lesion measurements obtained from either modality play a role in the initial staging and in the follow-up scans [2]. We aimed to determine the correlation in measured size of the breast lesion between the two modalities.

We found that the measured volume (LV) and the maximum diameter (D_{max}) for the breast lesions using ^{18}F-FDG-PET-CT and DCE-MRI are highly correlated, though the absolute value differs significantly. This suggests that either of the two modalities may be used in the response evaluation, provided a single modality is used consistently. Our findings are supported by data from studies which confirm that there is good correlation between breast DCE-MRI and PET-CT in the evaluation of the primary breast tumour size [24-26]. Pace *et al*, (2014) found a good correlation between PET-CT and PET-MRI hybrid systems for the lesion detection, SUV values and the metabolic tumour volume (MTV) of the primary breast tumour, even though the absolute values differed slightly between the two modalities [26].

Data from studies examining the diagnostic accuracy of breast DCE-MRI, hybrid PET-MRI and ^{18}F-FDG-PET-CT have shown that DCE-MRI is more sensitive but less specific than the ^{18}F-FDG-PET-CT for the evaluation of the primary tumour size and the detection of additional ipsilateral or contralateral cancers [16-21]. Studies using the same parameters for both modalities utilising the newer modality of hybrid PET-MRI rather than localised breast DCE-MRI to compare with PET-CT have yielded variable outcomes [16, 25-28]. Grueneisen et al (2015) found that PET-MRI was no better than MRI alone for local tumour staging. Furthermore, both PET-MRI and MRI alone delineated local tumour extent more accurately than PET-CT [27]. Botsikas et al (2015) showed that MRI alone was more sensitive for the primary tumour detection than the PET-MRI, but they found both modalities to be highly specific for nodal metastases detection [22].

A direct correlation of measured sizes has not been possible in other comparative studies of PET-CT and MRI where different parameters were used for each modality [17-20, 24, 29-

35], since the studies focused mainly on metabolic parameters for the ^{18}F-FDG-PET-CT, which are not available for DCE-MRI, and similarly for MRI-specific parameters. Magometschnigg *et al* (2015) compared the diagnostic accuracy of the two modalities using the SUV_{max} for ^{18}F-FDG PET-CT and the Breast Imaging Reporting and Data System (BI-RADS®)lexicon morphology patterns and enhancement kinetics [2] for DCE-MRI. They found that ^{18}F-FDG-PET-CT and breast DCE-MRI at 3T demonstrated equal diagnostic accuracies in breast cancer diagnosis, however for lesions <10mm, DCE-MRI was more sensitive but less specific than ^{18}F-FDG-PET-CT.

In our study, we used the same parameters for both modalities. Our results showed that the mean D_{max} and the mean LV were significantly higher when measured on the PET-CT images compared with the DCE-MRI. A similar observation was found by Pace et al (2015), in which the breast metabolic tumour volume (MTV) was 6% lower on the hybrid PET-MRI compared to PET-CT, even though the differences were not statistically significant and there was excellent correlation between the measurements [26]. They suggested that a systematic bias was responsible for the differences, but noted that the differences fell within 1.96 standard deviations of the mean and can be considered clinically unimportant. We propose a number of possible explanations for this. Firstly, although both modalities were performed in the prone position, the breasts hang freely in the dedicated breast coil during an MRI scan but tend to be compressed against the table on the prone PET scanning, which may result in some distortion of tissue and apparent magnification of the resultant image. Secondly, PET-CT suffers from a partial volume effect (PVE) which may result in overestimation or underestimation of the lesion size [36]. This appears unlikely as an explanation in our data since the deviation was unidirectional. Thirdly, intravenous contrast was used for DCE-MRI but not for PET-CT, which may contribute to the better delineation of the lesion on the MRI than on the PET.

The correct measurement of breast lesions with either or both PET-CT and MRI is the fundamental part of staging and monitoring of treatment in patients with breast cancer [8]. The tumour maximum diameter is one of the criteria used in the response evaluation criteria in solid tumours (RECIST) version 1.1, which is not only important in clinical practice but also in clinical trials evaluation [37]. Studies comparing PET-CT and MRI in breast cancer patients receiving neoadjuvant chemotherapy (NAC) also have variable findings [17, 21, 30, 33, 35, 38]. Some studies showed good correlation between the two modalities for response

evaluation [30, 33, 35], whilst others showed MRI to be better than PET-CT [17], others showed PET-CT to have better prediction of complete pathological response than MRI in luminal B type breast cancer [38].

While PET-CT is unlikely to replace breast MRI in clinical practice, it may prove a useful adjunct to it [18, 20]. It may also have a place as a staging modality in patients who have contraindications to MRI such as those who are claustrophobic and those with an implanted pacemaker [39, 40].

Our study has several limitations. Although our sample was small, we were able to show statistical significance; furthermore we note that the larger measure for PET-CT was present in every case, suggesting that the observation is real. Secondly, the images were read by consensus, and intra-operator and inter-operator differences were not evaluated.

In conclusion, we have shown that there is a strong correlation in the lesion measurement between ^{18}F-FDG-PET-CT and DCE-MRI for both the maximum diameter and the lesion volume using the 3-D measuring technique. It would therefore appear that one modality is as effective as the other in determining the size of a breast lesion. However, given that there was an absolute difference in size between the two modalities, it is important that measurements using a single modality are compared; it is inappropriate to compare measurements across modalities.

CONFLICT OF INTEREST

The authors declare no conflict of interest.

ACKNOWLEDGEMENTS

This publication was made possible by grant number: R24TW008863 from the Office of the U.S. Global AIDS Coordinator and the U. S. Department of Health and Human Services, National Institutes of Health (NIH OAR and NIH ORWH). Its contents are solely the responsibility of the authors and do not necessarily represent the official views of the government. Further funding for operational costs was obtained from the UKZN strategic funds

REFERENCES

1. Gradishar WJ, Anderson BO, Balassanian R, Blair SL, Burstein HJ, *et al.* Breast Cancer Version 2. 2015. *Journal of the National Comprehensive Cancer Network* 2015; **13**: 448-75.

2. D'Orsi C, Sickles E, Mendelson E, Morris E. ACR BI-RADS Atlas: Breast Imaging Reporting and Data System. Reston, VA: American College of Radiology 2013.

3. NHS Breast Screening Programme. Guidelines on organising the surveillance of women at higher risk of developing breast cancer in an NHS Breast Screening Programme. England2013; Available from: https://www.gov.uk/government/uploads/system/uploads/attachment_data/file/439634/nhsbsp73.pdf.

4. Sathekge M, Warwick JM, Doruyter A, Vorster M. Appropriate indications for positron emission tomography/computed tomography: College of Nuclear Physicians of the Colleges of Medicine of South Africa. *South African Medical Journal* 2015; **105**: 894-6.

5. Senkus E, Kyriakides S, Ohno S, Penault-Llorca F, Poortmans P, *et al.* Primary breast cancer: ESMO Clinical Practice Guidelines for diagnosis, treatment and follow-up. *Annals of Oncology* 2015; **26 Suppl 5**: v8-30.

6. Catana C, Procissi D, Wu Y, Judenhofer MS, Qi J, *et al.* Simultaneous in vivo positron emission tomography and magnetic resonance imaging. *Proceedings of the National Academy of Sciences of the United States of America* 2008; **105**: 3705-10.

7. Tabouret-Viaud C, Botsikas D, Delattre BM, Mainta I, Amzalag G, *et al.* PET/MR in Breast Cancer. *Seminars in Nuclear Medicine* 2015; **45**: 304-21.

8. Sardanelli F, Boetes C, Borisch B, Decker T, Federico M, *et al.* Magnetic resonance imaging of the breast: recommendations from the EUSOMA working group. *European Journal of Cancer* 2010; **46**: 1296-316.

9. Mann RM, Kuhl CK, Kinkel K, Boetes C. Breast MRI: guidelines from the European Society of Breast Imaging. *European Radiology* 2008; **18**: 1307-18.

10. Rosenkrantz AB, Friedman K, Chandarana H, Melsaether A, Moy L, *et al.* Current status of hybrid PET/MRI in oncologic imaging. *AJR: American Journal of Roentgenology* 2015; 1-11.

11. Society of Nuclear Medicine. 18F-fluorodeoxyglucose (FDG) PET and PET/CT Practice Guidelines in Oncology. 2013; Available from: http://www.snm.org/docs/PET_PROS/OncologyPracticeGuidelineSummary.pdf.

12. Gradishar WJ, Anderson BO, Blair SL, Burstein HJ, Cyr A, *et al.* Breast cancer version 3. 2014. *Journal of the National Comprehensive Cancer Network* 2014; **12**: 542-90.

13. Groheux D, Espie M, Giacchetti S, Hindie E. Performance of FDG PET/CT in the clinical management of breast cancer. *Radiology* 2013; **266**: 388-405.

14. Kuhl CK. MRI of breast tumors. *European Radiology* 2000; **10**: 46-58.

15. Nievelstein RA, Littooij AS. Whole-body MRI in paediatric oncology. *Radiologia Medica* 2015;

16. Catalano OA, Nicolai E, Rosen BR, Luongo A, Catalano M, *et al.* Comparison of CE-FDG-PET/CT with CE-FDG-PET/MR in the evaluation of osseous metastases in breast cancer patients. *British Journal of Cancer* 2015; **112**: 1452-60.

17. Choi JH, Lim HI, Lee SK, Kim WW, Kim SM, *et al.* The role of PET CT to evaluate the response to neoadjuvant chemotherapy in advanced breast cancer: comparison with ultrasonography and magnetic resonance imaging. *Journal of Surgical Oncology* 2010; **102**: 392-7.

18. Choi YJ, Shin YD, Kang YH, Lee MS, Lee MK, *et al.* The effects of preoperative (18)F-FDG PET/CT in breast cancer patients in comparison to the conventional imaging study. *Journal of Breast Cancer* 2012; **15**: 441-8.

19. Chou CP, Peng NJ, Chang TH, Yang TL, Hu C, *et al.* Clinical roles of breast 3T MRI, FDG PET/CT, and breast ultrasound for asymptomatic women with an

abnormal screening mammogram. *Journal of the Chinese Medical Association* 2015; **78**: 719-25.

20. Jung NY, Kim SH, Kim SH, Seo YY, Oh JK, *et al.* Effectiveness of breast MRI and (18)F-FDG PET/CT for the peoperative staging of invasive lobular carcinoma versus ductal carcinoma. *Journal of Breast Cancer* 2015; **18**: 63-72.

21. You S, Kang DK, Jung YS, An YS, Jeon GS, *et al.* Evaluation of lymph node status after neoadjuvant chemotherapy in breast cancer patients: comparison of diagnostic performance of ultrasound, MRI and (1)(8)F-FDG PET/CT. *British Journal of Radiology* 2015; **88**: 20150143.

22. Botsikas D, Kalovidouri A, Becker M, Copercini M, Djema DA, *et al.* Clinical utility of 18F-FDG-PET/MR for preoperative breast cancer staging. *European Radiology* 2015;

23. Lindholm H, Brolin F, Jonsson C, Jacobsson H. The relation between the blood glucose level and the FDG uptake of tissues at normal PET examinations. *EJNMMI Res* 2013; **3**: 50.

24. Magometschnigg HF, Baltzer PA, Fueger B, Helbich TH, Karanikas G, *et al.* Diagnostic accuracy of (18)F-FDG PET/CT compared with that of contrast-enhanced MRI of the breast at 3 T. *European Journal of Nuclear Medicine and Molecular Imaging* 2015; **42**: 1656-65.

25. Moon EH, Lim ST, Han YH, Jeong YJ, Kang YH, *et al.* The usefulness of F-18 FDG PET/CT-mammography for preoperative staging of breast cancer: comparison with conventional PET/CT and MR-mammography. *Radiol Oncol* 2013; **47**: 390-7.

26. Pace L, Nicolai E, Luongo A, Aiello M, Catalano OA, *et al.* Comparison of whole-body PET/CT and PET/MRI in breast cancer patients: lesion detection and quantitation of 18F-deoxyglucose uptake in lesions and in normal organ tissues. *European Journal of Radiology* 2014; **83**: 289-96.

27. Grueneisen J, Nagarajah J, Buchbender C, Hoffmann O, Schaarschmidt BM, *et al.* Positron emission tomography/magnetic resonance imaging for local tumor staging

in patients with primary breast cancer: A comparison with positron emission tomography/computed tomography and magnetic resonance imaging. *Investigative Radiology* 2015; **50**: 505-13.

28. Jeong JH, Cho IH, Kong EJ, Chun KA. Evaluation of Dixon Sequence on hybrid PET/MR compared with contrast-enhanced PET/CT for PET-positive lesions. *Nucl Med Mol Imaging* 2014; **48**: 26-32.

29. An YS, Kang DK, Jung YS, Han S, Kim TH. Tumor metabolism and perfusion ratio assessed by 18F-FDG PET/CT and DCE-MRI in breast cancer patients: Correlation with tumor subtype and histologic prognostic factors. *European Journal of Radiology* 2015; **84**: 1365-70.

30. An YY, Kim SH, Kang BJ, Lee AW. Treatment response evaluation of breast cancer after neoadjuvant chemotherapy and usefulness of the imaging parameters of MRI and PET/CT. *Journal of Korean Medical Science* 2015; **30**: 808-15.

31. Kim TH, Yoon JK, Kang DK, Lee SJ, Jung YS, *et al.* Correlation between F-18 Fluorodeoxyglucose positron emission tomography metabolic parameters and dynamic contrast-enhanced MRI-derived perfusion data in patients with invasive ductal breast carcinoma. *Annals of Surgical Oncology* 2015; **22**: 3866-72.

32. Minamimoto R, Loening A, Jamali M, Barkhodari A, Mosci C, *et al.* Prospective comparison of 99mTc MDP sintigraphy, combined 18F-NaF and 18F-FDG PET/CT and whole-body MRI in patients with breast and prostate cancers. *Journal of Nuclear Medicine* 2015;

33. Park SH, Moon WK, Cho N, Chang JM, Im SA, *et al.* Comparison of diffusion-weighted MR imaging and FDG PET/CT to predict pathological complete response to neoadjuvant chemotherapy in patients with breast cancer. *European Radiology* 2012; **22**: 18-25.

34. Schmidt GP, Baur-Melnyk A, Tiling R, Hahn K, Reiser MF, *et al.* [Comparison of high resolution whole-body MRI using parallel imaging and PET-CT. First experiences with a 32-channel MRI system]. *Radiologe* 2004; **44**: 889-98.

35. Tozaki M, Sakamoto M, Oyama Y, O'Uchi T, Kawano N, *et al.* Monitoring of early response to neoadjuvant chemotherapy in breast cancer with (1)H MR spectroscopy: comparison to sequential 2-[18F]-fluorodeoxyglucose positron emission tomography. *Journal of Magnetic Resonance Imaging* 2008; **28**: 420-7.

36. Anouan KJ, Lelandais B, Edet-Sanson A, Ruan S, Vera P, *et al.* 18F-FDG-PET Partial volume effect correction using a modified recovery coefficient approach based on functional volume and local contrast: Physical validation and clinical feasibility in oncology. *Quarterly Journal of Nuclear Medicine and Molecular Imaging* 2015;

37. An YY, Kim SH, Kang BJ, Lee AW, Song BJ. MRI volume measurements compared with the RECIST 1.1 for evaluating the response to neoadjuvant chemotherapy for mass-type lesions. *Breast Cancer* 2014; **21**: 316-24.

38. Pahk K, Kim S, Choe JG. Early prediction of pathological complete response in luminal B type neoadjuvant chemotherapy-treated breast cancer patients: comparison between interim 18F-FDG PET/CT and MRI. *Nuclear Medicine Communications* 2015; **36**: 887-91.

39. Kodali S, Baher A, Shah D. Safety of MRIs in patients with pacemakers and defibrillators. *Methodist Debakey Cardiovascular Journal* 2013; **9**: 137-41.

40. Mann RM, Balleyguier C, Baltzer PA, Bick U, Colin C, *et al.* Breast MRI: EUSOBI recommendations for women's information. *European Radiology* 2015; **25**: 3669-78.

FIGURE LEGENDS

Figure 1

^{18}F-FDG-PET-CT and breast DCE-MRI images of a 45 year old woman with left breast cancer (patient no.6). The measurements for the 3-D volume and the maximum diameter demonstrated.

(a-c): T1 weighted 3-D subtracted DCE-MRI images. **a)** Axial; **b)** Coronal; and **c** Sagittal images.

(d-e): Fused ^{18}F-FDG-PET-CT images. **d)** Axial; **e)** Coronal; and **f)** Sagittal images.

Figure 2

Comparison of the measurement of 3-D volume of breast lesions using DCE-MRI and PET-CT images respectively via linear regression; correlation of determination R^2=0.986.

Figure 3

Comparison of the measurement of 3-D diameter of breast lesions using DCE-MRI and PET-CT images respectively via linear regression; correlation of determination R^2=0.931.

TABLE 1

Local dynamic contrast-enhanced breast MRI protocol technical parameters. TSE=Turbo Spin Echo; GE=Gradient Echo; STIR=Short Tau Inversion Recovery.

MRI sequence	Acquisition plane	Repetition time (TR) (msec)	Echo Time (TE) (msec)	Inversion time (msec)	Matrix size	Field of view (FoV) (mm)	Slice thickness (mm)	Voxel size (mm)
Localizer	sagittal	7.6	3.53	-	384 x 512	400	6	2.1x1.6x6.0
T1 pre-contrast GE 3D	axial	8.6	4.70	-	299 x 384	320	1	1.0x0.7x1.0
T1 GE 3D dynamic sequences (1 pre& 5post contrast)	axial	9.1	4.76	-	299 x 284	340	1.5	1.1x0.9x1.5
T1 3D Dixon	axial	7.20	first 2.38; second 4.76	-	320 x 320	340	1.8	1.1x1.1x1.8
T1 fat sat	axial	680	10	-	224 x 320	320	4	1.4x1.0x4.0
T2 STIR	axial	5600	59.0	170	314 x 320	340	4	1.1x1.1x4.0
T2 TSE	axial	6100	111	-	384 x 512	320	4	1.7x1.3x4.0
DWI b values 0 & 800s/mm^2	axial	9200	86	180	150 x 192	380	4	2.0x2.0x4.0

TABLE 2

Comparison of ^{18}F-FDG-PET-CT and DCE-MRI in the evaluation of breast lesions in patients with either breast cancer or breast tuberculosis

Patient ID	Diagnosis	Maximum diameter (cm)		Volume (cm^3)	
		DCE-MRI	^{18}F-FDG-PET-CT	DCE-MRI	^{18}F-FDG-PET-CT
1	TB	5.1	5.8	51.5	64.6
2 first lesion	TB	12.2	14.9	190.8	234.3
second lesion	TB	4.7	5.3	30.3	46.2
third lesion	TB	5	5.2	39.4	58.8
3	TB	11.1	11.7	440.1	380.6
4	TB	13.9	20	1300.7	1382.2
5	TB	4.3	6.1	30.7	63.7
6	Cancer	9.2	10.2	283.7	391.5
7	Cancer	7.4	8.1	161.8	252.9
Mean ± SD		8.1 ± 3.6	9.7 ± 5.1 (p=0.032)	280.98 ± 406.8	319.4 ± 421.8 (p=0.052)
Correlation factor (R)		0.964 (p<0.0001)		0.993 (p<0.0001)	
Coefficient of determination (R^2)		0.931 (p<0.0001)		0.986 (p<0.0001)	

FIGURE 1

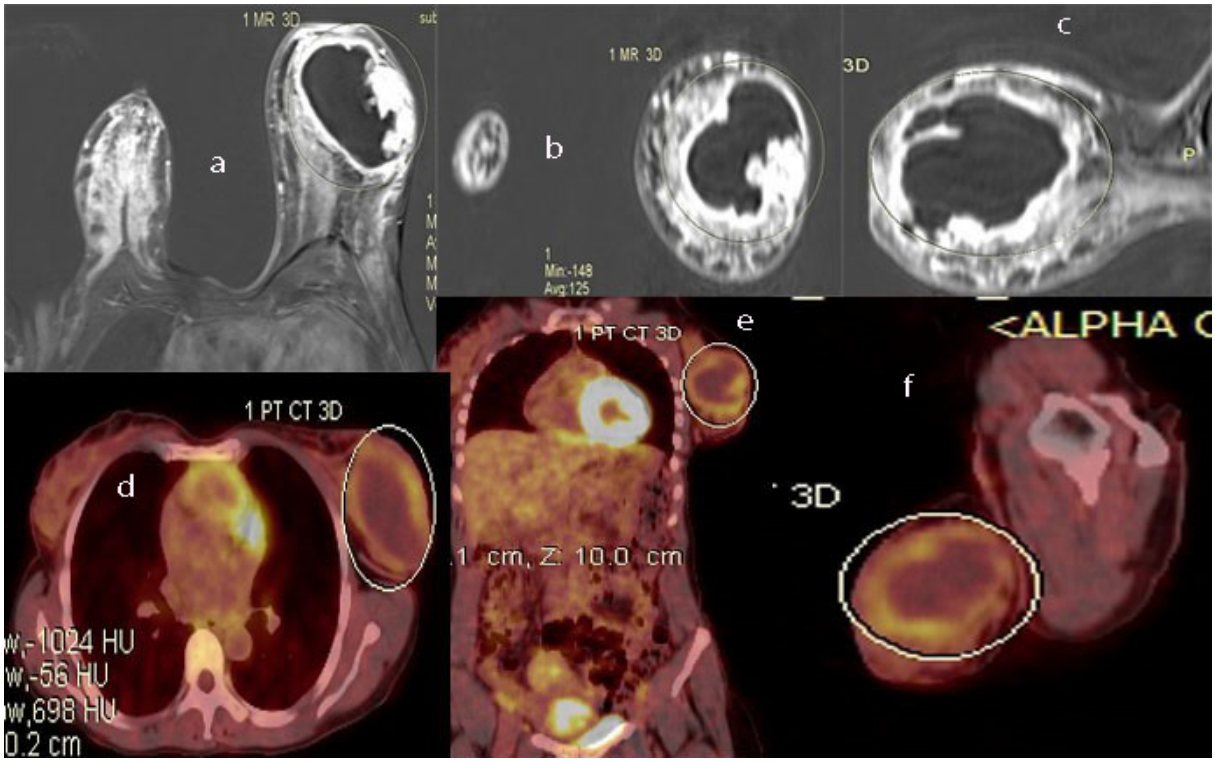
1 MR 3D
a
1 MR 3D
b
3D
c
1 PT CT 3D
d
1 PT CT 3D
e
f
3D
1 cm, Z: 10.0 cm
-1024 HU
-56 HU
698 HU
0.2 cm

FIGURE 2

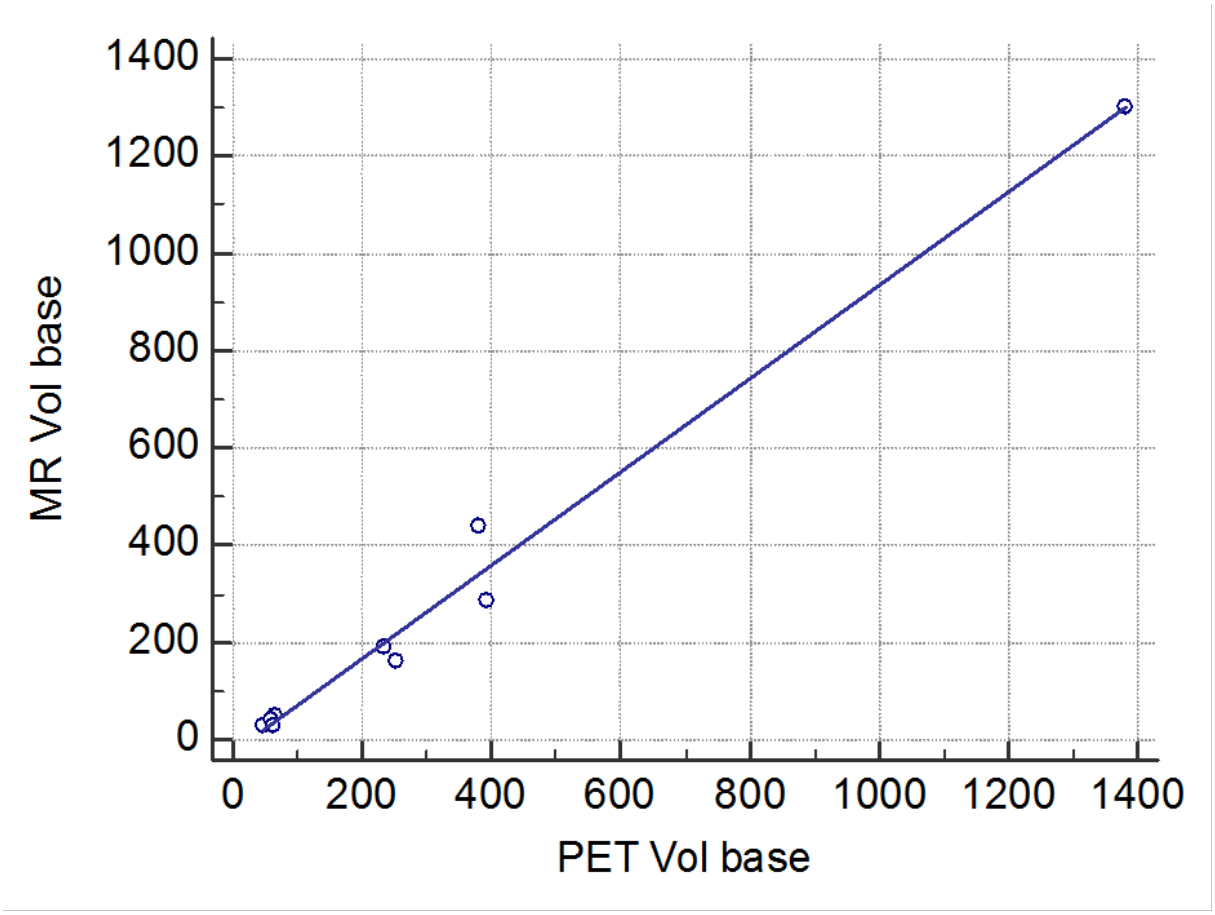

FIGURE 3

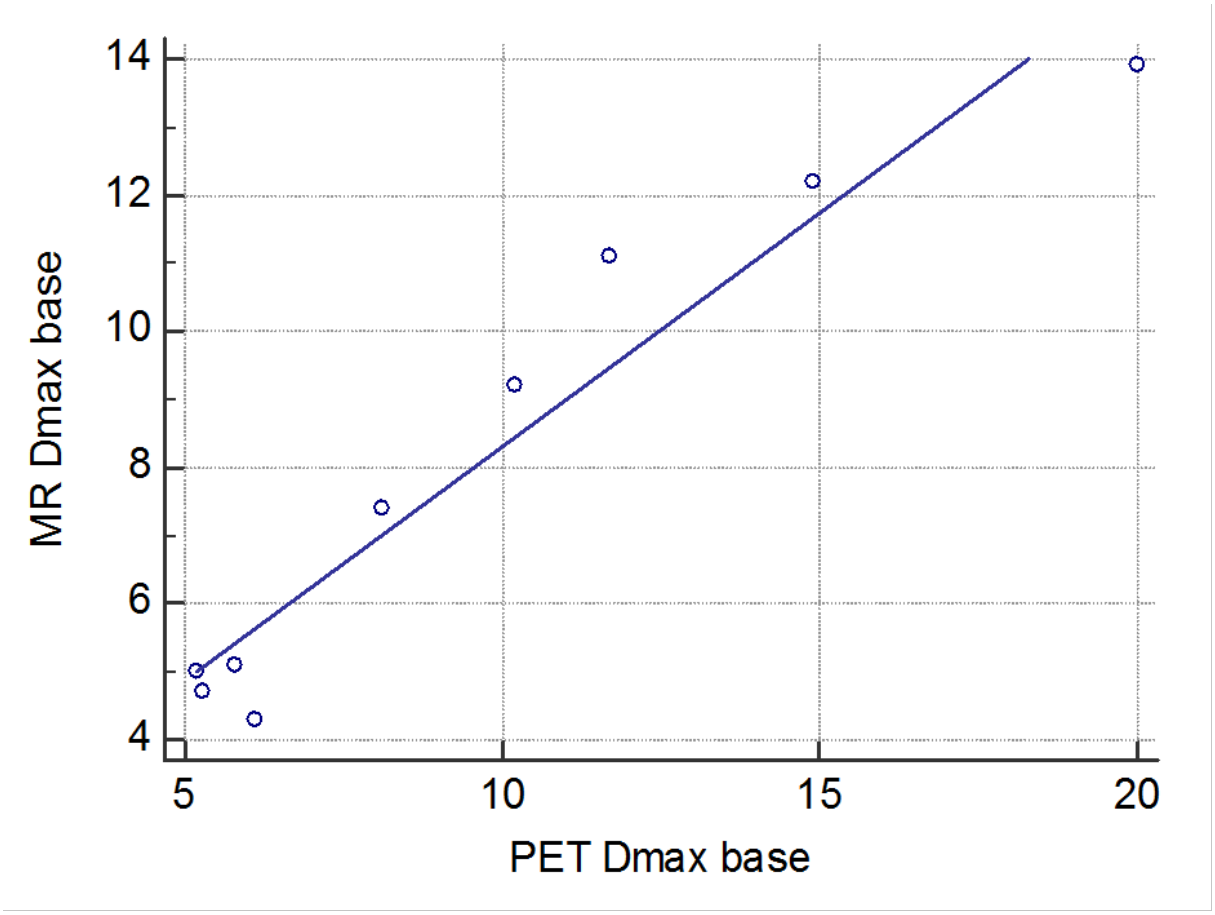

CHAPTER 8

SYNTHESIS AND DISCUSSION

SYNTHESIS AND DISCUSSION

INTRODUCTION

The purpose of this project was to evaluate the prevalence and spectrum of radiological manifestations of breast tuberculosis (BTB) in South African patients, drawing on a sample from two tertiary-level breast clinics in Durban, South Africa, to identify the radiological patterns manifest in these patients with a view to improving the specificity of diagnosis, with particular reference to the newer modalities of PET-CT and MRI, and to study the radiological markers indicating a satisfactory response to treatment. In the pages which follow, we have synthesised our findings into a number of conclusions and recommendations.

CONCLUSION 1

The prevalence of BTB is low.

The Addington surgical breast clinic is the major referral centre for the Ethekwini Municipality group of hospitals. However, even in this setting, the five-year period prevalence of BTB was found to be only 0.3% (Chapter 2). This finding emphasises that although the incidence of extrapulmonary tuberculosis (EPTB) is increasing in association with high rate of Human Immuno-Deficiency virus (HIV), the breast is still infrequently involved (*Yang et al.* 2004). Our findings are in line with other studies, which found the incidence of BTB to be low amongst patients presenting with breast disease (*Meerkotter et al.* 2011; *Tewari & Shukla* 2005). Shushtari *et al.* (2011) reported nine BTB cases in a total of 2235 over a five year period from 2005-2009. Due to the rarity of the disease, there is scanty literature to provide the clinician with adequate evidence based information.

One consequence of this low prevalence is the difficulty in recruiting large patient cohort for study. Indeed, in the further studies incorporated onto this thesis, we studied a small number of patients; a feature common to all previously published studies on this subject (*Oh et al.* 1998; *Popli et al.* 2010). Though ideal, recruitment of meaningfully large cohorts would be difficult, and would have to be multicentre, with the consequent problems of a prolonged

period of recruitment and the difficulties in overcoming differences between centres, particularly in terms of subjectivity in interpretation.

CONCLUSION 2

Current classifications of BTB are predominantly clinically based without any radiological correlation therefore we provide a descriptive framework based on clinical-radiological assessment which may be of more clinical utility.

Our data identified five clinical-radiological patterns of BTB based on mammography and ultrasound findings (Chapter 2). We retrospectively analysed 65 patient records on the prevalence study. Our data from the retrospective prevalence study identified the five distinct clinical-radiological patterns of BTB as: inflammatory/disseminated; axillary lymphadenitis with breast oedema (ALBE); abscess variety; nodular/focal mass; and the isolated axillary tuberculous lymphadenitis (IATL). Among the patients who had mammograms, the asymmetric density without nodes was the commonest observation in those found with the abscess variety on ultrasound. Although clinically IATL was not reported, it was seen in 12.1 % of mammograms. Our finding of IATL is similar to a smaller retrospective study of 21 patients with BTB that was done in Johannesburg (*Meerkotter et al.* 2011). In contrast, in studies performed outside South Africa, isolated axillary lymphadenitis was not specifically reported as the predominant presenting feature (*Mehta et al.* 2010; *Oh et al.* 1998). It is therefore important that the clinician is aware of the various presentations that can occur in the breast affected by TB, especially where TB is endemic like in this setting. Our various classifications reinforce the wide spectrum of presentation of BTB lesions. Furthermore, although there have been studies (*Harris et al.* 2006; *Meerkotter et al.* 2011) on the clinical-radiological features of BTB since the clinical classification of the disease by Tewari and Shukla (2005), the authors did not commit to any classification. Our data provided adequate information to allow us to re-classify the disease into the above categories. We therefore propose that the following classification framework be applied to BTB for research and clinical purposes: Table 8.1.

Pattern	Clinical	Mammogram description	Ultrasound description
Inflammatory/ disseminated	Diffuse inflammation & tenderness	Non-specific diffuse stromal thickening & axillary nodes	Diffuse hypoechoic trabecular thickening due to oedema& axillary nodes
ALBE	Enlarged breast, Oedema, no inflammation	Non-specific diffuse stromal thickening ± axillary nodes	Diffuse hypoechoic trabecular thickening due to oedema ± axillary nodes
Abscess	Focal tender mass	Asymmetric density	Complex solid-cystic heterogeneous mass
Nodular/focal mass	Focal firm mass	Irregular/smooth focal mass density	Hypoechoic/heterogeneous solid mass
IATL	Axillary swelling	Well defined dense mass	Oval hypoechoic solid thick cortex mass

Table 8.1 Proposed clinical-radiological classification of BTB, based on clinical, mammography and ultrasound examination.

CONCLUSION 3

The newer modalities of PET-CT and multiparametric MRI are potentially of value in the evaluation of BTB.

Appearances of BTB on ^{18}F-FDG-PET-CT and differentiation from BCA

We evaluated ^{18}F-FDG-PET-CT findings in five patients with BTB (Chapter 3 and 5). We conclude that the two patterns can be encountered on ^{18}F-FDG-PET-CT in patients with breast tuberculosis namely: a) the breast only pattern; and b) the combined breast/lymphatic pattern; The various patterns appear to have an association with patient clinical condition, whereby the breast only pattern is associated with general wellness and less severe disease, whereas the combined breast/lymphatic pattern represents the worse end of the spectrum of disease severity and debilitation. In the breast only pattern, the metabolic activity is localised to the breast region, with no significant association of pulmonary, lymph nodes or other organ involvement. The breast only pattern has not been previously described in other

studies which evaluated the patterns of TB on ^{18}F-FDG-PET-CT (*Martinez et al.* 2012; *Mehta* 2012; *Soussan et al.* 2012). In the combined breast/lymphatic pattern, there was predominance of ^{18}F-FDG avid lesions in the breast and widespread lymph nodes as well as other EPTB including hepato-splenic, bone and subcutaneous tissues. Although there may be evidence of pulmonary TB (PTB), the severity did not qualify for being classified under the lung pattern as described by (*Soussan et al.* 2012). There is limited data in the literature about the patterns of TB on ^{18}F-FDG-PET-CT. The lung and the lymphatic patterns were reported in the two studies (*Martinez et al.* 2012; *Soussan et al.* 2012), in which there was an association of the former with predominant pulmonary disease and the latter with more severe systemic disease (*Martinez et al.* 2012; *Soussan et al.* 2012). We also found similar association between the lymphatic pattern and the severity of the clinical findings. We additionally found a new pattern which has not been described previously, the breast only pattern.

Some parameters may play a role in the differentiation between BTB and breast cancer (BCA) (Chapter 5). The SUV_{max} can be used in for this purpose, in which the BCA patients displayed significantly higher values than the BTB patients for the ***breast lesions***. This finding has similarities to some recent studies that evaluated the role of ^{18}F-FDG-PET-CT in differentiating between benign and malignant pulmonary nodules (*Van Gomez Lopez et al.* 2015; *Yilmaz & Tastekin* 2015). Sadly, the same parameter, the SUV_{max}, was not useful in separating the ***TB axillary nodes*** from the malignant ones. This implies that we cannot yet prevent the futile biopsy of axillary nodes in patients with BCA. This is in agreement to a study done in a similar setting where TB is endemic, in which the SUV_{max} could not differentiate benign from malignant pulmonary nodules (*Sathekge et al.* 2010). The CT Hounsfield units (HU) were not useful in differentiating the breast lesions or the axillary nodes.

We conclude that ^{18}F-FDG-PET-CT has a role, especially in determining the pattern of whole body involvement with disease, whereby we described the previously unreported breast only pattern. A further role of ^{18}F-FDG-PET-CT is in the provision of a semi-quantitative differential guide in separating BCA from BTB with the use of SUV_{max}.

Appearances of BTB on DWI, T2W and DCE-MRI and differentiation from BCA

We analysed the MRI of six patients with BTB (Chapters 4 and 6). The use of multi-parametric MRI qualitative and semi-quantitative parameters has provided us with a guide description of the appearances of BTB lesions on this modality, as well as in the differential diagnosis between BTB and BCA. We have tabulated these findings in order to provide a tool for the reporting radiologist with differentiating features between BTB and BCA, with the following two cautions (Table 8.2).

MRI parameter	**BTB**	**BCA**
Pre-contrast T1W	Hypointense	Isointense/hypointense
Pre-contrast T2W morphology	Hyperintense/mixed signal	Hypointense
Pre-contrast T2W, T2SI value	Higher	Lower
Post contrast DCE-MRI (mass pattern)	Rim-enhancing with no internal solid elements	Rim-enhancing with internal solid elements
Post contrast DCE-MRI (non-mass pattern (NME))	Ring/rim enhancing axillary nodes	Solid axillary nodes
DWI ADC value	Higher	Lower
Axillary nodes	Ring/rim enhancing	solid

Table 8.2 MRI differential diagnosis of breast lesion in a patient suspected of having either BTB or BCA.

Caution 1: The features would mainly apply for the common breast cancer pathological type of invasive ductal cancers (IDC), other uncommon types may have variable appearances.

Caution 2: The significance of apparent diffusion coefficient (ADC) and T2 signal intensity (T2SI) values in separating BTB from BCA lesions appear to be influenced by whether the breast lesion enhancement pattern is mass or non-mass enhancement (NME), the parameters showing statistically significant differences between BTB and BCA for the mass pattern but not for the NME pattern. Many studies (*Dorrius et al.* 2014; *Yamaguchi et al.* 2015; *Zhao*

et al. 2015) that used the ADC value to discriminate between benign and malignant breast lesion were done on mass pattern, with only few (*Imamura et al.* 2010; *Partridge et al.* 2009) that evaluated the use of this parameter for both patterns. Partridge *et al* found that the ADC value was more beneficial for mass pattern than for NME, which is in agreement with our finding (*Partridge et al.* 2009).

Our finding of BCA pre-contrast T2W hypointense is in line with other studies (*Gribbestad et al.* 1994; *Kuhl et al.* 1999; *Malich et al.* 2005). We also found all patients with BTB to have ring/rim-enhancing necrotic axillary nodes, the finding that has been reported by other authors (*Lee et al.* 2012; *Williams et al.* 2010) . There is paucity of literature on the appearances of BTB on MRI, Apart from the study done on four patients to differentiate BTB from BCA on magnetic resonance spectroscopy (MRS) (*Popli et al.* 2010) and a case report to assess treatment response of one patient with BTB (*Fellah et al.* 2006), we found only one study that was performed on six patients with BTB in 1998 (*Oh et al.* 1998). Popli *et al* found BTB lesions to have absence of choline peak and presence of strong lipid peak (*Popli et al.* 2010). Oh *et al* reported similar findings to our study, from a total of seven breast lesions, four demonstrated ring/rim enhancement, however in contrast to ours, two had internal enhancement, and one lesion did not have any enhancement (*Oh et al.* 1998). Since 1998, there has been significant technological advancement involving all aspects of breast imaging, from equipment, to image acquisition and processing. These factors may play a role in the discordant reporting between our findings and those of *(Oh et al. 1998).*

The ADC value was a good discriminator between the BTB and the BCA group, with the latter demonstrating statistically significant lower values than the former (Chapter 6). Our results are in agreement with other studies (*Imamura et al.* 2010; *Qu et al.* 2015; *Woodhams et al.* 2005; *Yabuuchi et al.* 2010; *Yamaguchi et al.* 2015; *Yili et al.* 2009; *Zhao et al.* 2015), with few exceptions (*Chatterjee et al.* 2010). Peng *et al* found intracranial tuberculomas to have higher ADC value than high grade gliomas (*Peng et al.* 2012). In contrast, Chatterjee *et al* found no difference in the ADC values between brain tuberculomas and metastases (*Chatterjee et al.* 2010).

The T2SI value was a strong discriminator between the BTB and the BCA group, with the latter group displaying significant lower values than the former hence this parameter can be a valuable marker. The use of quantitative T2SI as a discriminator of malignancy has been

evaluated for other body parts other than the breast (*Henz Concatto et al.* 2015; *Peng et al.* 2014). Henz *et al* found that the mean T2SI ratio and the ADC values were significant in differentiating benign from malignant pulmonary nodules in a granulomatous endemic area (*Henz Concatto et al.* 2015).

We conclude that multiparametric breast MRI appears to add value beyond that of conventional imaging modalities in diagnosing BTB, specifically in assigning probabilities to the diagnosis of BTB vis a vis BCA and in defining disease extent.

Defining extent of disease with ^{18}F-FDG-PET-CT and DCE-MRI

The advantage of ^{18}F-FDG-PET-CT over conventional imaging of mammography, ultrasound and chest x-ray (CXR) is the ability to image the whole body instead of only imaging the localised body parts of breast and/or chest. It is therefore not surprising that more extensive disease spread was seen on ^{18}F-FDG-PET-CT than on conventional imaging, the extra sites being the lymph nodes, liver, spleen, skeleton and subcutaneous tissues (Chapters 3 and 4). This means that PET-CT can be used as an adjunct to mammography, ultrasound and CXR in patients suspected of having more widespread disease. The value of ^{18}F-FDG-PET-CT in evaluating the TB disease burden has been mainly studied in patients presenting with PTB

(*Coleman et al.* 2014)

(*Chen et al.* 2014; *Soussan et al.* 2014; *Stelzmueller et al.* 2015). Excluding case reports, there are few studies that evaluated the value of ^{18}F-FDG-PET-CT in extrapulmonary TB (EPTB), and none of the sites mentioned was breast (*Dureja et al.* 2014; *Martinez et al.* 2012; *Stelzmueller et al.* 2015). Stelzmueller *et al* compared the diagnostic accuracy of PET and CT components of ^{18}F-FDG-PET-CT in 35 patients with PTB or EPTB. The authors found comparable diagnostic performance on the initial baseline and follow up scans even though ^{18}F-FDG-PET demonstrated more abnormal findings than CT (*Stelzmueller et al.* 2015).

Breast DCE-MRI has many advantages over mammography and ultrasound including: better soft tissues contrast; ability to include chest wall in the imaging field; the use of intravenous (I.V.) contrast to improve lesion detection and characterisation (*Machida et al.* 2015). Again, it is not surprising that more local disease extent including chest wall involvement was revealed on DCE-MRI, yet was not seen on mammography and/or ultrasound (Chapter 4). However, unlike ^{18}F-FDG-PET-CT, DCE-MRI is focused on the breast/chest region only hence distant disease cannot be assessed.

Our conclusion is that both ^{18}F-FDG-PET-CT and DCE-MRI are valuable in providing the clinician with more information about disease extent than would not be possible with conventional imaging.

Monitoring response of BTB to anti-tuberculous therapy using ^{18}F-FDG-PET-CT and MRI

Response to treatment of BTB can be monitored using parameters derived from these two modalities.

Our conclusions following image review of five patients with BTB who had both ^{18}F-FDG-PET-CT and MRI at start of anti-tuberculous treatment (ATT) and at 4 months of treatment (Chapter 3 and 4) are that the ***breast lesion or axillary node*** maximum standardised uptake value (SUV_{max}) and maximum diameter (D_{max}) values can be used to separate the responders from the non-responders, the latter group displaying higher values than the former at baseline scan which demonstrated significant increase at 4 months follow-up scan. The SUV_{max} finding is similar to other ^{18}F-FDG-PET-CT studies done on PTB (*Coleman et al.* 2014; *Sathekge et al.* 2012; *Sathekge et al.* 2011) and EPTB (*Dureja et al.* 2014; *Martinez et al.* 2012) patients, hence it is used as a marker in TB treatment monitoring. Sathekge *et al* found the TB lymph nodes diameter to have significant role in differentiating the responders from the non-responders, in which the larger sized nodes were seen in non-responders (*Sathekge et al.* 2012).

The number of lymph node basins was not useful for separating the responders and the non-responders. In contrast, in a study done to predict response to first line ATT in TB-HIV co-infected patients, five or more lymph node basins could separate responders from non-

responders with a sensitivity and specificity of 88% and 81% (*Sathekge et al.* 2011). Other MRI parameters of ADC value and T2SI value were not useful for treatment monitoring.

We conclude that response to ATT may be monitored using ^{18}F-FDG-PET-CT and/or MRI using the following parameters: SUV_{max} and D_{max} for ^{18}F-FDG-PET-CT and D_{max} for MRI. Other parameters by contrast are unhelpful. We did not directly compare the older modalities with the newer modalities, since ^{18}F-FDG-PET-CT and MRI were used to assess interval change at 4 months, whereas conventional modalities were only assessed on completion of treatment, at 9 months. A direct comparison is now indicated, given the lower cost and wider availability of conventional imaging.

Correlation of lesion size determined by ^{18}F-FDG-PET-CT and DCE-MRI respectively

Either of these two modalities can be used in staging and treatment monitoring provided one modality is used consistently. We observed a strong correlation between the two modalities (Chapter 7). The measured lesion volume (LV) and maximum diameter (D_{max}) of the breast lesions were however higher on ^{18}F-FDG-PET-CT than on DCE-MRI, suggesting that absolute sizes should not be compared across modalities. We have suggested that differences in patient positioning, particularly the compression of the breast resulting from the undedicated prone position ^{18}F-FDG-PET-CT scanning as opposed to dedicated breast coil prone scanning on DCE-MRI, may account for this, as may the use of intravenous (I.V.) contrast for DCE-MRI. The partial volume effect suggested by (*Anouan et al.* 2015) does not appear to be a factor.

We conclude that apart from these slight differences between the two modalities, the excellent correlation implies that either modality can be used consistently in treatment monitoring. Although one modality cannot replace another, there are circumstances where either investigation cannot be used or is contra-indicated. Examples include patients who have MRI phobia and those with in situ pacemakers (*Kodali et al.* 2013; *Mann et al.* 2015). Our findings imply that ^{18}F-FDG-PET-CT can be an alternative treatment monitoring and/or staging investigation in these patients.

POTENTIAL BENEFITS OF THIS RESEARCH

We re-classified BTB into five distinct clinical-radiological patterns on mammography and ultrasound. We further classified it into two patterns on ^{18}F-FDG-PET-CT and described a new pattern which has not been previously reported. We described typical morphological appearances of BTB on multi-parametric MRI. We further identified potential markers for treatment response monitoring on both ^{18}F-FDG-PET-CT, DCE-MRI, T2W and DWI-MRI. It is hoped that this knowledge will aid the practicing clinician and the reporting radiologist to include the disease in the differential diagnosis when they encounter similar appearances. Knowledge of typical radiological appearances in the right setting will guide the radiologist towards the correct diagnosis. The identification of potential markers can play a role in effective monitoring of more severe infection.

FUTURE RESEARCH

The retrospective study (objective 1) can be extended to incorporate survival analysis of the cohort, which would require further funding and resources to track all the participants. In the analysis of the response to treatment (objectives 3 and 4), both studies can be further enhanced with the inclusion of control group consisting of TB patients who do not have BTB. In the two studies that evaluated the differences between BCA and BTB (objectives 5 and 6), a more in depth quantitative analysis can be performed with the use of newer quantitative software packages which we did not have funding for.

STUDY LIMITATIONS

Small sample size

This is difficult to avoid given the low prevalence of BTB. Many of our findings should be regarded as preliminary, and will require verification. This will require a large multicentre study. We were also limited in the number of scans that could be performed by the expense of these investigations. It would for example have been useful to repeat the ^{18}F-FDG-PET-CT and MRI study on completion of treatment in addition to the 4-month mark to identify further evolution of appearances.

Software

A higher level of quantitative analysis would be possible by utilising more advanced software packages such as the dedicated advanced breast MRI post-processing *Syngo-via MR Brevis* (*Siemens, Erlangen, Germany*) and the imaging biomarker experts *Icometrix* (*Icometrix, Leuven, Belgium)* quantitative imaging tools, access to which was limited by funding. Such analysis of the stored images may be possible in future should such software become available.

RECOMMENDATIONS

The study findings suggest the following recommendations:

1. The prevalence of BTB, though low, is not zero. It is important that clinicians and radiologists are primed to recognise the possibility of BTB and to respond appropriately in terms of diagnosis. The papers arising from this project will provide a valuable addition to the literature to guide clinicians under such circumstances.
2. The potential value of ^{18}F-FDG-PET-CT and MRI in the investigation of BTB should be recognised.
3. Patients with BTB suspected of having disease beyond the breast itself should be considered for ^{18}F-FDG-PET-CT and/or MRI imaging given their superiority in detecting extensive disease
4. When BTB and BCA appear in the differential diagnosis, ^{18}F-FDG-PET-CT and/or MRI imaging may assist in their differentiation. This may be particularly useful in the patient with known TB elsewhere who presents with a breast lesion.
5. When there is discordant result between clinical appearances and pathology, MRI should be considered.
6. All BTB patients who are clinically not responding to ATT at the follow-up appointment should be considered for ^{18}F-FDG-PET-CT and/or MRI imaging.

REFERENCES

REFERENCES

Afridi SP, Memon A, Rehman SU, Baig N. Spectrum of breast tuberculosis. *J. Coll. Physicians Surg. Pak.* 2009; 19: 158-61.

Afridi SP, Memon A, Shafiq ur R. Granulomatous mastitis: a case series. *J. Coll. Physicians Surg. Pak.* 2010; 20: 365-8.

Akbulut S, Sogutcu N, Yagmur Y. Coexistence of breast cancer and tuberculosis in axillary lymph nodes: a case report and literature review. *Breast Cancer Res. Treat.* 2011; 130: 1037-42.

Akcakaya A, Eryilmaz R, Sahin M, Ozkan OV. (2005). Tuberculosis of the Breast (Vol. 11, pp. 85-6): Wiley-Blackwell.

Akcay MN, Saglam L, Polat P, Erdogan F, Albayrak Y, *et al.* Mammary tuberculosis - importance of recognition and differentiation from that of a breast malignancy: report of three cases and review of the literature. *World J. Surg. Oncol.* 2007; 5: 67.

Al-Khawari HAT, Al-Manfouhi HA, Madda JP, Kovacs A, Sheikh M, *et al.* Radiologic Features of Granulomatous Mastitis. *Breast Journal* 2011; 17: 645-50.

Al-Marri MR, Almosleh A, Almoslmani Y. Primary Tuberculosis of the Breast in Qatar: Ten Year Experience and Review of the Literature. *Eur. J. Surg.* 2000; 166: 687-90.

Al-Roomi E, Jamal W, Al-Mosawi A, Rotimi VO. Mycobacterium Tuberculosis Breast Infection Mimicking Pyogenic Abscesses in Kuwait. *Med. Princ. Pract.* 2009; 18: 245-7.

Anouan KJ, Lelandais B, Edet-Sanson A, Ruan S, Vera P, *et al.* 18F-FDG-PET Partial volume effect correction using a modified recovery coefficient approach based on functional volume and local contrast: Physical validation and clinical feasibility in oncology. *Q. J. Nucl. Med. Mol. Imaging* 2015.

Atamanalp SS, Gündoğdu C, Polat P, Öztürk G, Aydinli B, *et al.* Clinical presentation of breast tuberculosis in eastern Anatolia. *Doğu Anadolu'da meme tüberkülozunun klinik sunumu.* 2010; 40: 293-7.

Aurum Institute. Managing TB in a new era of diagnosis Johannesburg, South Africa: Aurum Institute; 2013. Available from: http://www.sahivsoc.org/upload/documents/Aurum%20Managing%20TB%20in%20an%20era%20of%20new%20diagnostics.pdf.

Baharoon S. Tuberculosis of the breast. *Ann. Thorac. Med.* 2008; 3: 110-4.

Bakaris S, Yuksel M, Cıragil P, Guven MA, Ezberci F, *et al.* Granulomatous mastitis including breast tuberculosis and idiopathic lobular granulomatous mastitis. *Can. J. Surg.* 2006; 49: 427-30.

Bani-Hani KE, Yaghan RJ, Matalka, II, Mazahreh TS. Tuberculous mastitis: a disease not to be forgotten. *Int. J. Tuberc. Lung Dis.* 2005; 9: 920-5.

Ben Hassouna J, Gamoudi A, Bouzaiene H, Dhiab T, Khomsi F, *et al.* [Mammary tuberculosis: a retrospective study of 65 cases]. *Gynecol. Obstet. Fertil.* 2005; 33: 870-6.

Bhosale AA. Primary tuberculosis of breast: A case series. *Annals of tropical medicine and public health* 2012; 5: 1.

Centre for Disease Control and Prevention. Trends in tuberculosis--United States, 2012. *MMWR Morb. Mortal. Wkly. Rep.* 2013; 62: 201-5.

Centre for Disease Control and Prevention. Tuberculosis (TB). 2014.

Chalazonitis AN, Tsimitselis G, Tzovara J, Chronopoulos P. Tuberculosis of the Breast. *Breast Journal* 2003; 9: 327-9.

Chatterjee S, Saini J, Kesavadas C, Arvinda HR, Jolappara M, *et al.* Differentiation of tubercular infection and metastasis presenting as ring enhancing lesion by diffusion and perfusion magnetic resonance imaging. *J. Neuroradiol.* 2010; 37: 167-71.

Chauhan A, Kakkar S, Mahapatra S. Mammary tuberculosis — A case report. *Medical Journal Armed Forces India* 2006; 62: 385-6.

Chen RY, Dodd LE, Lee M, Paripati P, Hammoud DA, *et al.* PET/CT imaging correlates with treatment outcome in patients with multidrug-resistant tuberculosis. *Sci. Transl. Med.* 2014; 6: 9.

Cheng J, Du YT, Ding HY. [Granulomatous lobular mastitis: a clinicopathologic study of 68 cases]. *Zhonghua Bing Li Xue Za Zhi* 2010; 39: 678-80.

Chia BS LF, Rifat D, Herrera A, Kim EY, Sailer C, Torres-Chavolla E, Narayanaswamy P, Einarsson V, Bravo J, Pascale JM, Ioerger TR, Sacchettini JC, Karakousis PC. Use of Multiplex Allele-Specific Polymerase Chain Reaction (MAS-PCR) to Detect Multidrug-Resistant Tuberculosis in Panama. *PLoS One. 2012;7(7):e40456. Epub 2012 Jul 6.* 2012; 7.

Coleman MT, Chen RY, Lee M, Lin PL, Dodd LE, *et al.* PET/CT imaging reveals a therapeutic response to oxazolidinones in macaques and humans with tuberculosis. *Sci. Transl. Med.* 2014; 6: 9.

Cooper A. Illustrations of the Diseases of the Breast. 1829; Part1 London, Longman, Rees, Orme, Brown and Green: 73.

Da Silva BB, Lopes-Costa PV, Pires CG, Pereira-Filho JD, dos Santos AR. Tuberculosis of the breast: analysis of 20 cases and a literature review. *Trans. R. Soc. Trop. Med. Hyg.* 2009; 103: 559-63.

Dang PA, Freer PE, Humphrey KL, Halpern EF, Rafferty EA. Addition of tomosynthesis to conventional digital mammography: effect on image interpretation time of screening examinations. *Radiology* 2014; 270: 49-56.

Deepa H, Vijay S, Mishra P, Jai J, Chitra DH. Tubercular Mastitis is Common in Garhwal Region of Uttarakhand: Clinico athological Features of 14 Cases. *Journal of Clinical and Diagnostic Research* 2011; 5: 5.

del Agua C, Felipo F, Paricio J, Equizabal C, Delgado M. Tuberculosis of the Breast as a Pseudotumoral Image. *Breast Journal* 2006; 12: 180-.

Department of Health (South Africa). National tuberculosis management guidelines 2014. Pretoria: Department of Health; 2014 [cited 2015 3 December 2015]. Available from: http://www.hst.org.za/sites/default/files/NTCP_Adult_TB-Guidelines-27.5.2014.pdf.

Department of Health South Africa. (2009). *South African National TB Management Guideline*. Retrieved

from http://familymedicine.ukzn.ac.za/Libraries/Guidelines_Protocols/TB_Guidelines_2009.sflb.ashx.

Domingo C, Ruiz J, Roig J, Texido A, Aguilar X, *et al.* Tuberculosis of the breast: a rare modern disease. *Tubercle* 1990; 71: 221-3.

Dorrius MD, Dijkstra H, Oudkerk M, Sijens PE. Effect of b value and pre-admission of contrast on diagnostic accuracy of 1.5-T breast DWI: a systematic review and meta-analysis. *Eur. Radiol.* 2014; 24: 2835-47.

Dubar L-E. Des tubercules de la mamelle. In: R. C. o. S. o. England, editor. Tuberculosis, Breast Diseases: Paris: J.-B. Bailliere et fils; 1881. p. 130.

Dureja S, Sen IB, Acharya S. Potential role of F18 FDG PET-CT as an imaging biomarker for the noninvasive evaluation in uncomplicated skeletal tuberculosis: a prospective clinical observational study. *Eur. Spine J.* 2014; 23: 2449-54.

Farrokh D, Talab FR, Rastegar YF. Primary breast tuberculosis mimicking carcinoma: a case report. *Iranian Journal of Clinical Infectious Diseases* 2010; 5: 242-5.

Fellah L, Leconte I, Weynand B, Donnez J, Berlière M. Breast tuberculosis imaging. *Fertil. Steril.* 2006; 86: 460-1.

Fiorucci F, Conti F, Lucantoni G, Fiorucci C, Giannunzio G, *et al.* Sarcoidosis of the breast: a rare case report and a review. *Eur. Rev. Med. Pharmacol. Sci.* 2006: 4.

Gautier MF. Contribution a l'etude de l'Anatomie pathologique et de la Pathogenie de la Tuberculose mammaire de la Femme. Gazette Hebdomadaire De Medecine et de Chirurgie; Paris1896. p. 2.

Gill M, Chabbra S, Sangwan M, Singh S, Praveen, *et al.* Tuberculous mastitis–A great mimicker. *Asian Pacific Journal of Tropical Disease* 2012; 2: 348-51.

Gold RH. The evolution of mammography. *Radiol. Clin. North Am.* 1992; 30: 1-19.

Goyal M, Sharma R, Sharma A, Chumber S, Sawhney S, *et al.* Chest wall tuberculosis simulating breast carcinoma: Imaging appearance. *Australas. Radiol.* 1998; 42: 86.

Gribbestad IS, Nilsen G, Fjosne HE, Kvinnsland S, Haugen OA, *et al.* Comparative signal intensity measurements in dynamic gadolinium-enhanced MR mammography. *J. Magn. Reson. Imaging* 1994; 4: 477-80.

Gunal S, Yang Z, Agarwal M, Koroglu M, Arici ZK, *et al.* Demographic and microbial characteristics of extrapulmonary tuberculosis cases diagnosed in Malatya, Turkey, 2001-2007. *BMC Public Health* 2011; 11: 154.

Gupta R, Singal RP, Gupta A, Singal S, Shahi SR, *et al.* Primary tubercular abscess of the breast - an unusual entity. *J. Med. Life* 2012; 5: 98-100.

Halstead AE, Lecount ER. I. Tuberculosis of the Mammary Gland. *Ann. Surg.* 1898; 28: 685-707.

Harris SH, Khan MA, Khan R, Haque F, Syed A, *et al.* Mammary tuberculosis: Analysis of thirty eight patients. *ANZ J. Surg.* 2006; 76: 234-7.

Hartstein M, Leaf HL. Tuberculosis of the breast as a presenting manifestation of AIDS. *Clinical Infectious Diseases: An Official Publication Of The Infectious Diseases Society Of America* 1992; 15: 692-3.

Hendrick RE. Radiation doses and cancer risks from breast imaging studies. *Radiology* 2010; 257: 246-53.

Henz Concatto N, Watte G, Marchiori E, Irion K, Felicetti JC, *et al.* Magnetic resonance imaging of pulmonary nodules: accuracy in a granulomatous disease-endemic region. *Eur. Radiol.* 2015.

Hiremath BV, Subramaniam N. Primary breast tuberculosis: Diagnostic and therapeutic dilemmas. *Breast Dis.* 2015; 35: 187-93.

Imamura T, Isomoto I, Sueyoshi E, Yano H, Uga T, *et al.* Diagnostic performance of ADC for Non-mass-like breast lesions on MR imaging. *Magn. Reson. Med. Sci.* 2010; 9: 217-25.

Indumathi CK, Anand A, Chitra D, Priti Lata R. Tuberculosis of the beast in an adolescent Girl: A rare presentation. *J. Trop. Pediatr.* 2007; 53: 133-4.

Jah A, Mulla R, Lawrence FD, Pittam M, Ravichandran D. Tuberculosis of the breast: experience of a UK breast clinic serving an ethnically diverse population. *Ann. R. Coll. Surg. Engl.* 2004; 86: 416-9.

Kalaç N, Özkan B, Bayiz H, Dursun AB, Demirağ F. Breast tuberculosis. *The Breast* 2002; 11: 346-9.

Kaneria MV SP, Burkule D, Shukla A, Somani A, Nabar ST. Bilateral breast tuberculosis: A rare entity. *J Indian Acad Commun Med* 2006: 3.

Kant S, Mahajan V, Verma SK. Tubercular mastitis mimicking malignancy. *Internet Journal of Pulmonary Medicine* 2008; 9: 5-.

Kapan M, Toksöz Mt, BakIr ŞD, Sak ME, Evsen MS, *et al.* Tuberculosis of breast. *European Journal of General Medicine* 2010; 7: 216-9.

Khanna R, Prasanna GV, Gupta P, Kumar M, Khanna S, *et al.* Mammary tuberculosis: report on 52 cases. *Postgrad. Med. J.* 2002; 78: 422-4.

Khodabakhshi B, Mehravar F. Breast tuberculosis in northeast Iran: review of 22 cases. *BMC Womens Health* 2014; 14: 72.

Khurram M, Tariq M, Shahid P. Breast cancer with associated granulomatous axillary lymphadenitis: a diagnostic and clinical dilemma in regions with high prevalence of tuberculosis. *Pathol. Res. Pract.* 2007; 203: 699-704.

Kodali S, Baher A, Shah D. Safety of MRIs in patients with pacemakers and defibrillators. *Methodist Debakey Cardiovasc. J.* 2013; 9: 137-41.

Kolb TM, Lichy J, Newhouse JH. Comparison of the performance of screening mammography, physical examination, and breast US and evaluation of factors that influence them: an analysis of 27,825 patient evaluations. *Radiology* 2002; 225: 165-75.

Kuhl CK, Klaschik S, Mielcarek P, Gieseke J, Wardelmann E, *et al.* Do T2-weighted pulse sequences help with the differential diagnosis of enhancing lesions in dynamic breast MRI? *J. Magn. Reson. Imaging* 1999; 9: 187-96.

Kulchavenya E. Extrapulmonary tuberculosis: are statistical reports accurate? *Therapeutic advances in infectious disease* 2014; 2: 61-70.

Lacambra M, Thai TA, Lam CC, Yu AM, Pham HT, *et al.* Granulomatous mastitis: the histological differentials. *J. Clin. Pathol.* 2011; 64: 405-11.

Lancereaux, Charley. Tumeur tuberculeuse du sein, bulletin de la societe d anatomie. 1860.

Lee WK, Van Tonder F, Tartaglia CJ, Dagia C, Cazzato RL, *et al.* CT appearances of abdominal tuberculosis. *Clin. Radiol.* 2012; 67: 596-604.

Leeds IL, Magee MJ, Kurbatova EV, del Rio C, Blumberg HM, *et al.* Site of extrapulmonary tuberculosis is associated with HIV infection. *Clin. Infect. Dis.* 2012; 55: 75-81.

Machida Y, Tozaki M, Shimauchi A, Yoshida T. Two Distinct Types of Linear Distribution in Nonmass Enhancement at Breast MR Imaging: Difference in Positive Predictive Value between Linear and Branching Patterns. *Radiology* 2015; 276: 686-94.

Makanjuola D, Murshid K, Sulaimani SA, Saleh MA. Mammographic features of breast tuberculosis: The skin bulge and sinus tract sign. *Clin. Radiol.* 1996; 51: 354-8.

Malich A, Fischer DR, Wurdinger S, Boettcher J, Marx C, *et al.* Potential MRI interpretation model: differentiation of benign from malignant breast masses. *AJR Am. J. Roentgenol.* 2005; 185: 964-70.

Mann RM, Balleyguier C, Baltzer PA, Bick U, Colin C, *et al.* Breast MRI: EUSOBI recommendations for women's information. *Eur. Radiol.* 2015; 25: 3669-78.

Maroulis I, Spyropoulos C, Zolota V, Tzorakoleftherakis E. Mammary tuberculosis mimicking breast cancer: a case report. *J Med Case Rep* 2008; 2: 34.

Martinez V, Castilla-Lievre MA, Guillet-Caruba C, Grenier G, Fior R, *et al.* (18)F-FDG PET/CT in tuberculosis: an early non-invasive marker of therapeutic response. *Int. J. Tuberc. Lung Dis.* 2012; 16: 1180-5.

Mathur RV, M.V.; Chitimilla, S.K. Tuberculosis of breast: A case report. *The West London Medical Journal* 2009; 1: 4.

Mazurek GH, Jereb J, LoBue P, Iademarco MF, Metchock B, *et al.* Guidelines for Using the QuantiFERON®-TB Gold Test for Detecting Mycobacterium tuberculosis Infection, United States. *Centre for Disease Control* 2005; 54: 7.

McKendry RJ, . Giant cell arteritis (temporal arteritis) affecting the breast: report of two cases and review of published reports. *Annals of the rheumatic diseases [0003-4967]* 1990; 49: 1.

McKeown K, Wilkinson K. Tuberculous disease of the breast. *Br. J. Surg.* 1952; 39: 420.

Meerkotter D, Spiegel K, Page-Shipp LS. Imaging of tuberculosis of the breast: 21 cases and a review of the literature. *J. Med. Imaging Radiat. Oncol.* 2011; 55: 453-60.

Mehta G, Mittal A, Verma S. Breast tuberculosis- clinical spectrum and management. *The Indian Journal Of Surgery* 2010; 72: 433-7.

Mehta S. Patterns of systemic uptake of 18-FDG with positron emission tomography/computed tomography (PET/CT) studies in patients with presumed ocular tuberculosis. *Ocul. Immunol. Inflamm.* 2012; 20: 434-7.

Michell MJ, Iqbal A, Wasan RK, Evans DR, Peacock C, *et al.* A comparison of the accuracy of film-screen mammography, full-field digital mammography, and digital breast tomosynthesis. *Clin. Radiol.* 2012; 67: 976-81.

Mirsaeidi SM, Masjedi MR, Mansouri SD, Velayati AA. Tuberculosis of the breast: report of 4 clinical cases and literature review. *East Mediterr Health J* 2007; 13: 670-6.

Moskowitz M, Pemmaraju S, Fidler JA, Sutorius DJ, Russell P, *et al.* On the diagnosis of minimal breast cancer in a screenee population. *Cancer* 1976; 37: 2543-52.

NHS Breast Screening Programme. Guidelines on organising the surveillance of women at higher risk of developing breast cancer in an NHS Breast Screening Programme England2013. Available from: https://www.gov.uk/government/uploads/system/uploads/attachment_data/file/439634/nhsbsp73.pdf.

Oh KK, Kim JH, Kook SH, . Imaging of tuberculous disease involving breast *Eur. Radiol.* 1998; 8: 6.

Partridge SC, DeMartini WB, Kurland BF, Eby PR, White SW, *et al.* Quantitative diffusion-weighted imaging as an adjunct to conventional breast MRI for improved positive predictive value. *AJR Am. J. Roentgenol.* 2009; 193: 1716-22.

Peng J, Ouyang Y, Fang WD, Luo TY, Li YM, *et al.* Differentiation of intracranial tuberculomas and high grade gliomas using proton MR spectroscopy and diffusion MR imaging. *Eur. J. Radiol.* 2012; 81: 4057-63.

Peng Y, Jiang Y, Antic T, Giger ML, Eggener SE, *et al.* Validation of quantitative analysis of multiparametric prostate MR images for prostate cancer detection and aggressiveness assessment: a cross-imager study. *Radiology* 2014; 271: 461-71.

Peto HM, Pratt RH, Harrington TA, LoBue PA, Armstrong LR. Epidemiology of extrapulmonary tuberculosis in the United States, 1993-2006. *Clin. Infect. Dis.* 2009; 49: 1350-7.

Popli MB, Kumari A, Popli V. Proton magnetic resonance spectroscopy in breast tuberculosis. *European Journal of Radiology Extra* 2010; 74: e59-e63.

Qu RF, Guo DR, Chang ZX, Meng J, Sun Y, *et al.* Differential Diagnosis of Benign and Malignant Breast Tumors Using Apparent Diffusion Coefficient Value Measured Through Diffusion-Weighted Magnetic Resonance Imaging. *J. Comput. Assist. Tomogr.* 2015; 39: 513-22.

Rajagopala S, Agarwal R. Tubercular Mastitis in Men: Case Report and Systematic Review. *Am. J. Med.* 2008; 121: 539-44.

Rogalla P M, Kloeters C, MD, Hein P, MD. CT Technology Overview: 64-Slice and Beyond. *Radiol. Clin. North Am.* 2008; 47: 11.

Sakr AA, Fawzy RK, Fadaly G, Baky MA. Mammographic and sonographic features of tuberculous mastitis. *Eur. J. Radiol.* 2004; 51: 54-60.

Sathekge M, Maes A, D'Asseler Y, Vorster M, Gongxeka H, *et al.* Tuberculous lymphadenitis: FDG PET and CT findings in responsive and nonresponsive disease. *Eur. J. Nucl. Med. Mol. Imag.* 2012; 39: 7.

Sathekge M, Maes A, Kgomo M, Stoltz A, Van de Wiele C. Use of 18F-FDG PET to predict response to first-line tuberculostatics in HIV-associated tuberculosis. *J Nucl Med* 2011; 52: 880-5.

Sathekge M, Maes A, Pottel H, Stoltz A, Van de Wiele C. Dual time-point FDG PET/CT for differentiating benign from malignant solitary pulmonary nodules in a TB endemic area. *The South African medical journal* 2010; 100: 4.

Sen M, Gorpelioglu C, Bozer M. Isolated primary breast tuberculosis - Report of three cases and review of the literature. *Clinics (Sao Paulo)* 2009; 64: 607-10.

Shushtari MHS, Alavi SM, Talaeizadeh A. Breast tuberculosis: Report of nine cases of extra pulmonary tuberculosis with breast mass. *Pakistan Journal of Medical Sciences* 2011; 27: 582-5.

Soussan M, Brillet P-Y, Mekinian A, Khafagy A, Nicolas P, *et al.* Patterns of pulmonary tuberculosis on FDG-PET/CT. *Eur. J. Radiol.* 2012; 81: 2872-6.

Soussan M, Cyrta J, Pouliquen C, Chouahnia K, Orlhac F, *et al.* Fluorine 18 fluorodeoxyglucose PET/CT volume-based indices in locally advanced non-small cell lung cancer: prediction of residual viable tumor after induction chemotherapy. *Radiology* 2014; 272: 875-84.

Sriram K, Moffatt D, Stapledon R. Tuberculosis infection of the breast mistaken for granulomatous mastitis: a case report. *Cases J* 2008; 1: 273.

Stelzmueller I, Huber H, Wunn R, Hodolic M, Mandl M, *et al.* 18F-FDG PET/CT in the Initial Assessment and for Follow-up in Patients With Tuberculosis. *Clin. Nucl. Med.* 2015.

Tandon M, Chintamani, Panwar P. Breast tuberculosis at a tertiary care centre: a retrospective analysis of 22 cases. *Breast Dis.* 2014; 34: 127-30.

Tewari M, Shukla H. Breast tuberculosis: diagnosis, clinical features & management. *Indian J. Med. Res.* 2005; 122: 103.

The Royal College of Radiologists. Guidance on screening and sypmtomatic breast imaging. 2013.

Van Gomez Lopez O, Garcia Vicente AM, Honguero Martinez AF, Jimenez Londono GA, Vega Caicedo CH, *et al.* (18)F-FDG-PET/CT in the assessment of pulmonary solitary nodules: comparison of different analysis methods and risk variables in the prediction of malignancy. *Translational lung cancer research* 2015; 4: 228-35.

Veerysami M, Freeth M, Carmichael AR, Carmichael P. Wegener's granulomatosis of the breast. *Breast Journal* 2006; 12: 268-70.

Velpeau A. Traité des maladies du sein. Paris: Victor Masson; 1854.

Verfaillie G, Goossens A, Lamote J. Atypical Mycobacterium Breast Infection. *The breast journal* 2004; 10: 60-.

Williams A, Stockely H, Filobbos R. A pictorial review of the imaging findings in abdominal tuberculosis. European Congress of Radiology; Vienna2010.

Winzer K-J, Menenakos C, Braumann C, Guski H, Mueller JM. (2005). Breast mass due to pectoral muscle tuberculosis mimicking breast cancer in a male patient (Vol. 9, pp. 176-7).

Woodhams R, Matsunaga K, Kan S, Hata H, Ozaki M, *et al.* ADC mapping of benign and malignant breast tumors. *Magn. Reson. Med. Sci.* 2005; 4: 35-42.

World Health Organisation. Global Tuberculosis report 2014. World Health Organization, 2014.

World Health Organisation. Global tuberculosis report 2015. World Health Organisation, 2015.

World Health Organization. Interim WHO clinical staging of hiv/aids and hiv/aids case definitions for surveillance - African regions. 2005.

Woyke S, Domagala W, Gniewosz Z. Tuberculosis of the breast clinically mimicking carcinoma and diagnosed by thin needle aspiration biopsy. *Pathology - Research and Practice* 1980; 168: 256-61.

Yabuuchi H, Matsuo Y, Kamitani T, Setoguchi T, Okafuji T, *et al.* Non-mass-like enhancement on contrast-enhanced breast MR imaging: lesion characterization using combination of dynamic contrast-enhanced and diffusion-weighted MR images. *Eur. J. Radiol.* 2010; 75: e126-32.

Yamaguchi K, Schacht D, Nakazono T, Irie H, Abe H. Diffusion weighted images of metastatic as compared with nonmetastatic axillary lymph nodes in patients with newly diagnosed breast cancer. *J. Magn. Reson. Imaging* 2015; 42: 771-8.

Yang Z, Kong Y, Wilson F, Foxman B, Fowler AH, *et al.* Identification of risk factors for extrapulmonary tuberculosis. *Clin. Infect. Dis.* 2004; 38: 199-205.

Yili Z, Xiaoyan H, Hongwen D, Yun Z, Xin C, *et al.* The value of diffusion-weighted imaging in assessing the ADC changes of tissues adjacent to breast carcinoma. *BMC Cancer* 2009; 9: 18.

Yilmaz F, Tastekin G. Sensitivity of (18)F-FDG PET in evaluation of solitary pulmonary nodules. *Int. J. Clin. Exp. Med.* 2015; 8: 45-51.

Zandrino F, Monetti F, Gandolfo N. Primary tuberculosis of the breast. *Acta Radiol.* 2000; 41: 61-3.

Zhao J, Guan H, Li M, Gu H, Qin J, *et al.* (2015). Significance of the ADC ratio in the differential diagnosis of breast lesions. *Acta Radiol.* doi:10.1177/0284185115590286

APPENDIX

Breast tuberculosis: radiology spectrum with clinical correlation – a retrospective analysis of 65 patients

DP Ramaema

(Poster presented at European Congress of Radiology, Vienna, Austria, March 2015)

EPOS™
Electronic Presentation Online System
ESR
European Society of Radiology

Breast tuberculosis: radiology spectrum with clinical correlation - a retrospective analysis of 65 patients

Poster No.:	C-1154
Congress:	ECR 2015
Type:	Scientific Exhibit
Authors:	D. P. Ramaema, I. Buccimazza, R. J. Hift; Durban/ZA
Keywords:	Breast, Mammography, Ultrasound, Treatment effects, Infection, Inflammation
DOI:	10.1594/ecr2015/C-1154

Any information contained in this pdf file is automatically generated from digital material submitted to EPOS by third parties in the form of scientific presentations. References to any names, marks, products, or services of third parties or hypertext links to third-party sites or information are provided solely as a convenience to you and do not in any way constitute or imply ECR's endorsement, sponsorship or recommendation of the third party, information, product or service. ECR is not responsible for the content of these pages and does not make any representations regarding the content or accuracy of material in this file.
As per copyright regulations, any unauthorised use of the material or parts thereof as well as commercial reproduction or multiple distribution by any traditional or electronically based reproduction/publication method ist strictly prohibited.
You agree to defend, indemnify, and hold ECR harmless from and against any and all claims, damages, costs, and expenses, including attorneys' fees, arising from or related to your use of these pages.
Please note: Links to movies, ppt slideshows and any other multimedia files are not available in the pdf version of presentations.
www.myESR.org

Aims and objectives

Purpose:

Introduction:

It is estimated that over 1 billion people worldwide have tuberculosis (TB) [1]. However, breast tuberculosis (BTB) is a rare condition. The incidence is quoted as less than 0.1% of all surgical breast lesions seen in developed countries and 3-4.5% of breast lesions in countries where BTB is endemic [2-5], although even in this setting, carcinoma is far more commonly encountered [6]. While BTB is considered a manifestation of extrapulmonary tuberculosis (EPTB), it represents only about 0.1 % of the disease burden of EPTB. However, there has been a resurgence of EPTB due to Human Immune Deficiency (HIV), with estimated incidences as high as 50% in countries where HIV infection is endemic [7].

Both breasts are equally affected. In approximately 3% of cases, tuberculosis may be found bilaterally [8]. Up to 70% of cases may have associated axillary lymphadenopathy, often with visible axillary swelling [9]. Constitutional symptoms are unusual in the absence of systemic and particularly pulmonary tuberculosis [6].

There are no clinical or radiological features which are absolutely diagnostic of breast tuberculosis. The diagnosis is usually readily confirmed by biopsy with histology or fine needle aspiration and staining for acid-fast bacilli (AFB), Mycobacterial culture or the polymerase chain reaction (PCR). Whereas the main differential diagnosis is carcinoma, other considerations are idiopathic granulomatous mastitis and fungal infections. Most patients respond to standard anti-tuberculous therapy (ATT) [10]. It has been suggested that patients in endemic areas presenting with a breast mass in whom histology reveals granulomatous inflammation, should receive ATT, even if culture results are negative for TB [11]. There have been reports that occasionally sinuses, fistulae and deformities may require primary localised excision or simple mastectomy, but this is not standard care [6].

The aim of our study was to identify different radiological patterns of BTB, to assess available treatment options and response to treatment.

Methods and materials

We identified 64 patients with histological or cytological confirmed diagnosis of breast tuberculosis. One patient with discharging axillary nodes and breast oedema was included even though cytology was not confirmatory. Therefore 65 patients were included in the data analysis. Patients were diagnosed between 2000 and 2013. Collection of data from the Breast Clinic was performed. The study was approved by the institutional review board.

Retrospective chart and radiology review focused on demographic, clinical, mammographic and ultrasound patterns, diagnostic and treatment methods.

Mammograms Medio-Lateral Oblique (MLO) and Cranio-Caudal (CC) views were obtained from a standard analogue mammographic unit (+/- digital processing). Ultrasound images were obtained on the standard unit using 7.5 - 12.5 MHz linear probe. Classification of mammographic and ultrasound patterns is shown in (Fig. 1 and Fig. 2) respectively.

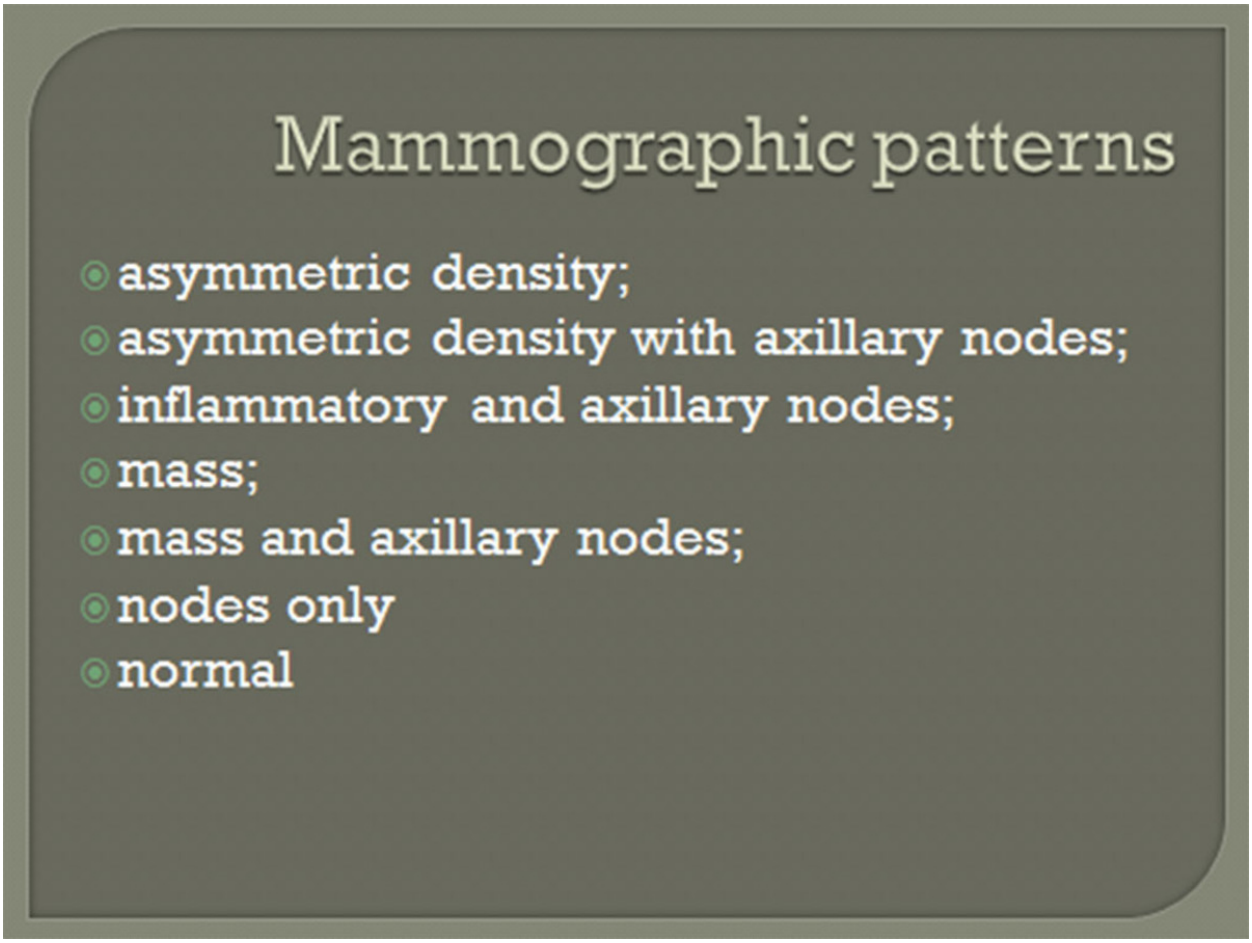

Fig. 1: Mammographic patterns.
References: Diagnostic Radiology, Nelson R Mandela School of Medicine - Durban/ZA

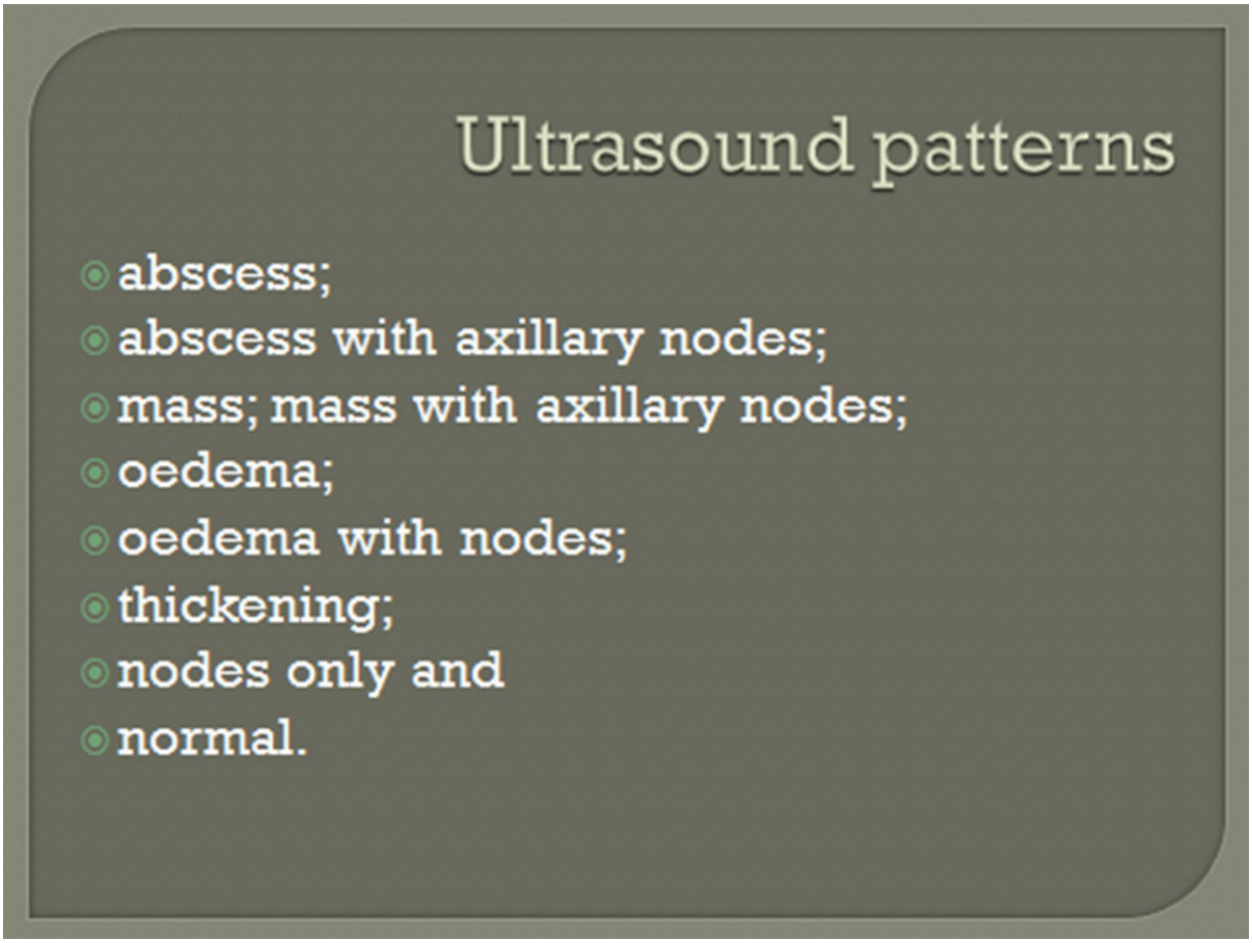

Fig. 2: Ultrasound patterns.
References: Diagnostic Radiology, Nelson R Mandela School of Medicine - Durban/ZA

Histological and microbiological diagnosis was done by obtaining core biopsy samples using 14Gauge needle. Cytological diagnosis was done by Fine Needle Aspiration (FNA). Lesion localisation was achieved by either palpation or ultrasound guided.

Statistical analysis

Medcalc statistical software using descriptive statistics was used to analyse results.

Images for this section:

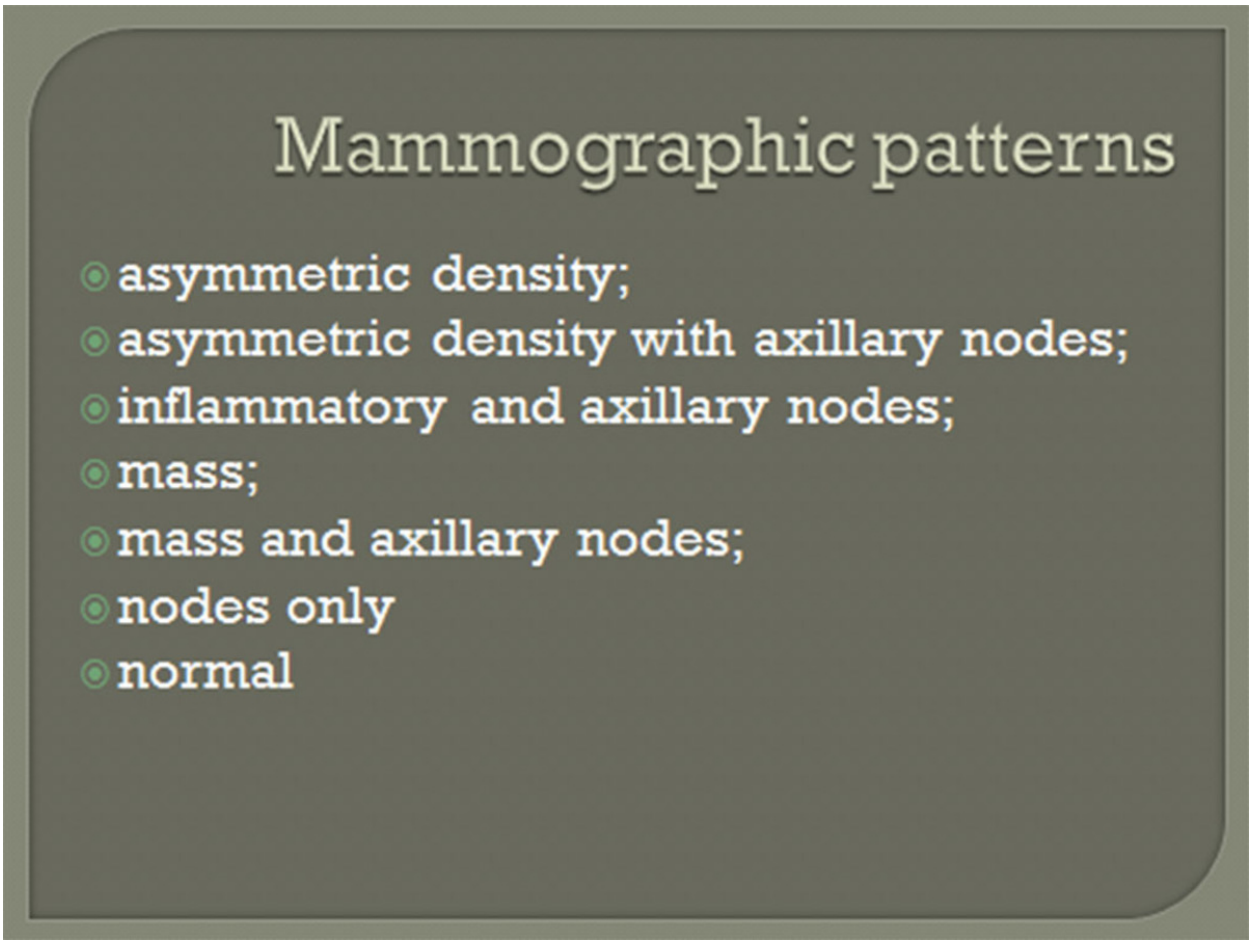

Fig. 1: Mammographic patterns.

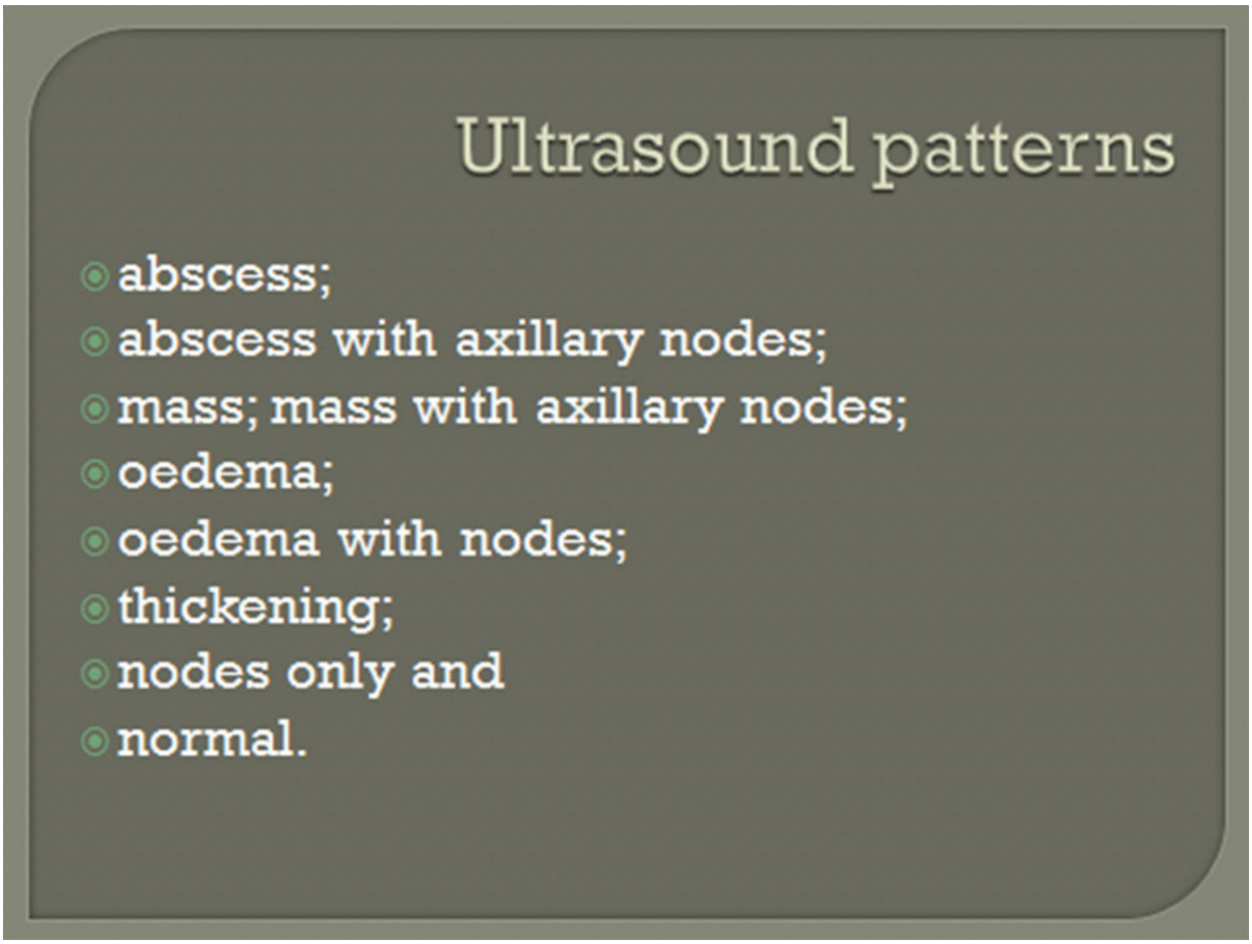

Fig. 2: Ultrasound patterns.

Results

Demographics and clinical presentation

Summary of demographics and clinical presentation is shown in Table 1.

Characteristics	**Total (*n* = 65*), n (*%)**
Gender	
Female (98.5%)	64 (98.5)
Male (1.5%)	1 (1.5)
Age at Presentation	
Range 23yr - 69 yr	
Mean (SD) 38.5yr (10.3	
Side	
Left	30 (46.2)
Right	33 (50.8)
Unknown	2 (3.1)
Axillary nodes	
Yes	21 (33.9)
No	41 (66.1)

Table 1: Age range was 23 to 69 years with a mean age of 38.5 years. There was no right or left side preference. Almost one third of patients had associated axillary nodes.

References: Diagnostic Radiology, Nelson R Mandela School of Medicine - Durban/ZA

Clinical Presentation

Proportions of clinical patterns is depicted in (Fig. 3). The most common presentation (40%) was an inflammatory mass, also termed diffuse/disseminated form. The second and third presentations were oedema with adenitis and the nodular (focal mass), both of which occurred in almost equal proportions, being 24.6% and 26.2% respectively.

Although on clinical assessment, the abscess variety was reported in only *n =2 (*3.1%) cases, on ultrasound this presentation was the most common, seen in *n =16* (39%), with or without adenitis. Based on our findings we propose to classify BTB into four forms;

- i) Inflammatory mass/disseminated,
- ii) Oedema with adenitis,
- iii) Abscess
- iv) Nodular (focal mass).
- Classifications i), iii, and iv) can occur with or without associated axillary lymphadenopathy.

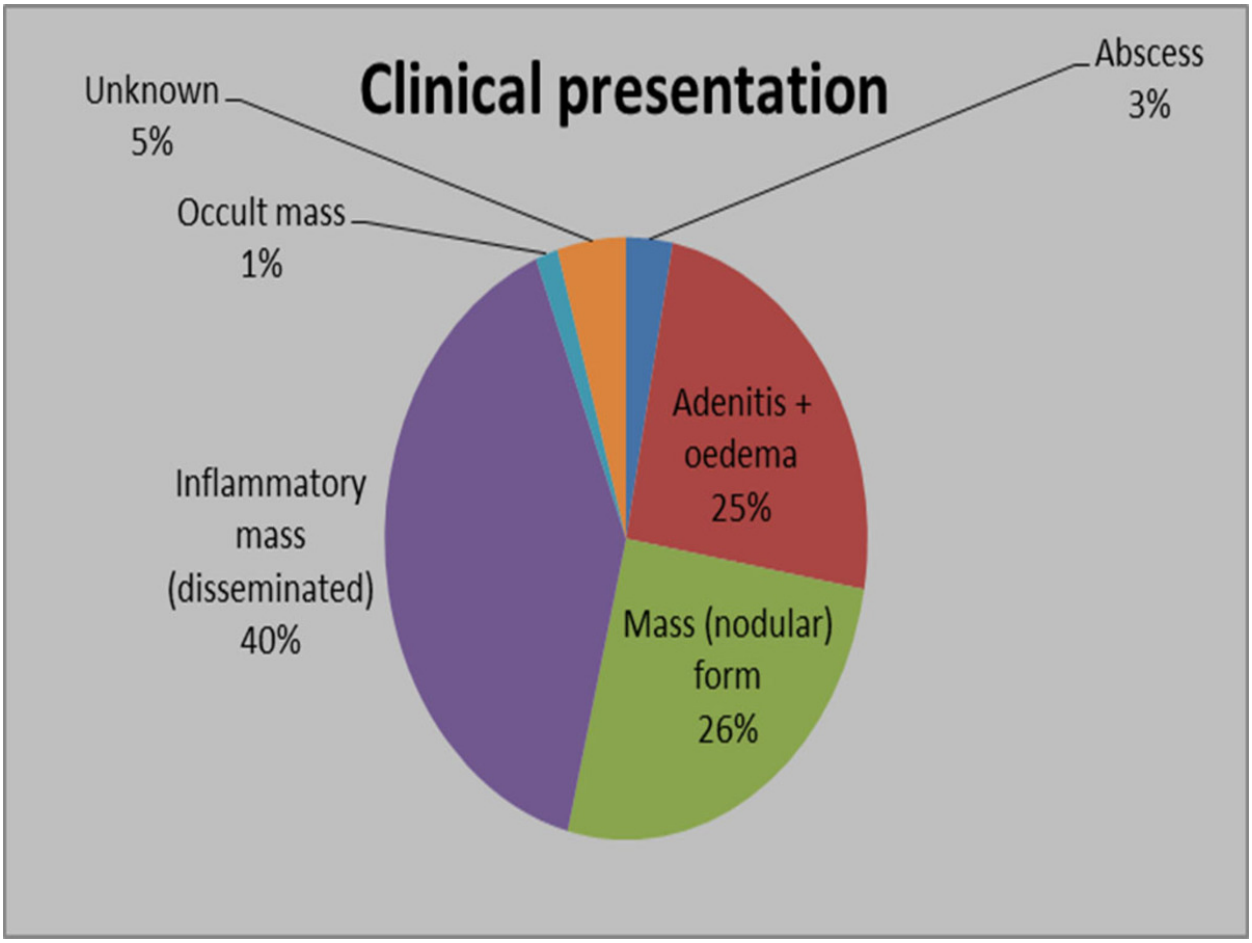

Fig. 3: Clinical presentation proportions.
References: Diagnostic Radiology, Nelson R Mandela School of Medicine - Durban/ZA

Associated clinical features

Record of associated clinical features are recorded in Table 2.

Characteristics	n (%)
History pulmonary TB (n = 47)	
CXR normal	32 (49.2)
CXR abnormal	15 (23.1)
Pregnant/lactating (n = 65)	
No	64 (98.5)
Yes	1 (1.5)
HIV Status (n = 47)	
Negative	12 (18.5)
Positive	34 (52.3)
Refused testing	1 (1.5)

Table 2: Amongst all 65 patients, only one was lactating, whereas 34 were HIV positive. Whilst 47 patients had history of prior pulmonary TB, only 15 had radiological evidence of either prior or concurrent pulmonary TB.

References: Diagnostic Radiology, Nelson R Mandela School of Medicine - Durban/ZA

Radiological features

Mammography and ultrasound findings are summarised in (Fig. 4 and Fig. 5) respectively.

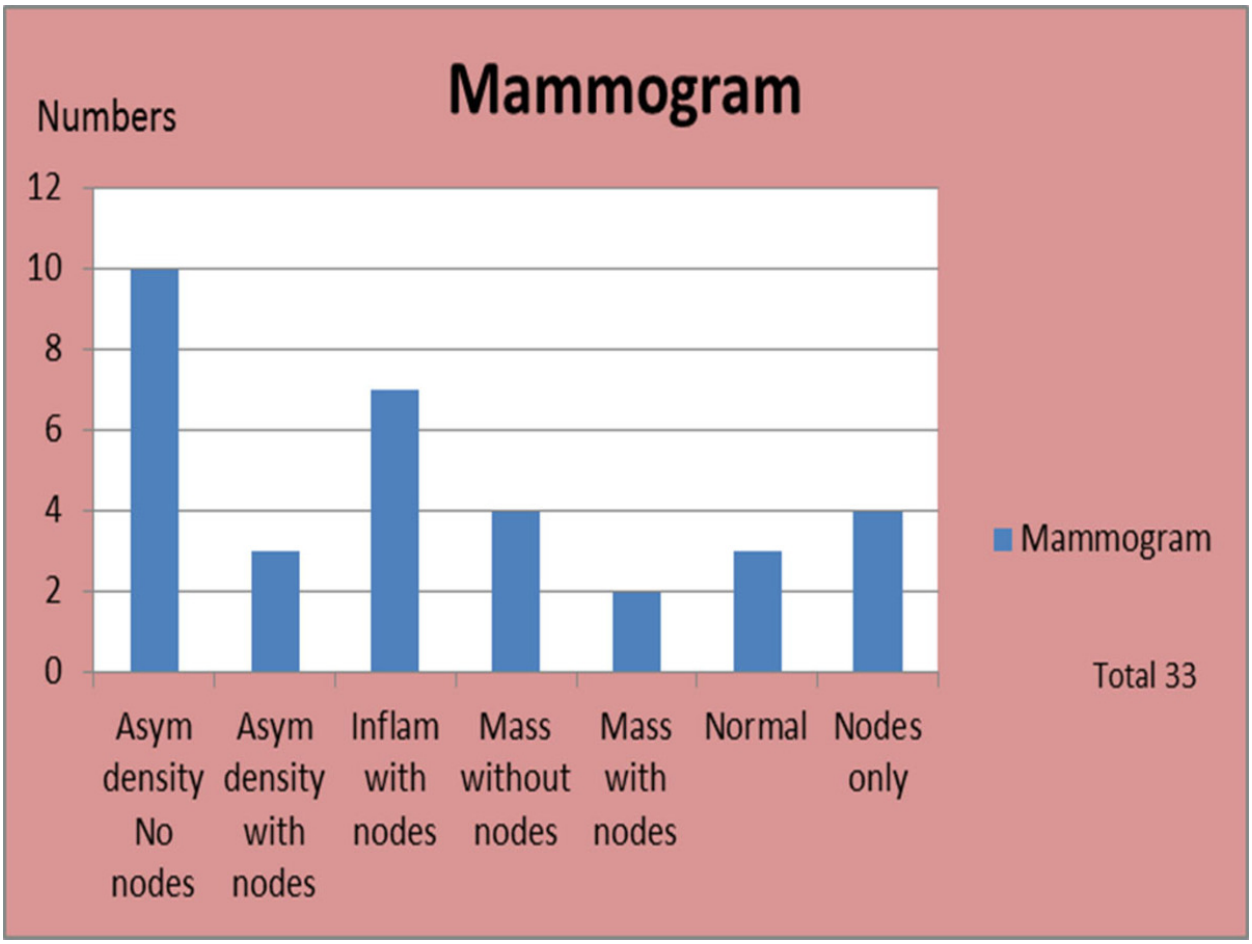

Fig. 4: Of 33 patients who had mammograms, 16 demonstrated ipsilateral or bilateral axillary lymphadenopathy. Asymmetric density pattern was seen in 13 cases.
References: Diagnostic Radiology, Nelson R Mandela School of Medicine - Durban/ ZA

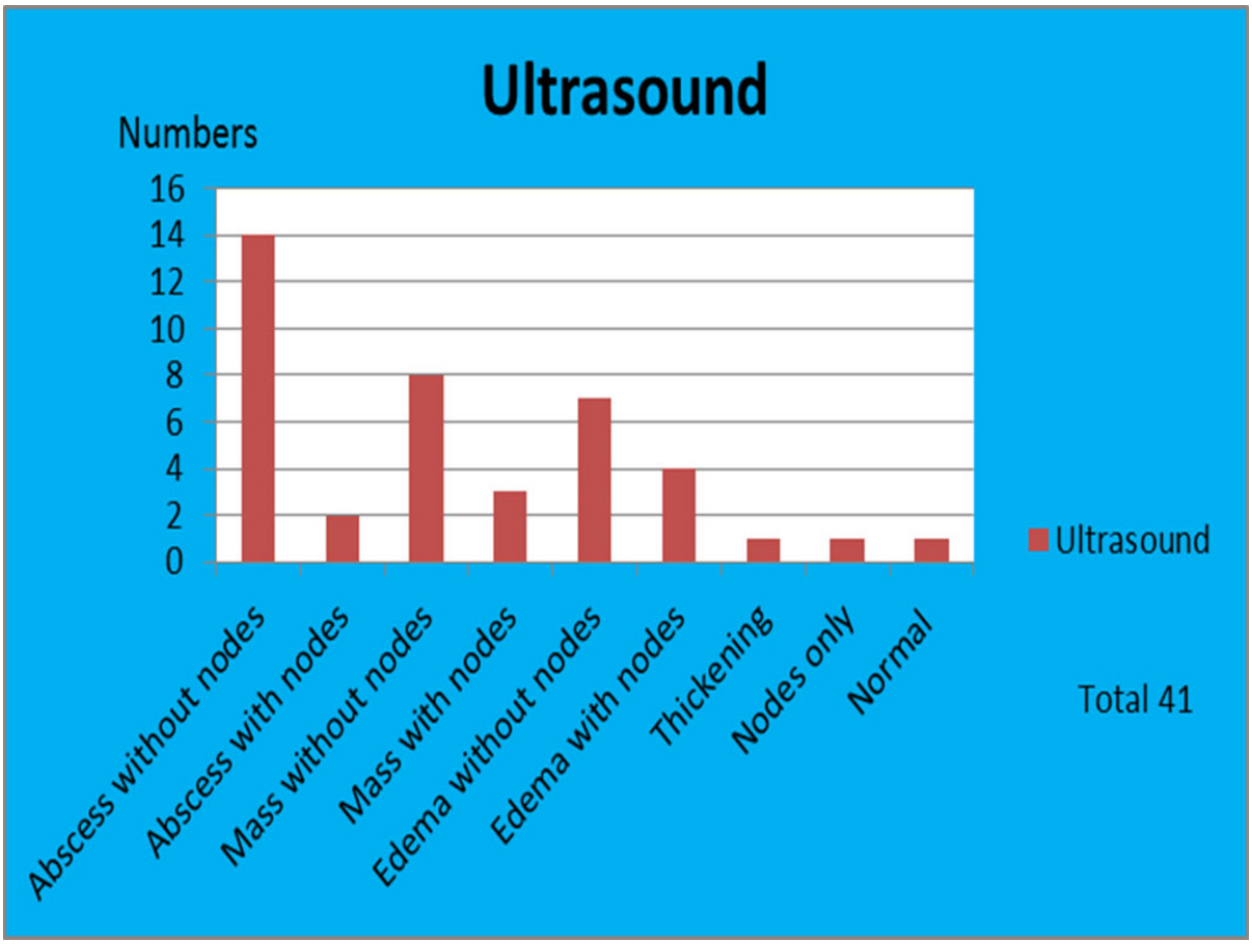

Fig. 5: Ultrasound was performed in 41 patients. The commonest pattern was abscess variety in 16 cases (39%).
References: Diagnostic Radiology, Nelson R Mandela School of Medicine - Durban/ZA

Clinical-radiological patterns

i) Inflammatory/Disseminated

This pattern was the most common clinical presentation. However, amongst those who had mammograms, this pattern was seen in 21.2% (Fig. 6).

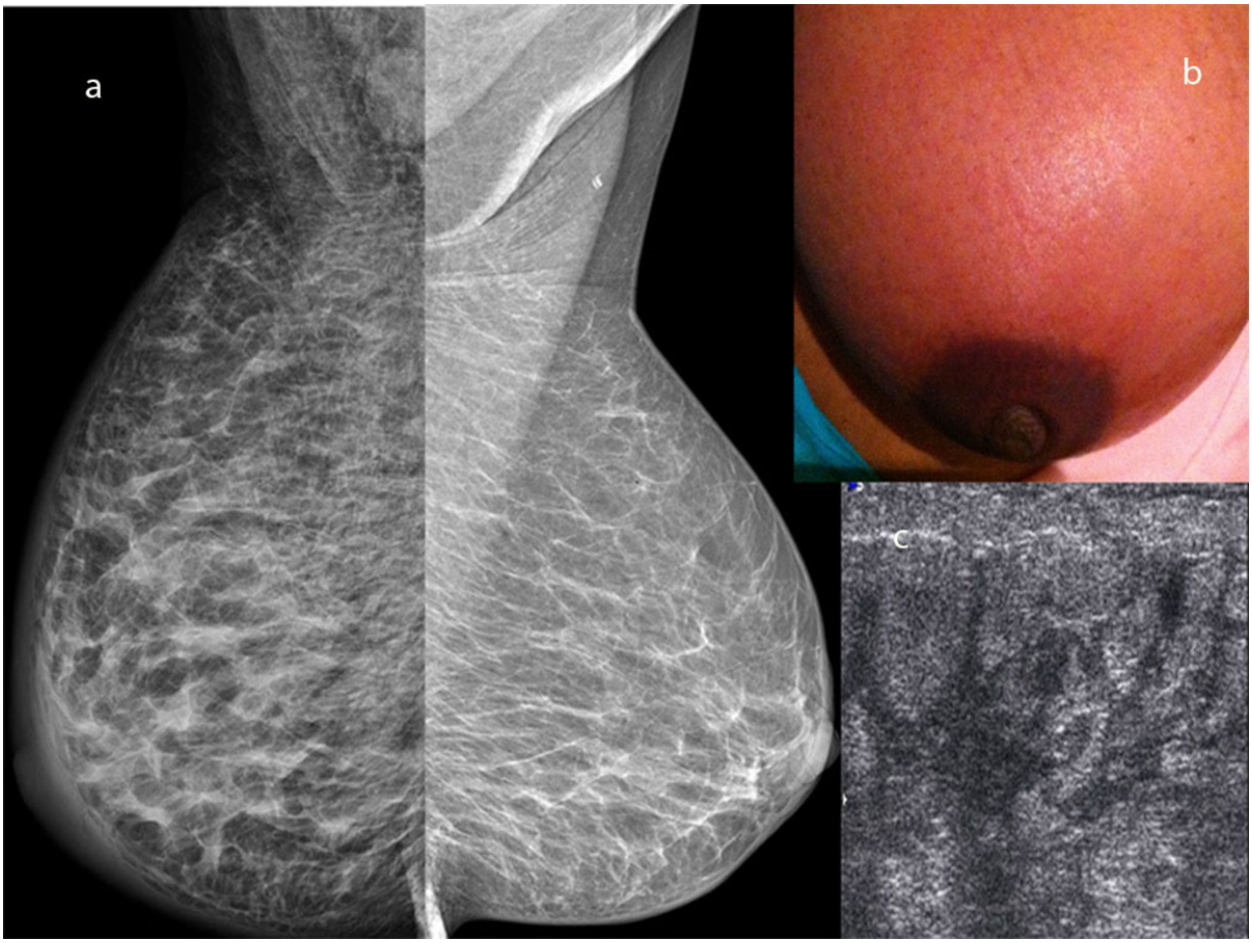

Fig. 6: Inflammatory/Disseminated Breast tuberculosis. Images taken from various patients. A. Mammogram MLO views. The right breast is enlarged. Non-specific diffuse stromal thickening and skin is oedema. B. Left breast photograph. Inflammatory skin change. C. Ultrasound images showing diffuse trabecular thickening with oedema as hypoechoic bands in between hyperechoic fibro-fatty tissue.
References: Diagnostic Radiology, Nelson R Mandela School of Medicine - Durban/ZA

We noted that all cases with inflammatory/disseminated form also had nodes. This supports the hypothesis that this form may be due to either reactive oedema, or retrograde spread from the axillary lymph nodes [12]. To date, there has not been a study to specifically determine whether AFBs are present within the oedematous or diffusely inflamed breast. The major differential diagnosis of this form is inflammatory breast cancer. However, the combination of an inflammatory breast lesion and sinuses or fistulae favours BTB from cancer [13]. On ultrasound some appeared as diffuse trabecular thickening and oedema (Fig. 6C), whereas others demonstrated a diffuse inflammatory mass.

Corresponding Magnetic Resonance Imaging (MRI) for the inflammatory BTB pattern appears as enlarged and oedematous breast (Fig. 7).

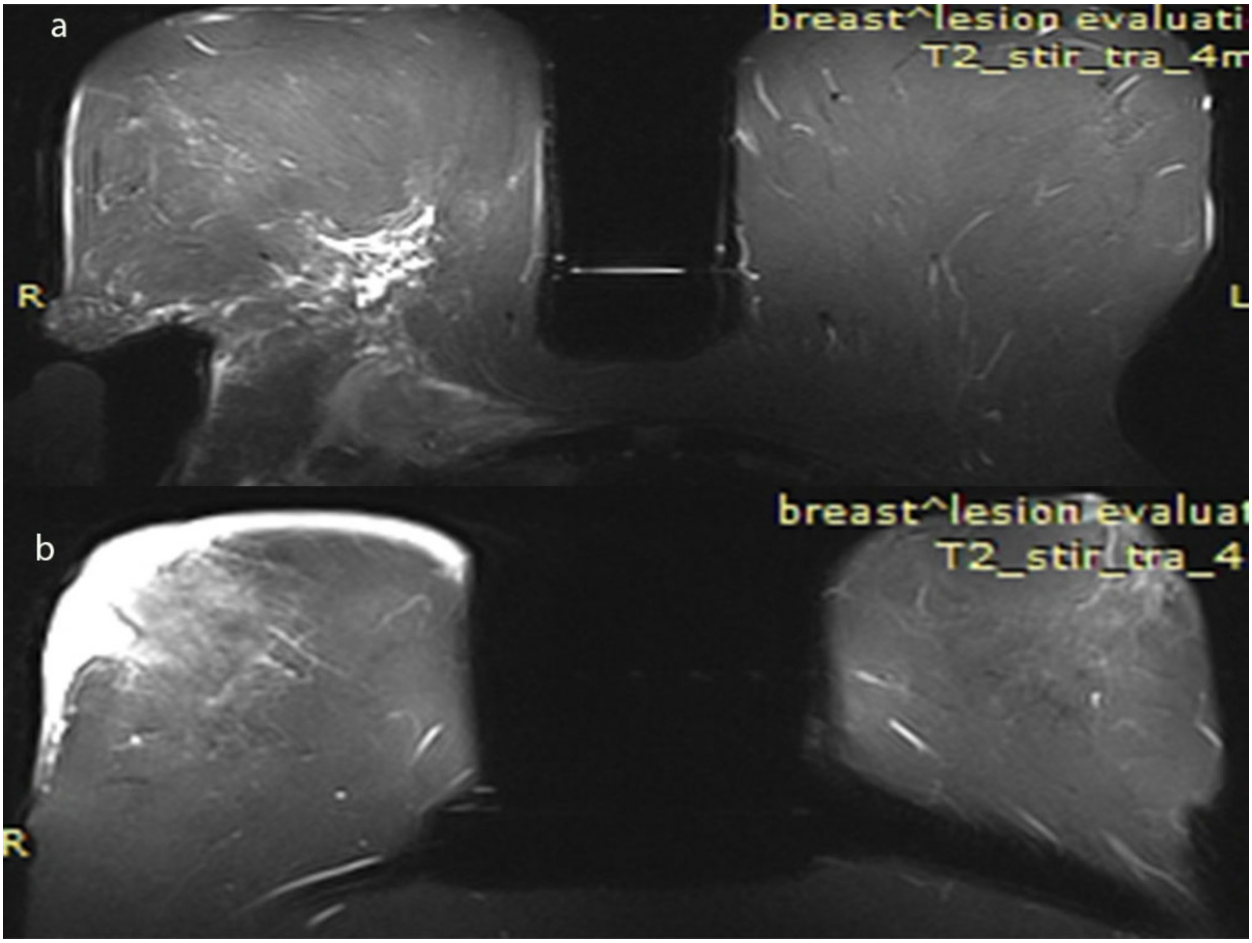

Fig. 7: Breast MRI T2 STIR axial image. A. The right breast has diffuse trabecular hyperintensity, more intense posteriorly abutting the pectoral muscles. B. Skin oedema. ***References:*** Diagnostic Radiology, Nelson R Mandela School of Medicine - Durban/ZA

ii) Oedema with adenitis

The clinical presentation of oedema was noted in 24.6% (Fig. 8). Ultrasound pattern of oedema was seen in *n=11* (26.9%). This pattern can be found in other forms of mastitis.

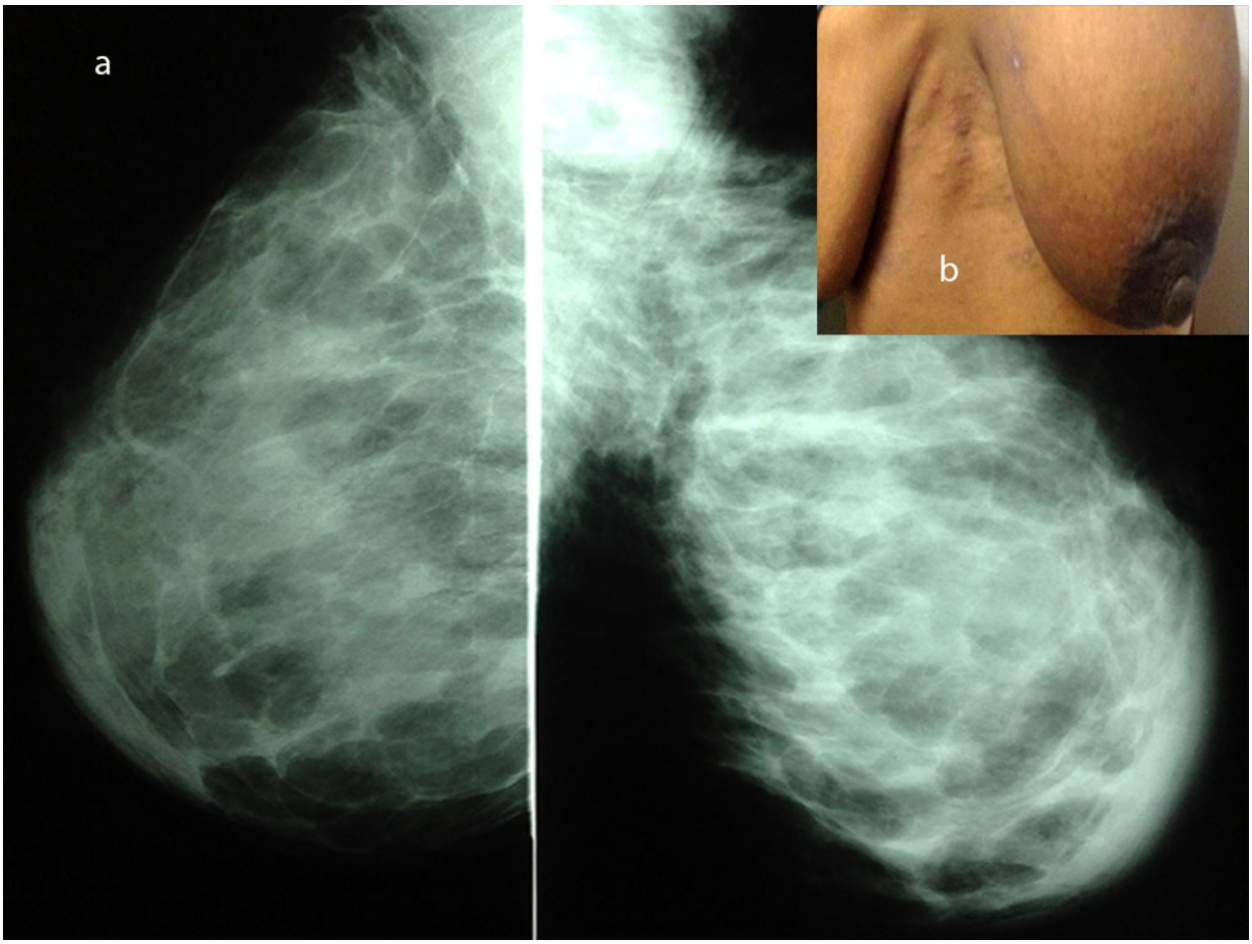

Fig. 8: A. Mammogram MLO views. The left breast is enlarged. Skin oedema and enlarged left axillary nodes are evident. B. Left breast photograph from same patient. The Left breast is larger than the right. (Note: No evidence of skin inflammation, in comparison to the inflammatory pattern).
References: Diagnostic Radiology, Nelson R Mandela School of Medicine - Durban/ZA

iii) Abscess variety

Even though clinical evaluation classified abscess variety in only 3.1%, ultrasound showed this pattern to be the most common, seen in *n= 18 (*39%), with or without adenitis.

On ultrasound it appears as complex solid-cystic heterogeneous hypoechoic mass and fluid collections. In our study, asymmetric density was the commonest mammographic pattern, *n= 13 (*39.4%) associated with this classification. The differential diagnosis is that of a pyogenic abscess, and indeed some of our patients had received antibiotics treatment, it was only after lack of response to this treatment that the diagnosis of tubercular abscess was considered. It is therefore important to obtain sample specifically

for TB analysis in all cases of non-lactational breast abscess, even if there is no history of TB elsewhere.

iv) Nodular (focal mass)

Clinically this form presented as a focal mass. On mammogram the focal mass opacities had variable outline, some had smooth margins, whilst others were irregular. Some were single, whereas others were multiple (Fig. 9A and B).

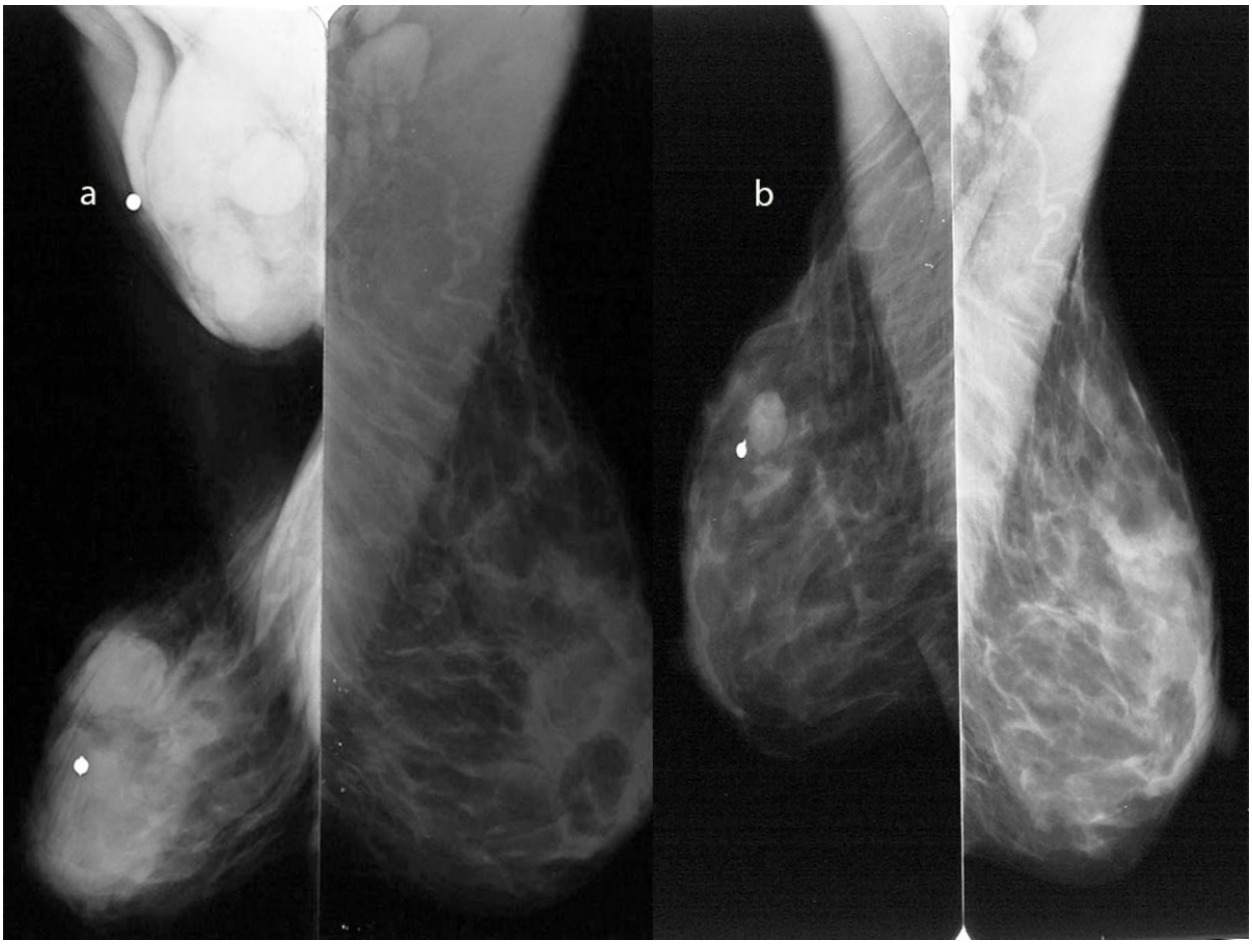

Fig. 9: Nodular form breast tuberculosis. Mammogram MLO views. A. At presentation. Multiple rounded mass opacities in right breast, and enlarged dense right axillary nodes. B. After 4 months of treatment with ATT. One small round mass opacity remains in upper part.
References: Diagnostic Radiology, Nelson R Mandela School of Medicine - Durban/ZA

This was the third commonest mammographic pattern seen in 18.2% of patients. On ultrasound this form appeared as a hypoechoic solid or heterogeneous mass with a

variable outline ranging from well-defined round to irregular. Lesion size based on ultrasound ranged from 0.9cm - 6.1cm. The differential diagnosis of this form can range from benign fibroadenoma to breast cancer depending on the lesion character on imaging. We did not find microcalcification to be a feature in our study.

v) Tuberculous lymphadenitis

Although isolated lymphadenitis was not reported on clinical presentation, it was seen in *n=4 (12.1%)* of mammograms and *n= 1 (2.4%)* of ultrasounds examinations. Nodes were intramammary, axillary or both (Fig. 10).

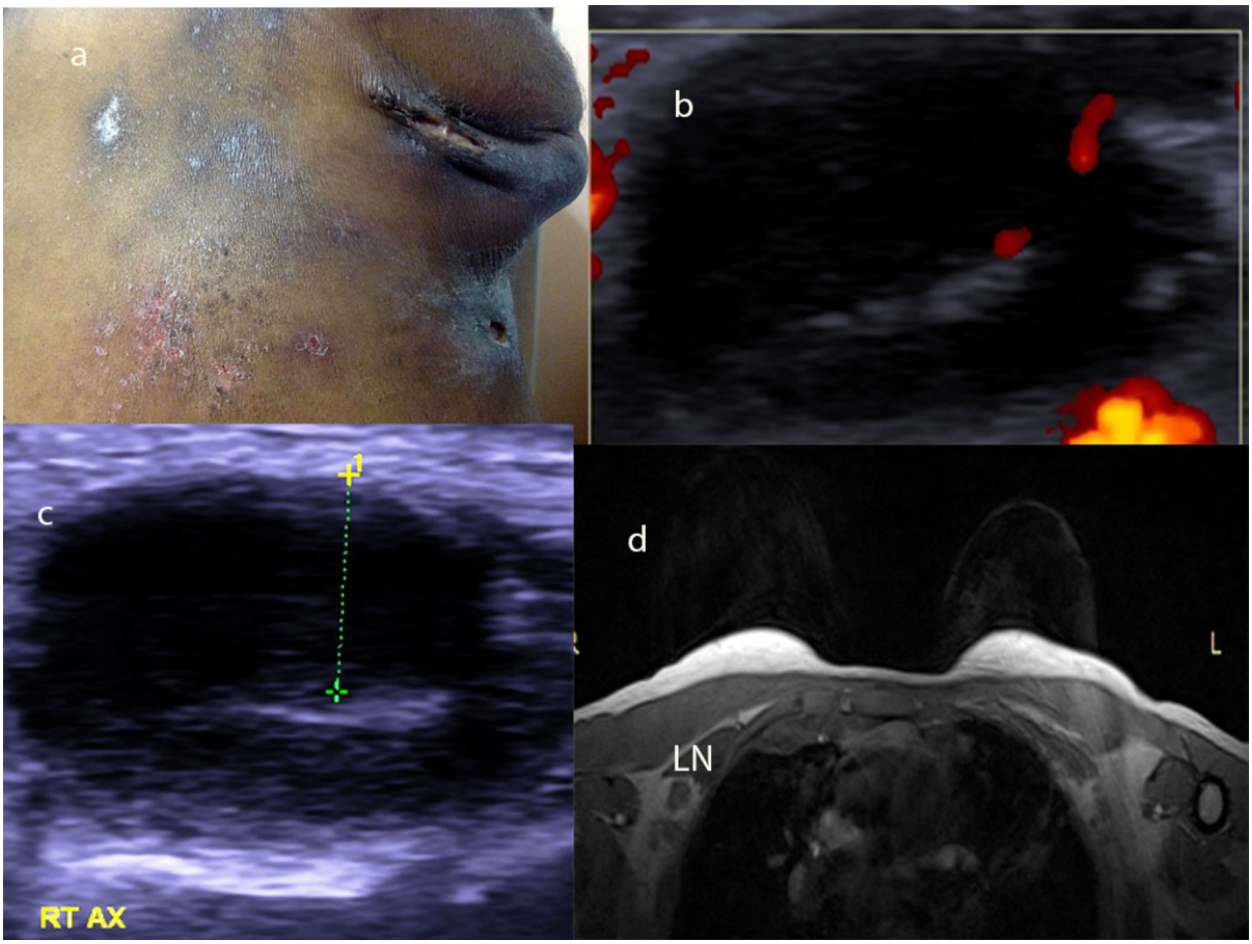

Fig. 10: Tuberculous lymphadenitis. A. Left axilla enlarged nodes discharging onto skin sinuses. B. Ultrasound Doppler, hilum vessel and thick cortex seen. C. Ultrasound shows node with thick 7mm cortex (callipers). D. Breast MRI T1 post contrast axial image. Right axillary nodes (LN) have peripheral rim enhancement and central low signal (PRECLO).

References: Diagnostic Radiology, Nelson R Mandela School of Medicine - Durban/ZA

Intra-mammary nodes appeared as well defined round dense masses on mammogram. These can be confused with a breast mass when they are solitary. Radiological differentiation of tuberculous axillary nodes from metastatic nodes remains difficult. In our series axillary nodes appeared as oval, hypoechoic solid masses with thick cortices and loss of normal fatty hilum. This ultrasound appearance cannot be differentiated from that of a malignant or metastatic lymph node. Another author described nodes to have peripheral enhancement with central low attenuation (PRECLO) on PET/CT [14].

Pathology

Histology diagnosis was 94% sensitive compared to 28% for cytology (Fig. 11).

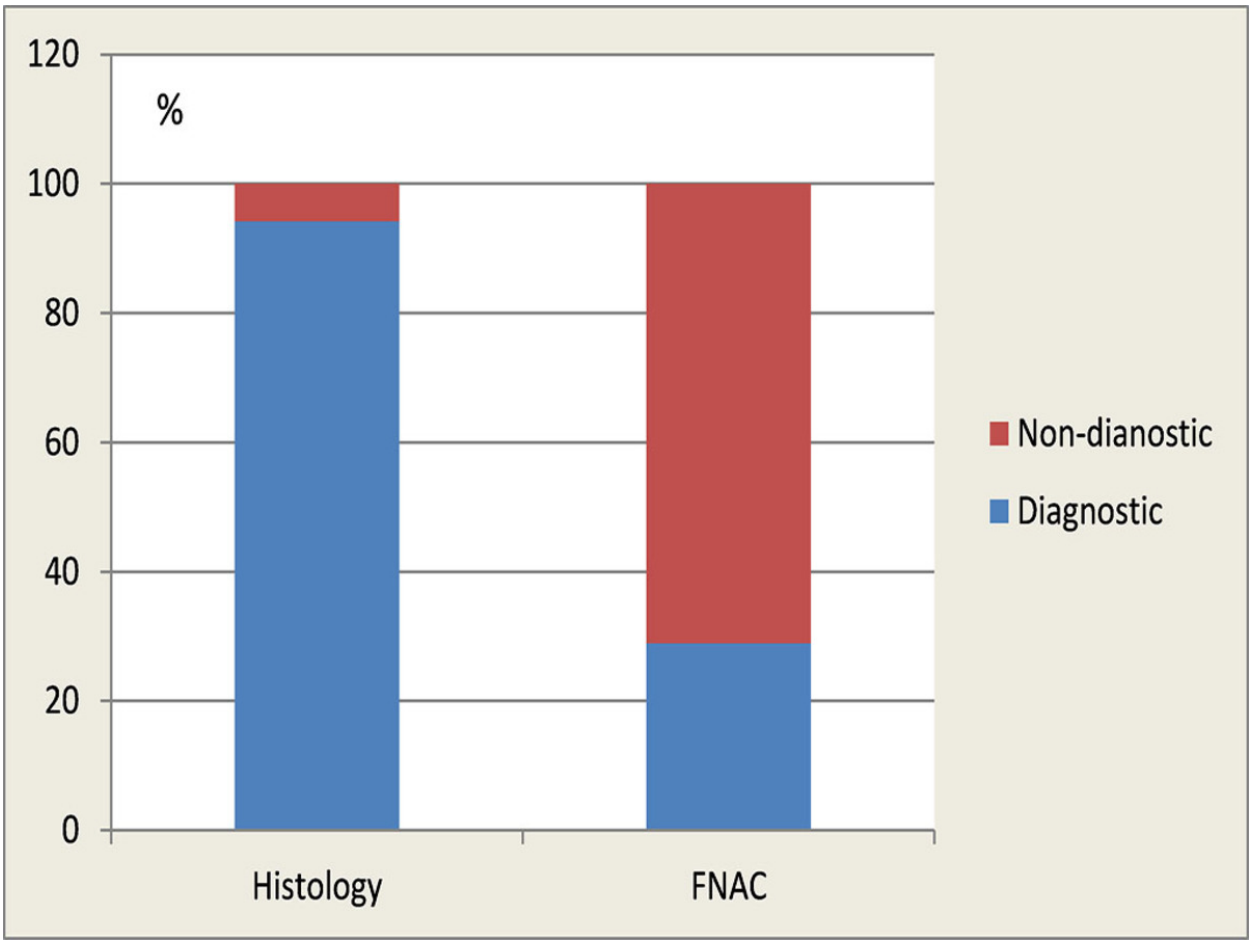

Fig. 11: Sensitivity for FNAC was 28% compared to 94% for histology. Necrotising granulomatous inflammation was seen in histology specimens.
References: Diagnostic Radiology, Nelson R Mandela School of Medicine - Durban/ZA

Diagnosis was confirmed by the presence of Acid Fast Bacilli (AFB) and caseating granulomas (Fig. 12).

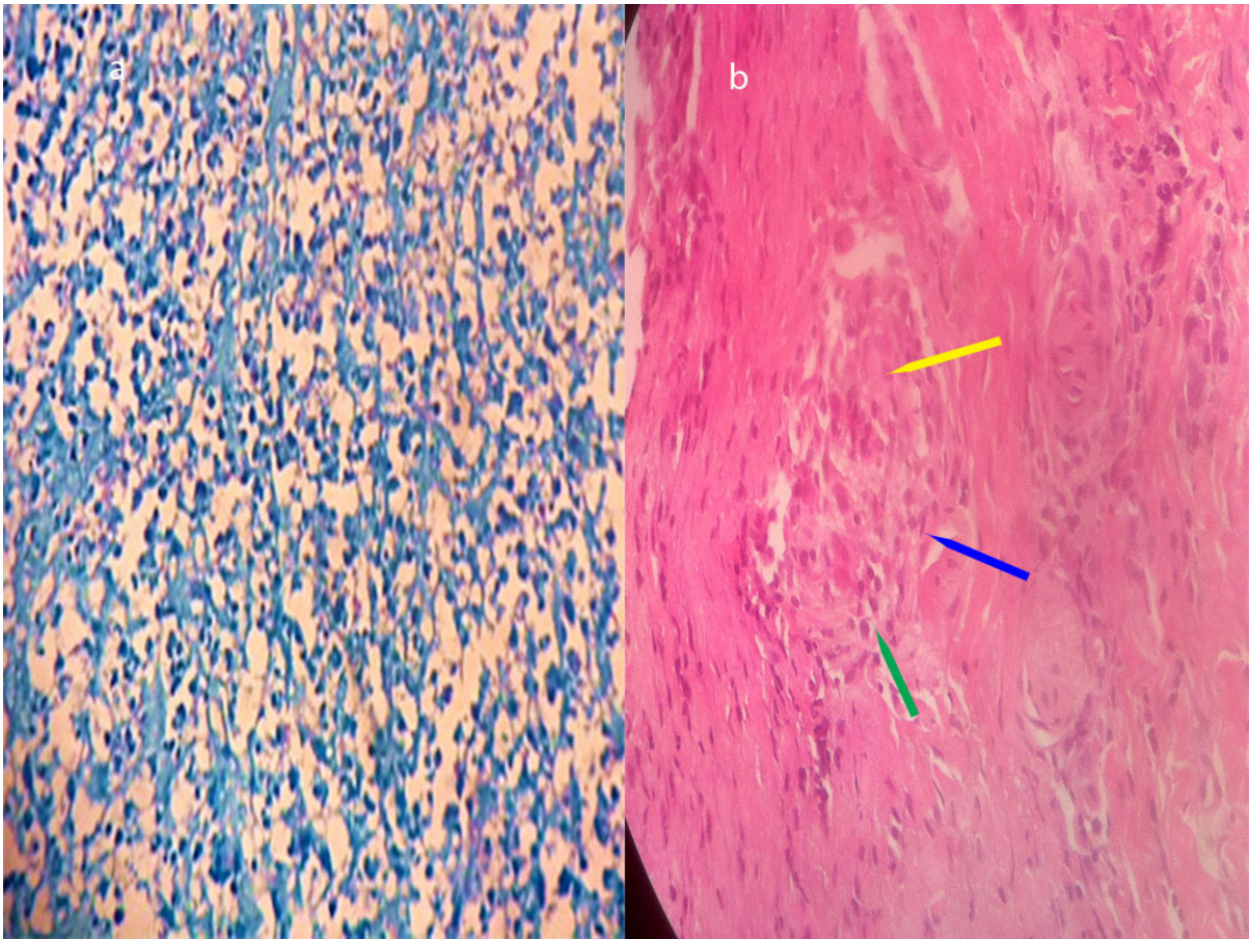

Fig. 12: A. 400x (High power) magnification. Clumps of acid-fast bacilli (red against a blue background) on Ziehl-Neelsen stain. B. Granuloma showing multinucleated histiocytic giant cells (yellow arrow), epitheliod histiocytes (blue arrow) and lymphocytes on the periphery (green arrow).
References: Diagnostic Radiology, Nelson R Mandela School of Medicine - Durban/ZA

In support of the literature, the yield of AFB in our study was low, being positive in 10.3% of cytology and 29.6% of histology specimens (Fig. 13). A single histological AFB detection was by polymerase chain reaction (PCR). Harris et al reported a 2% rate of positive Ziehl-Neelsen (ZN) smears for AFB from the tuberculous breast abscess fluid [15]. Furthermore, AFB-positive smear is not always adequate for a definitive diagnosis of *M. tuberculosis*, as it should be differentiated from other Mycobacterium species [16].

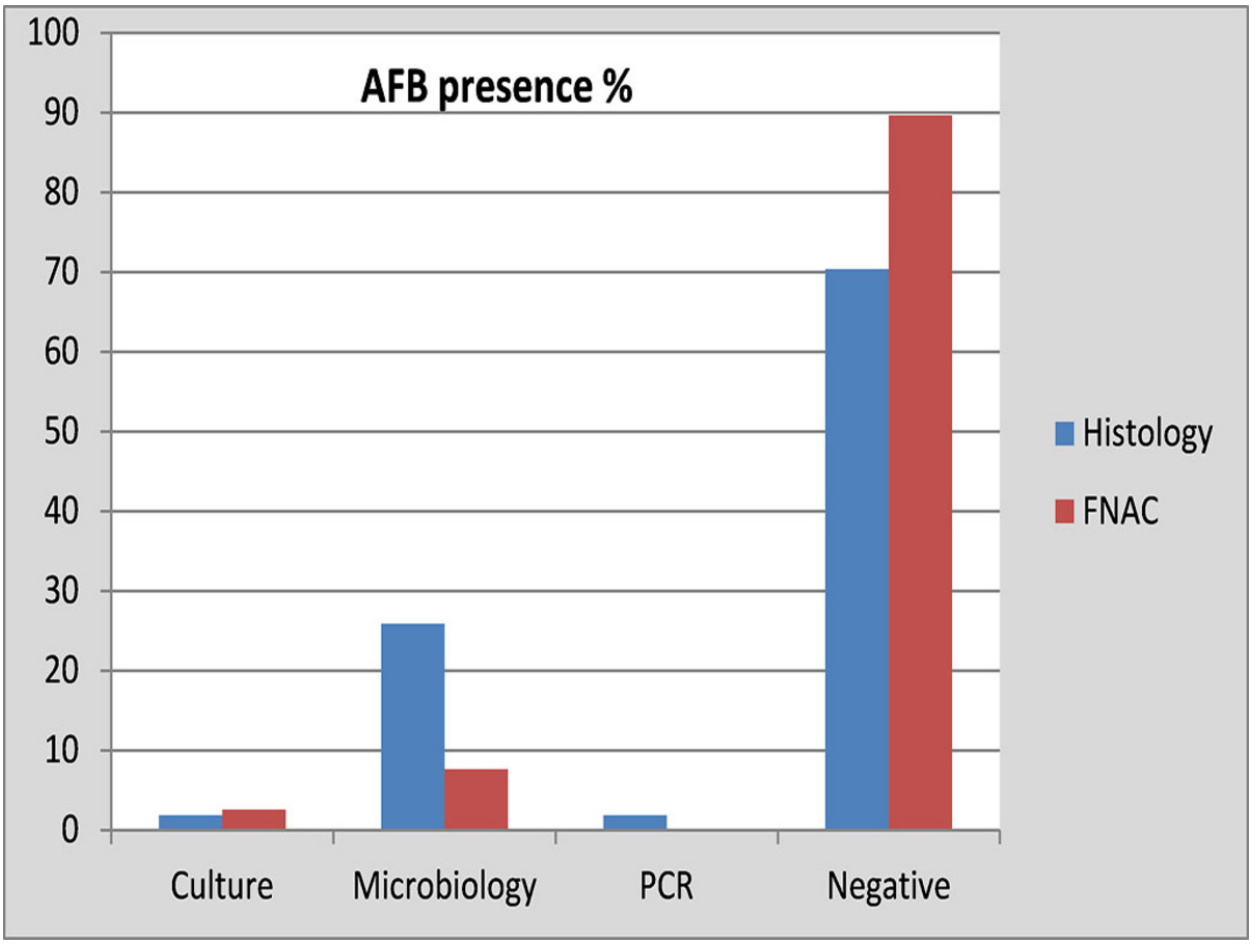

Fig. 13: Detection of AFB's in pathology samples.
References: Diagnostic Radiology, Nelson R Mandela School of Medicine - Durban/ZA

Treatment methods

Summarised in (Fig. 14).

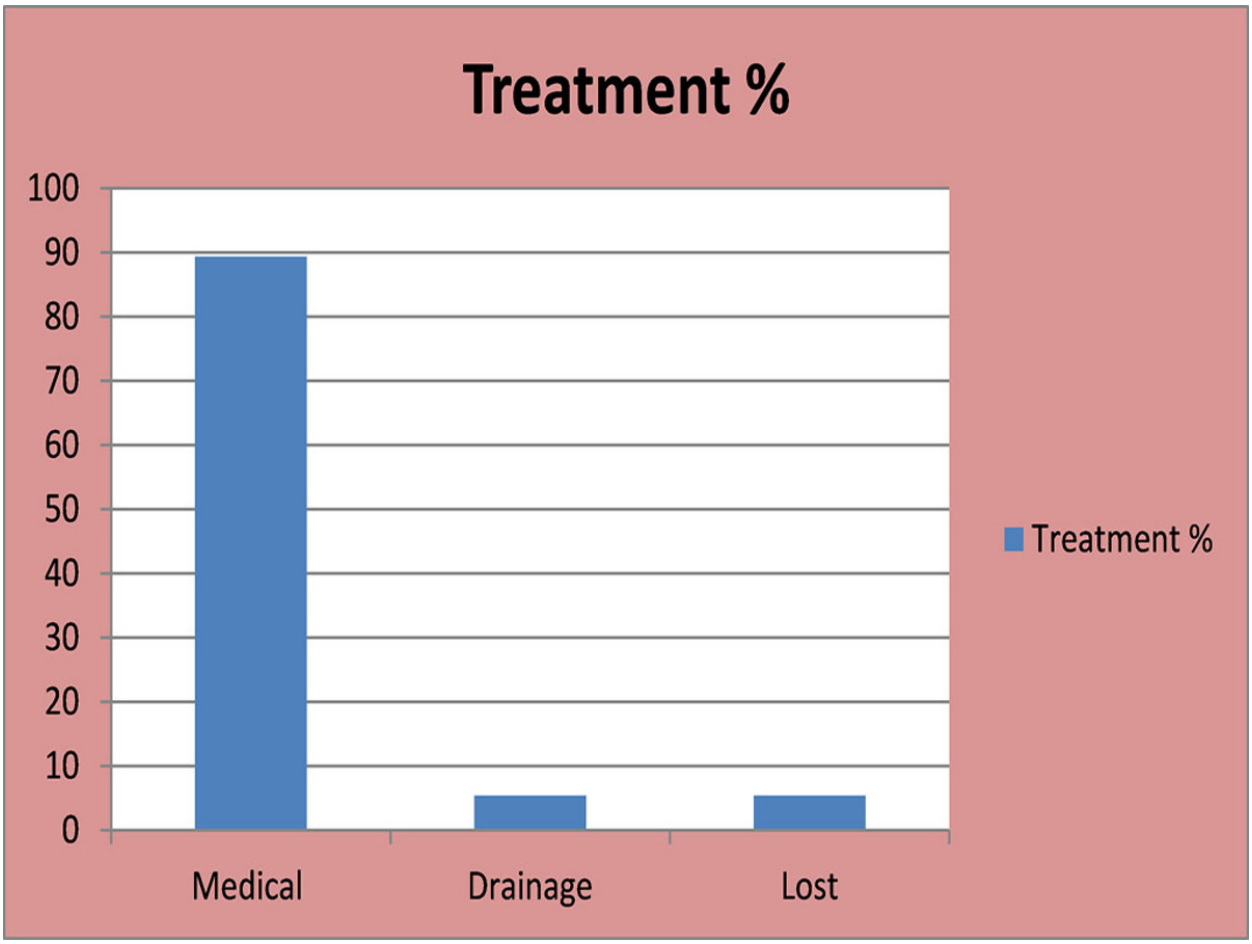

Fig. 14: Amongst all 65 patients, 59 received medical treatment comprising of 9 months of standard anti-TB treatment (ATT). Three patients received both medical and surgical intervention involving abscess drainage, whilst three were lost and were never treated following diagnosis.
References: Diagnostic Radiology, Nelson R Mandela School of Medicine - Durban/ZA

Treatment outcome

Summarised in (Fig. 15).

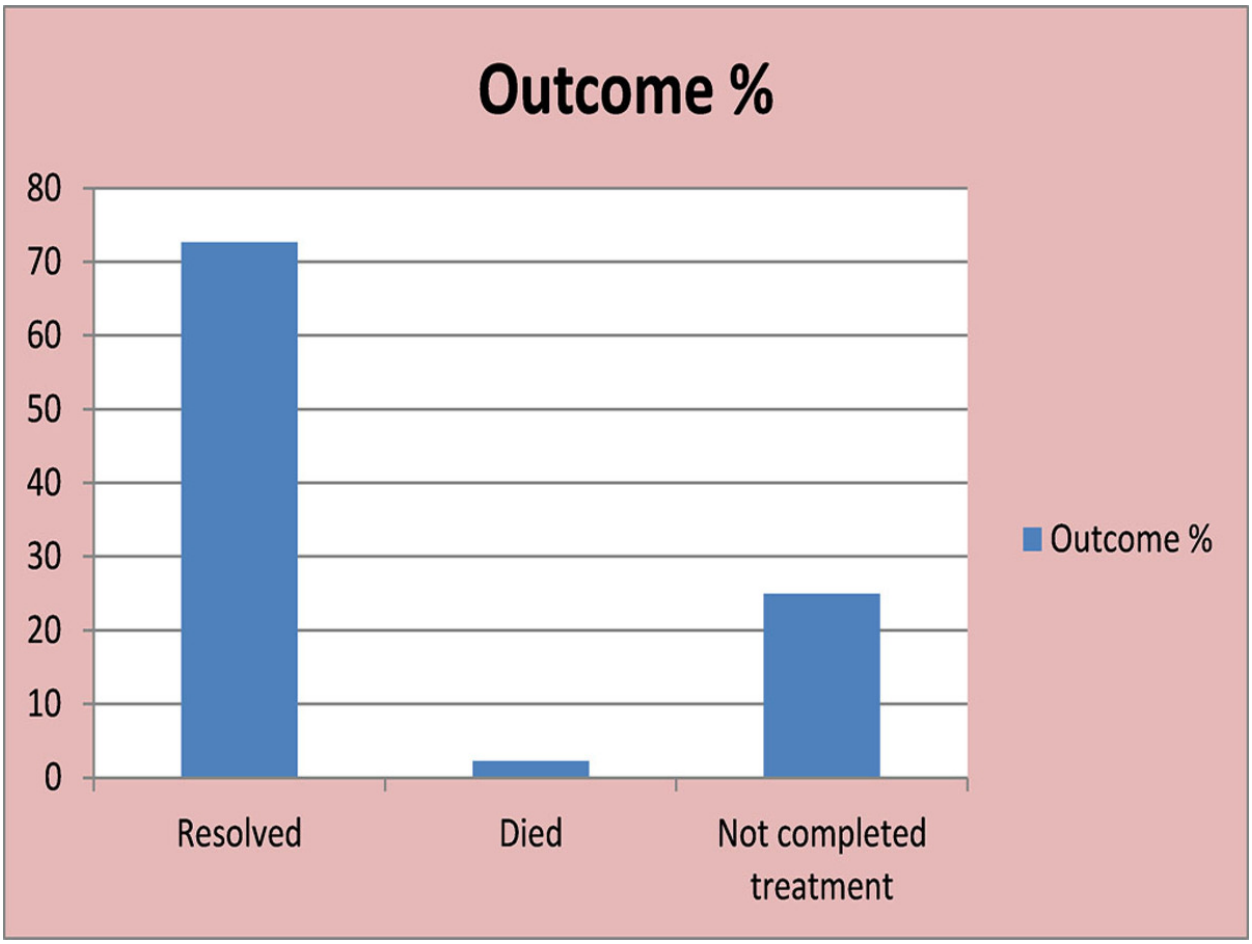

Fig. 15: Of those treated, 72.7% obtained full resolution, 25% did not complete treatment, and 2.3% died (n=1).
References: Diagnostic Radiology, Nelson R Mandela School of Medicine - Durban/ZA

Assessment of response to treatment was done by clinical examination and repeat of radiological investigations, including either ultrasound, mammography or both modalities. Although there are no documented criteria for radiological response, drug resistance may be suspected when lesions fail to reduce in size, or change their appearance on ultrasound or mammography. Ultrasound is especially useful in monitoring the abscess variety, to detect residual fluid collections. In single studies, both MRI [17] and PET CT [14] have shown promise as tools for monitoring response.

Images for this section:

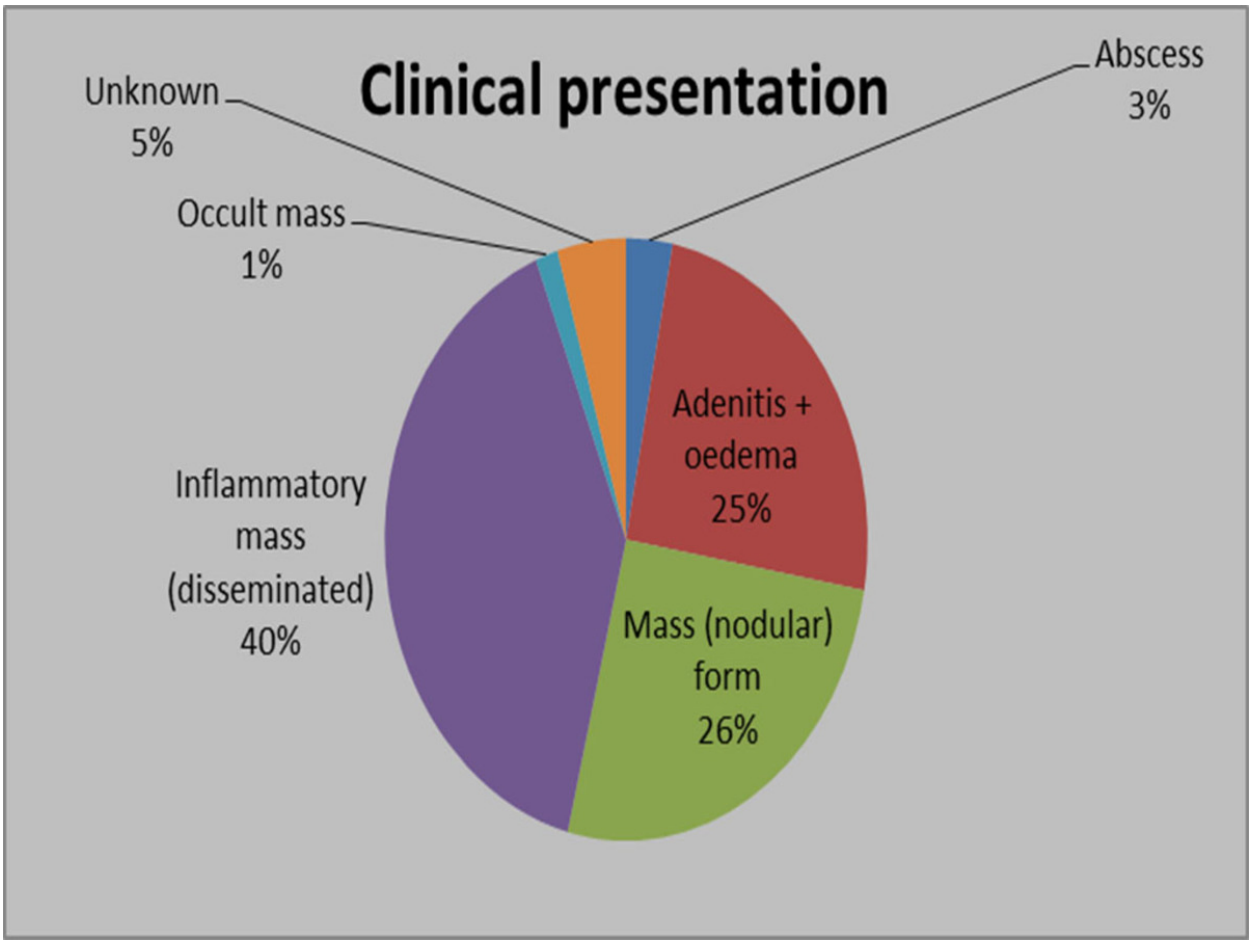

Fig. 3: Clinical presentation proportions.

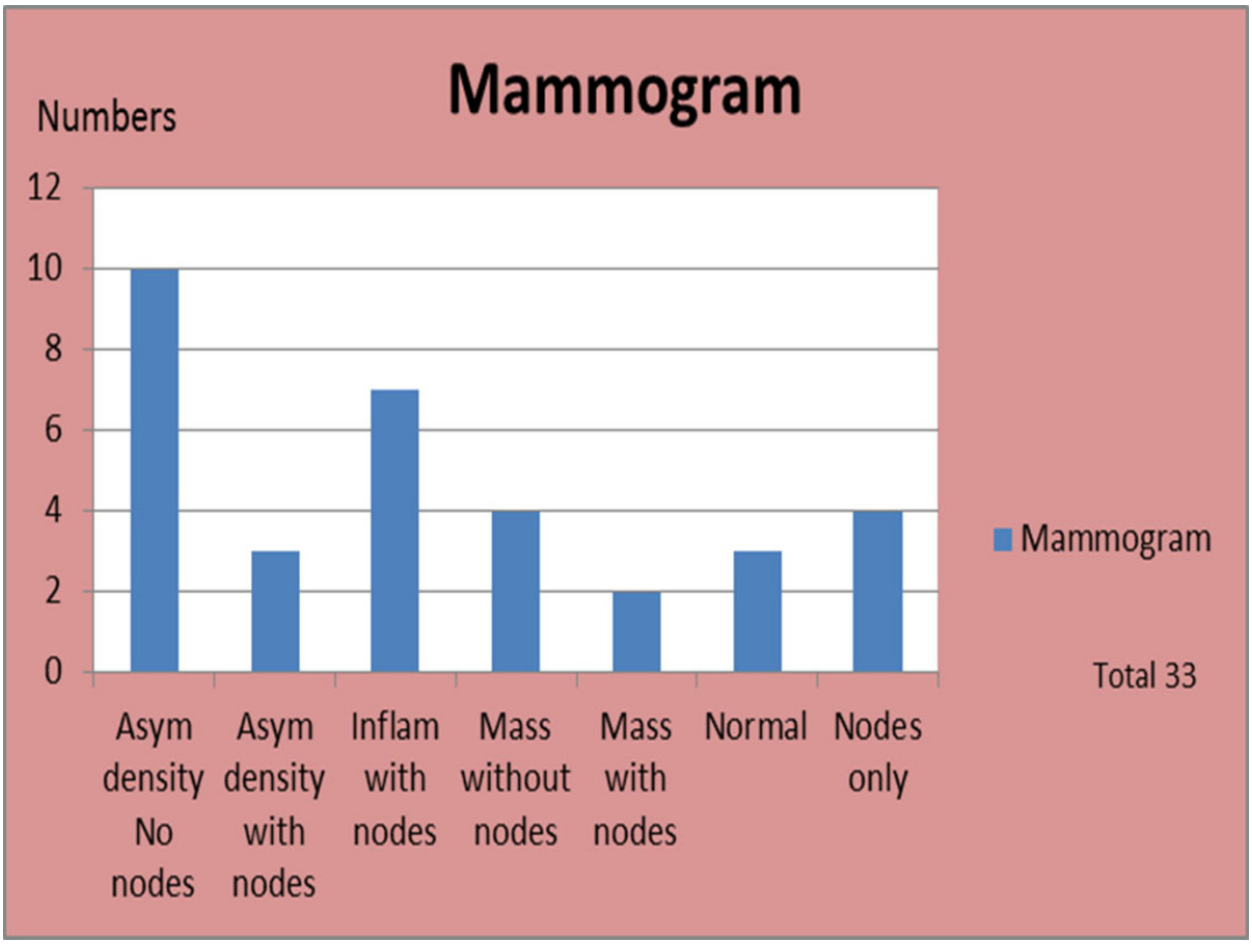

Fig. 4: Of 33 patients who had mammograms, 16 demonstrated ipsilateral or bilateral axillary lymphadenopathy. Asymmetric density pattern was seen in 13 cases.

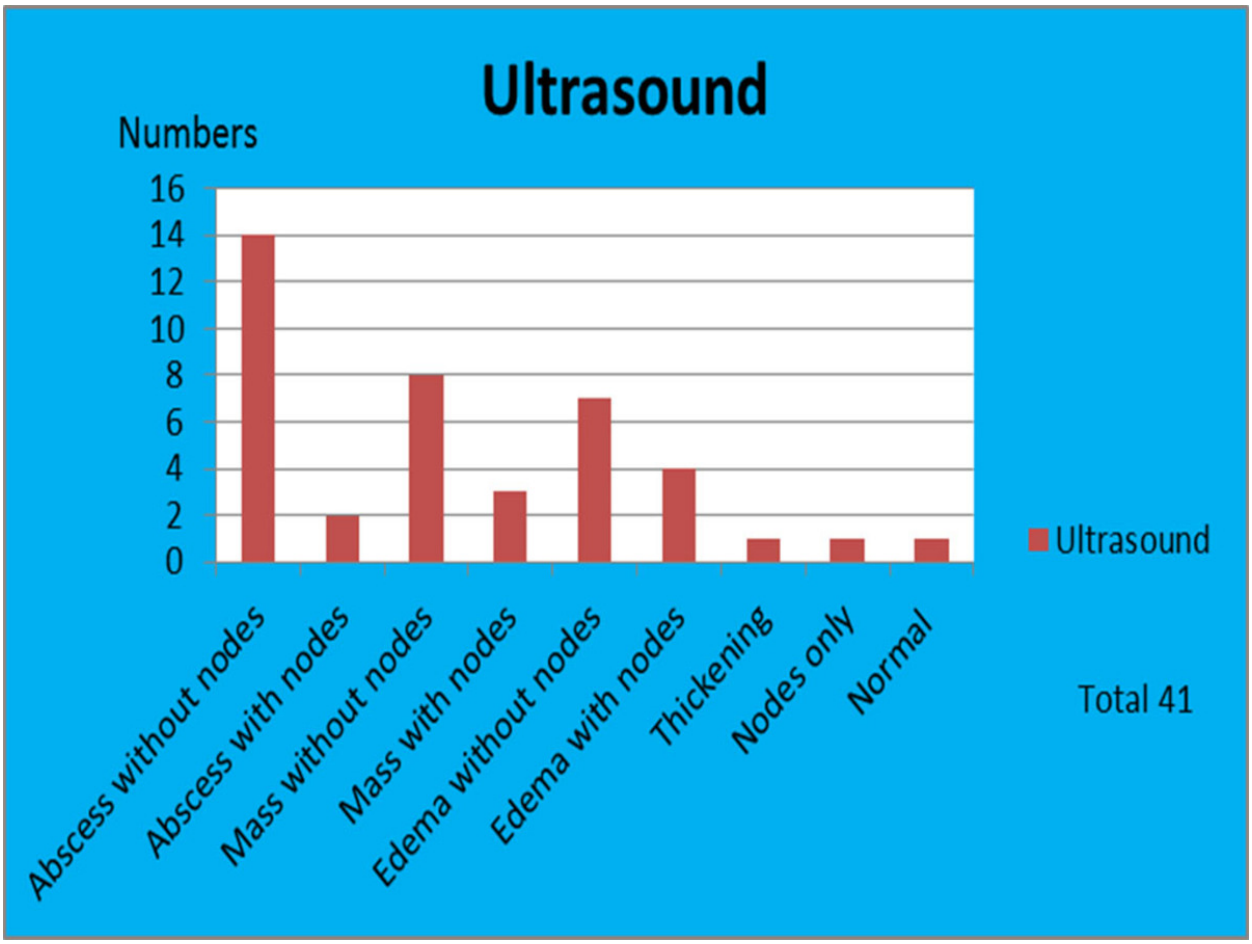

Fig. 5: Ultrasound was performed in 41 patients. The commonest pattern was abscess variety in 16 cases (39%).

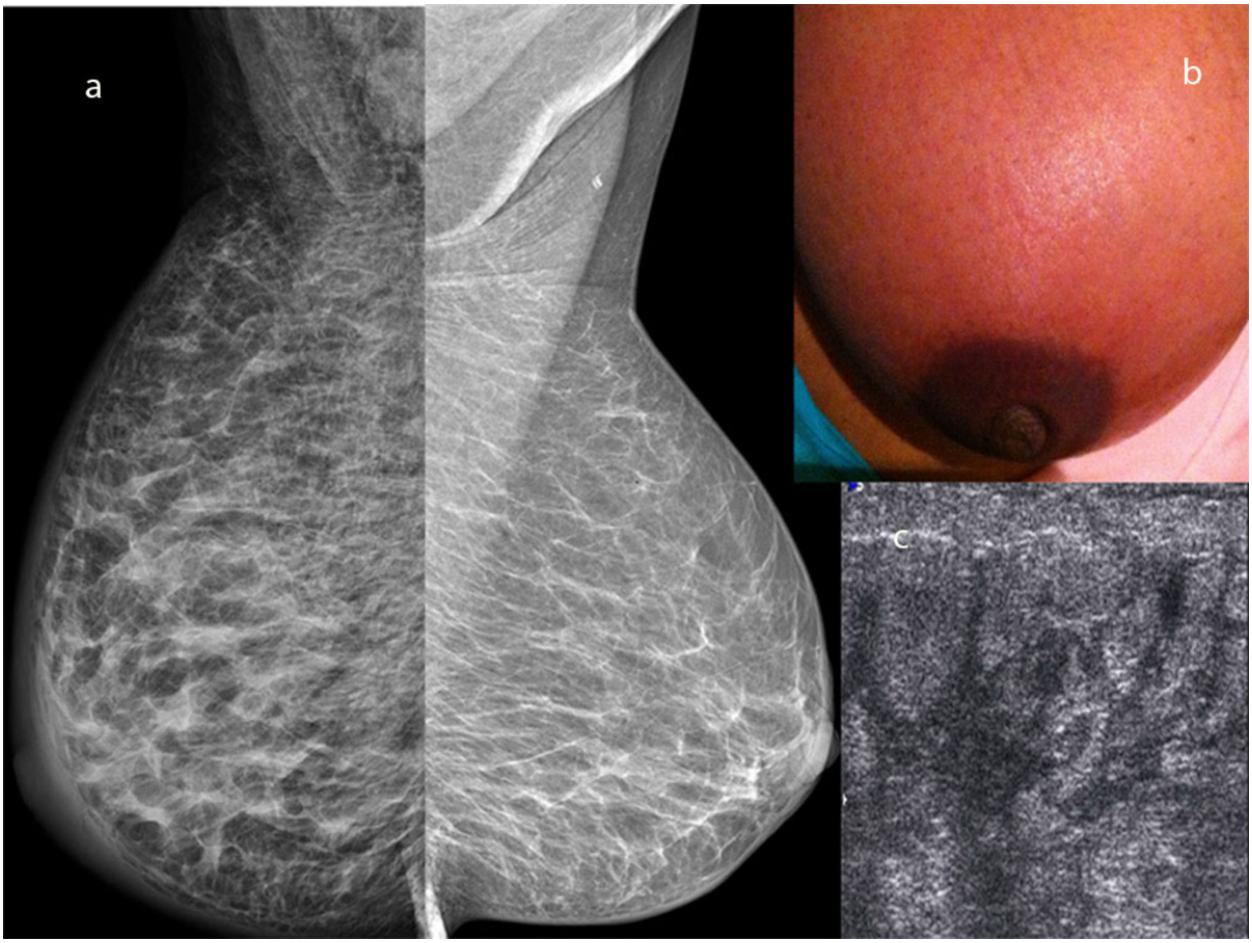

Fig. 6: Inflammatory/Disseminated Breast tuberculosis. Images taken from various patients. A. Mammogram MLO views. The right breast is enlarged. Non-specific diffuse stromal thickening and skin is oedema. B. Left breast photograph. Inflammatory skin change. C. Ultrasound images showing diffuse trabecular thickening with oedema as hypoechoic bands in between hyperechoic fibro-fatty tissue.

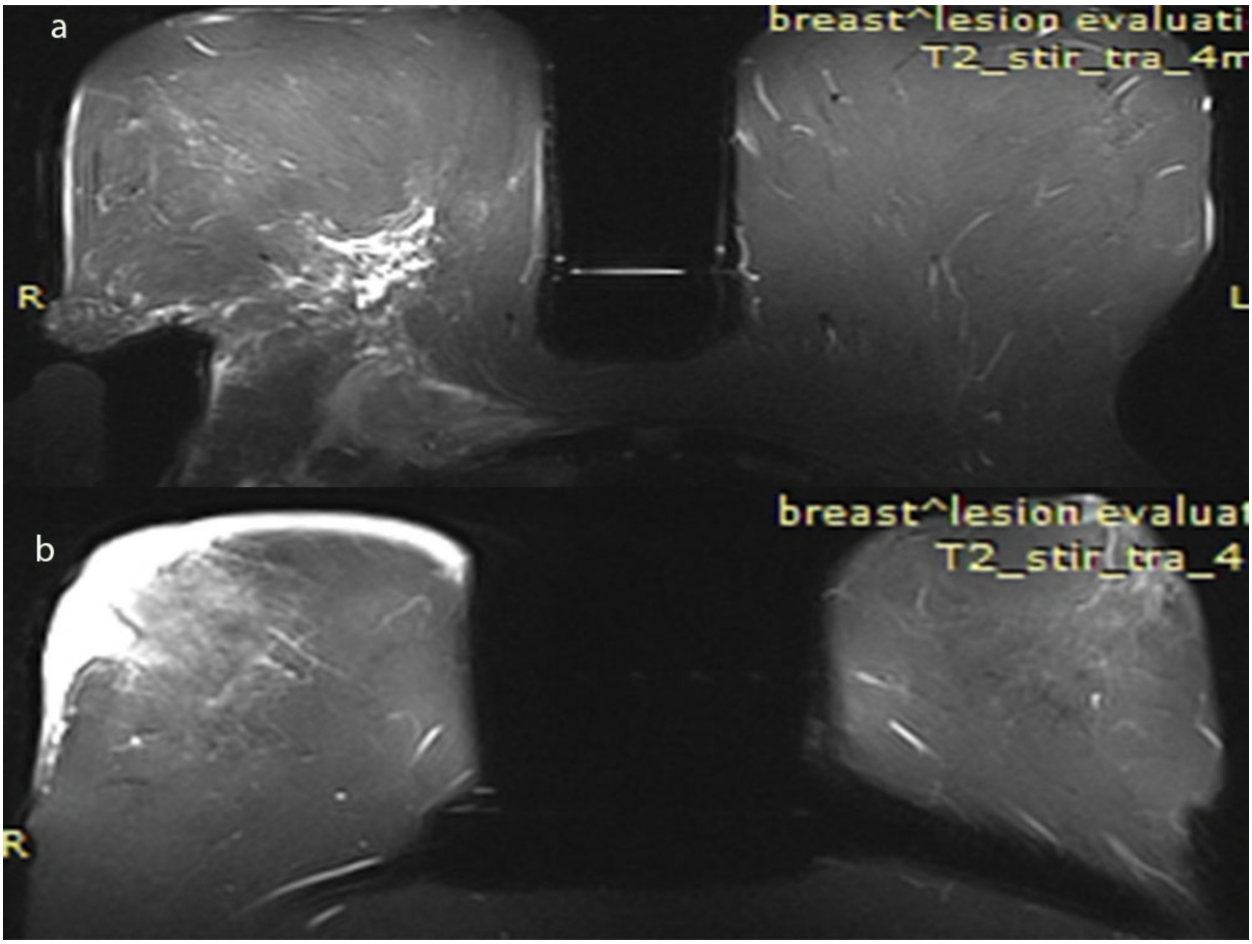

Fig. 7: Breast MRI T2 STIR axial image. A. The right breast has diffuse trabecular hyperintensity, more intense posteriorly abutting the pectoral muscles. B. Skin oedema.

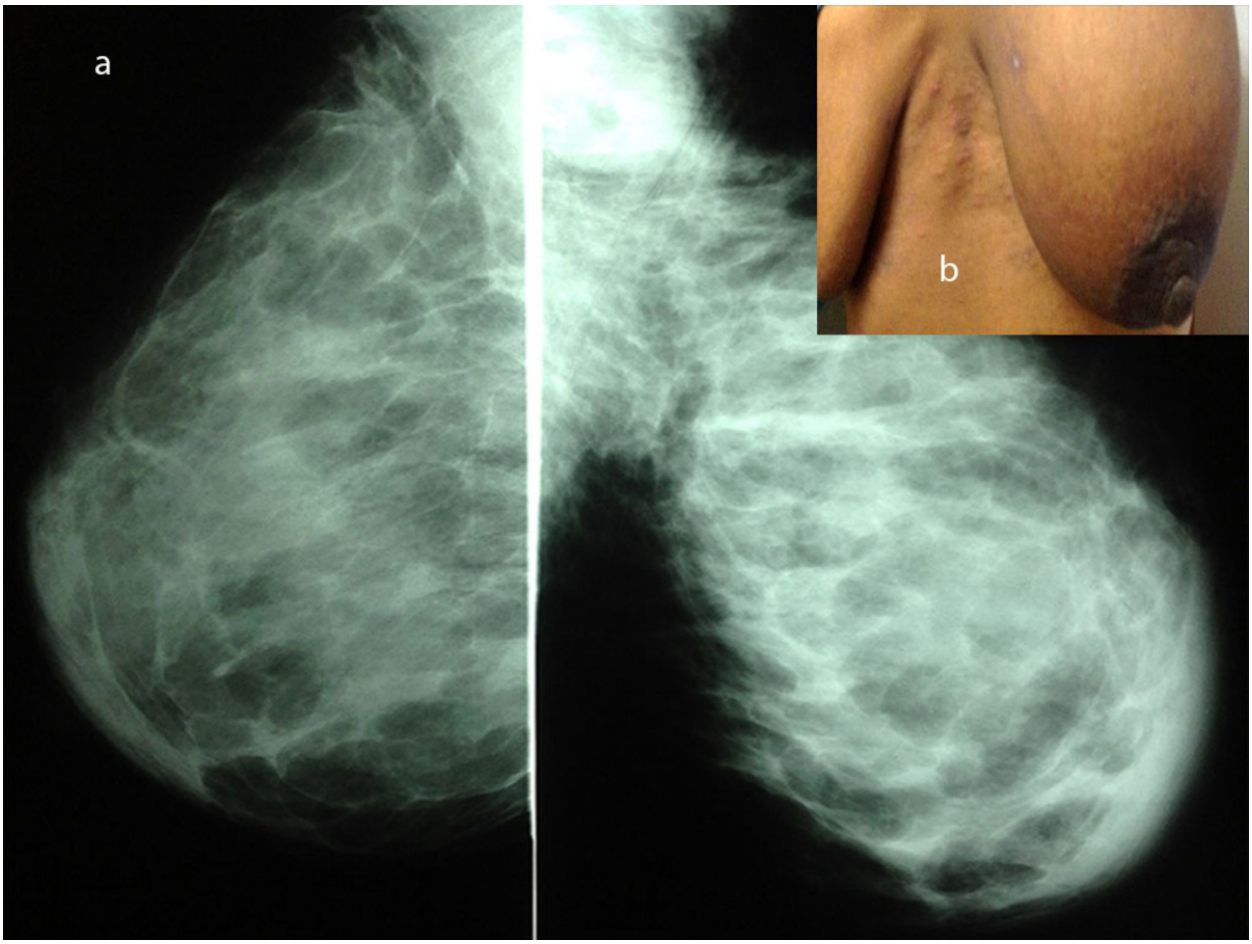

Fig. 8: A. Mammogram MLO views. The left breast is enlarged. Skin oedema and enlarged left axillary nodes are evident. B. Left breast photograph from same patient. The Left breast is larger than the right. (Note: No evidence of skin inflammation, in comparison to the inflammatory pattern).

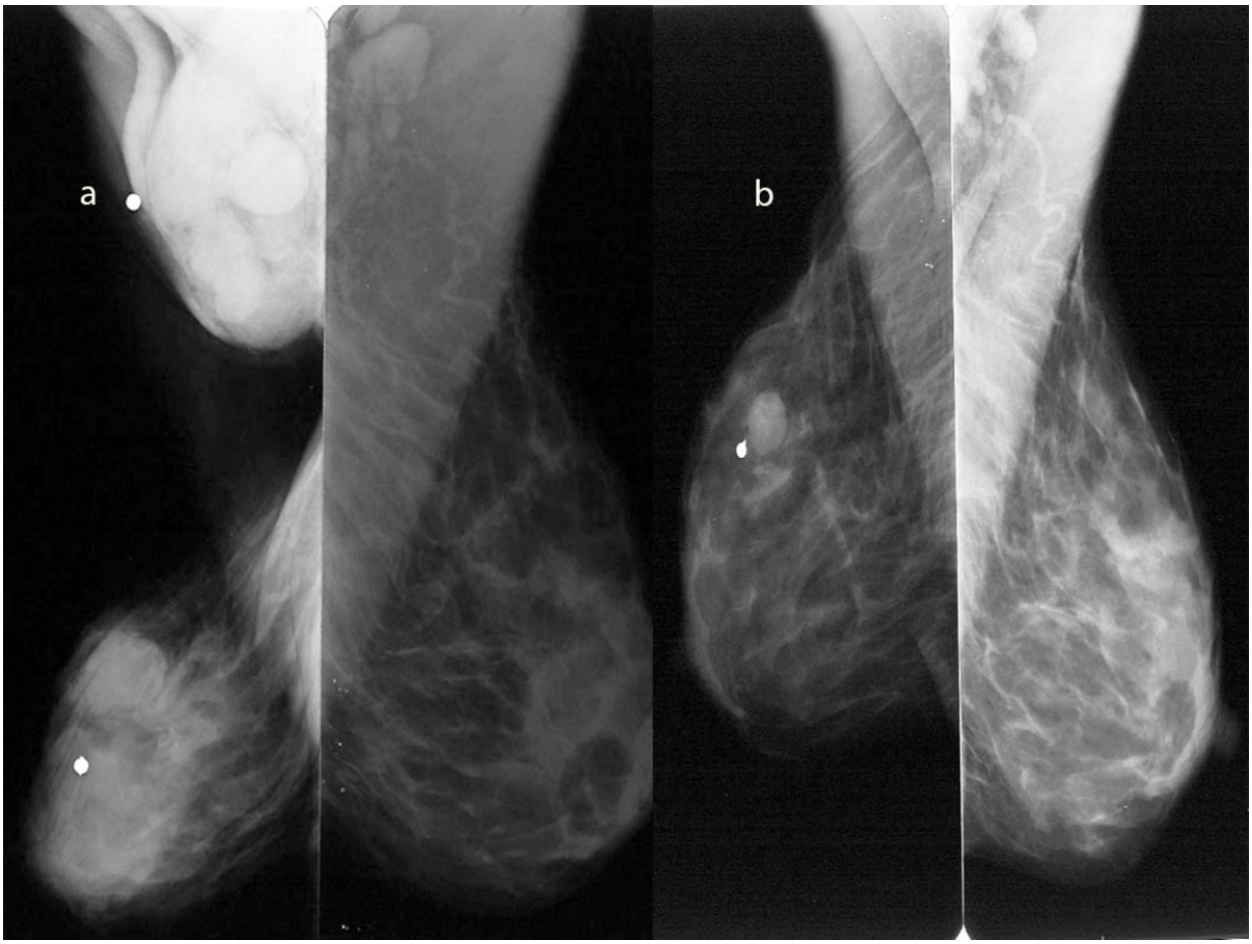

Fig. 9: Nodular form breast tuberculosis. Mammogram MLO views. A. At presentation. Multiple rounded mass opacities in right breast, and enlarged dense right axillary nodes. B. After 4 months of treatment with ATT. One small round mass opacity remains in upper part.

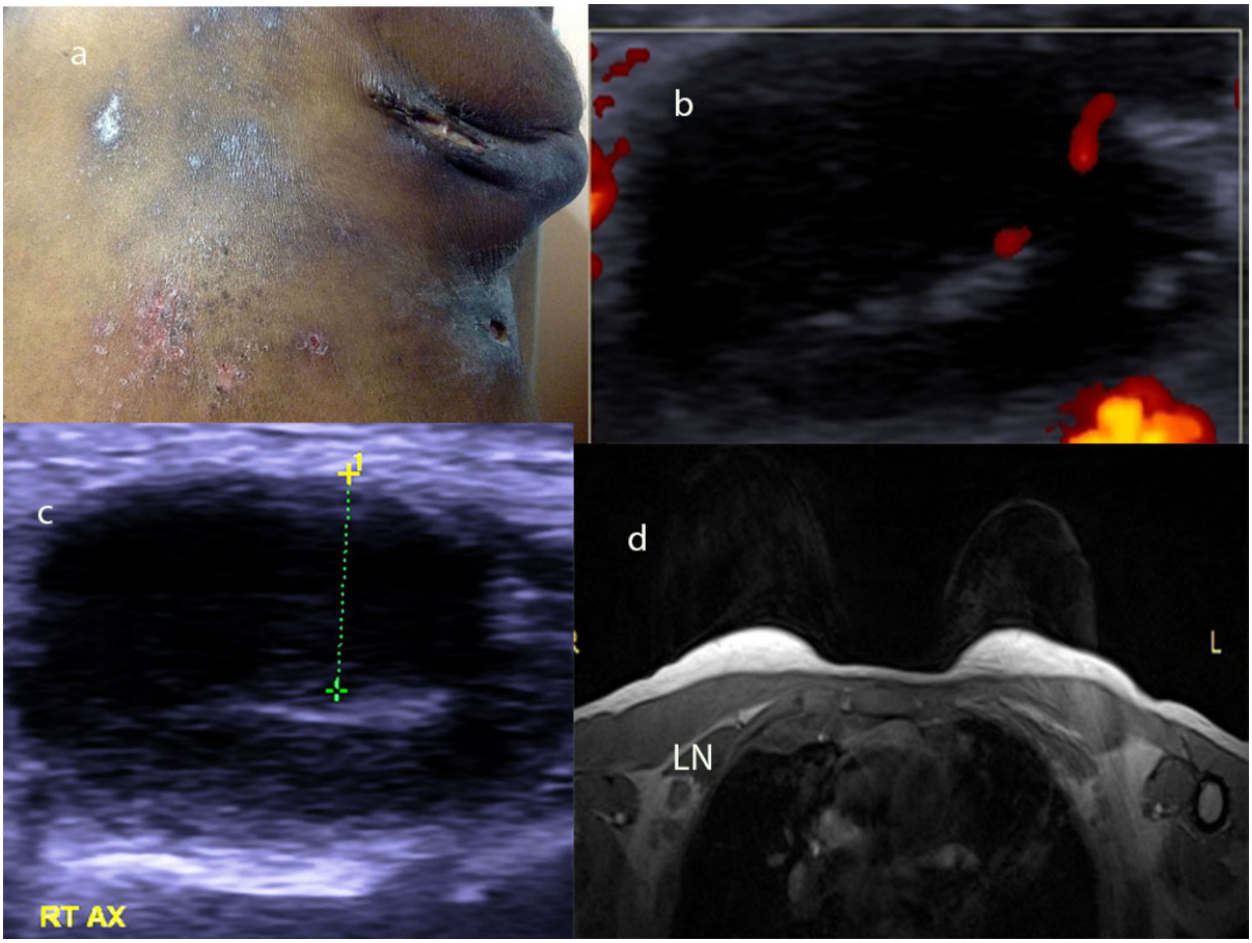

Fig. 10: Tuberculous lymphadenitis. A. Left axilla enlarged nodes discharging onto skin sinuses. B. Ultrasound Doppler, hilum vessel and thick cortex seen. C. Ultrasound shows node with thick 7mm cortex (callipers). D. Breast MRI T1 post contrast axial image. Right axillary nodes (LN) have peripheral rim enhancement and central low signal (PRECLO).

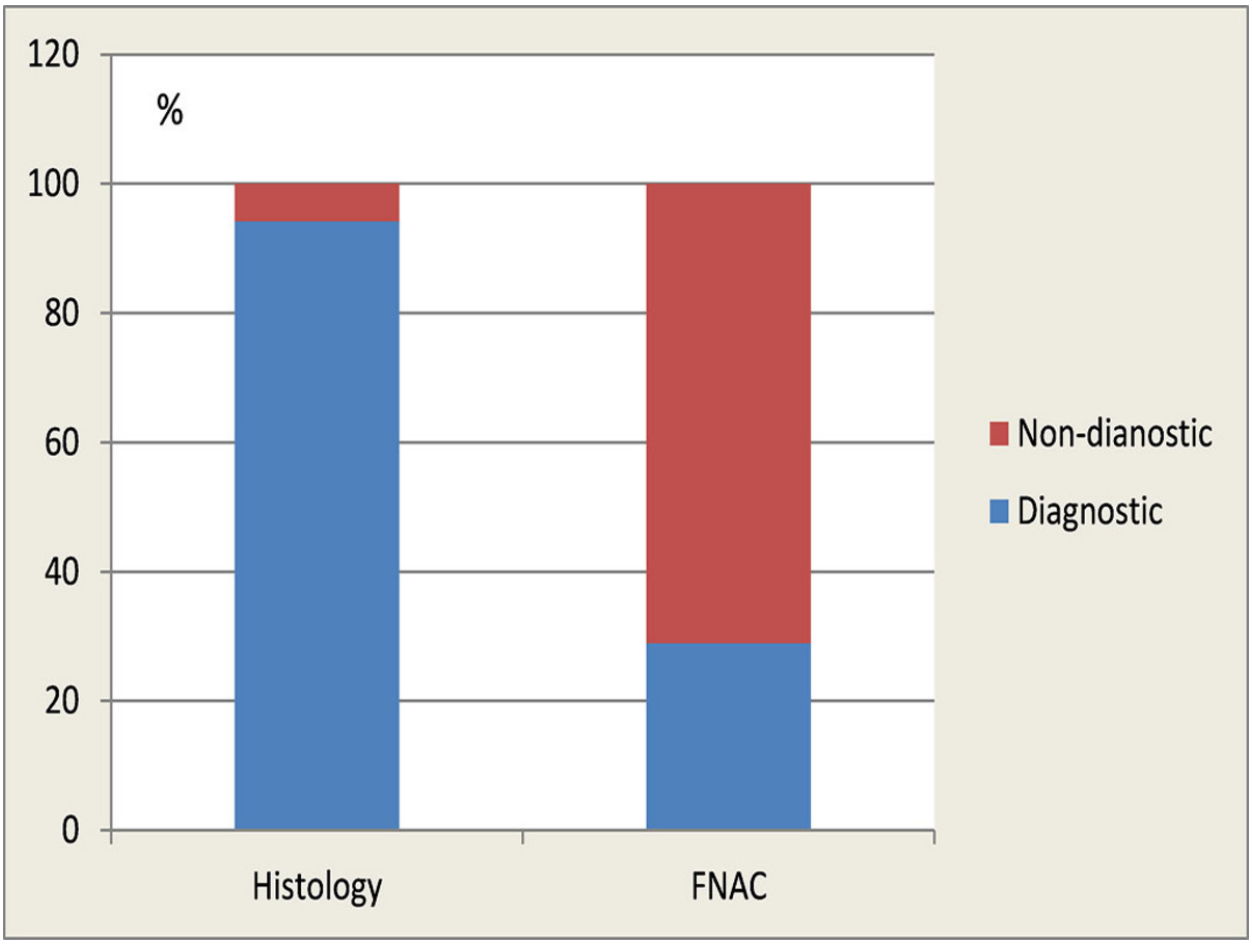

Fig. 11: Sensitivity for FNAC was 28% compared to 94% for histology. Necrotising granulomatous inflammation was seen in histology specimens.

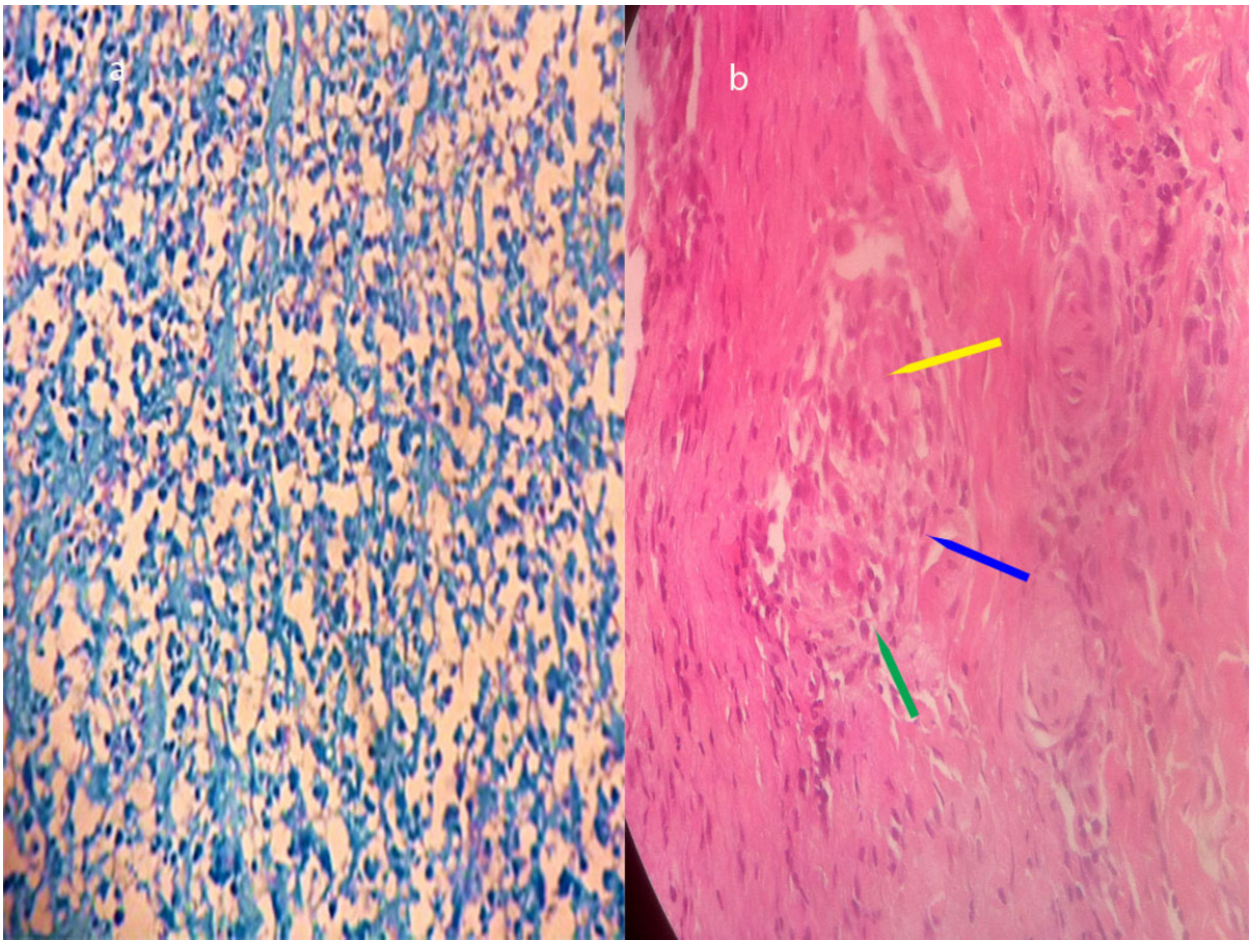

Fig. 12: A. 400x (High power) magnification. Clumps of acid-fast bacilli (red against a blue background) on Ziehl-Neelsen stain. B. Granuloma showing multinucleated histiocytic giant cells (yellow arrow), epitheliod histiocytes (blue arrow) and lymphocytes on the periphery (green arrow).

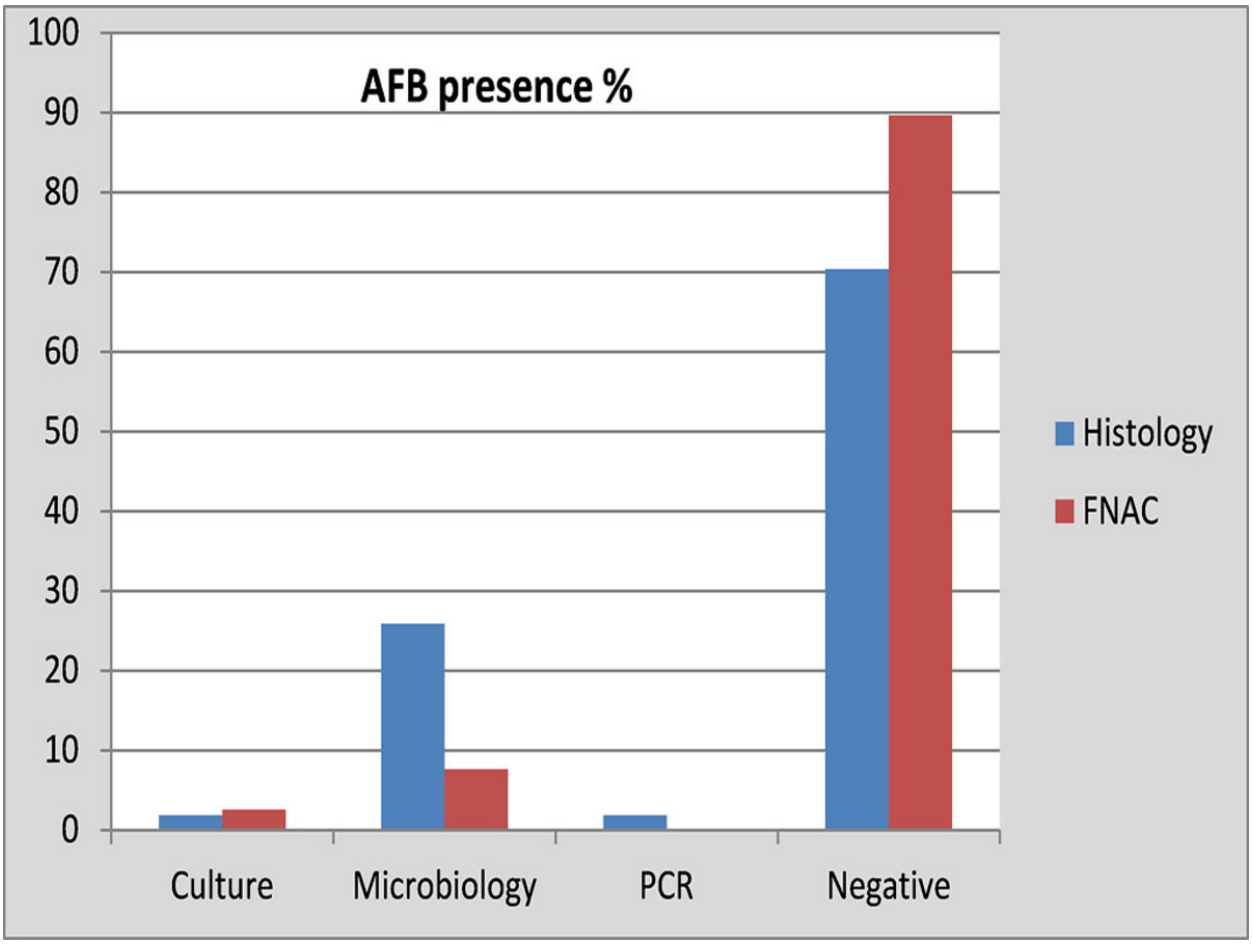

Fig. 13: Detection of AFB's in pathology samples.

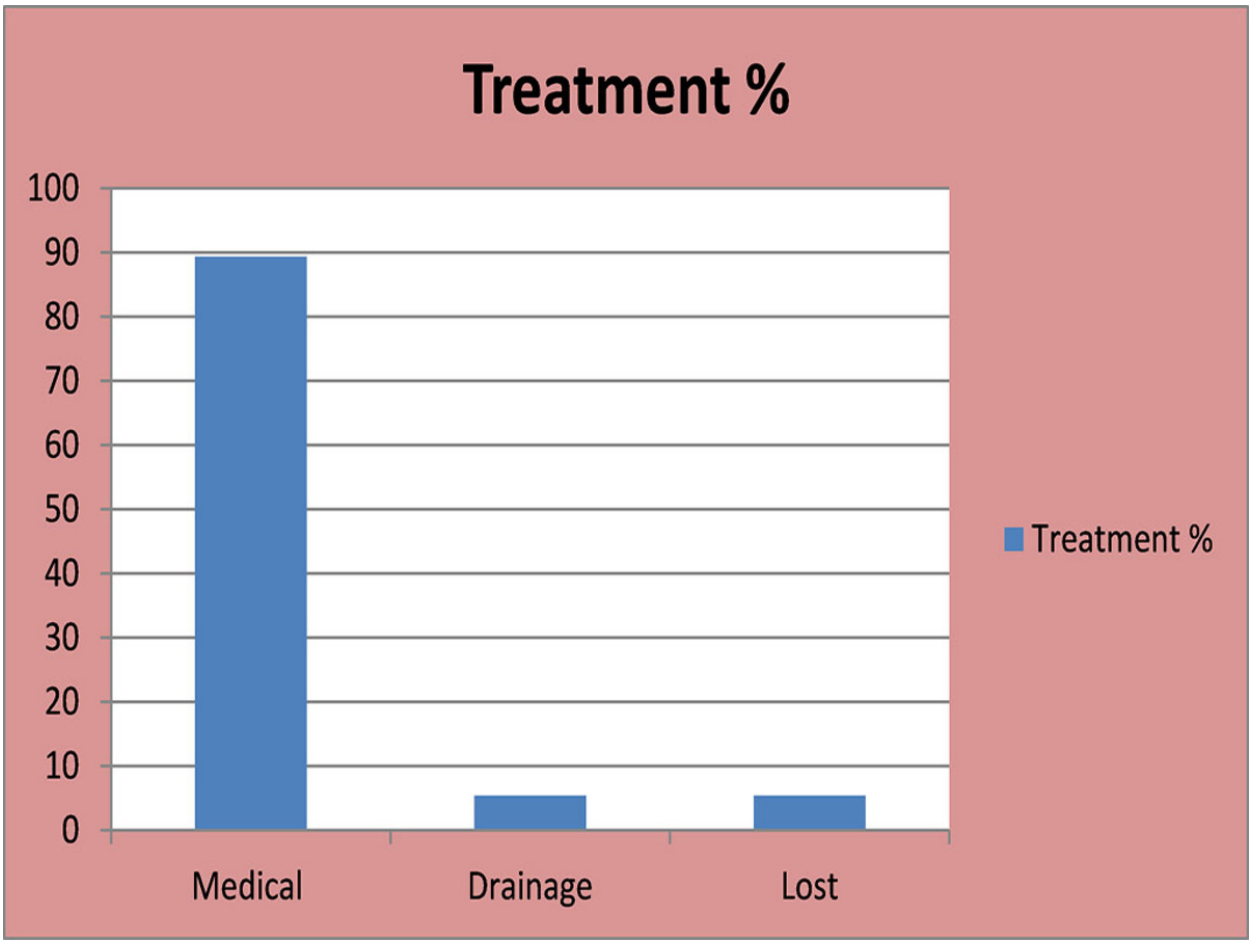

Fig. 14: Amongst all 65 patients, 59 received medical treatment comprising of 9 months of standard anti-TB treatment (ATT). Three patients received both medical and surgical intervention involving abscess drainage, whilst three were lost and were never treated following diagnosis.

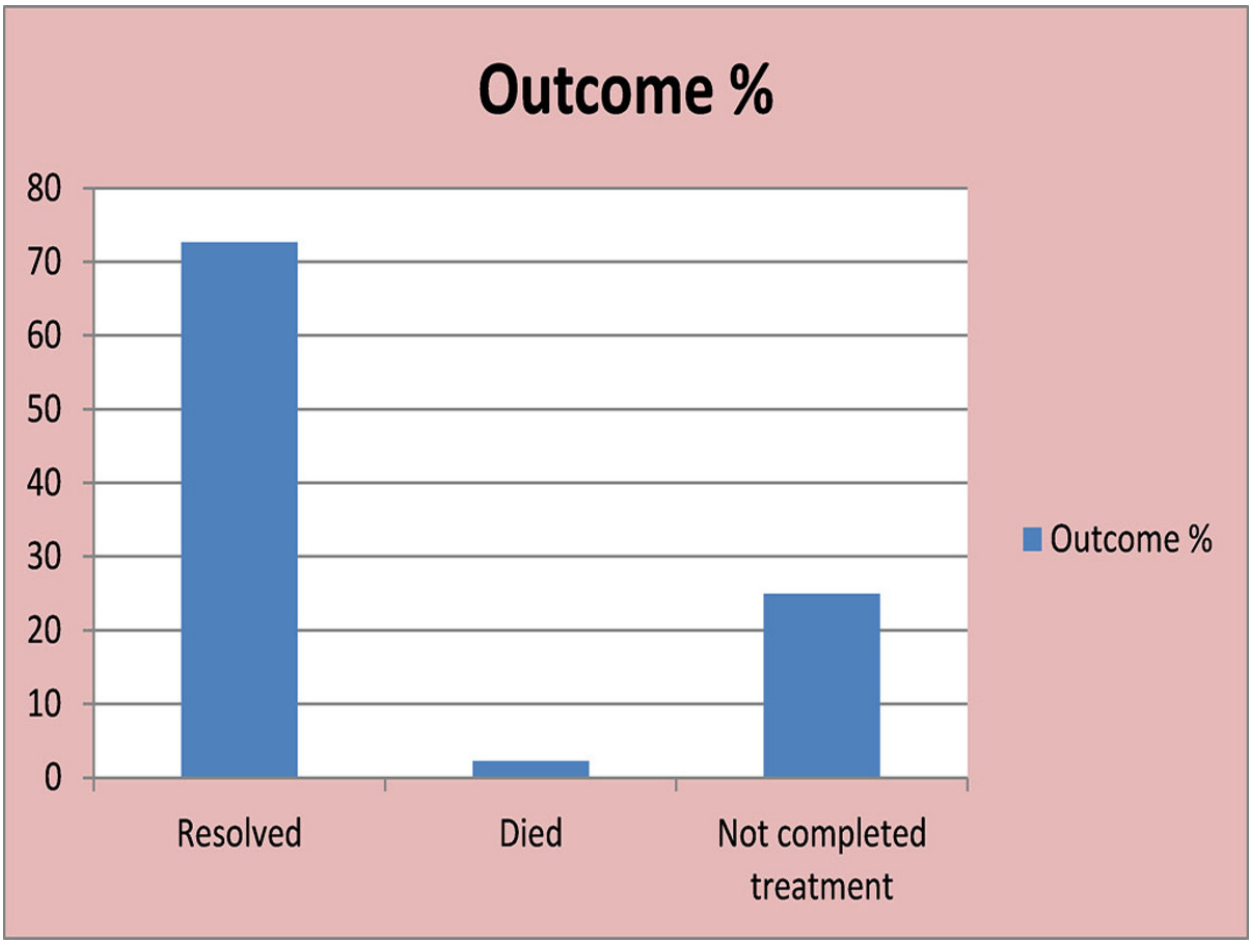

Fig. 15: Of those treated, 72.7% obtained full resolution, 25% did not complete treatment, and 2.3% died (n=1).

Conclusion

The varied clinical and radiological presentations of breast tuberculosis have been demonstrated. Early diagnosis can lead to full response following treatment with standard anti-TB treatment, averting more invasive surgical treatment or even breast disfigurement. The practising clinician requires an awareness of these patterns and a high index of suspicion if misdiagnosis and inappropriate management is to be avoided.

Limitations

Due to the study being retrospective, the data regarding follow up post completion of treatment was not complete, even though patients were scheduled for further visits.

Personal information

Dibuseng P. Ramaema FCRad (Diag) SA[1,*],

Ines Buccimazza FCS (SA), FACS[2],

Richard J Hift MMed (Med) PhD FCRP FCP (SA) [3]

Affiliations:

1. Division of Radiation Medicine (Radiology), Nelson R Mandela School of Medicine, University of KwaZulu-Natal, Durban, South Africa.

2. Division of General Surgery, Nelson R Mandela School of Medicine, University of KwaZulu-Natal, Durban, South Africa.

3. Division of Medicine, Nelson R Mandela School of Medicine, University of KwaZulu-Natal, Durban, South Africa.

***Corresponding author:**

Dibuseng P Ramaema, Radiology department, Nelson R Mandela School of Medicine, University of KwaZulu-Natal, Private Bag 7, Congella, Durban 4013, South Africa

Email: Ramaema@ukzn.ac.za

Tel: +27 31 2604301

Fax: +27 31 2604621

References

1. Gupta R, Singal R P, Gupta A, Singal S, Shahi S R and Singal R Primary tubercular abscess of the breast - an unusual entity. Journal of Medicine & Life.2012; 5: 98-100

2. Kalaç N, Ozkan B, Bayiz H, Dursun A B and Demira# F Breast tuberculosis. Breast (Edinburgh, Scotland).2002; 11: 346-349

3. Tewari M and Shukla H S Breast tuberculosis: diagnosis, clinical features & management. The Indian Journal Of Medical Research.2005; 122: 103-110

4. Singal R, Bala J, Gupta S, Goyal S, Mahajan N and Chawla A Primary breast tuberculosis presenting as a lump: a rare modern disease. Annals of medical and health sciences research.2013; 3: 110-2

5. Meerkotter D, Spiegel K and Page-Shipp L S Imaging of tuberculosis of the breast: 21 cases and a review of the literature. Journal of medical imaging and radiation oncology.2011; 55: 453-60

6. Mehta G, Mittal A and Verma S Breast tuberculosis- clinical spectrum and management. The Indian Journal Of Surgery.2010; 72: 433-437

7. Akbulut S, Sogutcu N and Yagmur Y Coexistence of breast cancer and tuberculosis in axillary lymph nodes: a case report and literature review. Breast Cancer Res Treat.2011; 130: 1037-42

8. Baslaim M M, Al-Amoudi S A, Al-Ghamdi M A, Ashour A S and Al-Numani T S Case report: Breast cancer associated with contralateral tuberculosis of axillary lymph nodes. World journal of surgical oncology.2013; 11: 43

9. Kumar M, Chand G, Nag V L, Maurya A K, Rao R N, Agarwal S, Babu S S and Dhole T N Breast tuberculosis in immunocompetent patients at tertiary care center: A case series. Journal of research in medical sciences : the official journal of Isfahan University of Medical Sciences.2012; 17: 199-202

10. Tanrikulu A C, Abakay A, Abakay O and Kapan M Breast Tuberculosis in Southeast Turkey: Report of 27 Cases. Breast Care (Basel).2010; 5: 154-157

11. Shushtari M H S, Alavi S M and Talaeizadeh A Breast Tuberculosis: Report of nine cases of extra pulmonary tuberculosis with breast mass. Pakistan Journal of Medical Sciences.2011; 27: 582-585

12. K. K. Oh J H K a S H K and Imaging of tuberculous disease involving breast European radiology.1998; 8: 6

13. Tewari M S H and Breast tuberculosis: Diagnosis, clinical features and management. Indian J Med Res.2005; 8

14. Mike Sathekge A M, Yves D'Asseler, Mariza Vorster, Harlem Gongxeka and Christophe Van de Wiele Tuberculous lymphadenitis: FDG PET and CT findings in responsive and nonresponsive disease European Journal of Nuclear Medicine and Molecular Imaging 2012; 39: 7

15. Harris S H, Khan M A, Khan R, Haque F, Syed A and Ansari M M Mammary tuberculosis: Analysis of thirty eight patients. ANZ Journal of Surgery.2006; 76: 234-237

16. Akcay M N, Saglam L, Polat P, Erdogan F, Albayrak Y and Povoski S P Mammary tuberculosis - importance of recognition and differentiation from that of a breast malignancy: report of three cases and review of the literature. World J Surg Oncol.2007; 5: 67

17. Fellah L, Leconte I, Weynand B, Donnez J and Berlière M Breast tuberculosis imaging. Fertility and Sterility.2006; 86: 460-461